OM PRAKASH PANDEY

TERRESTRIAL HEAT FLOW IN NEW ZEALAND

Submitted for the degree of

Doctor of Philosophy in Geophysics
Institute of Geophysics
Victoria University of Wellington
New Zealand

August, 1981

ABSTRACT

In this regional heat flow study of New Zealand temperatures have been measured in available boreholes using a specially constructed thermistor probe, and existing temperature information has been incorporated from various sources including oil prospecting boreholes. Thermal conductivity has been measured in the laboratory on 581 samples. Newly determined values of heat flow are given for 105 locations; values for the South Island are here presented for the first time.

Most of the heat flow values have been grouped in eight regions based on the level of heat flow. This classification can be related to the occurrence of certain surface manifestations and geophysical anomalies, and to regional plate tectonics. High heat flow in three regions is consistent with melting conditions being reached at depths between 35km and 45km. These are the Taranaki Region, the West Coast Region and the Great South Basin. The average regional heat flow for these regions varies from 86.4 mW/m^2 to 110.7 mW/m^2. Much lower heat flow is obtained in the Hikurangi and Marlborough-Canterbury Regions; these may possibly be interconnected. Elsewhere the heat flow is low to normal with isolated highs. The broad distribution of heat flow in the North Island is typical for an active subduction region.

Radioactive heat generation has been measured on rock types from various localities, and large variations have been found. The heat flow - heat generation relationship has been studied for 42 sites. A linear relationship is found only in the Taranaki and Hikurangi Regions. Temperature calculations show large differences in the deep-seated temperature distribution beneath New Zealand, and this has also been reflected in the distribution of "reduced heat flow". Temperature and heat flow can be correlated with upper mantle inhomogeneity.

The inferred variation of radioactive heat generation with depth has been studied for areas beneath the Western Canterbury Region. A mean heat generation of $1.56 \pm .07$ $\mu W/m^3$ has been found in a sequence which has been inferred to occur between 17km and 30km in depth under the region; this is very much higher than the usually adopted values for the lower crust.

Normal heat flow observed in the Western Cook Strait Region, and the existence of good seismic wave transmission beneath the same region, can be attributed to crustal and lithospheric thickening. The relevance of present study to petroleum occurrences has been examined and it is found that in areas of proven hydrocarbon potential the heat flow is high.

ACKNOWLEDGEMENTS

I am greatly indebted to Prof. F.F. Evison, Chairman, Institute of Geophysics and my supervisor, for his guidance, encouragement, help and unfailing patience throughout the study. I am also grateful to Dr T. Hatherton, Director, Geophysics Division, DSIR, for his supervision, interest and helpful discussions at various stages of the work. Discussions held with Prof. H.W. Wellman, Drs R.I. Walcott, C. Adams, J. Harper and Messrs A. Hull, R. Cook, K. Berryman and K.V.V.S. Murty were very helpful, and to them I extend my sincere thanks.

Mr T. Ball constructed the thermister probe and his assistance as well as that of Messrs W. Richardson, C. Brown and T. Stern during the field measurements is highly appreciated. Mrs M.C. Syms and Messrs J. Gumbley, G.E.K. Thompson, B. Hegan provided the temperature data for a few boreholes. I am grateful to Shell B.P. and Todd Oil Services Ltd., and the Petroleum Corporation of New Zealand Ltd., who kindly provided temperature and other pertinent data from some boreholes, and gave permission to use these data. Some unpublished heat flow results were provided by Dr R. Allis.

The permission accorded by Dr R.P. Suggate, Director, Geological Survey, DSIR, to examine petroleum reports and use borehole samples, and help rendered by Dr Peter Andrews in sample selection, are gratefully acknowledged. Drs D.N.B. Skinner, B. Waterhouse and Mr N. Fowke also provided samples from a few boreholes. Thermal conductivity measurements at high pressure were kindly performed by Prof. E.R. Decker at University of Wyoming (U.S.A.). Radioactive heat generation measurements were carried out at the University's Analytical Facility; help rendered by Mr K. Palmer is appreciated. Some unpublished heat generation data have been kindly supplied by Dr R. Grapes and Mr B. Roser.

Thanks are also due to Director, National Geophysical Research Institute, Hyderabad, India for granting study leave, and the University Grants Committee of New Zealand for the award of a Commonwealth Scholarship. I record my gratitude to Miss D.L. Anderson, Secretary, Scholarship Committee, for her help at various stages. Financial support was also provided by the internal research grant of this University.

I am extremely thankful to Mrs M. Penning for her help in the preparation of the drafts and Mrs M. Cooper for typing the thesis. Finally, I am indebted to my wife Kamala and daughter Manisha for their patience during hard times.

CONTENTS

LIST OF FIGURES

LIST OF TABLES

CHAPTER 1

INTRODUCTION

1.1 HISTORICAL

Studies of terrestrial heat flow and its relationship with other geological and geophysical parameters provide useful information about the thermal state of the earth's crust and upper mantle. The surface heat flow is closely related to the deeper temperature regime and is thus helpful in the mapping of geothermally controlled properties inside the earth (Ádám, 1978). It also has a direct relevance to regional tectonic interpretation, and plays an important role in the location of geothermal fields.

Although studies of underground temperatures and thermal conductivity have a long history (Beck, 1965; Bullard, 1965), no systematic investigations of heat flow were reported till the classical works of Benfield (1939) and Bullard (1939), and in oceanic areas heat flow was first successfully measured in 1950 (Revelle and Maxwell, 1952). Numerous investigations have since been carried out over the surface of the earth and enormous amounts of data have been compiled and interpreted by various authors (e.g. Lee and Uyeda, 1965; Simmons and Horai, 1968; Horai and Simmons, 1969; Lee, 1970; Negi and Pandey, 1974; Jessop et al., 1976). On the global scale correlations of high heat flows with unstable, younger regions and low heat flows with stable and older regions have been noted. The most important single result of the above investigations is the near equivalence of continental and oceanic heat flows. The correlation with tectonics has suggested the possibility of large regional differences in the constitution of the upper mantle. It is normally possible to explain most of the continental heat flow with the help of radioactivity from an upper crust of granitic composition, while in oceanic areas the major share must originate from below the basaltic crust, which is far less radioactive than the upper continental crust.

The distribution of heat flow measurements up to the present day is very uneven. Many of the large numbers of boreholes drilled every year cannot be used either because of regulations requiring them to be sealed, or because of financial considerations, under which casing is pulled out and the borehole collapses before thermal equilibrium is re-established, which often requires a long time compared to drilling operations (Bullard, 1947; Jaeger, 1955-56; Lachenbruch and Brewer,

1959; Cheremenski, 1960; Beck, 1965). High cost inhibits measurement in many desirable areas by means of specially drilled holes, although this has been managed by some workers (Studt and Thompson, 1969; Jaeger, 1970; Cermák and Jessop, 1971). The problems and techniques associated with satisfactory heat flow measurements on land have been critically reviewed by Beck (1965).

The most important areas lacking in detailed heat flow investigations are some of those with present tectonic, volcanic and seismic activity, such as island arcs and their surroundings. Large variations in heat flow over short horizontal distances may be anticipated in these areas. Nevertheless the average heat flow of island arcs is only 71.7 mW/m^2, which is very close to the world mean of 74.3 mW/m^2 (Jessop et al., 1976). But an important feature is the areal distribution by which low and high heat flows are associated with outer and inner arcs respectively (Uyeda and Horai, 1964; Vacquier, et. al., 1967; Uyeda, 1977; Watanabe et al., 1977). This suggests a connection between heat flow and the subduction process. In many cases, however, the distribution is extremely complicated (Watanabe et al., 1970; Yasui et al., 1970; Sugimura and Uyeda, 1973) and requires very detailed study.

New Zealand is one of the few areas where this problem can readily be studied through detailed heat flow mapping. It offers distinct advantages over other subduction regions since the effect of continued subduction can be traced in finer detail by means of land-based geological and geophysical observations.

1.2 PREVIOUS STUDIES IN NEW ZEALAND

Heat flow measurements in New Zealand have mainly been concentrated on special areas, and the overall distribution has been insufficient to allow a general interpretation. In the North Island, studies were first undertaken in the form of natural heat flow measurements in the geothermal areas of the Taupo Volcanic Zone, using the techniques described by Dawson (1964) and Dawson and Dickinson (1970). Later, the regional heat flow pattern was studied from borehole measurements by Studt and Thompson (1969), who found that most values of heat flow were below normal to the southeast, and above normal to the northwest, of the volcanic belt. Within and adjacent to this belt, observed heat flow is nearly everywhere zero owing to convective water circulation; this result has been supported by further geothermal gradient studies (Thompson, 1977, 1980). Within the narrow confines of each particular thermal area, of course, there is a very high convective heat flow.

In addition, heat flow has been measured by Calhaem (1973) in several lakes of the Taupo Volcanic Zone, using a modified oceanic technique. Exceedingly high values (up to 52 W/m^2) have been reported from some lakes; these values are interpreted in terms of underlying hydrothermal systems. In the South Island, although there have been some very early and more recent temperature measurements (Henderson, 1917; Hilgendorf et al., 1919; Thompson, 1966), no values of heat flow have previously been reported.

1.3 PRESENT INVESTIGATION

In the present project every opportunity has been taken to obtain sufficient heat flow measurements to support a detailed mapping of both Islands. This has involved the measurement of temperature in available boreholes drilled for other purposes, by means of a specially constructed thermistor probe, and also the collection of temperature information from various sources. Some gaps still exist due to inaccessibility or to a lack of suitable boreholes. Equilibrium temperatures have been measured by thermistor probe in a number of boreholes which have been standing long enough to be sufficiently free from transient thermal perturbation. Many of these holes were found, however, to be hydrologically disturbed. Much additional information was obtained from oil company reports containing records of bottom hole temperatures. These temperatures are measured at a number of depths during conventional geophysical logging and formation testing operations in deep exploration wells, occasionally reaching to the basement. A considerable number of oil prospecting boreholes have been drilled in offshore regions, and these give a valuable opportunity for heat flow investigation, since the water is too shallow to permit conventional oceanic measurements, the water temperature at the bottom being more or less variable. The usefulness of bottom hole temperatures has recently been demonstrated by a number of studies (Girdler, 1970; Evans and Tammemagi, 1974; Matsubayashi and Uyeda, 1979; Carvalho et al., 1980 etc.).

CHAPTER 2

PLATE-TECTONIC SETTING, REGIONAL GEOLOGY AND GEOPHYSICAL ANOMALIES

2.1 INTRODUCTION

To understand fully the significance of terrestrial heat flow distribution a knowledge of the geological and geophysical features of the study area is essential. A brief summary of the relevant features is presented below.

2.2 PLATE-TECTONIC SETTING

In plate tectonic terms the North Island forms part of the Indian plate, under which the Pacific plate is subducted along the Hikurangi Trench; the Trench is thus the surface trace of the boundary between the two plates. The North Island possesses all the important features typically associated with a subduction zone (Reyners, 1978). However, the geometry of the subducted plate differs considerably from most others in that (i) it dips less steeply until well beneath the central part of the island (Adams and Ware, 1977), (ii) it seems to have some curvature of strike (Gibowicz, 1974), and (iii) the deeper part of the Benioff zone, if extrapolated to the earth's surface, intersects at an unusually large distance (about 200km) from the trench (Hamilton and Gale, 1968). Seismological studies of this region have been made by Eiby (1958, 1964, 1971), Hamilton and Gale (1968, 1969), Hatherton (1970a), Mooney (1970), and Gibowicz (1972).

The plate boundary in the central South Island is represented by the Alpine Fault which is described as a zone of oblique continental convergence (Scholz et al., 1973). Further south, in Fiordland, the plate boundary lies offshore near the coast. Here again the characteristic features of a subduction region are present: seismicity at shallow and intermediate depths, large gravity anomalies, and a quarternary volcano (Hamilton and Evison, 1967). But here the Indian plate is being subducted under the Pacific plate (Smith, 1971). The plate tectonic setting of New Zealand and its surroundings is shown in fig. 2.1, and important features of the New Zealand landmass are shown in fig. 2.2.

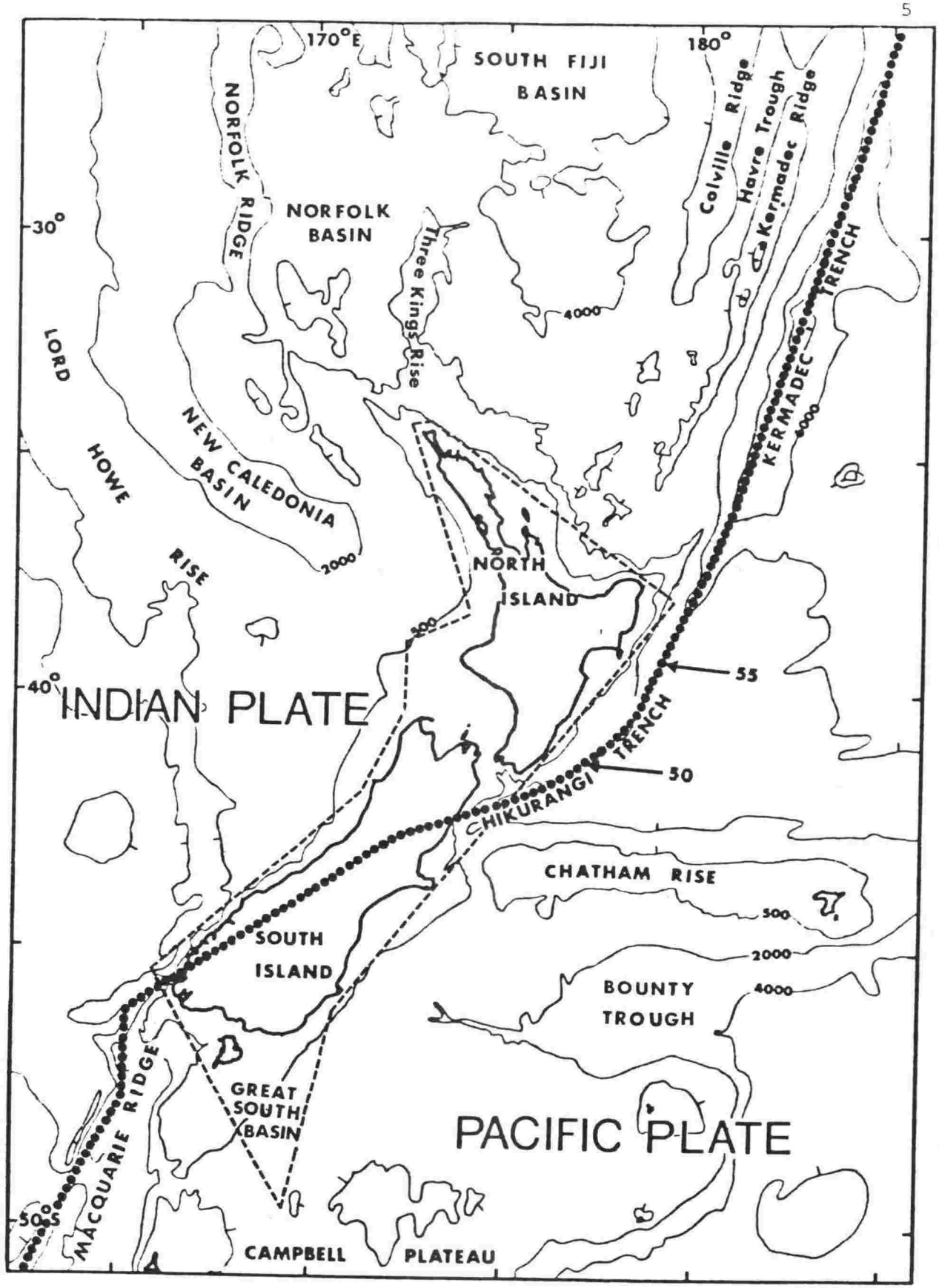

Fig. 2.1 Plate-tectonic setting of New Zealand. Area of the present study is shown by dashed line. Bathymetry in metres, is taken from Lawrence (1967). Approximate boundary between the Pacific and Indian plates is shown by dotted line (Walcott, 1978). Arrows indicate the estimated velocity (in mm/yr) of the Pacific plate relative to the Indian plate (Chase, 1978).

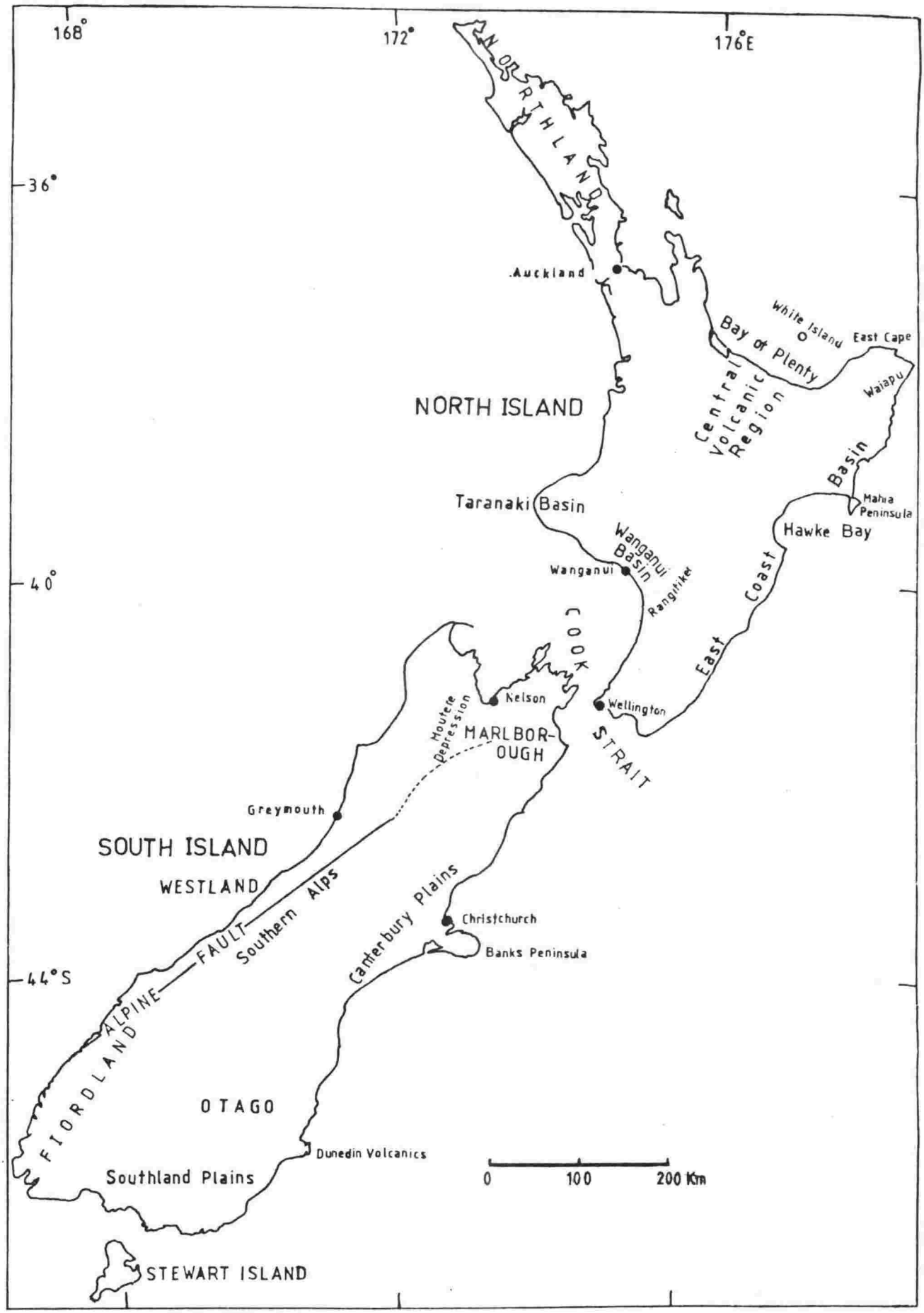

Fig. 2.2 Map of New Zealand showing locations of important features and places.

2.3 REGIONAL GEOLOGY AND TECTONICS

Geotectonically New Zealand belongs to an unstable mobile belt with extensive diastrophism, volcanism, faulting, erosion and deposition. Enormous piles of sediment which have been formed since the Cambrian cover about three-fourths of the country's area. Volcanic activity has produced in the North Island very large quantities of ash, ignimbrite, rhyolitic lava, and andesite, and in the South Island substantial andesite lavas at Banks Peninsula and basalts at Timaru and Dunedin. Large elevation changes have occurred from time to time, most recently in the South Island along the Southern Alps and the Kaikouras (figs. 2.3, 2.4). The broad geological features of both islands, together with major shallow seismicity and major gravity anomalies, are presented in figs. 2.5 and 2.6.

In the North Island the oldest rocks are predominantly folded and faulted greywackes and argillites, mainly Mesozoic in age, and Permian in a few places. Very widespread at the surface are younger sediments and volcanics. The thickest sedimentary sequences occur in the Rangitikei, Taranaki, and East Coast basins. In the Central Volcanic Region (a complex volcano-tectonic rift) the surface rocks are mainly volcanics of late Pliocene-Pleistocene age. The oldest rocks in the South Island (some as old as Precambrian (Adams, 1975) occur in Nelson, Westland, Fiordland and Stewart Island, in the form of diorite, granite, schist, gneiss, greywacke and argillite. These are separated by the Alpine Fault from mainly younger sedimentary and igneous rocks to the east; the Fault offsets certain geological features by some 400km. In the east, greywackes and argillites of Triassic - Jurassic age occur from Marlborough to north Otago, merging into schist and gneiss across Otago and the western flanks of the Southern Alps, into Permian tuffs and tuffaceous greywackes in Southland. Thick piles of younger sedimentary formations are recorded in eastern and western parts of Southland and in the Great South Basin. Young deposits (Pleistocene-Recent) are also found in the Moutere Depression (Nelson) and in the plains of Canterbury and Southland. The detailed geotectonics of both islands have been described by Wellman (1956), Kingma (1959a,b), Brown et al. (1968) and Suggate et al. (1978).

2.4 GEOPHYSICAL CHARACTERISTICS

2.4.1 Crustal Thickness

Bullen (1939) made the first estimate of the crustal thickness in New Zealand and obtained about 30km. Numerous investigators (Thomson and Evison, 1962; Reilly, 1962; Garrick, 1968; Calhaem

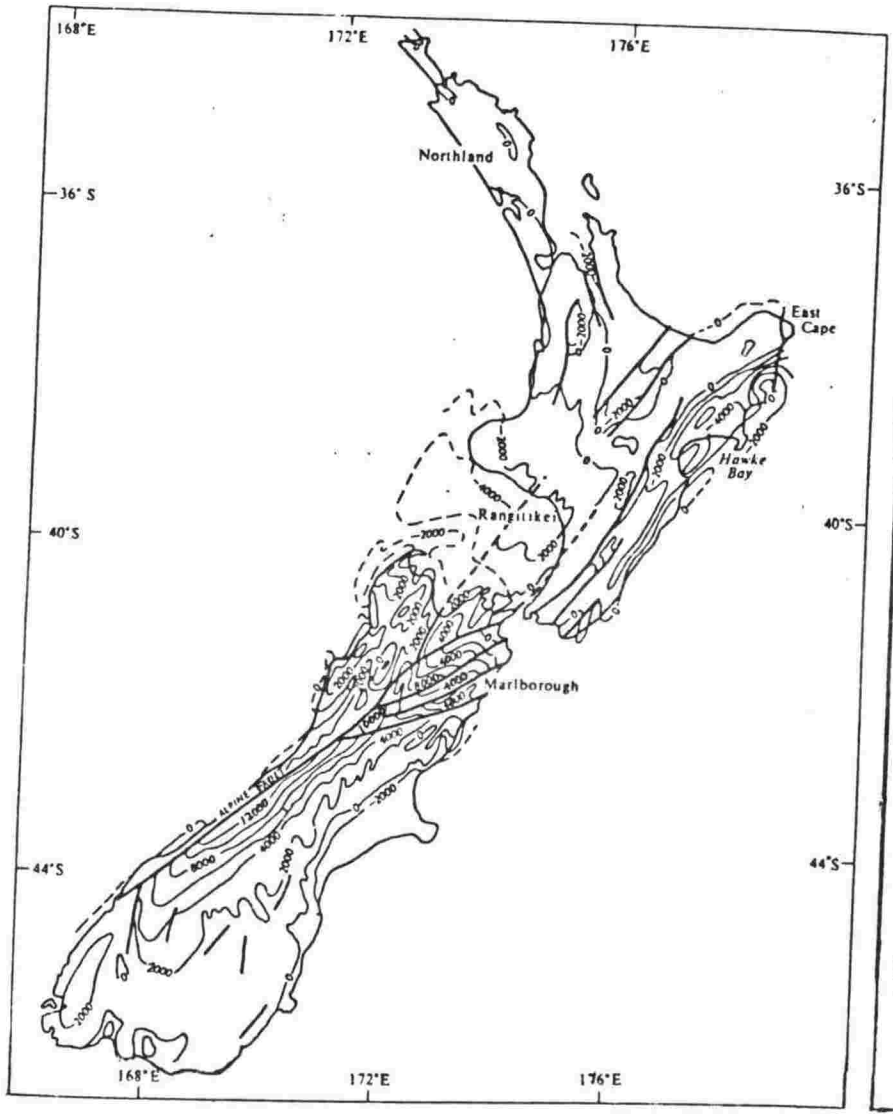

Fig. 2.3 Gross vertical changes (in metres) during Neogene in New Zealand (after Lensen, Suggate and Wellman, pers. comm.).

Fig. 2.4 Estimated uplift rates (mm/yr) in the South Island (Wellman, 1979).

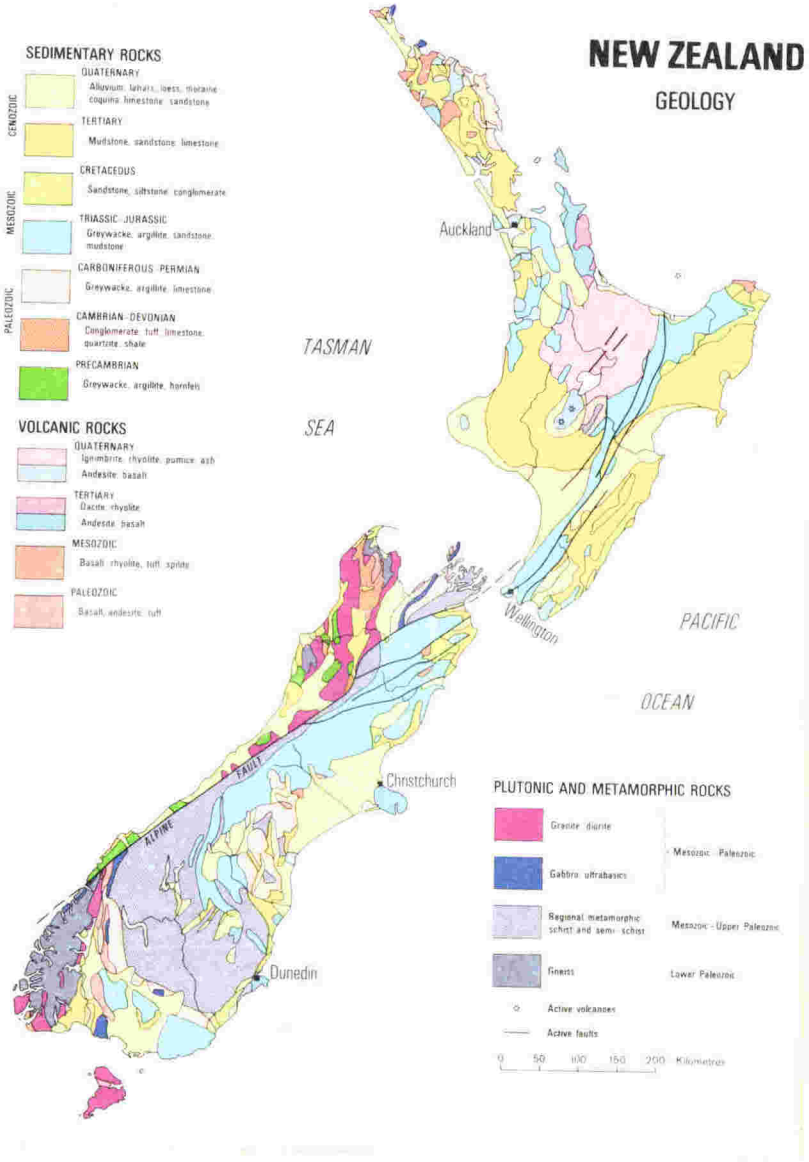

Fig. 2.5 Simplified geological map of New Zealand (N.Z. Geol. Surv., 1973).

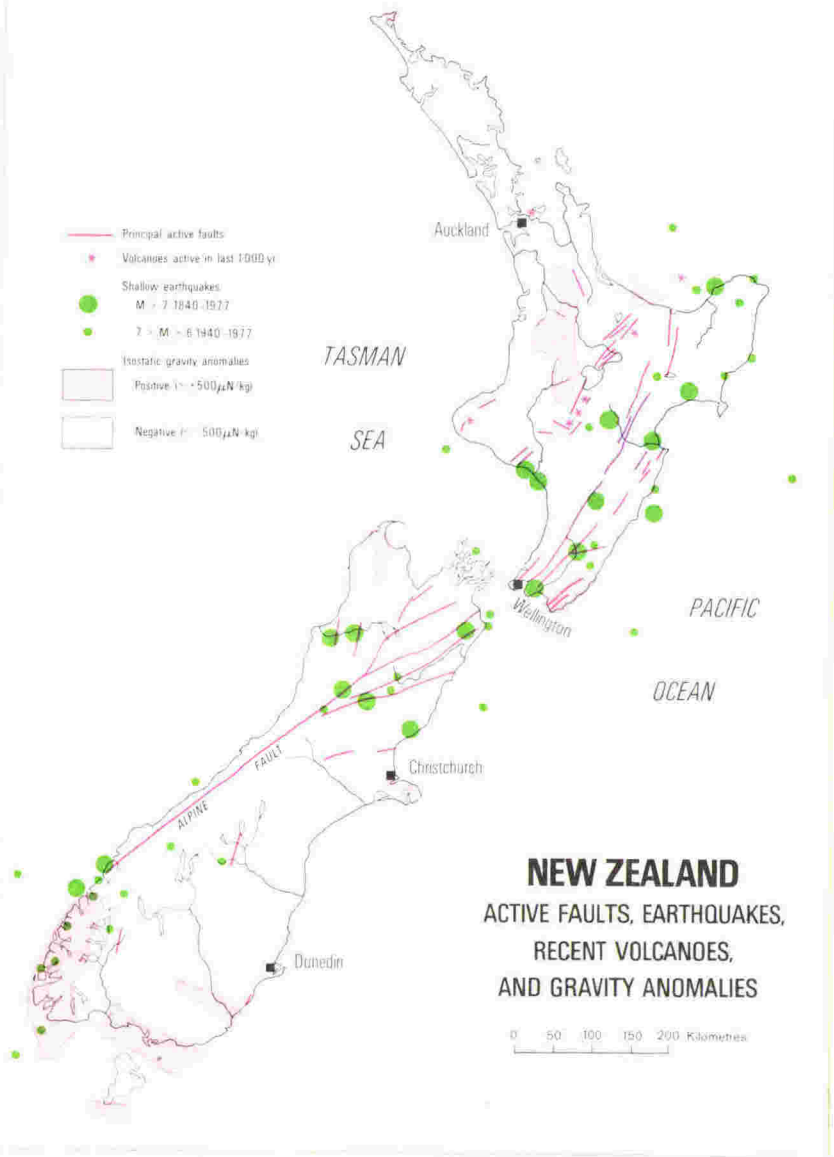

Fig. 2.6 Distribution of large shallow earthquakes and major isostatic gravity anomalies in New Zealand (N.Z. Geol. Surv., 1977).

et al., 1977; Woodward, 1979) have since obtained thicknesses of 30 to 35km over most of New Zealand from seismic and gravity observations. The average thickness in the South Island is a little greater than in the North Island (Reilly, 1962); under the Southern Alps the thickness reaches 40-45km (Woodward, 1979). A much lower estimate (18-19km) was reported by Eiby (1955, 1957) and by Officer (1955), but these results have been revised to 36km by Garrick (1968). Despite some local fluctuations (Smith, 1970), all studies confirm the continental nature of the crust beneath New Zealand.

2.4.2 Hikurangi Trench

The Hikurangi trench, which forms the southwest extension of Tonga-Kermadec trench system, is, as mentioned above, a feature of the active margin of the North Island and northern South Island (fig. 2.7). The trench becomes progressively shallower to the south, and ends in the northeastern part of the South Island (fig. 2.1). The trench is shallower than most, being at most 2.5km deep.

2.4.3 Volcanism

The North Island has five andesite volcanoes which have been active in recent times (fig. 2.7), and extensive andesitic and rhyolitic volcanism has occurred over the northwestern and central parts of the North Island (fig. 2.8). Andesitic volcanism commenced about 18 Myr ago (Schofield, 1968; Stipp and Thomson, 1971; Balance, 1976) on an axis which appears to have rotated clockwise and migrated eastwards (Calhaem, 1973). According to Midha (1979) the Indian-Pacific plate boundary in the North Island was oriented nearly NW-SE between 18 Myr and 3 Myr ago, and then changed rapidly to its present orientation. Andesitic volcanism and lithospheric subduction is intimately connected, and a close association exists between the potash content of the andesite and the depth to the Benioff zone (Dickinson and Hatherton, 1967; Hatherton, 1969). There is no active volcanism in the South Island, where the youngest volcanics are the Late Miocene andesites of Bank Peninsula.

2.4.4 Thermal Springs

The locations of thermal springs and their relation to the main lava areas are shown in fig. 2.8. In the North Island, the springs are chiefly distributed within the Central Volcanic Region and further north-west. A few springs of presumed tectonic origin occur in East Coast areas. In the South Island, numerous springs have been found, mainly associated with the mountain ranges.

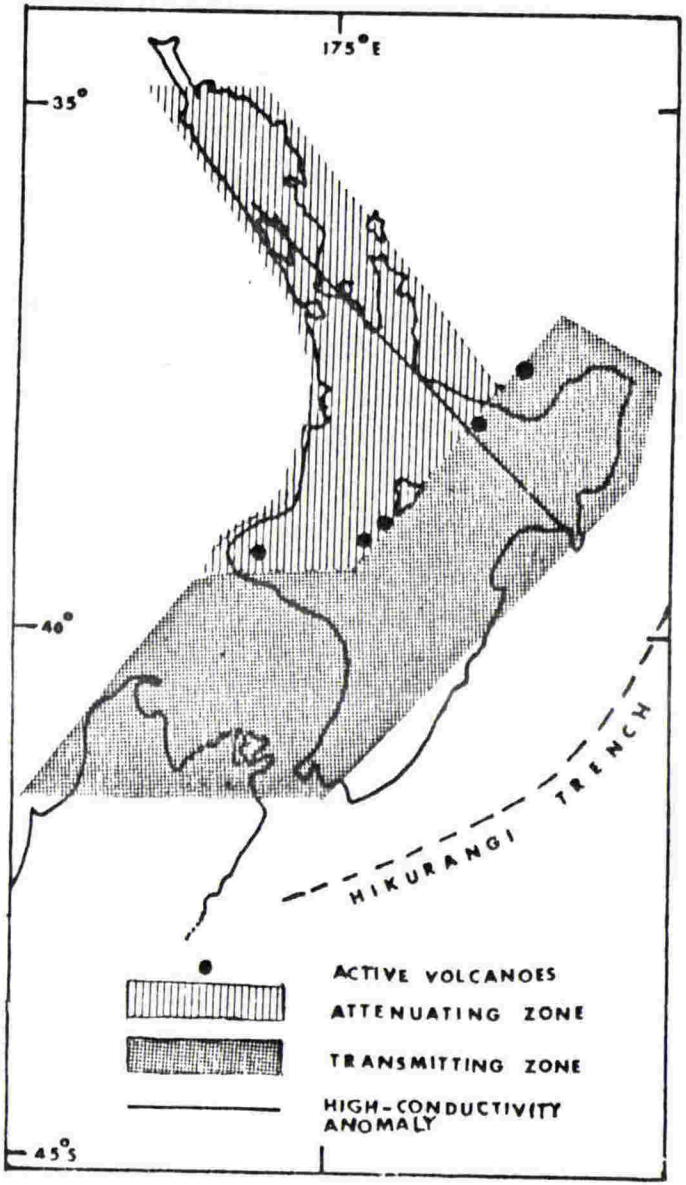

Fig. 2.7 Locations of active volcanoes, high conductivity anomaly, attenuating/ transmitting zones of Mooney (1970), and Hikurangi trench.

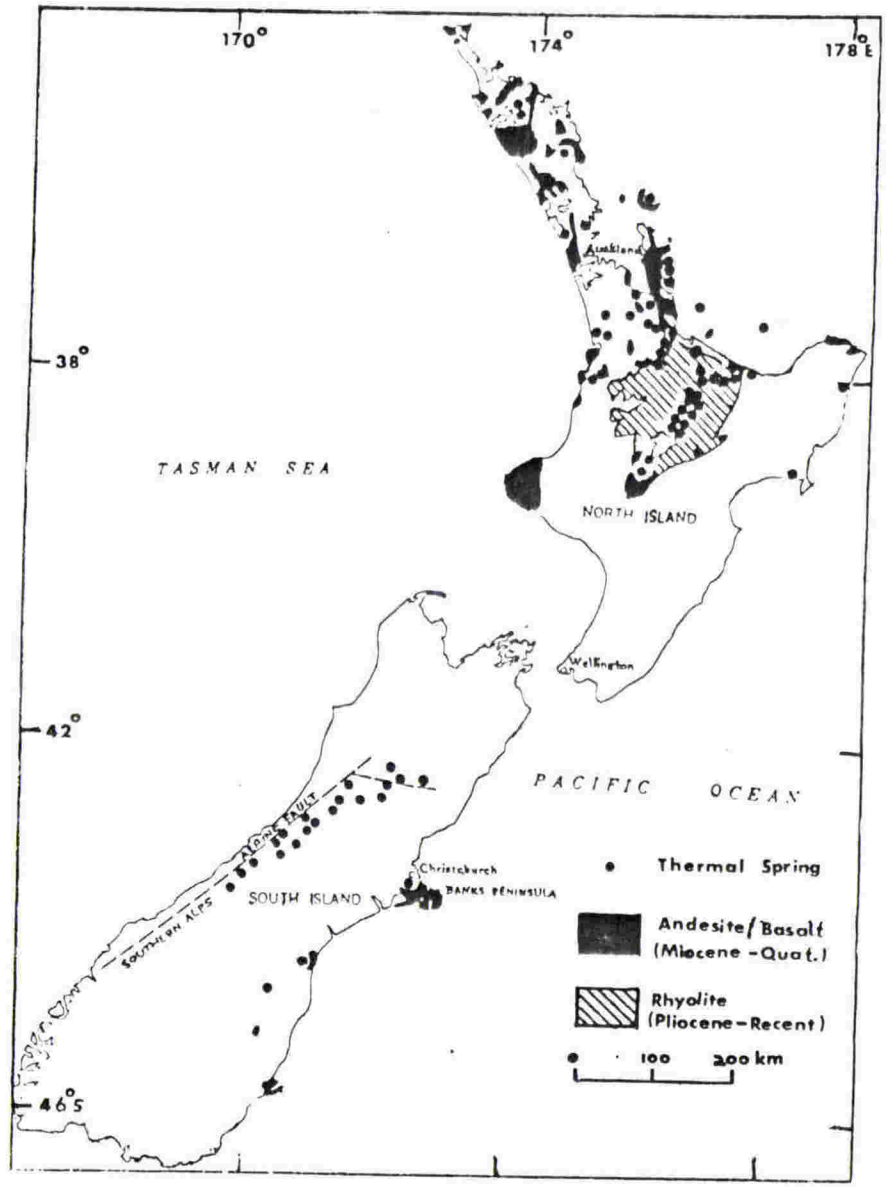

Fig. 2.8 Distribution of Andesitic, basaltic and rhyolitic volcanism and thermal springs in New Zealand.

2.4.5 Geoelectromagnetic Induction Studies

Earlier studies of Marriot (1969) and Hurst (1974) in the southern part of the Taupo Volcanic Zone have been extended by Midha (1979) to cover the entire Central Volcanic Region. A high-conductivity anomaly has been interpreted as due to a conductivity of about 1 mho/m extending from 20km to 80km in depth and trending southeast from Northland to Mahia Peninsula (fig. 2.7). This anomaly has been attributed to an earlier subduction zone.

2.4.6 Seismicity

New Zealand is a region of moderate seismic activity (figs. 2.9 and 2.10). The distribution of earthquakes has been studied by Eiby (1958, 1964, 1970, 1971), Hamilton and Gale (1968, 1969), Hatherton (1970a, 1980), Smith (1971), Scholz et al. (1973) and Adams and Ware (1977), among others. Microearthquake studies have been carried out by Arabasz and Robinson (1976), Evison et al. (1976), Reyners (1978) and Smith (1979). New Zealand earthquakes occur at both shallow and intermediate depths; shocks deeper than 350km are rare.

Three seismic regions have been distinguished: the Main Seismic Region, the central South Island, and Fiordland. The Main Seismic Region is associated with the subduction of the Pacific plate under the Indian plate in the North Island and northern part of the South Island. The Fiordland seismicity is associated with the subduction of the Indian plate under the Pacific plate in the far southwest of the country. These two regions are separated by the central South Island region, where shallow activity is comparatively slight and there are no sub-crustal earthquakes (figs. 2.9, 2.10). In the Main Seismic Region, Hatherton (1970a) has drawn attention to an "aseismic corridor" and to a general change in the directional trend of crustal seismicity from the northern to the southern parts of the Region (fig. 2.9).

2.4.7 Seismic Wave Propagation

Mooney (1970) studied the frequency content of seismic waves from intermediate earthquakes under the Main Seismic Region, and found that a transmitting zone for high frequencies underlies the eastern and southern parts of the Region, while an attenuating zone exists in the depth range of 75 to 125km in the northern parts (fig. 2.7). The attenuating zone evidently lies beneath the region of Upper Tertiary to Recent volcanism.

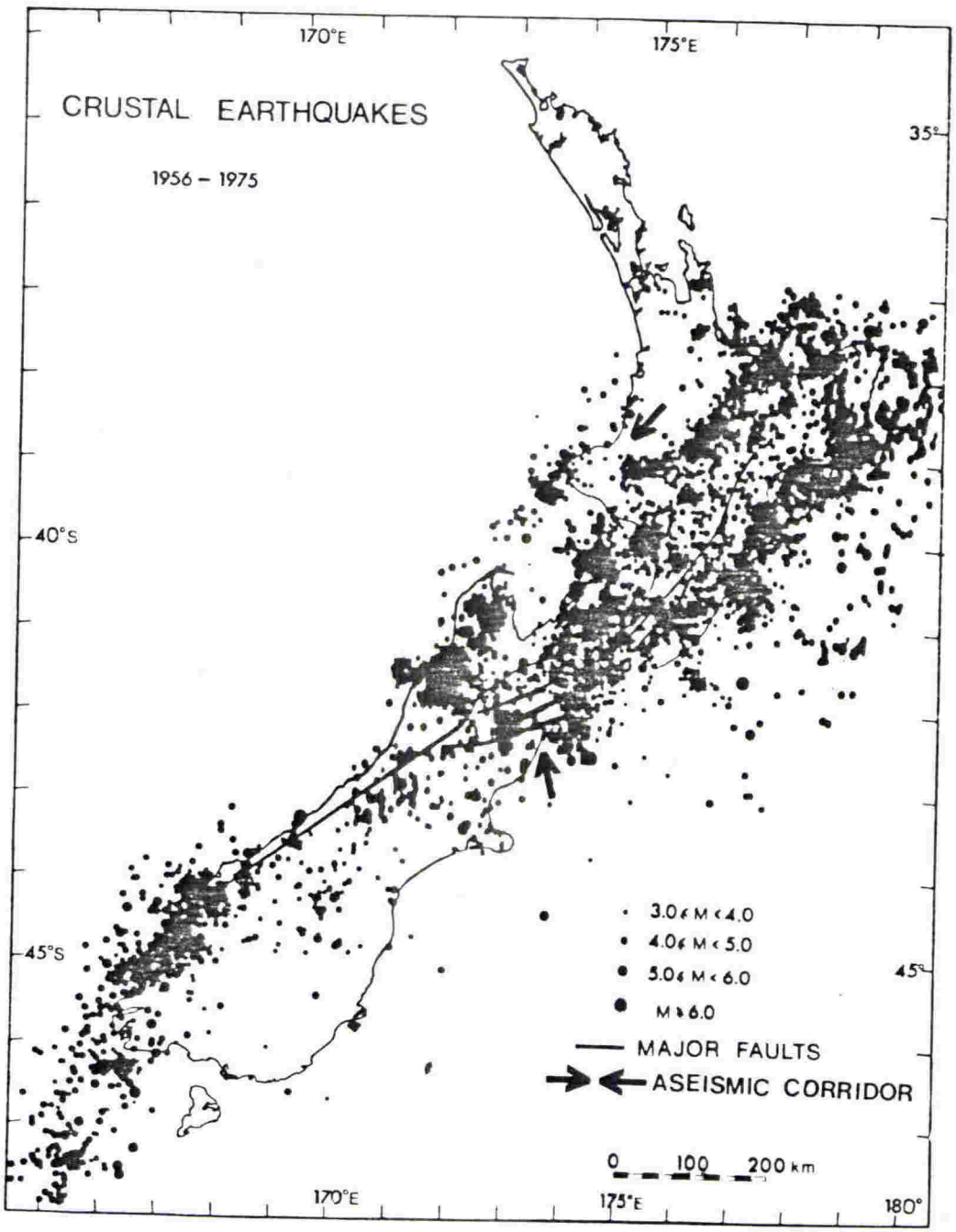

Fig. 2.9 Crustal seismicity in New Zealand from 1956 to 1975 (Hatherton, 1980).

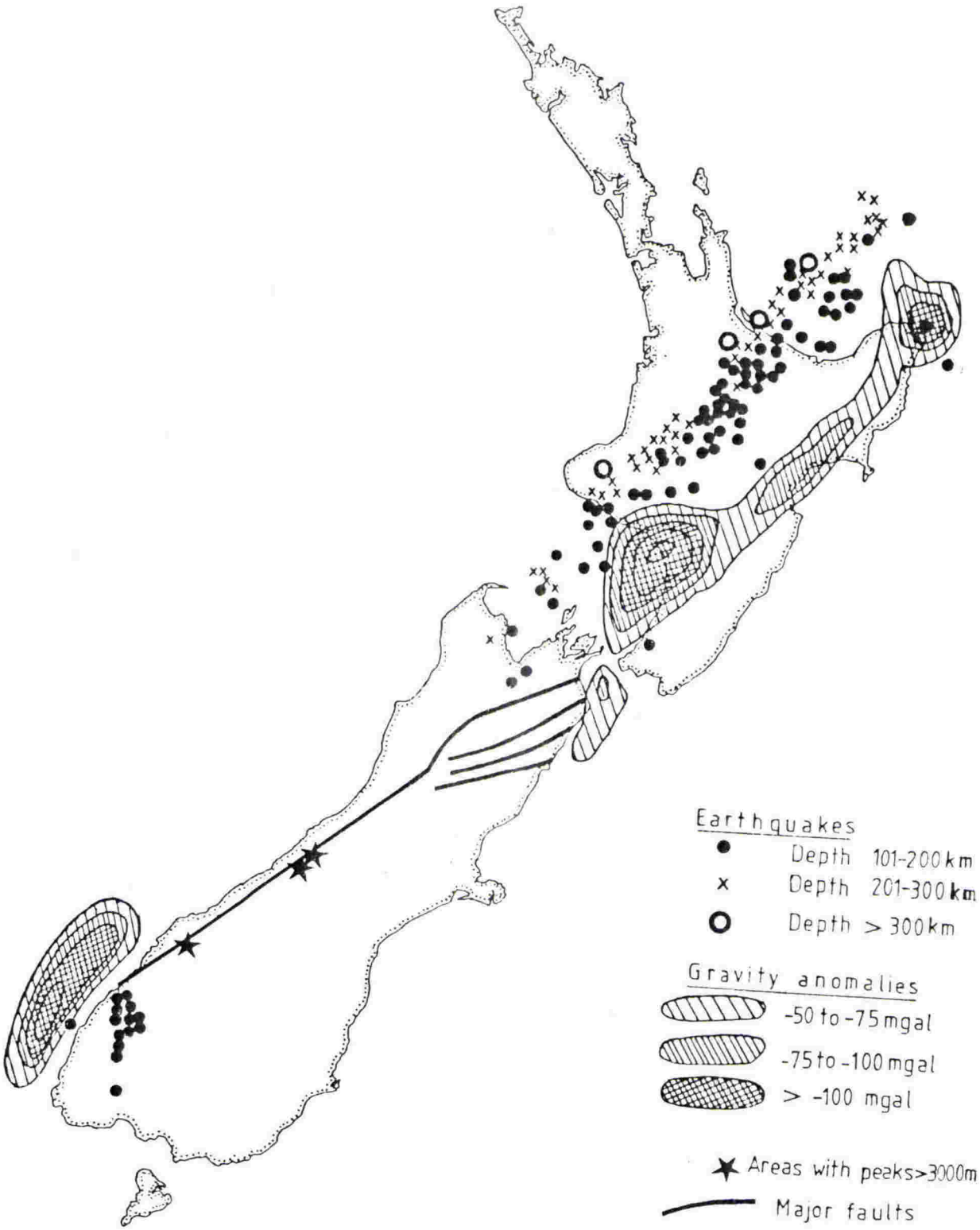

Fig. 2.10 Intermediate earthquake distribution and major negative gravity anomalies in New Zealand (Adapted from Hatherton, 1978).

2.4.8 Velocity Distribution

Upper mantle velocity variations beneath New Zealand were first discussed by Hamilton (1969), and studied in detail by Haines (1979), who obtained lateral variations in the Pn velocity from 7.4 to 8.7km/s, and in the Sn velocity from 3.95 to 4.8km/s (fig. 2.11).

2.4.9 Travel-Time Residuals

The lateral inhomogeneities which are associated with subduction under the Main Seismic Region (Hatherton, 1970b; Mooney, 1970) are reflected in velocity anomalies (Hamilton, 1969; Adams and Ware, 1977). These anomalies have been studied by Robinson (1976), who has calculated teleseismic residuals for the permanent seismograph stations of the North Island and the northern part of the South Island. Average P-wave teleseismic residuals, relative to Wellington seismograph station, show a large spatial variation (up to 3s), decreasing from west to east (fig. 2.12).

2.4.10 Gravity Anomalies

The Bouguer and isostatic anomaly maps of New Zealand are presented in figs. 2.13 and 2.14 respectively (Reilly, 1965). In general, anomalies are closely related to the sedimentary cover, volcanics and crustal thickness (Robertson and Reilly, 1958) and exhibit a close relationship with the attenuating and transmitting zones of Mooney (1970). The anomalies across the subduction zone have been modelled by Hatherton (1970b). The Bouguer map is dominated by two major negative anomalies and one large positive anomaly (Robertson and Reilly, 1958);

(i) Rangitikei-Waiapu negative anomaly, trending northeast across the axial mountain ranges of the North Island, with an unknown deep-seated origin. Robertson and Reilly (1958) postulated that this anomaly is related to the Tonga-Kermadec Trench negative anomaly. However, it has now been shown by Hatherton and Syms (1975) that any connection can only be across a gravity saddle on which isostatic anomalies are less negative than -25 mgal.

(ii) Alpine negative anomaly, related to the Southern Alps.

(iii) Fiordland positive anomaly, reaching up to +175 mgal.

Isostatic corrections account for most of the negative anomaly over the Southern Alps but have little affect on the anomalies in the North Island and Fiordland.

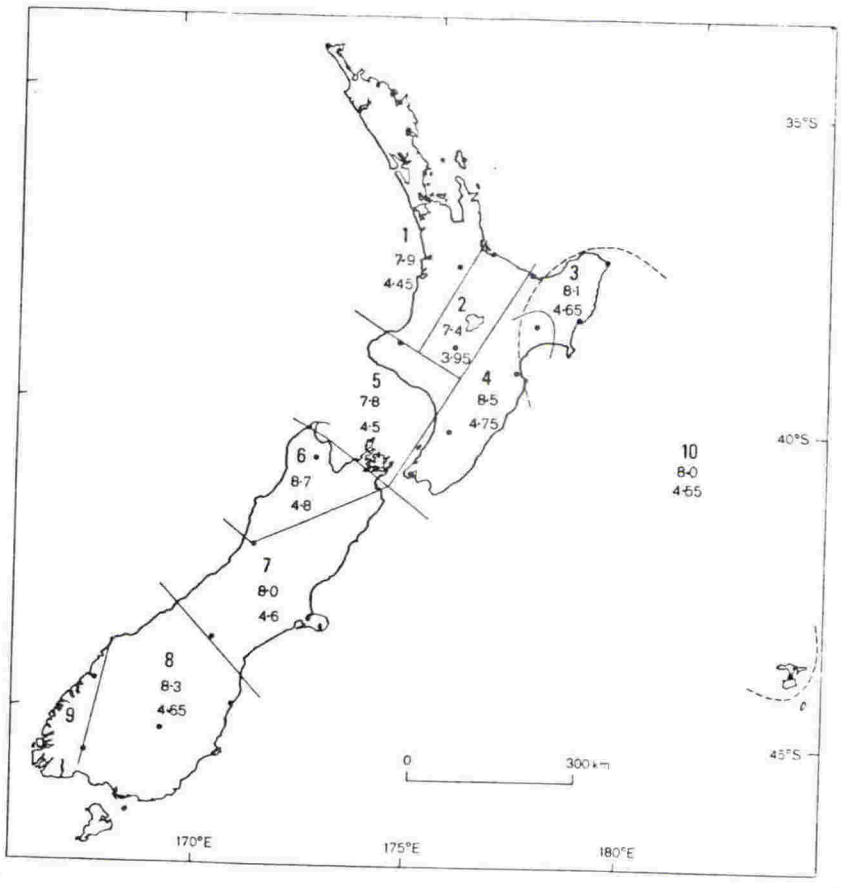

Fig. 2.11 Distribution of Pn and Sn velocities (km/s) in New Zealand (Haines, 1979).

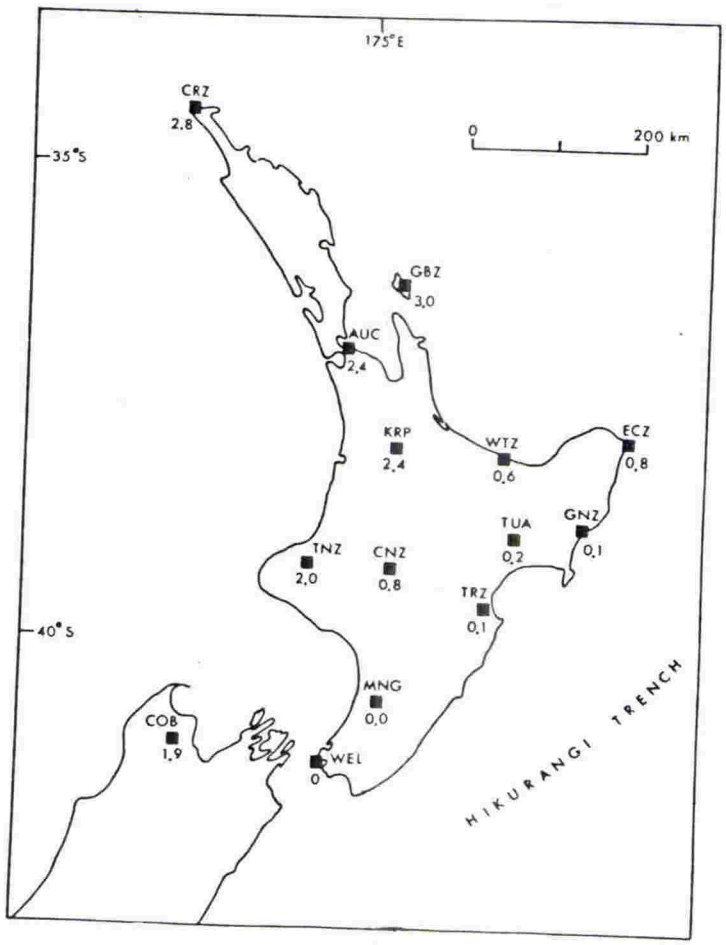

Fig. 2.12 Average P wave teleseismic residuals (in seconds) relative to Wellington seiomograph station (Robinson, 1976).

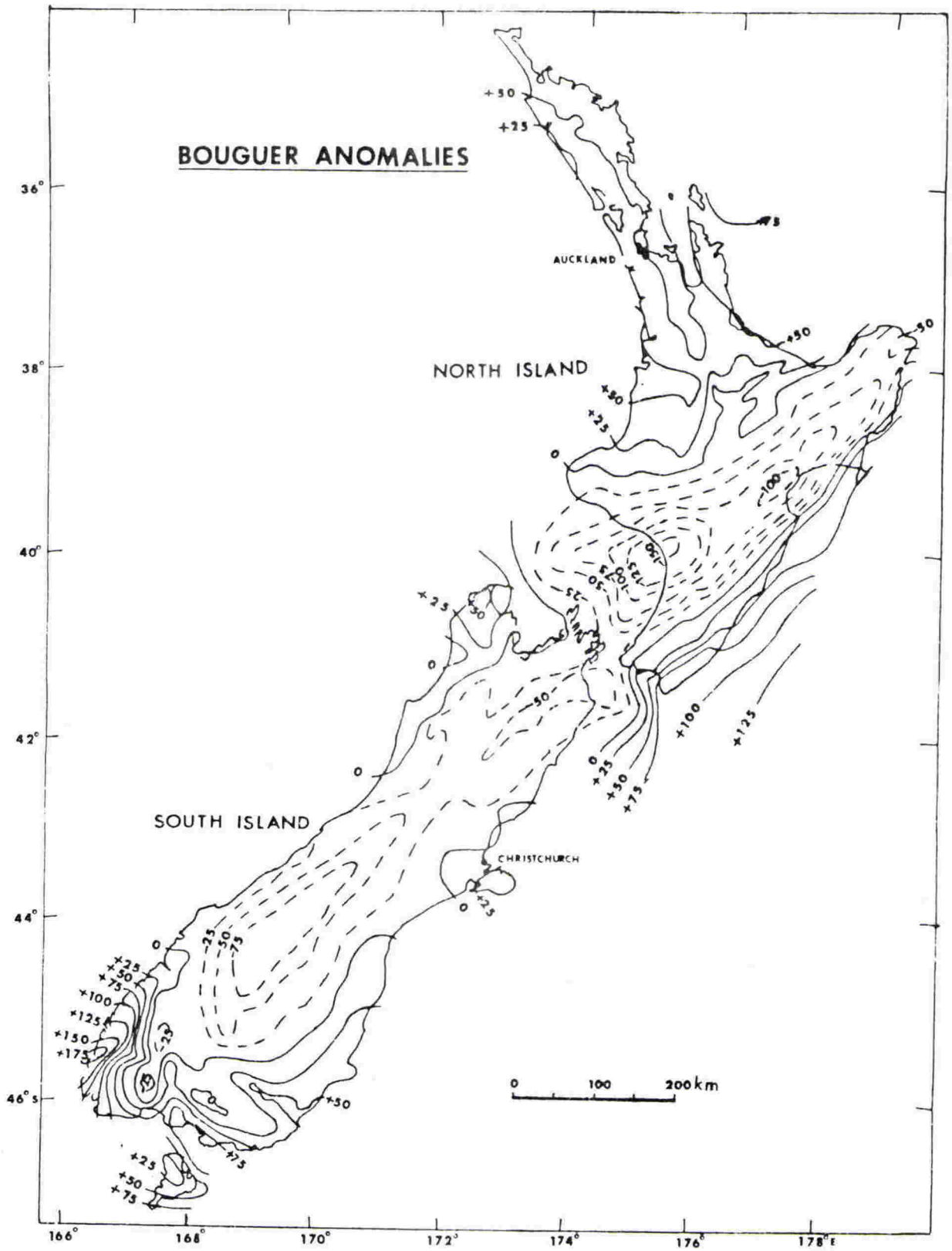

Fig. 2.13 Bouguer gravity anomaly map of New Zealand (in mgal) (redrawn after Reilly, 1965).

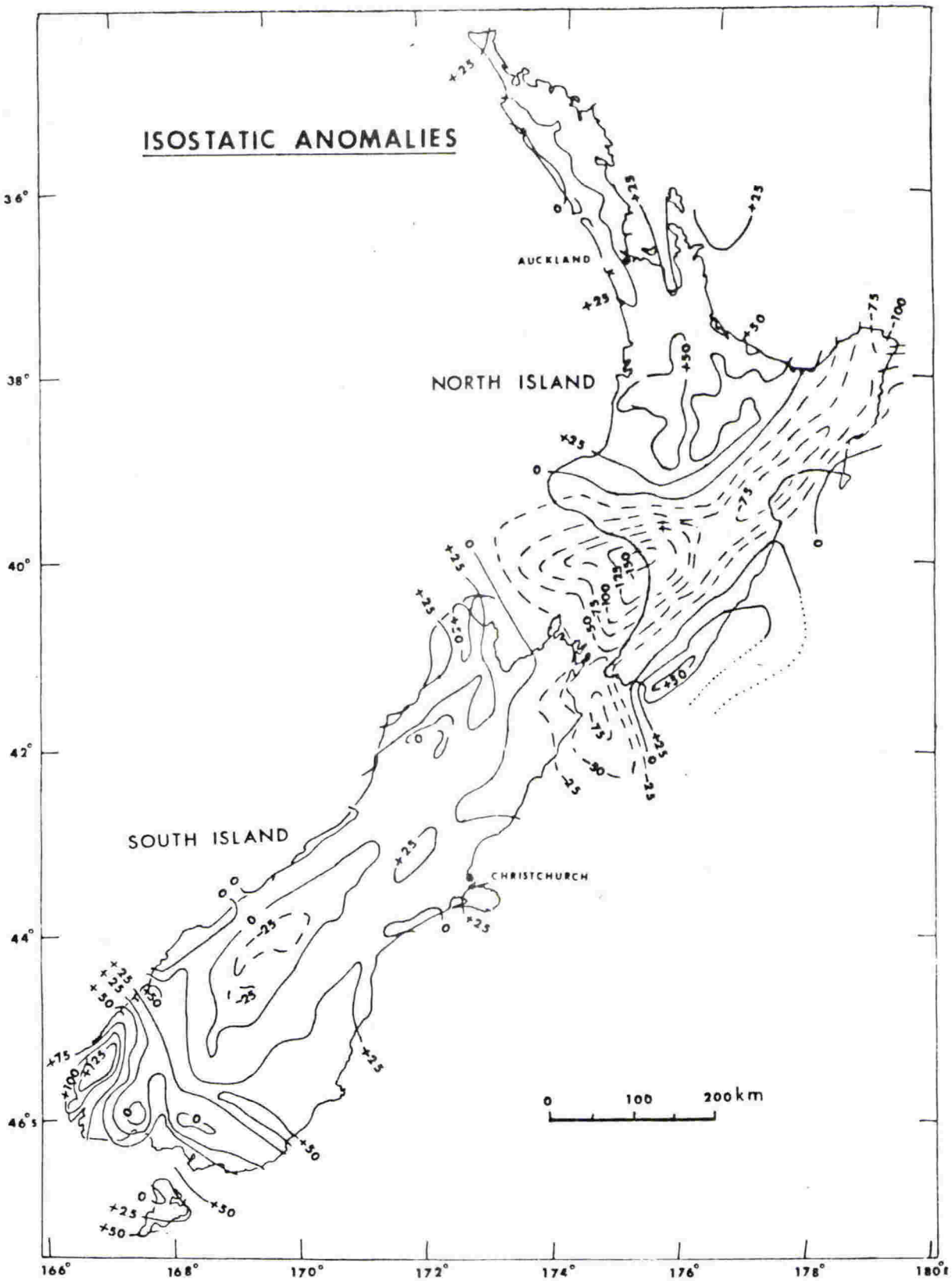

Fig. 2.14 Isostatic gravity anomaly map of New Zealand (in mgal) (redrawn after Reilly, 1965).

CHAPTER 3

MEASUREMENT PROCEDURES, DATA REDUCTION AND STATISTICAL TECHNIQUES

3.1 INTRODUCTION

Terrestrial heat flow is here defined as the rate of heat transfer per unit area by conduction from the earth's interior to the surface; it is expressed in units of mW/m^2. The equation of flow of heat in one dimension can be written as:

$$q = -K \frac{\partial T}{\partial z} \qquad (3.1)$$

where q is the heat flow vertical to the earth's surface, K is the thermal conductivity of the rock, T is the temperature and z is the depth. $\frac{\partial T}{\partial z}$ is called the geothermal gradient. The detailed theory of heat conduction is given in Ingersoll et al. (1954) and in Carslaw and Jaeger (1959).

3.2 TEMPERATURE MEASUREMENT

To obtain the geothermal gradient an accurate knowledge of the temperature variation with depth is essential. On land this can be achieved through measurements in tunnels, mines, lake bottoms or boreholes. Where suitable boreholes are available the measurement is rapid, convenient and accurate. In favourable circumstances, reliable heat flow can be estimated from boreholes as shallow as 200 m (Roy et al., 1972; Sass et al., 1968). The present study is based entirely on borehole measurements.

3.2.1 Borehole Temperature Measurement

The commonest devices used for measurement of temperature in boreholes are maximum thermometers, platinum resistance thermometers, thermocouples, and thermistor probes. Thermistor probes have the advantage of sensitivity, accuracy, and simplicity of operation and design, and they have no serious drawbacks (Beck, 1965). A thermistor probe has been constructed specially for the present study.

There are several well-known sources of error in the measurement of heat flow in boreholes. Circulation of ground water is the commonest of these. The upper portion of a borehole is often disturbed. The effect of metal casing in the borehole can be neglected at depths greater than a few meters (Misener and Beck, 1960). In recently drilled holes the temperatures are affected to an important extent by the drilling operation. The time required to attain thermal equilibrium may be shorter for diamond drilled holes, because less circulating fluid is

needed; after about a day the measured heat flow should be accurate to within 5% (Jaeger, 1961). Errors due to drilling operations have been analysed by Bullard (1947), Jaeger (1955-56), Lachenbruch and Brewer (1959), Cheremensky (1960), Kutarov (1968), and Kappelmeyer and Haenel (1974). Recent geological changes and present topography are a further source of error in some areas. The appropriate corrections for such cases will be discussed in detail later.

3.2.2 Apparatus

The probe has been designed for measurements at depths down to 1000 m. The apparatus is portable; the weight including wire and winding apparatus is about 40 kgm. The salient features of the instrument, which is illustrated in figs. 3.1 and 3.2, will now be described.

(i) Probe

The active element is a thermistor, accommodated in an aluminium jacket with 4 mm outside diameter, bored to 2 mm. The cavity has been pumped full of silicone grease to eliminate air space and improve thermal contact. The thermistor and jacket are screwed into a larger aluminium tube, diameter 19.05 mm, wall thickness 1 mm, using an O-ring and washers to form a seal. Inside this, the thermistor leads are connected to the main cable and insulated with silicone rubber. The cable is brought into the probe body through tapered holes sealed with araldite plugs. The probe body is packed with silicone rubber.

At room temperature the thermistor resistance is approximately 12 kilohm and the power dissipation is approximately 83 μW. The probe was designed to withstand pressures up to about 270 bars and has been tested in the laboratory to 150 bars. The probe is equipped with a sinker.

(ii) Voltage source

The circuit diagram of the voltage source is shown in fig. 3.3. The voltage reference is buffered with a low drift operational amplifier. The voltage output of the source, which is powered by twelve size A dry cells, is 1.0 volt, and the largest current available is 4.0 mA. (The current drawn by the probe at room temperature is approximately 83 μA.) Current drain when the reference is in its stable state is 2-3 mA. Monitoring circuits with LED warning lamps indicate abnormal conditions.

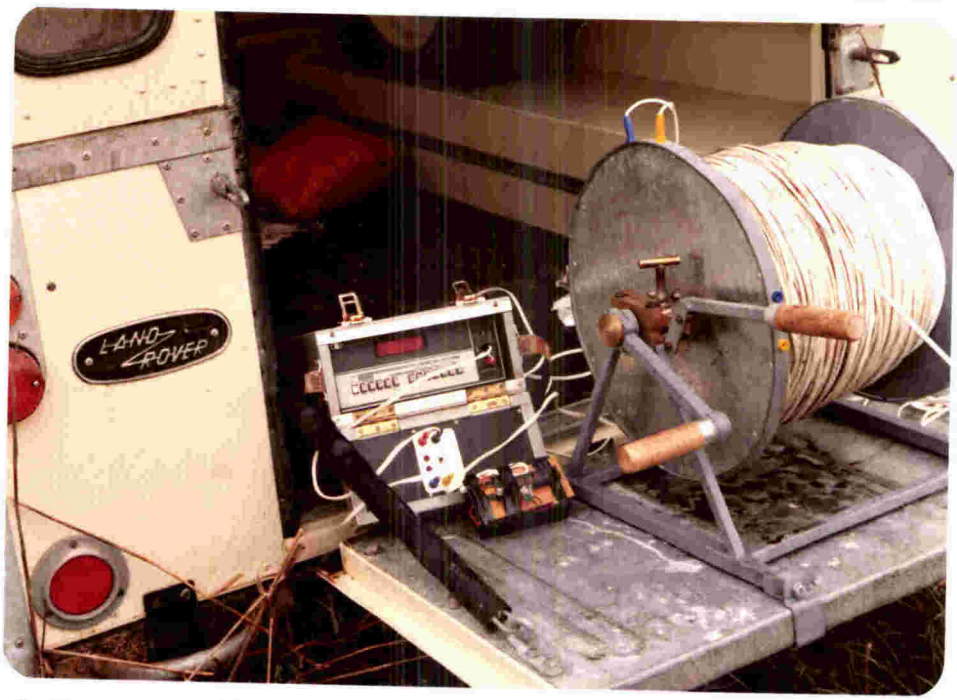

Fig. 3.1 Photographs showing borehole temperature measurement by thermistor probe.

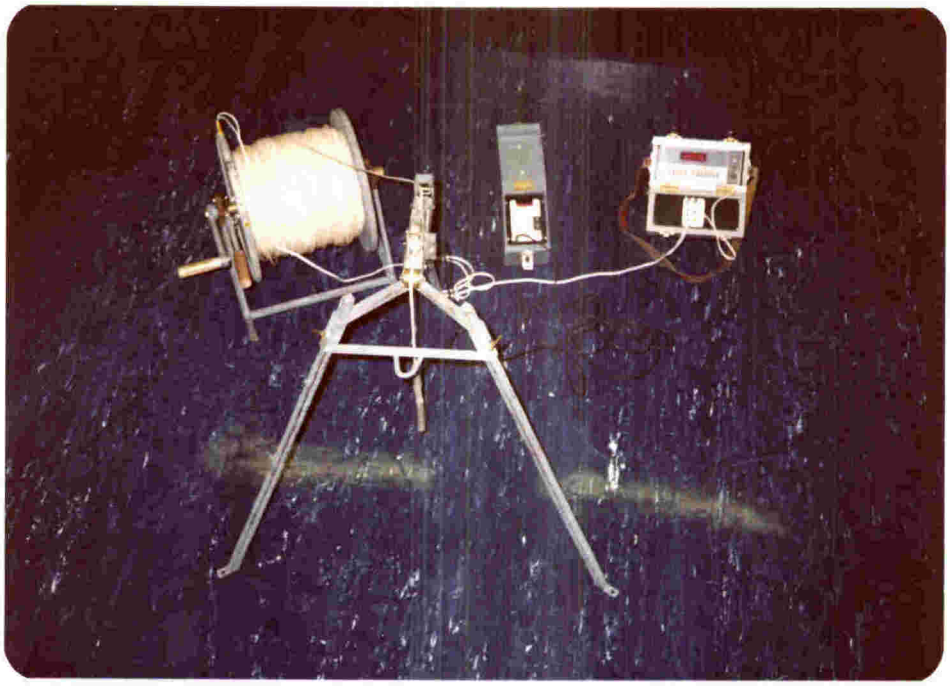

Fig. 3.2 Complete temperature measuring equipment.

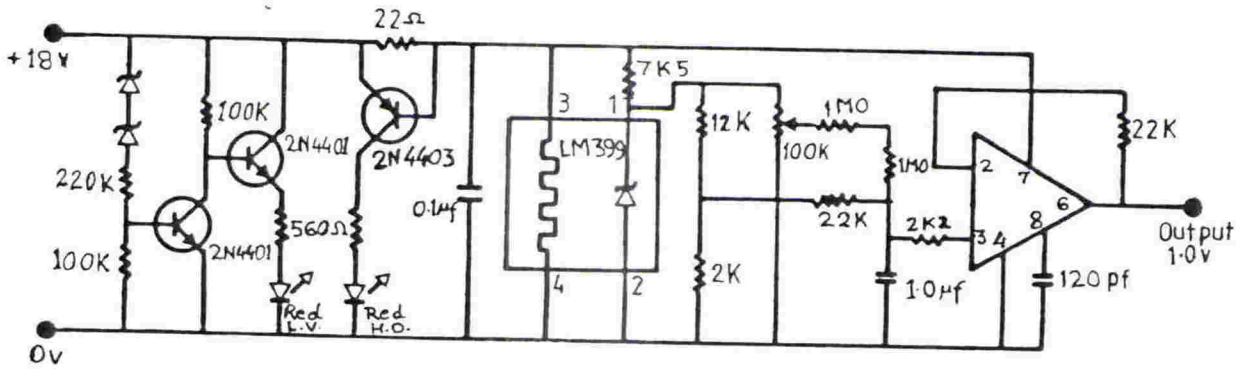

Fig. 3.3 Schematic diagram of voltage source.

(iii) Meter

The current is monitored at the well head by connecting a meter in series with the voltage source and the probe. The meter used is a Hewlett Packard digital multimeter type 3465A. This is mainly used on its most sensitive range (100 μA), where the value is indicated to 0.01 μA. The certified accuracy of the meter in the 100 μA and 1 mA ranges is ± (0.07% of reading + 0.01% of range).

(iv) Cable drum

A winding reel capable of holding 1000 m of wire (copper, 0.673 sq.mm) can be clamped on the tailgate of a landrover for anchorage and transportation. The wire connection is made by means of banana sockets on the periphery of one drum end. A hand brake with a screw clamp is provided to control the cable.

(v) Well-head equipment

This assembly is a tripod that supports an output pulley at the centre. It also holds a pulley of calibrated circumference and an idler for measuring the length of wire as it passes into the well. A small magnet connected to the side of the calibrated pulley activates a reed relay once every revolution. The relay closures are counted electronically to give the wire length, which is indicated to the nearest 100 mm. Any number can be set on the display as a starting point.

3.2.3 Field Procedure

With the probe lowered to the desired depth the voltage source and meter are connected to the drum and switched on, and the desired current range is selected. After waiting about a minute in order to allow the probe to equilibrate sufficiently, the meter reading is recorded. A depth reading is also recorded. Output in μA is converted into temperature from the calibration chart. The reading interval of 0.01 μA corresponds to about 0.005°C. Repeatability was found to be within 0.05 μA, corresponding to 0.025°C.

Measurements in boreholes were made only while the probe was going down, so as to avoid any appreciable disturbance of the water column. The measurement interval was chosen between 2 m and 10 m, depending upon the depth and lithology. In many boreholes the temperature was disturbed at depths less than 100 m, and sometimes the temperature graph exhibited a curvature, as has also been observed by Cermák and Jessop (1971), Uyeda and Horai (1964), Studt and

Thomson (1969), Rao et al. (1970), and Roy et al. (1972). Such curvatures can be caused by hydrological, environmental or man-made effects (Roy et al., 1972) or by post-glacial warming (Cermák, 1971). Temperatures measured in air filled holes were erratic, presumably because of air movements and lack of equilibrium between thermistor and air. No such measurements were used.

3.2.4 Bottom Hole Temperatures

Three types of data were available from deep exploration wells:

(i) Bottom hole temperatures measured during routine logging, which is carried out at appropriate intervals of time in the course of drilling,

(ii) temperatures recorded during formation testing, and

(iii) temperatures measured after several months or more.

Bottom hole temperatures are recorded usually by a maximum thermometer during each logging operation, after several hours from the cessation of drilling. Due to mud settlements, measurements are made about 5 to 10 m from the bottom, where the thermal disturbance is least. Such measurements, in general, do not correspond to static temperatures because of cooling effects of the circulating fluid, and drilling disturbances (Fertl and Wichmann, 1977; Timko and Fertl, 1972). Stabilised conditions are rarely reached by the time logs are run and therefore they are typically lower by up to 40^{o}C (fig. 3.4) from the static temperatures, depending mainly on the properties of the borehole fluid and surrounding rocks, on the drilling history, and on the natural temperature regime.

In New Zealand, bottom hole temperatures have been measured down to depths greater than 5km. However, detailed inspection has revealed that in many cases measurements are disturbed in the upper 600 m; this has been confirmed by Dr John Harrison, Petroleum Corporation of New Zealand Ltd. (Pers.comm.). In order to utilise the bottom hole temperature data for heat flow determinations a correction must be made to obtain the static value. Various methods have been developed (Cooper and Jones, 1959; Oxburgh et al., 1972; Albright, 1976; Nwachukwu, 1976; Fertl and Wichmann, 1977; Middleton, 1979 etc.). The method of Fertl and Wichmann (1977) (see also Timko and Fertl, 1972) has most commonly been used although it has some limitations, as the authors point out.

Four of these methods have been tested on the data from several deep holes which were drilled many years ago and for which the static

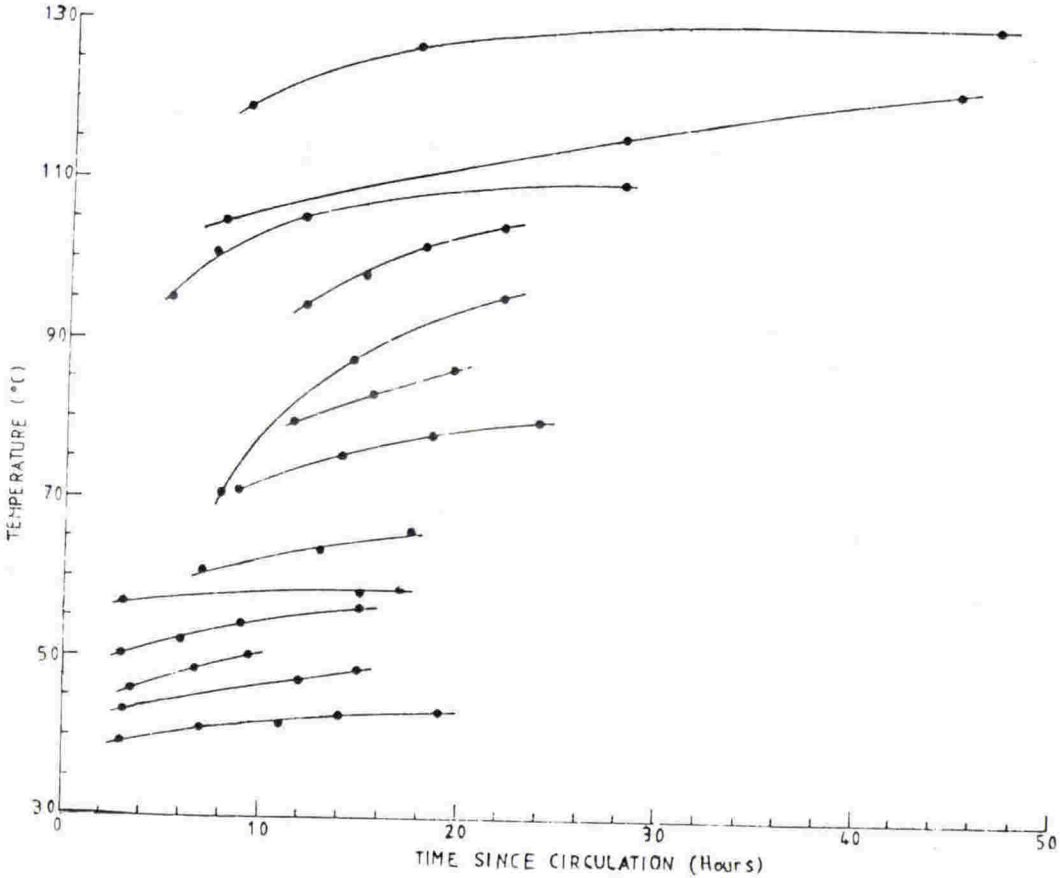

Fig. 3.4 Trends of bottom hole temperature stabilisation with time.

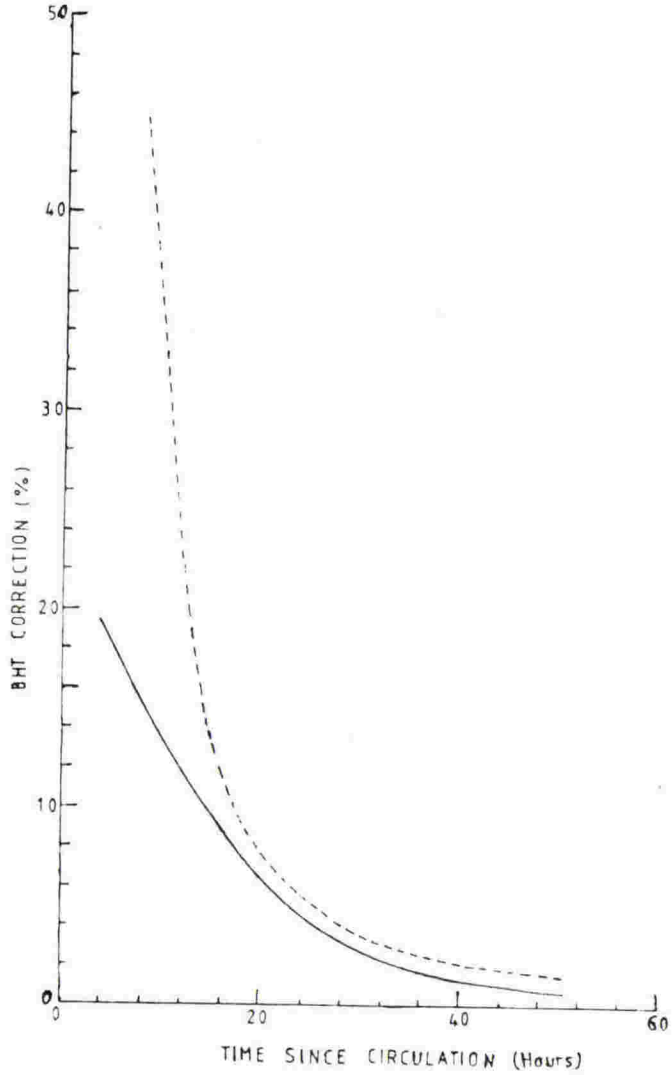

Fig. 3.5 Bottom hole temperature correction curves for the Great South Basin (dashed curve) and rest of New Zealand (solid curve).

bottom temperature had been determined. All methods require a graph of temperature versus time. No other parameter is needed in the method of Nwachukwu (1976), while thus looks the simplest. Additional information is needed in other methods, e.g. circulation times after cessation of drilling in the method of Fertl and Wichmann (1977), and physical properties of the borehole fluid and its surroundings, along with borehole radius, in the methods of Cooper and Jones (1959) and Middleton (1979). Circulation times after drilling were not known in most cases, but in normal practice it is between 4 and 6 hours. Estimates of the other parameters were usually available, but these appear to have been unsatisfactory, since the calculated temperature values were not in good agreement with the known values.

Thus for this study, correction curves had to be prepared from the measured static and formation-test temperatures, for which corresponding time sequential bottom-hole measurements had also been recorded previously. Two trends emerged, one in the Great South Basin and the other in the rest of the New Zealand region as shown in fig. 3.5. This figure reveals that (i) the corrections are significantly larger in the Great South Basin, where the geothermal gradients and heat flow are high compared to elsewhere in New Zealand. (ii) the amount of the correction drops rather sharply as the elapsed time increases, and apparently becomes negligible after about 50 hours; and (iii) deviations from static temperatures are smaller at shallower depths. A similar relationship to that in (i) above has been reported by Fertl and Wichmann (1977). Stabilising trends of bottom hole temperatures are shown in fig. 3.4 for a few cases.

Estimated static temperatures using these curves (fig. 3.5) will be accurate to about 4%. Their application is useful even if only one bottom hole temperature has been measured. Similar curves are sometimes used by Petroleum companies, and a standard correction graph kindly supplied by Petrocorp (N.Z.) Ltd., agrees satisfactorily with the curve presented here for the rest of New Zealand.

Since the temperatures measured during formation or production tests are very close to the static formation temperatures (Cornelius, 1975; Gable, 1979; Matsubayashi and Uyeda, 1979), and corrected bottom hole temperatures correlate well with those measured during testing operations at the same depths, no correction is applied. Besides these temperatures, some other available data measured by conventional probes have also been used for a few bore holes, and were found satisfactory for heat flow determination.

3.2.5 Gradient Determination

Disturbed sections of profiles were discarded and only sections showing a continuous temperature increase were used. In the case of deep exploration wells, corrected bottom hole temperatures were used. Gradients have been calculated using least squares techniques. In a few cases where only one bottom hole temperature was measured, the gradient was calculated in the usual way, taking the ground surface temperature as $1^{o}C$ higher than the mean air temperature. This procedure is satisfactory when the difference between the bottom temperature and the estimated surface temperature is greater than $20^{o}C$ (Bullard, 1939).

For thermistor probe measurements, allowing for the accuracies of temperature and depth measurements, an error of less than 1% in the gradient determination is incurred under normal circumstances. However, considering the accuracy of estimating static bottom hole temperatures, an error of up to ± 4% could be assigned to the gradient calculated by this means. Although this error is larger than for probe measurements there is the advantage that the gradients are unlikely to be affected by near surface effects such as ground water circulation, which can contribute significant errors in shallow boreholes. In any case, much larger errors can result from limitations in conductivity sampling.

3.2.6 Geological Corrections

Heat flow determination involves the measurement of undeground temperatures which are often influenced by past geological processes, and systematic errors may thus be introduced. These include the effects of topography, uplift, sedimentation, erosion, past climatic changes, refraction and groundwater movements. A knowledge of these effects is needed. Up till now much attention has been paid to the effect of topography. Some other effects which may be significant in the present work will be discussed below, although it is difficult to assess the reliability of computed errors since estimates of the various parameters involved are often somewhat subjective.

(i) Topographic correction

The correction is significant only in mountainous areas, and comes mainly from the area within 2km of the place of observation (Bullard, 1938). The correction may be positive or negative. It has been applied in relevant areas to a distance of 40 times the depth of the borehole (Decker, 1966), with a maximum of 20km, following the method described by

Kappelmeyer and Haenel (1974). The effects of hills and valleys tend to cancel each other in areas of moderate relief.

(ii) Erosion and sedimentation

These effects are treated using the heat conduction equation in a moving medium. In general the effects are small but they may be serious, if due to rapid rates. The effect of erosion is to increase and that of sedimentation is to reduce the geothermal gradient relative to the equilibrium value. The correction has been applied wherever found necessary, following Jaeger (1965).

(iii) Uplift

Uplift raises the underground temperature gradient above its equilibrium value, as does the erosional process. The effect is of importance in large uplift areas like the Southern Alps. A correction may be applied, following Kappelmeyer and Haenel (1974).

A method of combining the effects of topography, uplift and erosion was developed by Birch (1950) and is useful for areas where all these effects are found, as in orogenic regions.

(iv) Past climate

Benfield (1939) was the first to apply this correction. The effect has been studied by Crain (1968), Horai (1969), Sass et al. (1971a), Beck (1977), Allis (1978), and other workers. A large correction is sometimes needed. The correction is most significant in shallow holes (Beck, 1977), the main cause being that of climatic changes during glacial times. Sass et al. (1971a) found no such effect in about a 3km deep hole in the Canadian shield, in spite of strong evidence about the past climatic changes.

The nature of past climatic changes in New Zealand is not accurately known. Evidence of the effect is lacking in temperature profiles (chapters 5 and 6). The correction has been attempted, following Beck (1977) but found unnecessary, and thus altogether neglected. Its non-application will not affect the regional pattern and will only tend to increase the values by a few percent.

3.2.7 Change of Temperature with Altitude

Knowledge of this parameter is essential in order to apply geological corrections. For this study it has been calculated from the meteorological observations of 1941 to 1970 (N.Z. Met. S. Misc. Pub., 1978). It varies between 3.5 and 10°C/km in different parts of New Zealand.

3.3 CONDUCTIVITY MEASUREMENT

To obtain a reliable heat flow, one needs to know the thermal conductivity of the same rock formations as those in which the temperature gradient is measured. A considerable problem is faced in assigning a mean value for a particular hole, and this involves a larger error than does the uncertainty in temperature gradient. It is often found that apparently similar rocks from the same formation have different conductivities. No anisotropic effects were observed in the present study. The problem of determining the conductivity is acute for deep holes.

3.3.1 Sampling - A New Method

Rock samples were available for most of the bore holes. They were in the form of cores and cuttings. Since it is not practicable to sample the entire length of every borehole a new sampling method has been devised which is particularly useful for deep wells from which cuttings are available. The depth range is divided into a number of zones 50 to 200 m thick. It is preferred that each zone be lithologically homogeneous. Then from each zone nearly equal amounts of cuttings are collected at every 5 to 10 m, and a composite sample is prepared for measurement.

3.3.2 Methods of Measurement

Steady-state, quasi steady-state and transient methods have been used by various workers to measure thermal conductivity in the laboratory (Powells, 1957; Beck, 1957, 1965; Von Herzen and Maxwell, 1959; Lubimova et al., 1961; Schröder, 1963; Zierfuss, 1963; Jaeger and Sass, 1964; etc.). A steady-state device in the form of a divided bar has been most common(Beck, 1957, 1965). Steady-state methods are relatively more accurate than others but involve tedious sample preparation and are unsuitable for friable rocks (although Sass et al., (1971b) use a divided bar apparatus on cuttings). There is also a problem with contact resistance (Beck, 1965).

A more rapid method suitable for cores as well as cuttings is the transient needle probe method (Von Herzen and Maxwell, 1959; Beck, 1965; Jaeger, 1965; Langseth, 1965). The theory has been given in detail by Blackwell (1954), Bullard (1954), Jaeger (1956) and Carslaw and Jaeger (1959). In addition to seafloor and lakefloor studies, the needle probe is becoming popular in studies of heat flow on land (Woodside and Messmer, 1961; Sass et al., 1968; Horai and Baldridge, 1972a; Kings and Simmons, 1972; Boccalitti et al., 1977; Veliciu et al., 1977; Balling, 1979, etc.). Measurements by transient and steady-state methods agree to between 3 and 10% (Von Herzen and Maxwell, 1959; Christoffel and Calhaem, 1969; Combs and Simmons, 1973; Balling, 1979).

Conductivity can also be estimated indirectly in the laboratory by determining the rock composition (Horai and Baldridge, 1972b) and the physical and thermal properties; this method has been used for five of the present samples. Field methods (Beck et al., 1956; Blackwell, 1956; Jaeger, 1956) have also been developed but have been seldom used.

3.3.3 The Needle Probe

A complete probe apparatus with control box and circuit diagram is shown in figs. 3.6, 3.7 and 3.8. The probe itself consists of a hypodermic needle 7 cm long and 2 mm in outside diameter with a heater and thermistor mounted halfway down the inside. It is connected by means of a four-core cable to the control box, which houses the power supply for the heater and a bridge network with biasing control. From about 10 sec. after the heater power is turned on, the temperature T (^{o}C) of the thermistor as a function of time t (sec.) is given by

$$T = (Q/4\pi K) ln(t) + C \qquad (3.2)$$

where Q(W/m) is the power per unit length of heater, K(W/m^{o}C) is the thermal conductivity, and C is a constant. A measurement is made by inserting the probe in the sample, switching on the heater, and measuring the thermistor output (in mv.) for up to about 5 min. The output is then converted into temperature by means of a calibration chart. A plot is then made between $ln(t)$ and T; this is theoretically a straight line (fig. 3.9) with slope equal to $\frac{Q}{4\pi K}$, although because of finite sample size the relationship may eventually become non-linear (fig. 3.9). Q is known since the current, resistance and length of

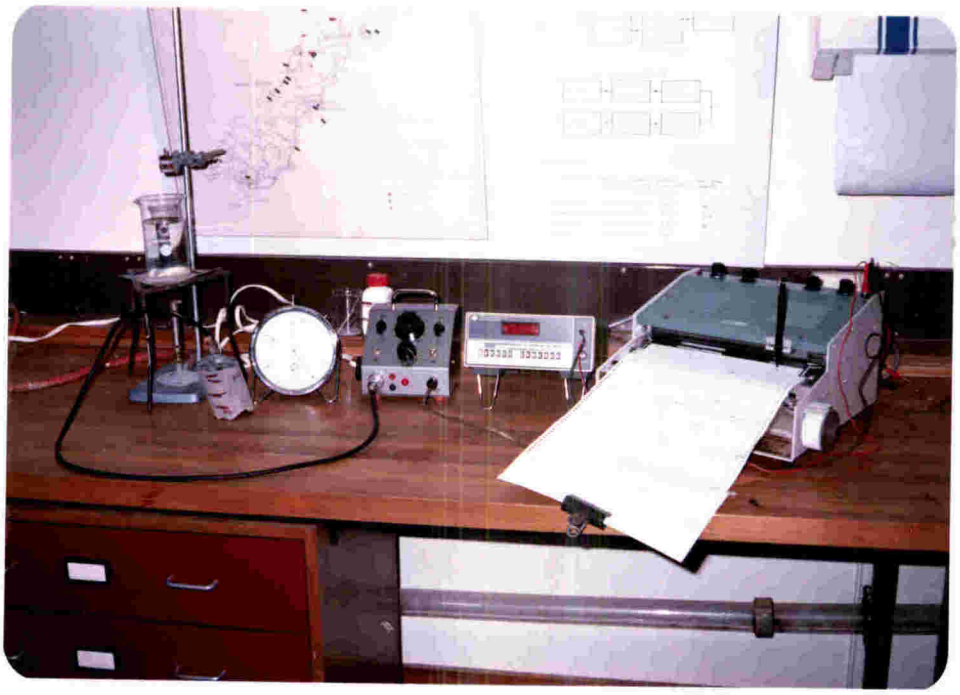

Fig. 3.6 Laboratory set-up for measurement of thermal conductivity by needle probe.

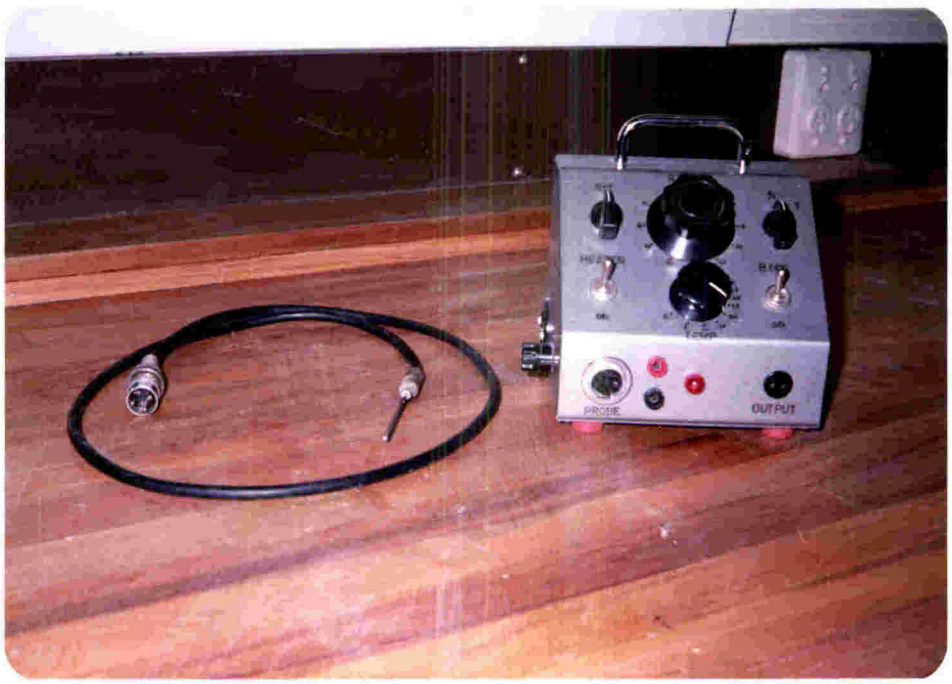

Fig. 3.7 Needle probe and control box.

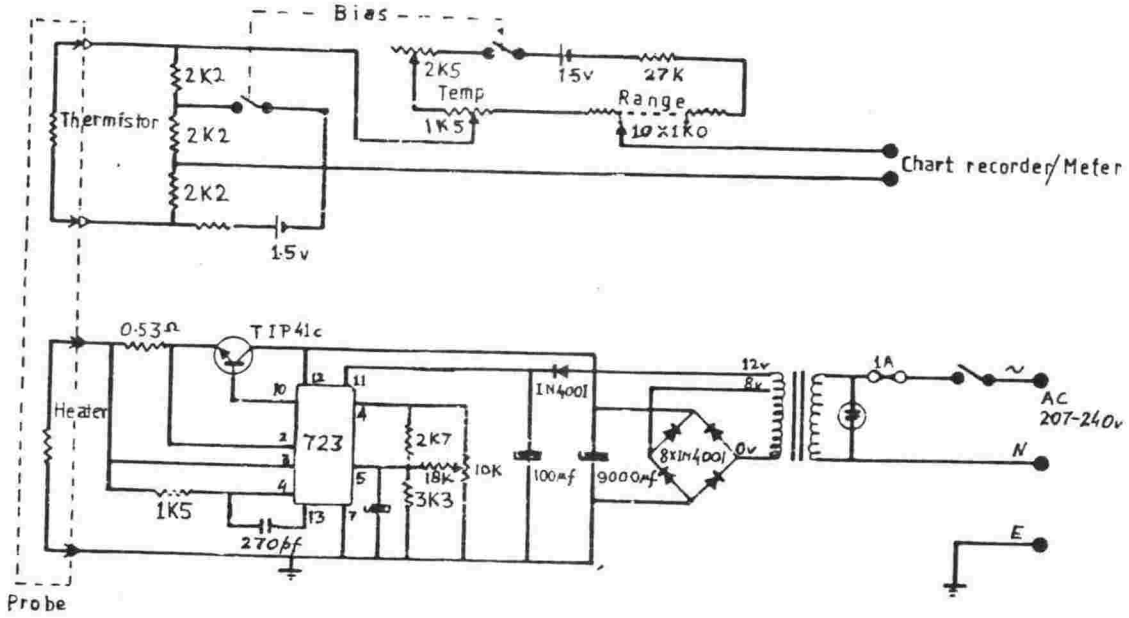

Fig. 3.8 Circuit diagram of needle probe.

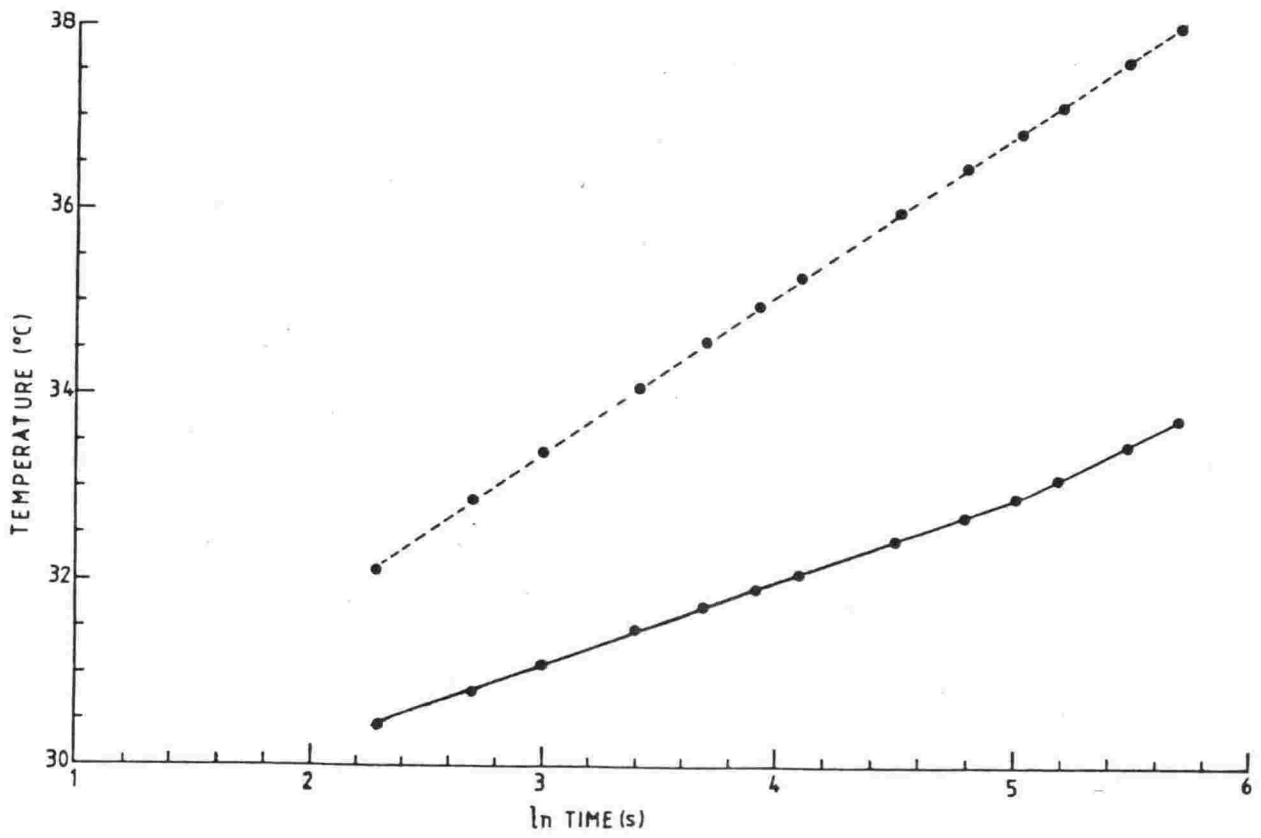

Fig. 3.9 Temperature vs ln time(s) for typical measurements on mudstone (dashed line) and sandstone (solid line).

the heater are known. Thus K can be calculated. In most cases the temperature rise is about 2 to 6°C depending upon the material; in a high conductivity material the rise in temperature is smaller.

Measurement procedure

All measurements were made at room temperature (15°-20°C). In the case of a solid core a hole about 7 cm deep and 3.5 mm diameter was made in the centre and the conductivity was measured both in the dry and wet states. Wood's metal (melting point = 74°-76°C) is used (Woodside and Messmer, 1961) as a contact material between the probe and the core. Water has also been tried (Balling, 1979), but sometimes it tends to lower the estimate due to lack of a perfect contact, and it has not been used in the present work. Prior to measurement the cores were oven-dried at about 100°C for 12 to 15 hours. For wet determinations the cores were then saturated with water under partial vacuum for 24 to 48 hours. Some samples disintegrated while soaking, and for these the wet conductivity was estimated from wet/dry ratios for similar types of rock.

For measurements on cuttings (King and Simmons, 1972) they were first crushed into fine powder, then packed into a 100 ml beaker and saturated with distilled water under partial vacuum. Then the thermal conductivity of the mixture was determined by means of the probe. The density was measured and the volume fraction of water determined from dry and wet weights. To get the thermal conductivity of the rock in its natural porous state, porosity was either measured or calculated from sonic, formation density, and neutron porosity well logs. The conductivity was then calculated from the following equations:

$$(Km) = (Kr)^{1-\phi}(Kw)^{\phi} \qquad (3.3)$$

and

$$(Kpr) = (Kr)^{1-\phi_o}(Kw)^{\phi_o} \qquad (3.4)$$

where Km = Thermal conductivity of rock powder and water mixture

Kw = Thermal conductivity of water (0.61 W/m°C)

Kr = Weighted geometric mean conductivity of solid constituents of the mixture.

Kpr = Thermal conductivity of rock in its natural state

ϕ = Volume fraction of water in the mixture

ϕ_o = Porosity of rock sample in uncrushed state.

In cases of zero porosity, the conductivity is expressed by Kr, and if there is a natural porosity (ϕo) then by Kpr.

Repeatability and accuracy

In the interests of accuracy each sample was measured several times in the dry and wet states, and a mean was adopted. In most cases repeatability was better than ±3%. Considering the accuracy of measurement of current, resistance and length of heater, the probe is capable of measuring to ±2% accuracy. The probe has been checked by comparing results with thermal conductivities determined by other methods. An example of thermal conductivities measured by different methods on the samples cut from the same core is presented in table 3.1.

3.3.4 Effect of Temperature and Pressure on Conductivity

These effects are negligible in the case of shallow holes for a wide variety of rocks. However for deeper wells they could be serious. The effect of temperature is to decrease the thermal conductivity while pressure tends to increase it. The effects thus cancel each other to some extent as the depth increases.

(i) Effect of temperature

The effect is considerable in high gradient areas. In order to apply this correction, data on temperature dependence have been compiled for various rock types using the values from Birch and Clark (1940), Ensor (1931), Kawada (1964), Winkler (1952) and Moissenko (1968). The relationship is shown in fig. 3.10; it is found that at 200°C the conductivity of some rocks has decreased by as much as 30%.

(ii) Effect of pressure

The effect is small within the pressure range prevailing in the drill holes used in this study. A linear dependence between pressure and thermal conductivity can be assumed (Kappelmeyer and Haenel, 1974):

$$K = Ko \quad (1 + \delta p) \qquad (3.5)$$

where Ko = thermal conductivity at normal pressure ($\simeq$ 1kg/cm^2).

δ = pressure coefficient of thermal conductivity ($kg^{-1}cm^2$)

p = pressure ($kg\ cm^{-2}$).

δ values have been adopted from Clark (1941). Pressure curves for the correction were computed for the two North Island wells (Ruakituri -1 and Midhurst-1) using density data from Garrick (1969) and from the present study.

Table 3.1 Comparison of thermal conductivity by different methods.

Sample Number	Rock Type	Thermal Conductivity ($W/m^{\circ}C$)		
		Needle Probe, using Wood's Metal	Needle Probe, using chip method	Divided bar*
281	Siltstone	2.81	2.92	-
323	Andesite	1.46	-	1.51
324	Greywacke	2.29	-	2.09
325	Schist	2.79	-	2.76
326	Sandstone	2.18	-	1.89

* Measured by Prof. E.R. Decker at the University of Wyoming (U.S.A.), at 1000 psi except for sample number 326, which was measured at 500 psi.

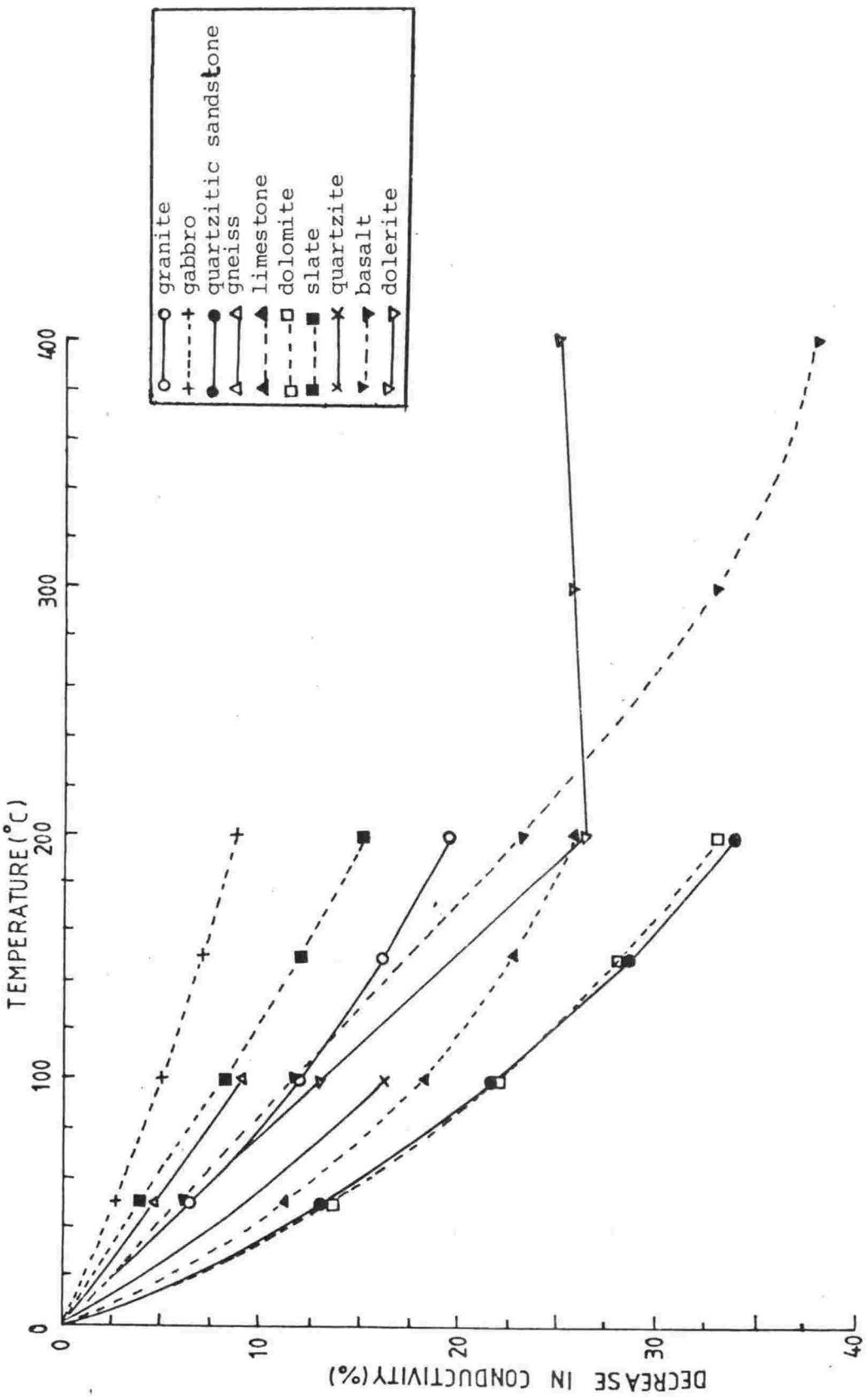

Fig. 3.10 Decrease in thermal conductivity with temperature for different rock types.

3.4 OTHER MEASUREMENTS

The densities and porosity of all samples, and the concentrations of U, Th, K and SiO_2 in selected samples, were measured. Procedures and results of these measurements will be presented in chapters 4 and 7.

3.5 STATISTICAL TECHNIQUES

Means, correlation coefficients, and parameters of least squares straight-line, with their standard errors, have been computed by the usual procedures. Methods of computation have been given in Spiegel (1961), Macfadyen (1963), Meyer (1975) and Negi and Pandey (1976).

3.6 HEAT FLOW CALCULATION

3.6.1 Methods

Three main methods can be used to combine geothermal gradient (G) with thermal conductivity (K) in order to determine heat flow (Beck, 1965; Jaeger, 1965). These are:

(i) the G-K method, which involves the multiplication of mean gradient with mean conductivity for the useful depth range,

(ii) the interval method, where an average heat flow is calculated from the gradient and conductivity of several depth intervals, and

(iii) the thermal resistance integral method (Bullard, 1939), in which observations are combined according to equation

$$Tz = To + q\sum_{i=1}^{n} (Di/Ki) \qquad (3.6)$$

where Tz is the temperature at depth z, Ki is the thermal conductivity of the i th layer, of thickness Di, To is constant, and q is the mean heat flow which can be found from the slope of the line plotted between Tz and $\sum_{i=1}^{n}(Di/Ki)$.

Here the G-K and resistance integral methods have been utilised in the calculation of heat flow; no significant difference was noticed when both methods were applied to the same location. The choice of method depended upon the nature of the temperature profile. In the case of a constant gradient with depth (especially in massive homogenous rocks), with no systematic changes of conductivity, a mean conductivity of all the samples (sometimes a weighted mean) is combined with the least squares gradient. In the case of stratified rocks having distinct differences of conductivity (as reflected in the temperature profile) the resistance integral method has been used.

3.6.2. Presentation of Results

'Mean' in this thesis refers to the unweighted arithmetic mean of all the samples used. N is the number of samples. Sometimes, if the sampling is very uneven, a weighted mean is used. Gradients, corrected for the geological history of the area wherever desirable, refer to the corresponding depth interval only. Attached errors are the standard errors of the gradient calculation.

Where standard errors (shown as ±) have been assigned they represent only statistical errors and relate to the internal consistency of the measurements.

The tabulated standard errors of heat flow combine the standard errors of mean gradient and mean conductivity; in the resistance integral method this corresponds to the error of the slope. In inclined boreholes the vertical component of the depth was used. Depths are given in meters from ground surface in land areas and from the sea floor in offshore areas. All elevations are from mean sea level. In the tables of heat flow, an indication of whether or not geological corrections were necessary is given. Wherever heat flow is calculated by resistance integral method, quoted conductivities are weighted means.

CHAPTER 4

RESULTS OF THERMAL CONDUCTIVITY AND DENSITY MEASUREMENTS AND RELATIONSHIP WITH OTHER PARAMETERS

4.1 INTRODUCTION

A knowledge of rock thermal conductivity and density is essential in the study of various geophysical problems. Thermal conductivity plays a particularly important role in the calculation of deep-seated temperatures. The main sources of compiled information of thermal conductivity and density are those given by Daly et al. (1966), Clark (1966) and Kappelmeyer and Haenel (1974). In this chapter we have attempted to summarize the results of thermal conductivity and density measurements on New Zealand rocks, and to study the relationships with other parameters such as geologic age, depth, porosity and composition. Such relationships could lead to the estimation of thermal conductivity in cases where only such other parameters are known. Results of regression analyses of these parameters are given in table 4.1.

4.2 DENSITY OF ROCKS AND ITS RELATIONSHIP WITH GEOLOGIC AGE, DEPTH AND POROSITY

4.2.1 Measurements of Density and Porosity

Dry, wet and particle densities have been measured using conventional methods. To obtain the dry density, the dry weight of the sample was measured after oven-drying for 12 to 15 hours at 100°C. The sample was then placed in water under partial vacuum for 24 to 48 hours. After saturation the wet weight and volume of the sample were measured and the densities calculated using following relation:

dry density = dry weight/volume

wet density = wet weight/volume

This enables us to calculate the particle density from the relation

particle density = dry density/(1 + dry density - wet density)

in which water is taken as having unit density.

For friable specimens, dry density was measured using wax as a coating material, and particle density was measured by pycnometer. Then the calculation of wet density was made using the relation

wet density = 1 + dry density - (dry density/particle density)

In these measurements, weights were measured correct to 0.01 gm.

Table 4.1 Parameters of regression analysis

Parameters	Rock type	Number of data	Correlation Coefficient	F Value (Critical F value at 95% level)	Linear equation*	Fig.
Wet density and Porosity	Sandstone	37	0.86	100.18 (~ 4.00)	$\rho = (-2.17 \pm .22)\phi_o + 2.63$	4.1
Wet density and Porosity	Mud-mudstone siltstone, shale, clay	49	0.79	79.73 (~ 4.00)	$\rho = (-1.59 \pm .18)\phi_o + 2.56$	4.1
Wet density and Porosity	Rest other rocks	55	0.87	169.58 (~ 4.00)	$\rho = (-2.26 \pm .17)\phi_o + 2.65$	4.1
Wet density and Porosity	All data	141	0.84	336.97 (~ 4.00)	$\rho = (-1.96 \pm .11)\phi_o + 2.62$	4.1
Wet thermal conductivity and depth	Sandstone Mud-mudstone silt-siltstone	55	0.62	33.46 (~ 4.00)	$K = (.54 \pm .09)10^{-3}D + 2.01$	4.2
Wet thermal conductivity and porosity	Sandstone	58	0.49	18.14 (~ 4.00)	$K = (-4.94 \pm 1.16)\phi_o + 4.23$	4.3
Wet thermal conductivity and porosity	Mudstone	66	0.57	30.60 (~ 4.00)	$K = (-3.07 \pm .55)\phi_o + 3.00$	4.3
Wet thermal conductivity and porosity	Siltstone	39	0.53	14.16 (~ 4.00)	$K = (-2.60 \pm .69)\phi_o + 3.02$	4.3
Wet thermal conductivity and porosity	All data	163	0.52	59.77 (~ 4.00)	$K = (-4.38 \pm .57)\phi_o + 3.58$	4.3
Wet thermal conductivity and wet density	Mud-mudstone siltstone, shale, clay	49	0.74	56.04 (~ 4.00)	$K = (2.11 \pm .28)\rho - 2.33$	4.4
Wet thermal conductivity and SiO_2 content	Schist	7	0.99	170.90 (~ 5.99)	$K = (.15 \pm .01)S - 5.90$	4.5
Wet thermal conductivity and SiO_2 content	Sandstone	25	0.61	13.68 (~ 4.20)	$K = (.55 \pm .15)10^{-1}S + .48$	4.6
Wet thermal conductivity and SiO_2 content	All data	101	0.44	24.15 (~ 4.00)	$K = (.50 \pm .10)10^{-1}S + .25$	4.7
Mean wet thermal conductivity vs mean SiO_2 content	Sedimentary rocks	9	0.68	6.15 (~ 5.12)	$K = (.73 \pm .30)10^{-1}S - 1.26$	4.8

ρ = wet density (g/cm^3)

ϕ_o = porosity

K = Wet thermal conductivity (W/m^oC)

D = Depth (m)

S = SiO_2 content (%)

* = Obtained from linear regression using a statistical package (Nie et al., 1975).

Finally, the porosity was obtained by subtracting dry density from wet density. This is called the natural porosity; it is concerned with pores to which groundwater has access in natural conditions.

4.2.2 Density Results and Relationships with Other Parameters

The results of density measurements on New Zealand rocks are summarized in table 4.2, which reveals large variations. In the sedimentary rocks the wet density is lowest for clayey rocks (apart from coal) and highest for argillite. Among the igneous rocks the lowest densities are for pumice and the highest for diorites. In general, the densities of the sedimentary rocks tend to increase with the age, as shown in table 4.3, which includes only those data where the geologic age was known accurately from the stratigraphic logs. The youngest rocks (Pliocene-Holocene) have a wet density of 2.21 g/cm^3, and densities increase to 2.68 g/cm^3 for the Paleozoics, similar to the value used in gravity corrections.

There appears a possibility that the relation between density and age may not always hold for the Paleocene and Eocene periods, when some densities are considerably lower. Since this inference is based on a small number of data, it may arise due to inadequate sampling. However, it must be mentioned here that some unusually low wet densities (as low as 2.16 g/cm^3) have been measured for Kapuni sandstone in the Taranaki region, which belong to an Eocene-L.Oligocene age. Lower densities for these periods have also been reported by Hatherton and Leopard (1964) and Garrick (1969). No such relation between geologic age and density is apparent in the igneous and metamorphic rocks. In general the rock densities increase with depth. This increase is due to the increase in overburden pressure, with progressive loss of porosity. The relationship between the wet density and the natural porosity is shown in fig. 4.1, which indicates how the density decreases as the porosity increases, for all rock types.

4.3 RELATIONSHIP OF THERMAL CONDUCTIVITY WITH DENSITY, POROSITY, GEOLOGIC AGE, AND SiO_2 CONTENT

4.3.1 Thermal Conductivity of New Zealand Rocks

The results of thermal conductivity measurements on 581 samples have been summarized in table 4.4. Attention is drawn to the following points:

Table 4.2 Measured Densities (g/cm^3)

Rock Type	Dry Density			Wet Density			Particle Density		
	n	Range	Mean	n	Range	Mean	n	Range	Mean
Mud - mudstone	34	1.38 - 2.66	2.17±.06	34	1.77 - 2.67	2.32±.04	74	1.85 - 3.12	2.53±.02
Silt-siltstone	15	1.61 - 2.66	2.32±.08	15	2.01 - 2.67	2.42±.06	45	2.03 - 2.87	2.54±.03
Sand-sandstone	44	1.10 - 2.66	2.34±.05	44	1.51 - 2.70	2.43±.04	77	1.87 - 2.81	2.55±.07
Shale	3	2.32 - 2.63	2.43±.10	3	2.34 - 2.65	2.47±.09	14	2.37 - 2.73	2.53±.03
Coal	1	-	1.27	1	-	1.35	2	1.31 - 1.40	1.35±.04
Argillite	6	2.33 - 2.70	2.59±.06	6	2.40 - 2.71	2.62±.05	8	2.52 - 2.75	2.68±.03
Clay_claystone	3	1.45 - 1.97	1.70±.15	3	1.84 - 2.23	2.04±.11	9	2.28 - 2.85	2.55±.06
Greywacke	10	2.27 - 2.71	2.53±.05	10	2.38 - 2.72	2.58±.04	14	2.28 - 2.76	2.63±.04
Limestone	4	2.19 - 2.63	2.46±.10	4	2.34 - 2.67	2.53±.07	6	2.57 - 2.76	2.67±.03
Conglomerate	2	2.54 - 2.57	2.56±.01	2	2.55 - 2.58	2.57±.01	5	2.54 - 2.61	2.58±.01
Bentonite	-	-	-	-	-	-	1	-	2.19
Gravels	-	-	-	-	-	-	12	2.60 - 2.84	2.71±.02
Dolerite	1	-	2.45	1	-	2.58	1	-	2.82
Tuff	1	-	2.04	1	-	2.18	2	2.36 - 2.52	2.44±.08
Basalt	3	1.59 - 2.73	2.34±.38	3	1.95 - 2.74	2.48±.26	4	2.49 - 2.83	2.67±.07
Andesite	9	1.58 - 2.72	2.30±.12	9	2.03 - 2.70	2.42±.07	10	2.36 - 2.88	2.59±.05
Breccia	1	-	1.31	1	-	1.67	2	2.03 - 2.69	2.36±.33
Granite	2	2.51 - 2.56	2.54±.03	2	2.52 - 2.58	2.55±.03	7	2.38 - 2.85	2.61±.06
Ignimbrite	2	1.75 - 2.19	1.97±.22	2	1.99 - 2.29	2.14±.15	2	2.29 - 2.43	2.36±.07
Rhyolite	1	-	2.03	1	-	2.06	1	-	2.09
Diorite	2	2.62 - 2.94	2.78±.16	2	2.63 - 2.94	2.78±.16	3	2.64 - 2.96	2.75±.10
Volcanics	-	-	-	-	-	-	1	-	2.52
Pumice	1	-	1.18	1	-	1.54	1	-	1.86
Schist	3	2.54 - 2.76	2.68±.07	3	2.57 - 2.80	2.71±.07	7	2.60 - 2.88	2.71±.04
Gneiss	1	-	2.76	1	-	2.77	2	2.37 - 2.78	2.57±.21
Mixed Rocks	8	1.41 - 2.58	2.14±.18	8	1.77 - 2.61	2.28±.13	73	2.00 - 2.89	2.51±.02

n is the number of depths or sites

± indicates a standard error

Table 4.3 Age and density of sedimentary rocks

AGE	MEAN DENSITIES (g/cm^3)					
	n	DRY	n	WET	n	PARTICLE
Holocene-Pliocene	26	1.99 ± .07	26	2.21 ± .05	56	2.57 ± .03
Miocene	24	2.32 ± .04	24	2.41 ± .03	66	2.56 ± .01
Oligocene	10	2.51 ± .05	10	2.56 ± .04	31	2.52 ± .03
Eocene	3	2.07 ± .22	3	2.43 ± .10	25	2.41 ± .07
Paleocene	1	1.77	1	2.05	4	2.47 ± .07
Mesozoic	21	2.47 ± .03	21	2.53 ± .02	47	2.59 ± .02
Paleozoic	2	2.65 ± .01	2	2.68 ± .00	4	2.71 ± .03

n is the number of depths or sites

± indicates a standard error

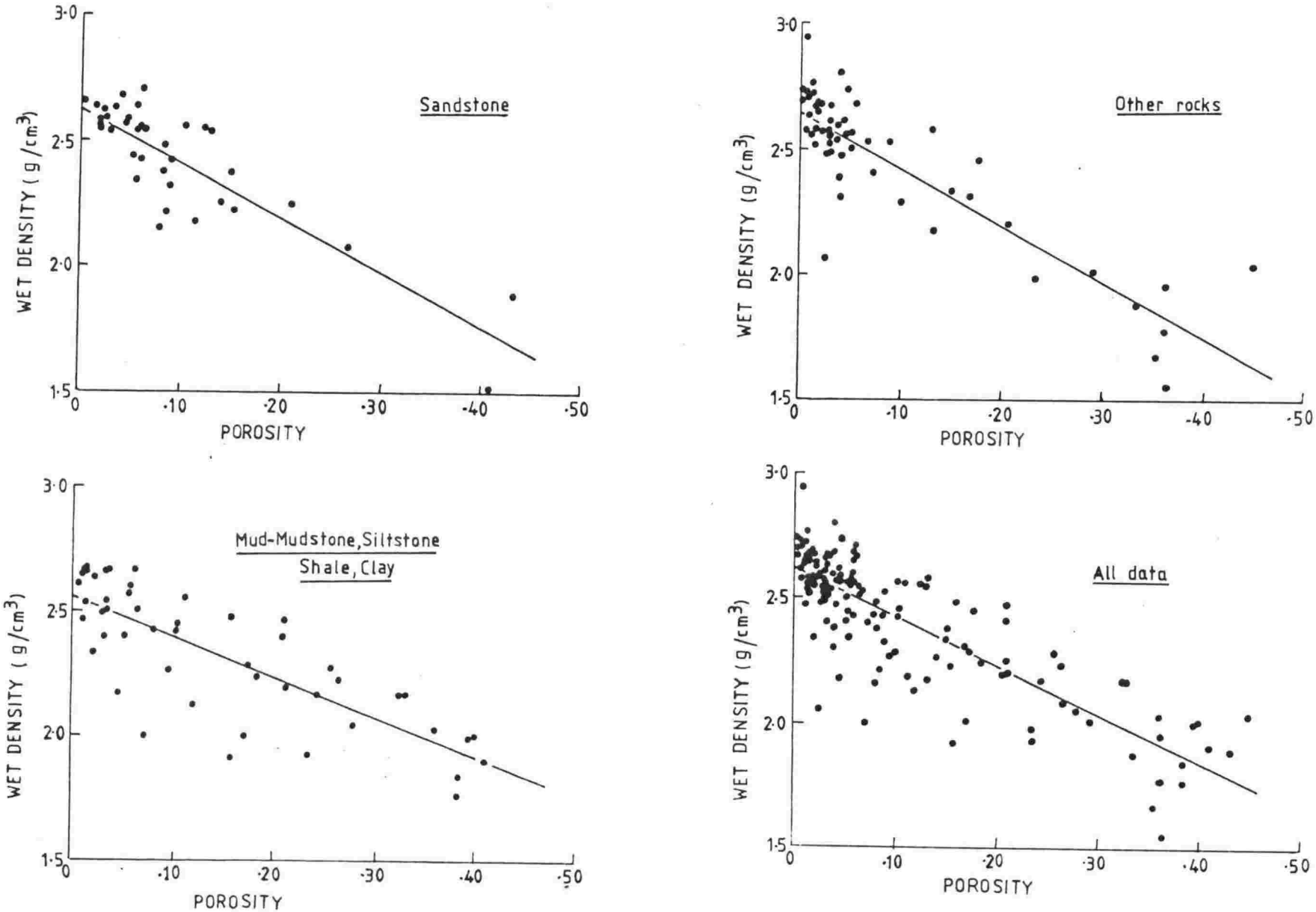

Fig. 4.1 Wet density vs porosity.

Table 4.4 Wet Thermal Conductivity ($W/m^{o}C$)

ROCK TYPE	N(n)	RANGE	MEAN
Mud - Mudstone	126(74)	1.38 - 4.50	2.45 ± .07
Sand - Sandstone	99(77)	1.46 - 6.55	3.54 ± .13
Silt - Siltstone	87(46)	1.73 - 3.98	2.63 ± .08
Limestone	8(6)	2.06 - 4.18	3.17 ± .30
Greywacke	17(13)	1.58 - 3.09	2.22 ± .12
Argillite	11(9)	2.23 - 6.06	3.96 ± .40
Shale	24(14)	1.90 - 3.28	2.65 ± .13
Clay - Claystone	13(9)	1.76 - 3.05	2.24 ± .13
Bentonite	3(1)	-	2.53
Coal	3(2)	0.39 - 0.65	0.52 ± .13
Gravel	13(12)	1.58 - 2.68	1.95 ± .08
Conglomerate	7(5)	3.08 - 5.51	3.94 ± .43
Mixed Rocks	115(72)	1.39 - 4.75	2.87 ± .10
Breccia	3(2)	1.63 - 2.00	1.82 ± .19
Tuffs	2(2)	1.64 - 1.79	1.72 ± .08
Pumice	1(1)	-	1.38
Volcanics	1(1)	-	2.10
Dolerite	1(1)	-	2.12
Basalt	4(4)	1.70 - 2.93	2.29 ± .33
Granite	11(7)	2.44 - 5.33	3.59 ± .40
Diorite	4(3)	2.42 - 3.91	2.92 ± .50
Andesite	10(10)	1.46 - 2.29	1.90 ± .09
Ignimbrite	2(2)	2.22 - 2.44	2.33 ± .11
Rhyolite	1(1)	-	2.50
Schist	10(7)	2.79 - 6.14	3.92 ± .47
Gneiss	1(1)	-	2.84

Note:- N is total number of samples measured
n is the number of depths or sites
Mean refers to n and ± indicates a standard error

(i) The conductivity of a particular lithological type can vary by up to four times or more. The largest variation, from 1.46 to 6.55 W/m^{o}C has been recorded in sandstones. This has a mean of 3.54 W/m^{o}C; Kappelmeyer and Haenel (1974) have reported a mean of 3.24 W/m^{o}C at 50^{o}C.

(ii) Surprisingly, the highest conductivity has been found for argillite (3.96 W/m^{o}C), conglomerate (3.94 W/m^{o}C) and schist (3.92 W/m^{o}C). This is because many of the samples were quartzose in nature. Sandstones are normally regarded as the most highly conductive rocks.

(iii) As expected, the lowest conductivity, 0.52 W/m^{o}C is associated with coal.

(iv) The mean conductivities of the various volcanic rocks (1.38 - 2.50 W/m^{o}C) are on average lower than those of sedimentary rocks (1.95 - 3.96 W/m^{o}C) and metamorphic rocks (2.84 - 3.92 W/m^{o}C).

4.3.2 Geologic Age, Depth of Overburden and Porosity

According to Kappelmeyer and Haenel (1974), the thermal conductivity of rocks in Germany increases with age, and this in general seems to be valid for New Zealand rocks also (table 4.5). The sedimentary rocks show a few exceptions, but these are possibly due to inadequate sampling. Conductivity also seems to increase with depth. Such a relation is shown in fig. 4.2 for a few rock types from the Taranaki basin; a similar relation holds true for other basins. Evans (1977) and Matsubayashi and Uyeda (1979) obtained similar results for the North Sea and for offshore Malaysian regions.

These relationships are consistent with an increase of compactness with depth, as is also often indicated by sonic well logs, in which transit-time usually decreases with depth. The decrease in thermal conductivity with porosity can be seen for a few rock types from fig. 4.3; this is in conformity with the earlier studies of Woodside and Messmer (1961) and Plewa (1976).

4.3.3 Relationship between Thermal Conductivity and Density

Horai (1971) found that for most minerals, conductivity is a linear function of density for constant mean atomic weight. An increase of conductivity with density in rocks has also been reported by Cermak (1973), Hurtig and Schlosser (1976), and Parasnis (1976). Here we consider the measured wet thermal conductivity and wet density of specimens to see if any relationship exists between them. The plot between the two parameters (fig. 4.4) reveals that:

Table 4.5 Variation of wet thermal conductivity ($W/m^{o}C$) with geological age.

Rock type	Holocene-Pliocene		Miocene		Oligocene		Eocene		Paleocene		Mesozoic		Paleozoic	
	n	Mean	n	Mean	n	Mean	n	Mean	n	Mean	n	Mean	n	Mean
Mud - mudstone	17	1.90±.07	18	2.66±.15	3	2.12±.37	8	2.75±.14	1	1.51	5	2.90±.34	-	-
Sand - sandstone	7	2.57±.30	20	3.23±.21	7	3.16±.46	6	3.59±.33	1	3.04	9	4.37±.25	1	4.71
Silt - siltstone	4	2.36±.21	12	2.62±.14	7	3.15±.29	4	2.09±.15	1	1.88	3	3.16±.27	-	-
Limestone	2	3.56±.62	-	-	4	2.98±.35	-	-	-	-	-	-	-	-
Greywacke	-	-	-	-	-	-	-	-	-	-	10	2.28±.13	-	-
Argillite	-	-	-	-	-	-	-	-	-	-	2	3.82±1.08	4	4.24±.83
Shale	-	-	1	3.00	3	2.33±.04	1	2.44	1	2.08	1	2.98	-	-
Clay-claystone	5	2.02±.08	-	-	1	3.05	1	2.25	-	-	1	2.73	-	-
Bentonite	-	-	-	-	-	-	1	2.53	-	-	-	-	-	-
Coal	-	-	-	-	-	-	1	0.39	-	-	-	-	-	-
Gravel	12	1.95±.08	-	-	-	-	-	-	-	-	-	-	-	-
Conglomerate	3	4.28±.65	-	-	-	-	-	-	-	-	2	3.43±.35	-	-
Mixed rock	5	2.19±.21	16	2.65±.20	5	2.65±.16	3	1.96±.31	-	-	14	3.32±.14	-	-
Breccia	-	-	-	-	-	-	-	-	-	-	1	2.00	-	-
Tuffs	-	-	1	1.64	-	-	-	-	1	1.79	-	-	-	-
Dolerite	-	-	-	-	1	2.12	-	-	-	-	-	-	-	-
Basalt	2	1.73±.03	-	-	-	-	-	-	-	-	-	-	-	-
Granite	-	-	-	-	-	-	-	-	1	3.29	3	4.55±.42	2	2.86±.42
Diorite	-	-	-	-	-	-	-	-	-	-	-	-	1	3.91
Andesite	10	1.90±.09	-	-	-	-	-	-	-	-	-	-	-	-
Ignimbrite	2	2.33±.11	-	-	-	-	-	-	-	-	-	-	-	-
Schist	-	-	-	-	-	-	-	-	-	-	-	-	5	4.09±.62

n is the number of depths or sites and ± indicates a standard error.

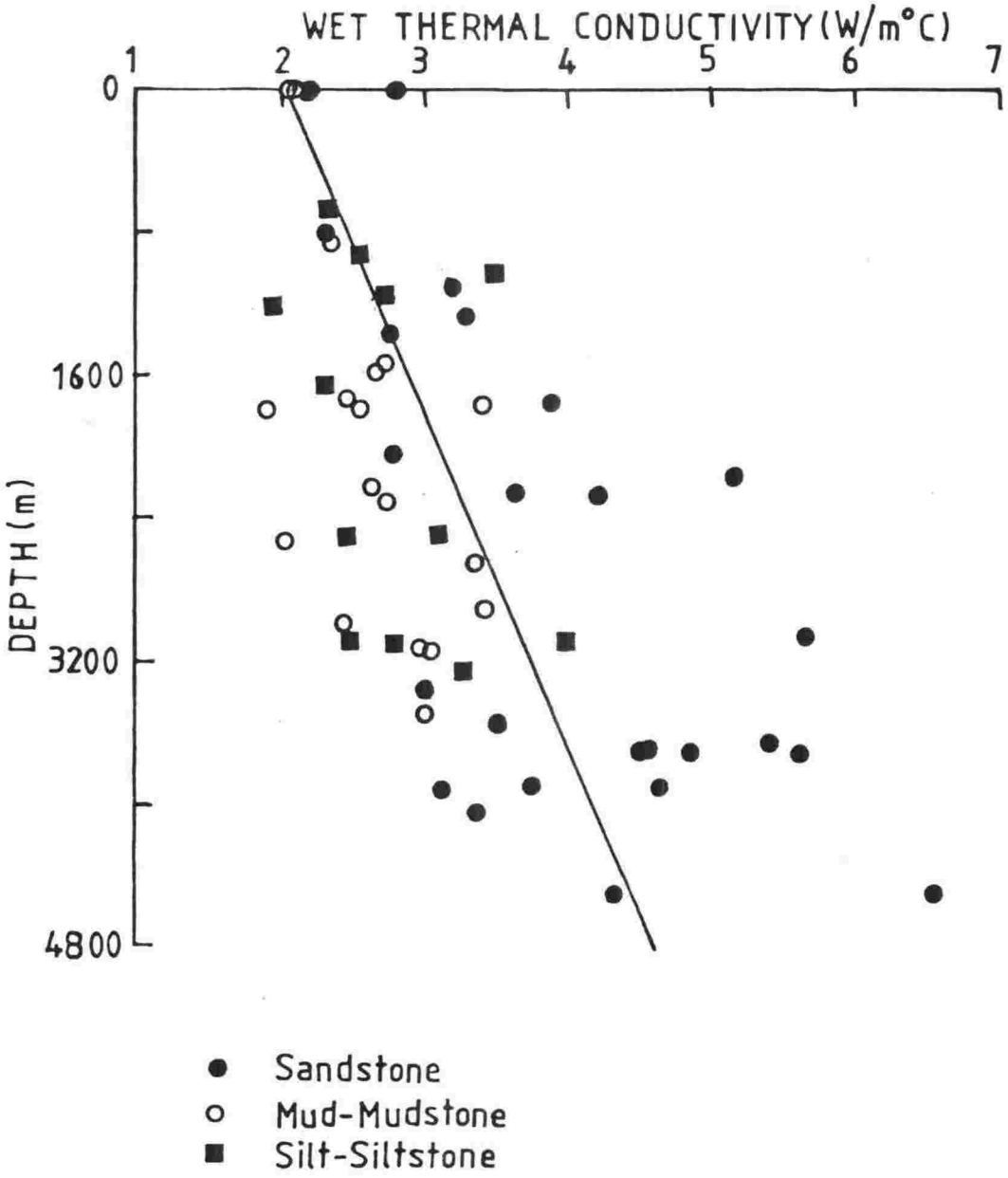

Fig. 4.2 Thermal conductivity vs depth: Taranaki Basin.

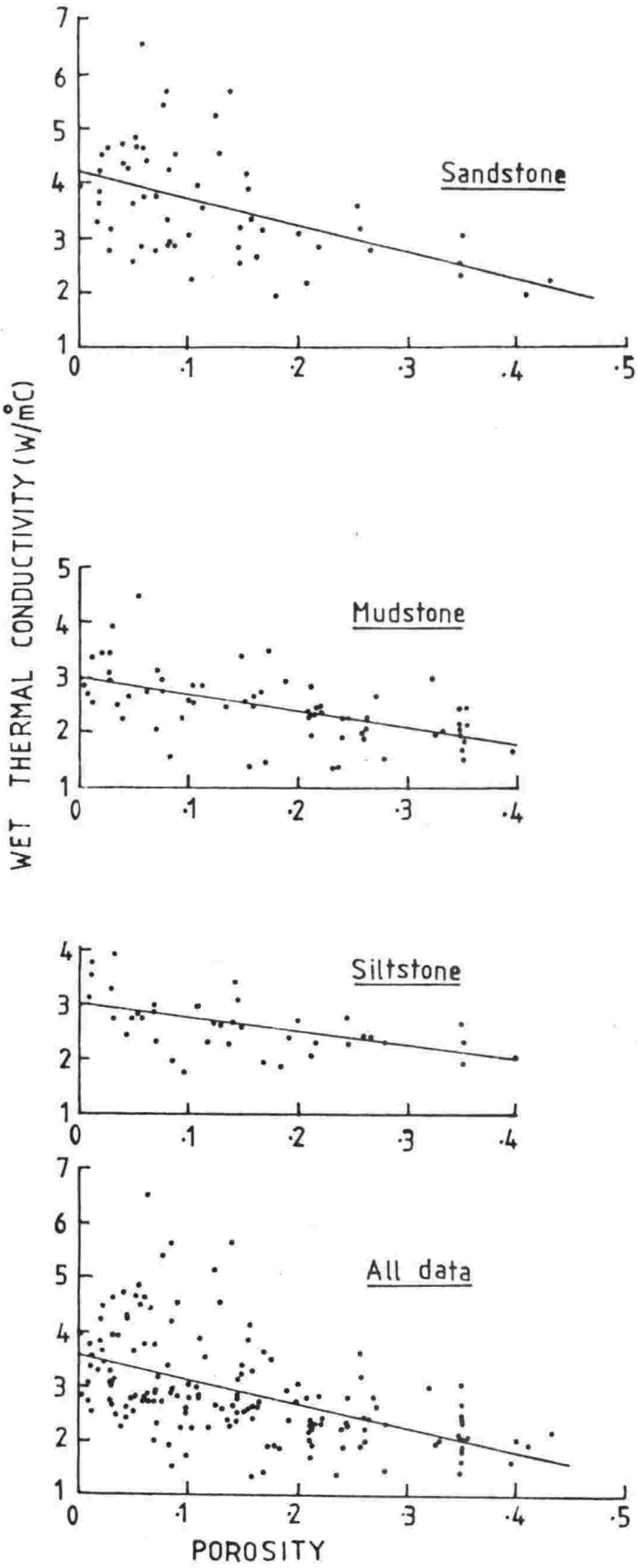

Fig. 4.3 Thermal conductivity vs porosity.

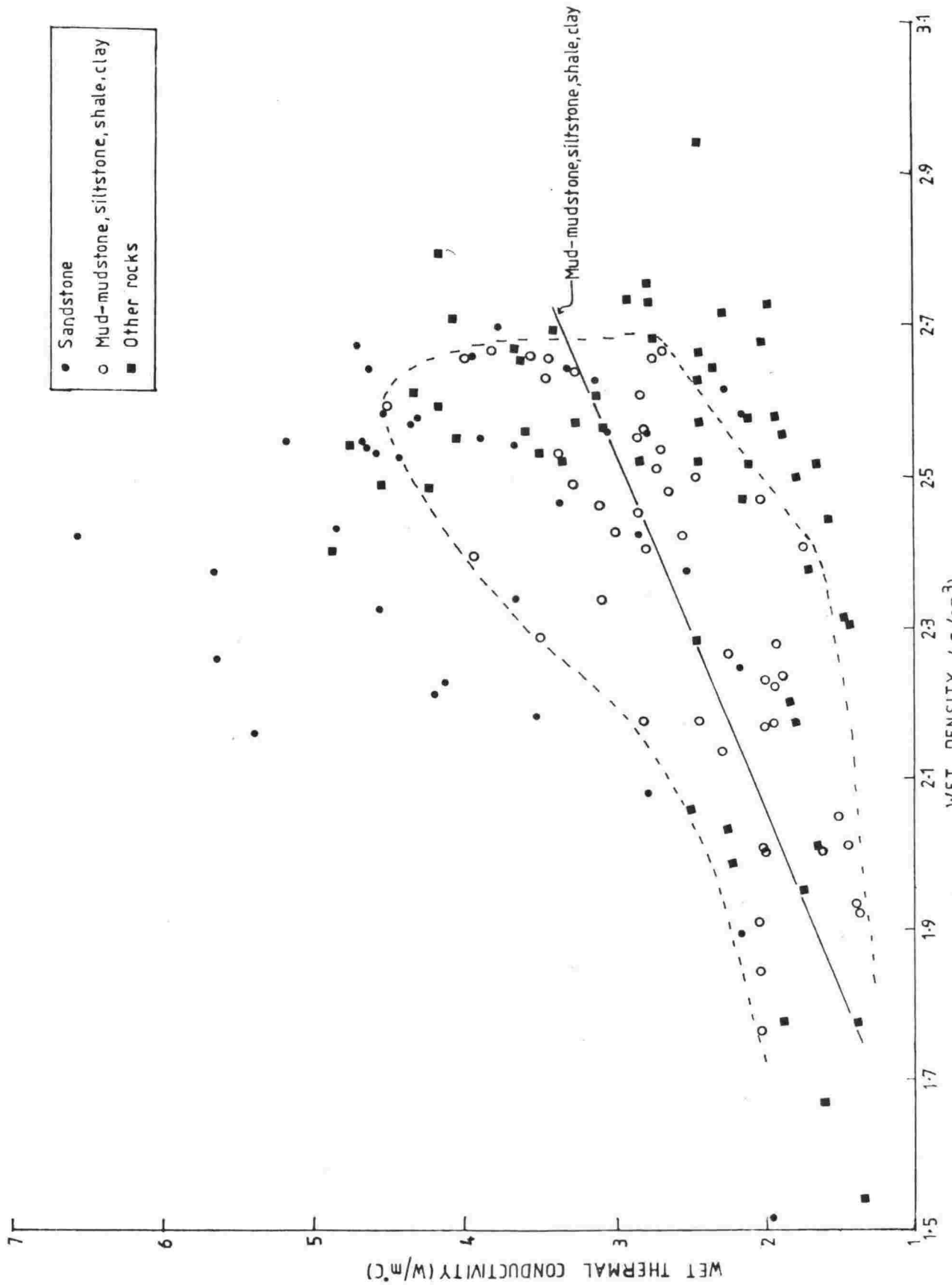

Fig. 4.4 Wet thermal conductivity vs wet density. The spread of data for clayey rocks is shown by dashed envelop.

(i) the thermal conductivity of clayey rocks (shale, mud - mudstone, siltstone and clay) seems to increase with density. The spread of data for these rock types is shown by a dashed envelope in fig. 4.4.

(ii) the thermal conductivity of other rocks may increase initially until the density reaches about 2.2 g/cm^3, after which the conductivity is governed by other factors such as composition.

4.3.4 Thermal Conductivity and SiO_2 Content

Previous studies have shown that sandstone normally has higher conductivity than most other rocks because it is largely made up of quartz. During the conductivity measurements, it also appeared that rocks having higher quartz content showed higher conductivity. So while measuring the U, Th and K content of samples we also measured the SiO_2 content in the hope of finding a relation between SiO_2 content and thermal conductivity. In addition to quartz, however, the SiO_2 content may be affected by other minerals, such as are commonly present in clay. The accuracy of measurement of SiO_2 content was about ±1%.

The plot of thermal conductivity against SiO_2 content is shown in fig. 4.5 for schists and in fig. 4.6 for sandstones. The trend is more or less clear. In fig. 4.7 the plot for all data is shown. Here the wide scatter is due to the igneous rocks. The trend is again clear in fig. 4.8, in which the average values of SiO_2 content and of conductivity are plotted for each of the nine different types of sedimentary rock.

The above correlations suggest that if the porosity were constant there should be a simple relationship between thermal conductivity and SiO_2 content, in the rocks where SiO_2 is present mainly in the form of quartz, as in sandstones and quartzites. The highest conductivity occurs when the SiO_2 content is high and porosity is low. The strong correlation for schists (fig. 4.5) is due to the fact that all the samples were quartzose in nature. However, the relationship may not hold good in cases where most of the SiO_2 is present in other forms, such as volcanic glass (rhyolite, ignimbrite, and andesite), clay minerals (mudstone, siltstone, sandstone, greywacke, altered andesites), orthoclase (ignimbrite, rhyolite, granite, etc.), plagioclase (granite, andesite), and pyroxene (andesites). Somewhat similar conclusions were drawn by Sass et al. (1968) and Kappelmeyer and Haenel (1974).

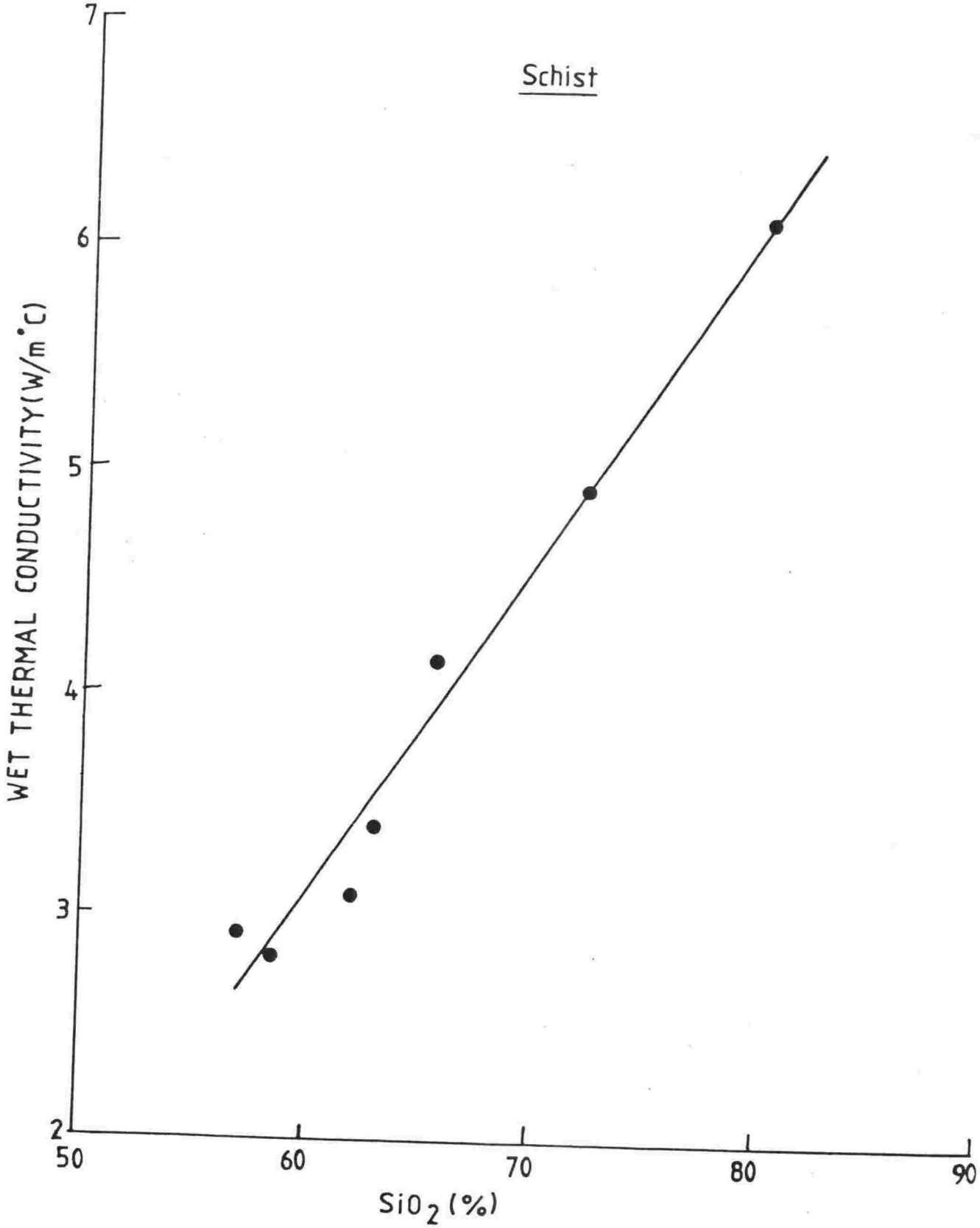

Fig. 4.5 Relationship between wet thermal conductivity and SiO_2 content for schists.

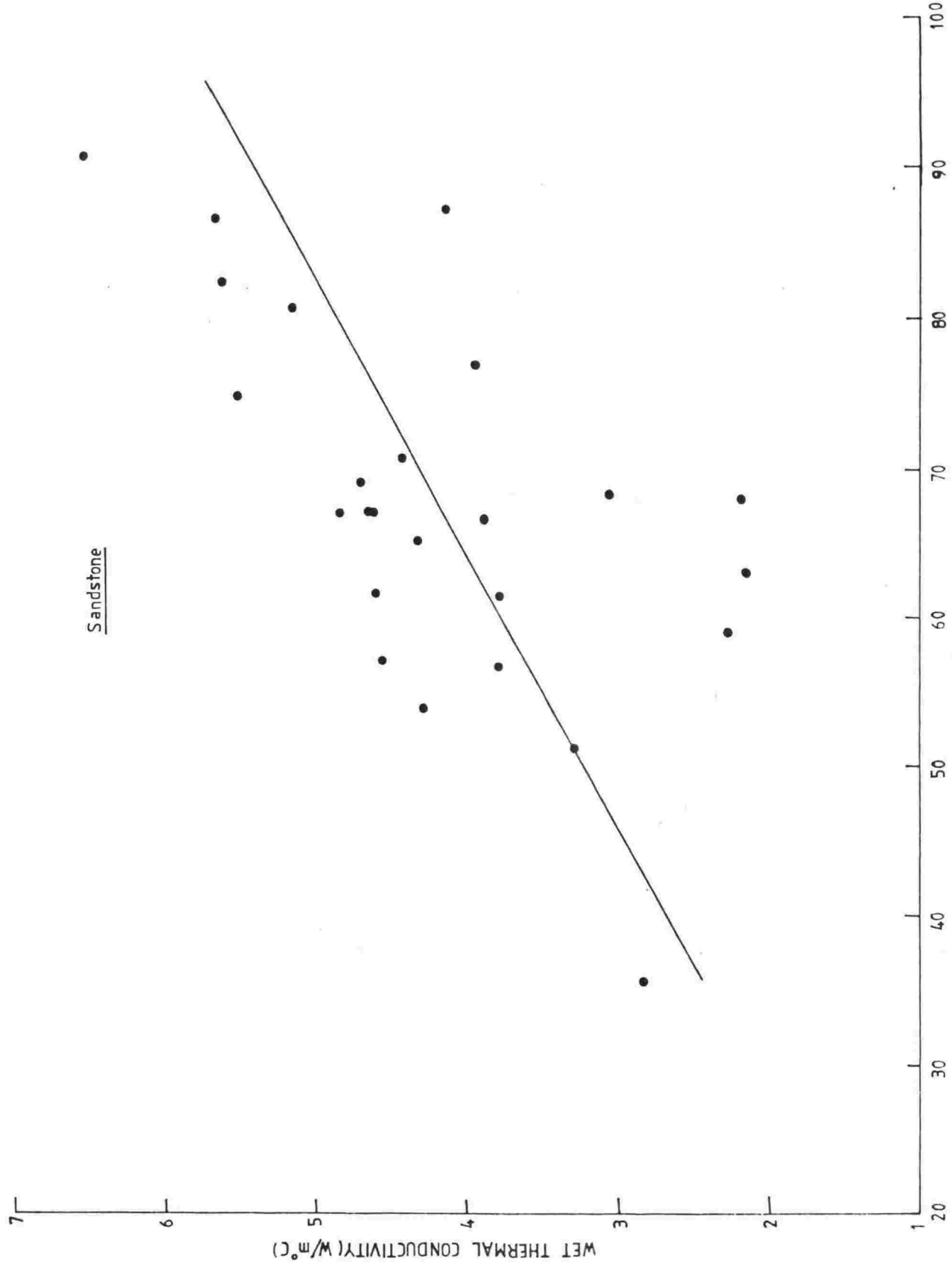

Fig. 4.6 Relationship between wet thermal conductivity and SiO_2 content for sandstones.

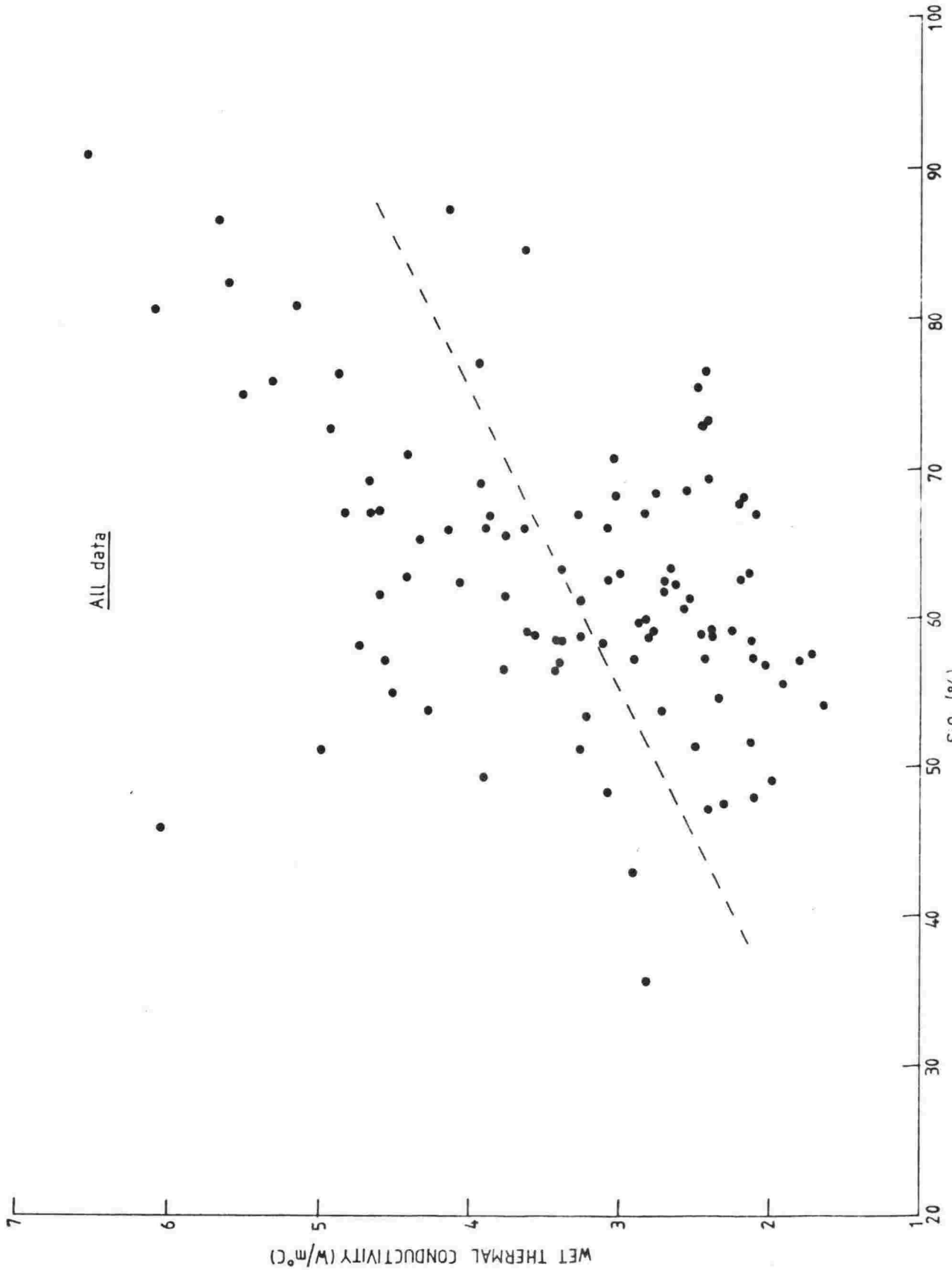

Fig. 4.7 Relationship between wet thermal conductivity and SiO_2 content: All data.

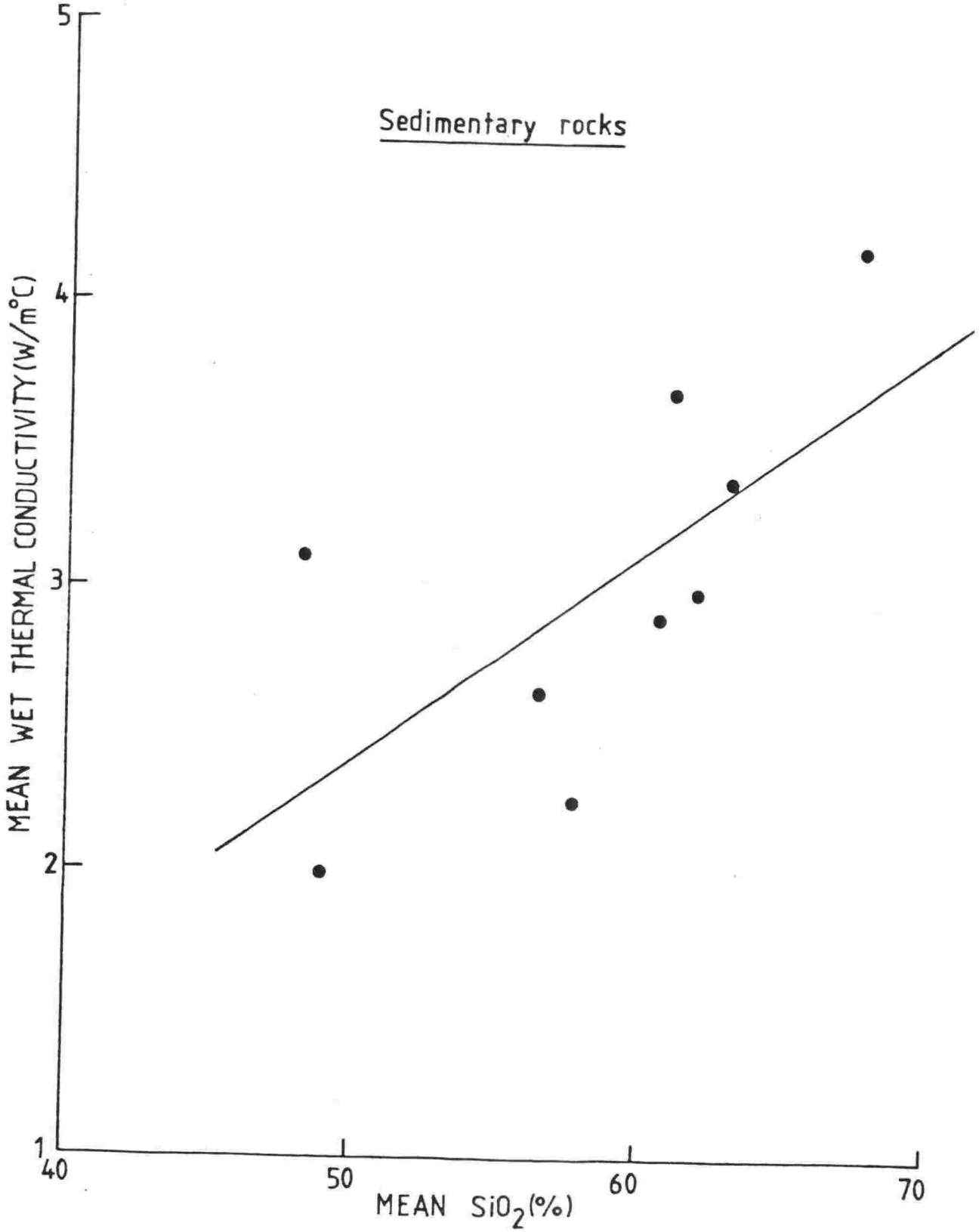

Fig. 4.8 Relationship between mean wet thermal conductivity and mean SiO_2 content: sedimentary rocks.

4.4 CONCLUSION

New Zealand rocks exhibit a large variation in density and thermal conductivity (tables 4.2 and 4.4). The densities are closely related to age, depth, and porosity. There is a possibility that the Eocene-Paleocene rocks might be associated with lower densities than those of Oligocene and Miocene ages. In general increased density is also related to increased conductivity, especially in clay rocks. It appears that the conductivity of sedimentary rocks and also of schists is primarily a function of SiO_2 content if the SiO_2 is present in the form of quartz, but it also depends on density, porosity, age and depth. It is thus possible to make an estimate of thermal conductivity if the values of these related parameters are known, but such estimates are of limited accuracy.

CHAPTER 5

TERRESTRIAL HEAT FLOW IN THE NORTH ISLAND

5.1 INTRODUCTION

The heat flow results from this study are presented in two groups: (i) North Island (chapter 5); and (ii) South Island (chapter 6). The majority of sites are located in eight major sedimentary basins (fig. 5.1) which have been explored in detail by petroleum companies. The North Island contains four of these basins: Northland, Waikato, Taranaki-Wanganui, and East Coast. All heat flow results for the North Island, along with pertinent details, are summarized in Table 5.1, and the regional distributions of geothermal gradient and heat flow are shown in figs. 5.2 and 5.3 respectively.* Temperature profiles and lithologs for specimen boreholes are shown in figs. 5.4-5.11, 5.13-5.24 and 5.27-5.28 to which reference is included in the table. Basic temperature data for all the locations are included in Appendix I. Additional details and comments are given for some boreholes in sections 5.2 to 5.8.

5.2 NORTHERN PART OF THE NORTH ISLAND

5.2.1 Northland-Auckland region

Much of this region is occupied by the Northland Basin, which extends over the Auckland Peninsula from south of the Manukau Harbour to North Cape. Permian-Jurassic basement is overlain by marine Upper Cretaceous and Tertiary rocks. The southern portion of the basin extends for about 120km north-south and contains 600-900 m of Lower Miocene Waitemata beds, probably lying directly over the basement. In the central and northern portions the Waitemata beds lie either directly on the basement (greywacke and argillites) or on Lower Tertiaries which rest on basement.

Northland -1

This borehole penetrated mainly shale with a small amount of sandstone and mudstone, before reaching volcanic basement composed of basalt at 578.2 m.

Bridgeman's -2 (Waiwera)

In the small coastal town of Waiwera, several bores drilled for private and commercial use yield thermal ground water whose origin is unknown. A volcanic origin is precluded by chemical and other evidence; the source depth is suggested to be less than 2200 m (Auckland Regional Water Board Report, 1980). The main rock formations

* See Appendix 3, p.175a.

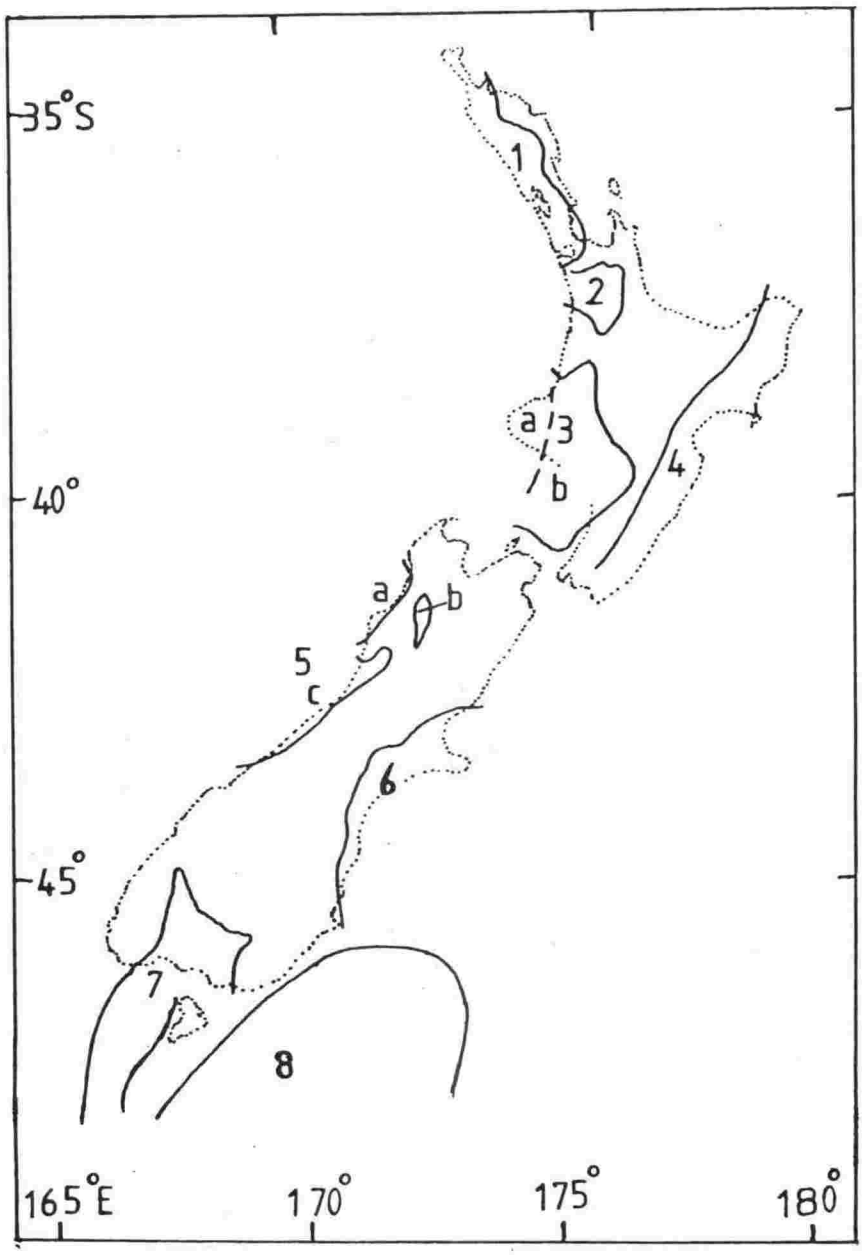

Fig. 5.1 Sedimentary basins of New Zealand: (1) Northland, (2) Waikato, (3a) Taranaki, (3b) Wanganui, (4) East Coast, (5a) Westport-Karamea, (5b) Murchison, 5(c) Greymouth, (6) Canterbury, (7) Southland-Solander, (8) The Great South.

Table 5.1 Heat flow data: North Island

Name of borehole	Location Lat. (S)	Location Long. (E)	Elevation (m)	Depth range (m)	N	Mean thermal conductivity (W/m°C)	Geothermal gradient (°C/km)	Heat flow (mW/m²)	Type of temperature data	Fig.
Northland-Auckland Region										
Northland -1	35°06'	173°27'	85.5	0-620	6	2.11	46.76	98.7	BHT+	-
Waimamaku -2	35°34'	173°28'	152.7	1402.6-3347.3	17	2.54	35.75	90.8±6.9	BHT*	5.4
Bridgeman's -2 (Waiwera)	36°33'	174°43'	2.5	-	2	3.09±.04	disturbed	disturbed	Probe	5.4
L. Harvey's (Orewa)	36°35'	174°41'	3.0	220-420	13	2.21 .16	29.26±.30	64.7±4.7	Probe+	5.5
Kumeu	36°47'	174°33'	-	45.3-90.0	-	2.31	36.66±.74	84.7	Probe+	5.6
Penrose (Auckland)	36°56'	174°50'	-	80-140	-	2.40	25.39±.78	60.9	Probe+	5.6
Pukekohe	37°13'	174°52'	-	115-195	6	1.72±.07	32.52±.66 32.52±.66T	55.9±2.5 55.9±2.5T	Probe+	5.7
Waikato Basin										
Huntly 6534	37° 32	175°10'	-	115-225		2.43	37.65	91.5±1.7	CL*	5.8
Huntly 8123	37°29'	175°09'	10	130-335		2.51	39.76	99.8±1.3	CL*	5.8
Huntly 8178	37°25'	175°09'	11.7	-	25	2.77	disturbed	disturbed	CL	5.9
Huntly 9022	37°16'	175°11'	60.9	60-155		2.29	27.73	63.5±1.3	CL*	5.9
Huntly 8333	37°24'	175°08'	23.9	180-700		2.87	28.23±2.06	81.0	Probe+	5.10
Huntly 9674	37°30'	175°11'	-	70-89		2.28	37.75±1.95	86.1	Probe+	5.10
Waikato -1	37°42'	175°15'	43	0-1032.1	-	2.36	26.60	62.8	BHT+	-
Waikato -2	37°47'	175°13'	61	0-1018		2.55	26.00	66.3	BHT+	-
Waikato -4	37°42'	175°19'	31.7	0-594.4	-	2.36	33.83	79.8	BHT+	-
Waikato -5	37°41'	175°13'	26.5	0-1012.2	-	2.36	48.09	113.5	BHT+	-
Te Rapa -1	37°45'	175°11'	33.5	0-1566.1	5	2.21±.14	30.32	67.0±4.2	BHT+	-
Coromandel Region										
DD2 (Whitianga)	36°50'	175°42'	-	85.3-195.1	4	1.72±.13	62.4±1.86 62.4±1.86T	107.3±8.7 107.3±8.7T	Probe+	5.11
Western Platform										
MoA -1B	38°30'	173°21	-158.2	1964.4-3375.7	10	2.69±.17	29.85±1.93	80.3±7.3	BHT+	-
Tane -1	38°56'	172°38'	-153.9	0-4354.1	10	2.93±.39	29.1±.41	85.3±11.4	BHT+	5.13
Maui -1	38°40'	173°19'	-110.6	827.5-3380.5	5	3.24	24.04	77.9±6.9	BHT*	5.13
Maui -2	39°37'	173°27'	-109.4	950.40-3424.1	8	3.42	25.94	88.7±8.4	BHT*	-
Maui -3	39°32'	173°27'	-109.4	1697.4-3253.1	6	3.22	24.19	77.9±7.5	BHT*	-
Cook -1	40°27'	172°17'	-124.4	969.6-2534.4	7	3.85±.42	35.49±1.97	136.6±16.7	BHT+	5.14
Taranaki Graben										
Turi -1	38°30'	174°26'	-57	1140.3-4004.5	9	3.15	31.97	100.7±7.1	BHT*	5.14
Urenui -1	39°01'	174°21'	64.6	913.5-3803.9	16	3.25±.40	26.78±1.65	87.0±12.00	BHT+	5.15
Republic New Plymouth -1	39°04'	174°02'	4.0	0-962.4	-	2.53	30.86±4.08	78.1	BHT+	-
Republic New Plymouth -2	39°04'	174°02'	4.3	0-911	-	2.30	41.37	95.20	BHT+	-
Republic New Plymouth -3	39°04'	174°02'	4.3	0-745.8	-	2.28	36.50	83.2	BHT+	-
Republic New Plymouth -4	39°04'	174°02'	3.2	0-947.2	1	2.28	34.3±2.18	78.2	BHT+	-
Mangahewa -1	39°04'	174°19'	172.5	1584.4-4086.8	8	3.36±.56	29.66±1.19	99.7±17.1	BHT+	5.15
New Plymouth-2	39°05'	174°03'	41.6	239.4-4420.7	14	2.88	31.32	90.2±5.6	BHT*	5.16
McKee -1	39°06'	174°20'	91	1831-3897.4	-	3.17	25.33	80.3±5.2	BHT*	5.16
Inglewood -1	39°13'	174°12'	310.3	2514-5051.1	8	2.93	36.28	106.3±4.0	BHT*	5.17

Table 5.1 Heat flow data: North Island (Continued)

Name of borehold	Location Lat. (S)	Location Long. (E)	Elevation (m)	Depth range (m)	N	Mean thermal conductivity (W/m°C)	Geothermal gradient (°C/km)	Heat flow (mW/m²)	Type of temperature data	Fig.
Toko -1	39°19'	174°22'	200	1666-4882	9	2.96	26.86	79.5±4.2	BHT*	5.17
Kapuni -1	39°29'	174°11'	186.5	1339.6-3967.9	8	3.12	30.87	96.3±5.6	BHT*	5.18
Kapuni -2	39°30'	174°10'	152.1	1639.2-4112.1	7	3.07	27.75	85.2±11.9	BHT*	-
Kapuni -3	39°31'	174°11'	131.7	1708.1-3682.9	10	3.06	29.71	90.9±4.6	BHT*	-
Kapuni -3A	39°31'	174°10'	131.6	2332.9-3649.4	-	3.03	34.22	103.7±1.8	BHT*	-
Kapuni -4	39°27'	174°10'	229.8	1671.5-3895.3	6	3.08	33.12	102±21.9	BHT*	-
Kapuni -5	39°30'	174°11'	167.8	761.5-3698.8	-	3.11	22.70	70.6±10.5	BHT*	-
Kapuni -6	39°30'	174°11'	152	754-3723.7	-	3.09	21.46	66.3±.3	BHT*	-
Kapuni -7	39°29'	174°11'	187.3	0-3728.9	-	3.01	24.85	74.8±.6	BHT*	-
Kapuni -8	39°26'	174°11'	265.1	2437.7-4071.7	1	3.07	29.35 29.35T	90.1±3.3 90.1±3.3T	BHT*	-
Kapuni -9	39°29'	174°12'	177.3	912.4-3741.7	-	3.12	23.85	74.4±6.0	BHT*	-
Kapuni -10	39°29'	174°11'	169	2354.5-3689.9	-	3.01	34.98	105.3±1.7	BHT*	-
Kapuni -11	39°30'	174°11'	151.7	0-3688.1	-	2.98	24.36	72.6±.8	BHT*	-
Maui -4	40°02'	173°14'	-103.6	1253-3784.7	8	2.38	22.18	52.8±4.5	BHT*	5.18
Kupe -1	39°50'	174°08'	-29.3	925.9-3641.9	-	3.02	15.93	48.1±10.4	BHT*	5.19
North Tasman -1	40°12'	173°16'	-86	448.2-2613.5	5	2.65±.55	2649±1.62	70.2±15.2	BHT+	-
Tasman -1	40°19'	173°24'	-74.4	0-1520.6	6	2.19	34.75	76.1	BHT*	-
Fresne -1	40°21'	173°05'	-73	1183.2-2413	7	2.58±.10	25.61±2.90	66.1±7.9	BHT+	-
Surville -1	40°43'	173°27'	-50.5	949-2140	7	3.39±.36	16.02	54.3±5.8	BHT+	-
Patea-Tongaporutu High										
Kiore -1	39°14'	174°34'	182.9	0-532.8	6	1.89±.13	59.4	112.3±7.7	BHT+	-
Patea	39°45'	174°29'	-	60-90	-	-	51.40±3.27	-	Probe	5.19
North Wanganui Basin										
Waikaka -1	38°43'	175°03'	173.7	0-975.1	-	2.36	39.93	94.2	BHT+	-
Ararimu -1	38°51'	175°08'	305.4	0-1054.0	6	2.38±.1	31.56	75.1	BHT+	-
Whakamaro -1	38°54'	175°10'	≈166.7	0-912.3	-	2.46	38.29	94.2	BHT+	-
Tatu -1	38°55'	174°55'	359.7	0-854	11	2.53±.24	45.87	116.1±11.0	BHT+	-
Koporongo -1	39°06'	175°19'	277.6	0-586.7	-	2.82	33.42	94.2	BHT+	-
Tupapakurua -1	39°11'	175°17'	314.9	0-1146	4	2.89±.29	27.97	80.8±8.1	BHT+	-
Puniwhakau -1	39°19'	174°43'	220.4	903.4-2135.1	11	3.33	25.20	83.9±4.5	BHT*	5.20
South Wanganui Basin										
Parikino -1	39°48'	175°09'	24.1	1222.9-2311	10	2.79	28.79±.89 35.50S	80.3 99.0S	BHT+	5.20
Santoff -1A	40°12'	175°13'	7.6	1628.1-2627.5	5	2.90	12.37±.81 16.94S	35.9 49.1S	BHT+	-
East Coast Basin										
Te Horo -1	37°48'	178°28'	≈ 2.7	0-1800.8	-	2.25	25.11	56.5	BHT+	-
Rotokautuku -1	37°53'	178°19'	59.7	350.3-619.4	6	2.48±.11	55.56 55.56T	137.8±6.1 137.8±6.1T	BHT+	-
Te Puia -1	38°02'	178°16'	209.6	0-2035	9	1.92±.23	32.41±2.63	62.2±9.0	BHT+	-
Waitangi Station -1	38°22'	177°54'	273.7	1051-2128.1	6	2.46±.17	20.41	50.2±3.5	BHT+	-
Ruakituri -1	38°48'	177°29'	101.8	887.3-2740.8	13	2.67±.15	15.53±1.50	41.5±4.6	BHT+	5.21
Mangaone -1	38°58'	177°45'	≈259.4	339.5-1264	9	3.04±.30	34.66±3.58	105.4±15.1	BHT+	5.21

Table 5.1 Heat flow data: North Island (Continued)

Name of borehole	Location Lat. (S)	Long. (E)	Elevation (m)	Depth range (m)	N	Mean thermal conductivity ($W/m^{\circ}C$)	Geothermal gradient ($^{\circ}C/km$)	Heat flow (mW/m^2)	Type of temperature data	Fig
Opoutama -1	39°04'	177°49'	18.3	1722.3-2743	14	3.56±.28	16.77	59.7±4.7	BHT+	5.22
Hawke Bay -1	39°17'	177°20'	-57	1294.3-1762.1		3.04	17.19	52.3	BHT+	-
Taradale -1	39°33'	176°49'	15.8	526.4-1652	-	-	disturbed	disturbed	BHT	-
Mason Ridge -1	39°40'	176°36'	236.2	310-1877	10	1.88±.17	15.64±.49 19.60S	29.4±2.7 36.8S	BHT+	5.22
Ongaonga -1	39°54'	176°25'	203	403.3-1567	11	2.01±.21	14.93±.35 17.73S	30±3.2 35.6S	BHT+	5.23
Takapau -1	39°59'	176°19'	262.7	198.1-1053.4	8	1.82	17.80±.98 19.99S	32.4 36.4S	BHT+	5.23
Rangipo										
R-240	39°09'	175°50'	-	55-89	5	3.69±.20	30.74±1.28 23.75T	113.4±7.7 87.6T	Probe+	5.24
Central Volcanic Region										
Tokaanu F-5A	38°59'	175°45'	-	39.6-150	4	1.94±.18	189.66±2.48 189.66±2.48T	367.9±34.5 367.9±34.5T	Probe+	5.27
Tokaanu F-5C	38°60'	175°45'	-	170.7-201.2	-	1.95±.11	213.29±24.95	415.9±54.0	Probe+	-
Tokaanu F-10	38°60'	175°45'	-	225.6-260.6	3	1.95±.14	212.43±4.22	414.2±30.9	Probe+	-
Petone-Lower Hutt										
UW -1	41°14'	174°52'	14.0	110-140	5	1.99±.18	20.79±.32 23.20S	41.4±3.8 46.2S	Probe+	5.28
UW -3	41°14'	174°54'	13.1	115-175		1.99±.18	21.58±.24 23.03T,S	42.9±3.9 45.8T,S	Probe+	5.28

± Refers to standard error

N Total number of samples

+ G-K method

* Resistance integral method

BHT Bottom hole temperature

Probe Conventional temperature probe

CL Continuous temperature log

T Corrected for topographic effects

S Corrected for sedimentation effects.

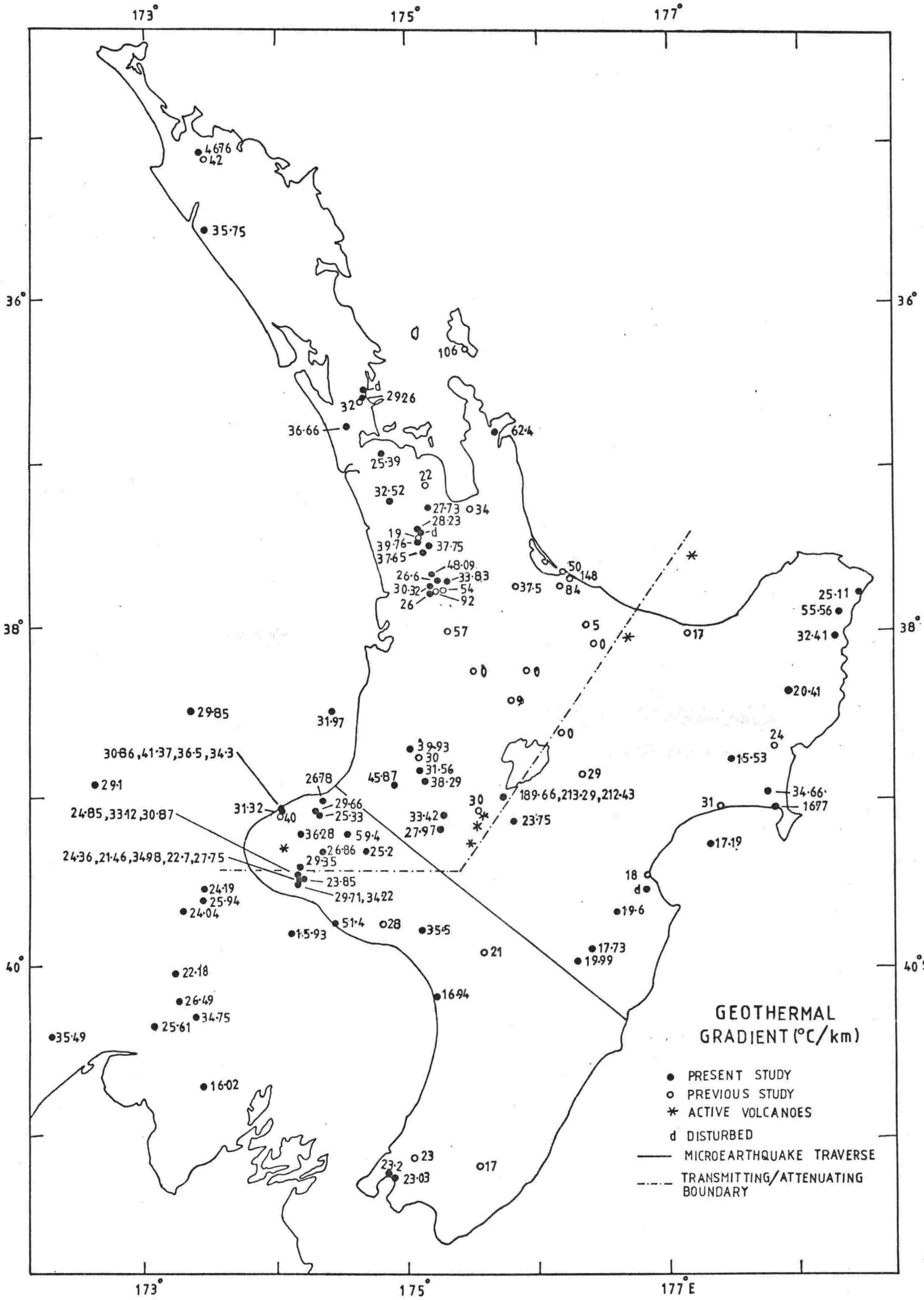

Fig. 5.2 Geothermal gradients: North Island. Data from previous studies are taken from Studt and Thompson (1969), Thompson (1977), Hegan (1978) and Dr R. Allis, pers. comm.

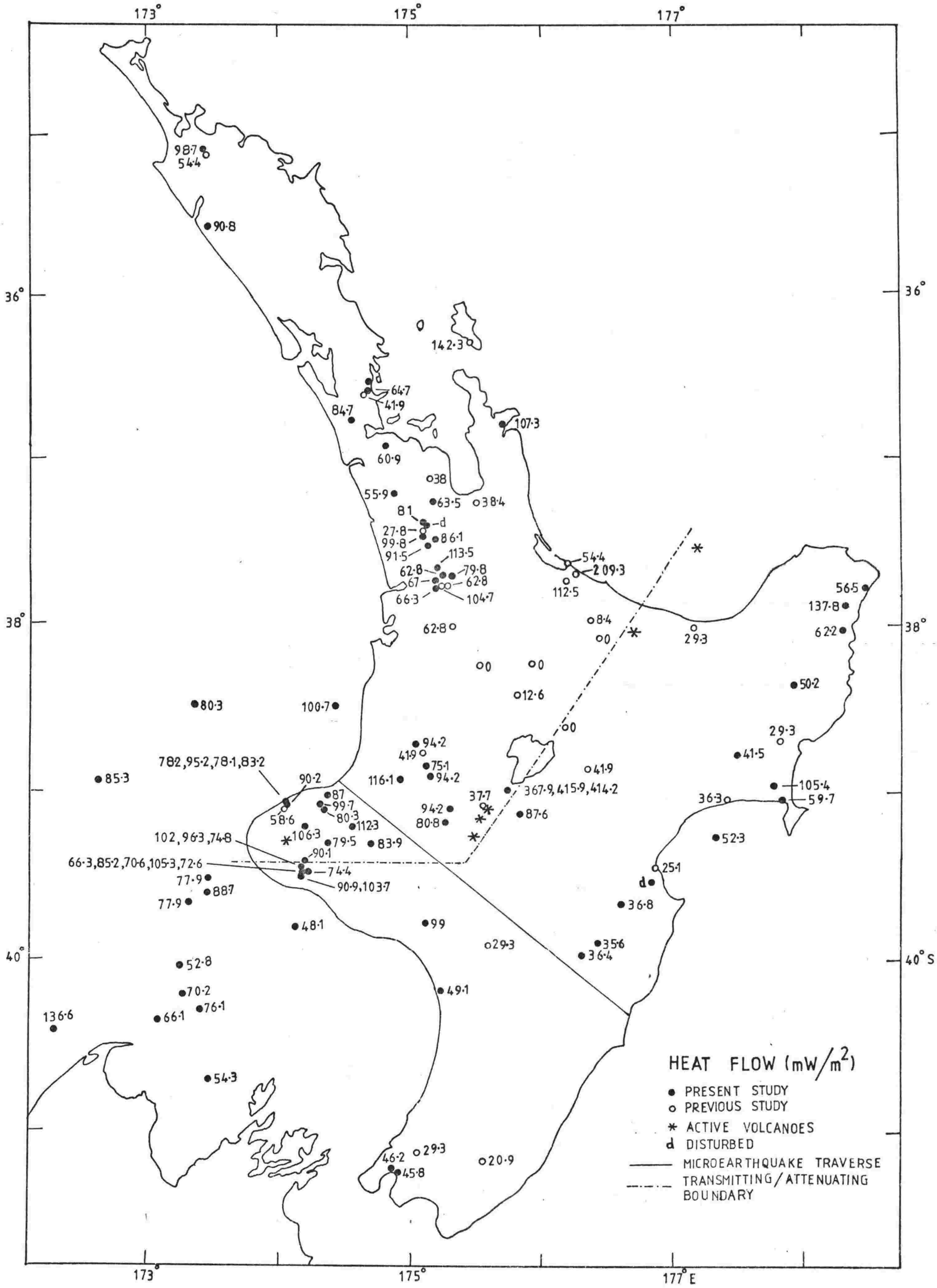

Fig. 5.3 Terrestrial heat flow: North Island. Data from previous studies are taken from Studt and Thompson (1969), Thompson (1977) and Dr R. Allis, pers. comm.

at Waiwera are the Waitemata sandstone and siltstone, which rest on greywacke basement. Waitemata rocks are folded and fractured and form an aquifer for the thermal waters. The temperature was measured in a borehole which has been standing unused for several months. The temperature profile and litholog as shown in fig. 5.4 are similar to those in nearby wells (Simpson, 1980).

The temperature profile obtained in this hole is a classical example of the effect of a faulted aquifer, by which ground water flows up to a much shallower level, giving, above that level, a geothermal gradient which is much steeper than normal for the region. It will be noted that the observed temperature gradient near the surface is about seven times greater than in two holes at Orewa (fig. 5.5; Studt and Thompson, 1969), situated ≃ 7km away. This appears to support the evidence mentioned above, that the source depth for the water in the aquifer is rather less than 2200 m.

L. Harvey's (Orewa)

This borehole was drilled to a depth of 875.5 m and penetrated the Waitemata group, comprising predominantly interbedded Miocene sandstone and siltstone, resting on the Mesozoic greywacke basement at 860 m. We measured the temperature (fig. 5.5), about 16 months after drilling, to a depth of 420 m, below which the hole seems to have collapsed.

Kumeu

Temperature measurements were carried out about 11 months after drilling. The profile and litholog are shown in fig. 5.6. No samples were available. We therefore estimated the thermal conductivity from the Orewa borehole, which penetrated similar rocks, and from two representative samples of Waitemata sandstone and siltstone kindly supplied by Dr B. Waterhouse, N.Z. Geological Survey, Otara, Auckland.

Penrose (Auckland)

This 426 m deep borehole is in Auckland city. The temperature profile was measured after the lapse of a few years to a depth of 140 m, below which the hole seems to have collapsed. The temperatures and litholog are shown in fig. 5.6. Since no samples were available the thermal conductivity was estimated in a similar manner to that of Kumeu, as the rocks penetrated were also Waitemata sandstone and siltstone.

Pukekohe

This borehole was drilled on the Pukekohe plateau. Temperatures were measured after about 5 months, and are shown in fig. 5.7. The temperatures were disturbed down to about 105 m, the top 60-65 m being in air. A topographic correction was calculated for this location but was found

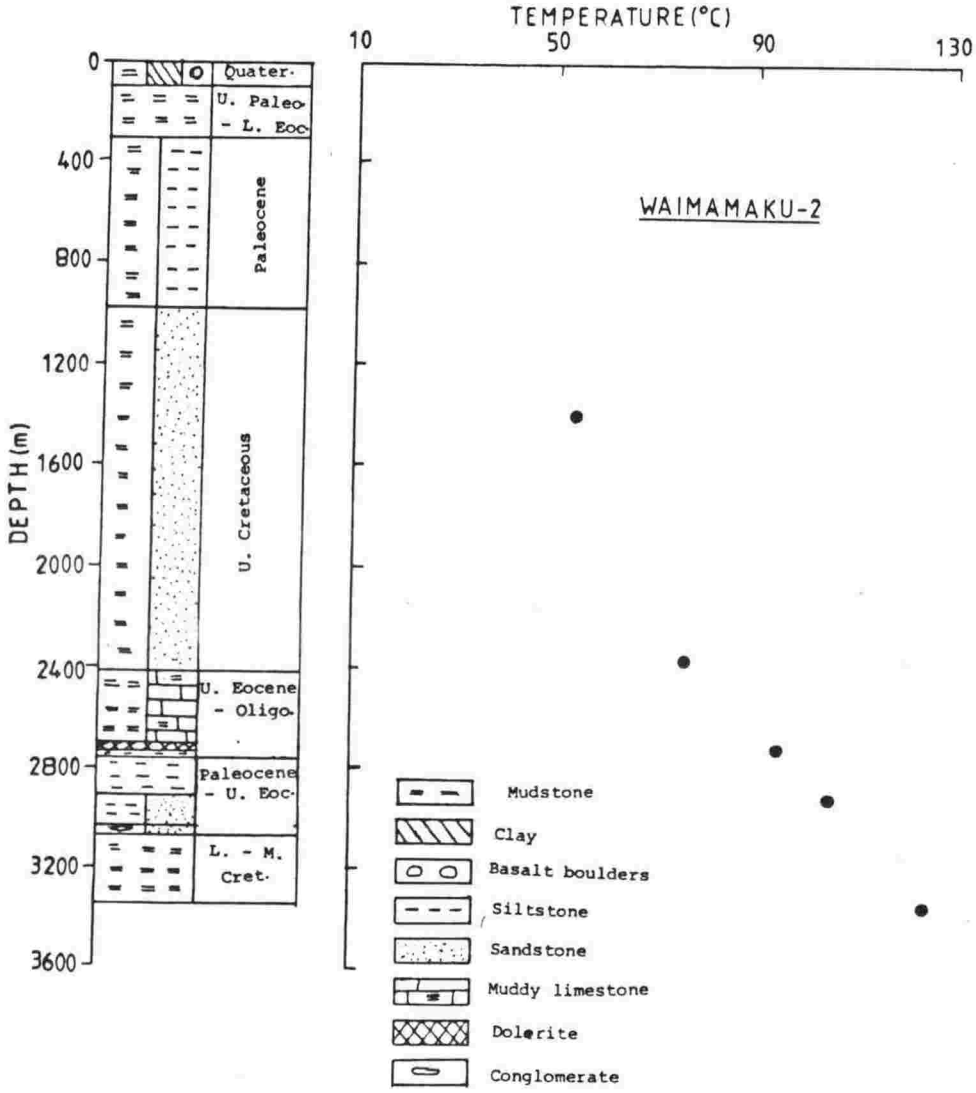
TEMPERATURE (°C)
10
50
90
130
WAIMAMAKU-2
DEPTH (m)
0
400
800
1200
1600
2000
2400
2800
3200
3600
Quater.
U. Paleo - L. Eoc.
Paleocene
U. Cretaceous
U. Eocene - Oligo.
Paleocene - U. Eoc.
L. - M. Cret.
Mudstone
Clay
Basalt boulders
Siltstone
Sandstone
Muddy limestone
Dolerite
Conglomerate

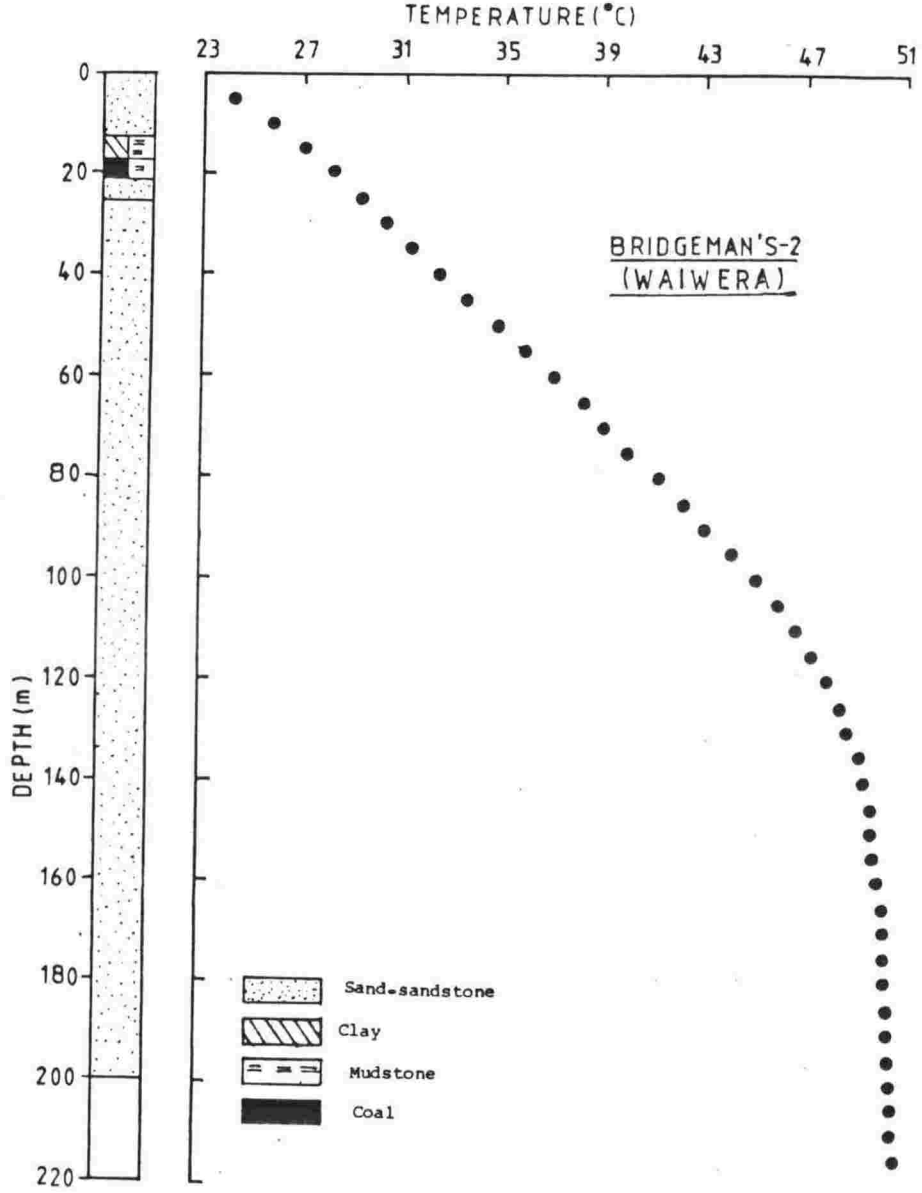
TEMPERATURE (°C)
23
27
31
35
39
43
47
51
BRIDGEMAN'S-2
(WAIWERA)
DEPTH (m)
0
20
40
60
80
100
120
140
160
180
200
220
Sand-sandstone
Clay
Mudstone
Coal

Fig. 5.4

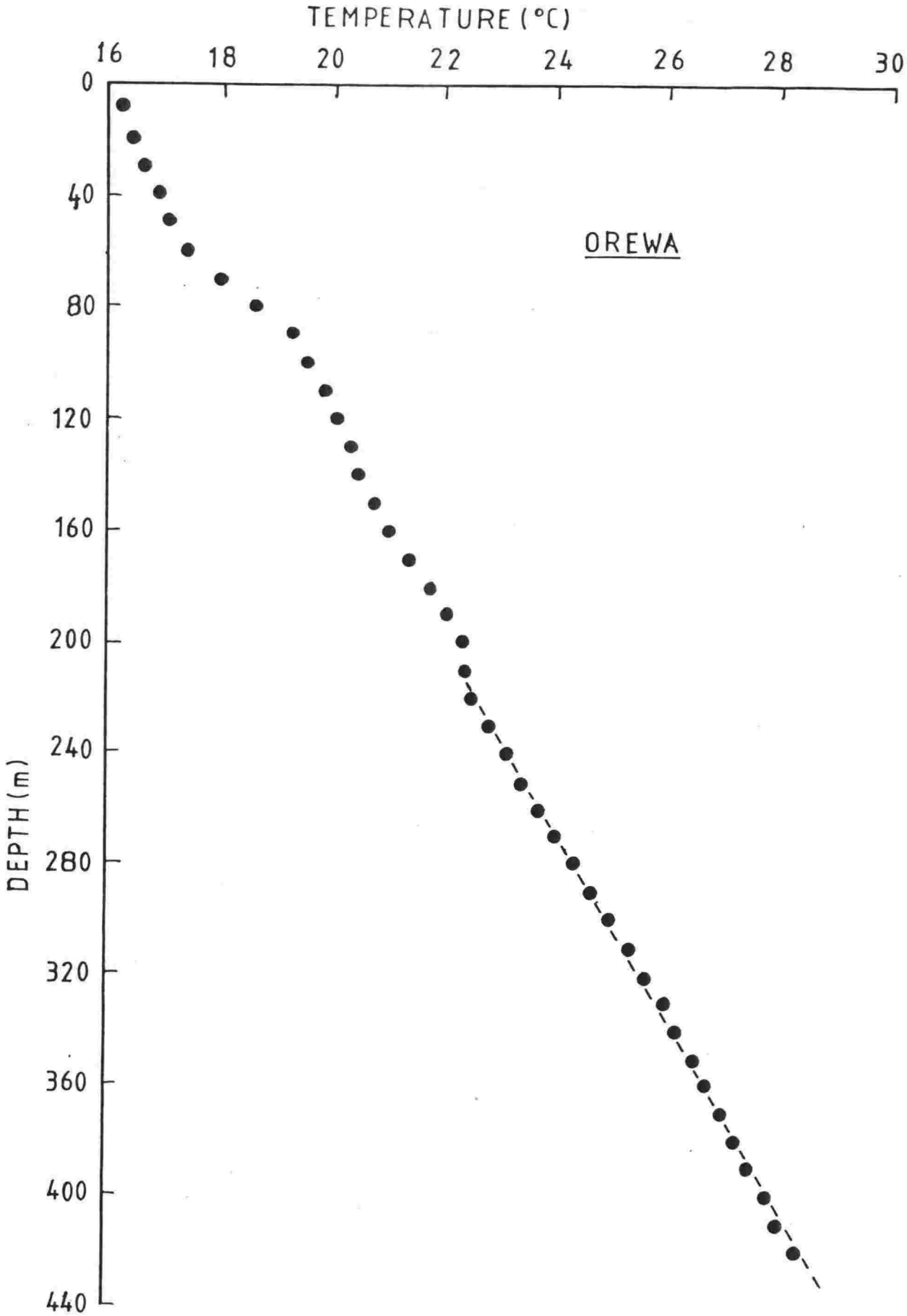
TEMPERATURE (°C)
16
18
20
22
24
26
28
30
0
40
80
120
160
200
240
280
320
360
400
440
DEPTH (m)
OREWA

Fig. 5.5

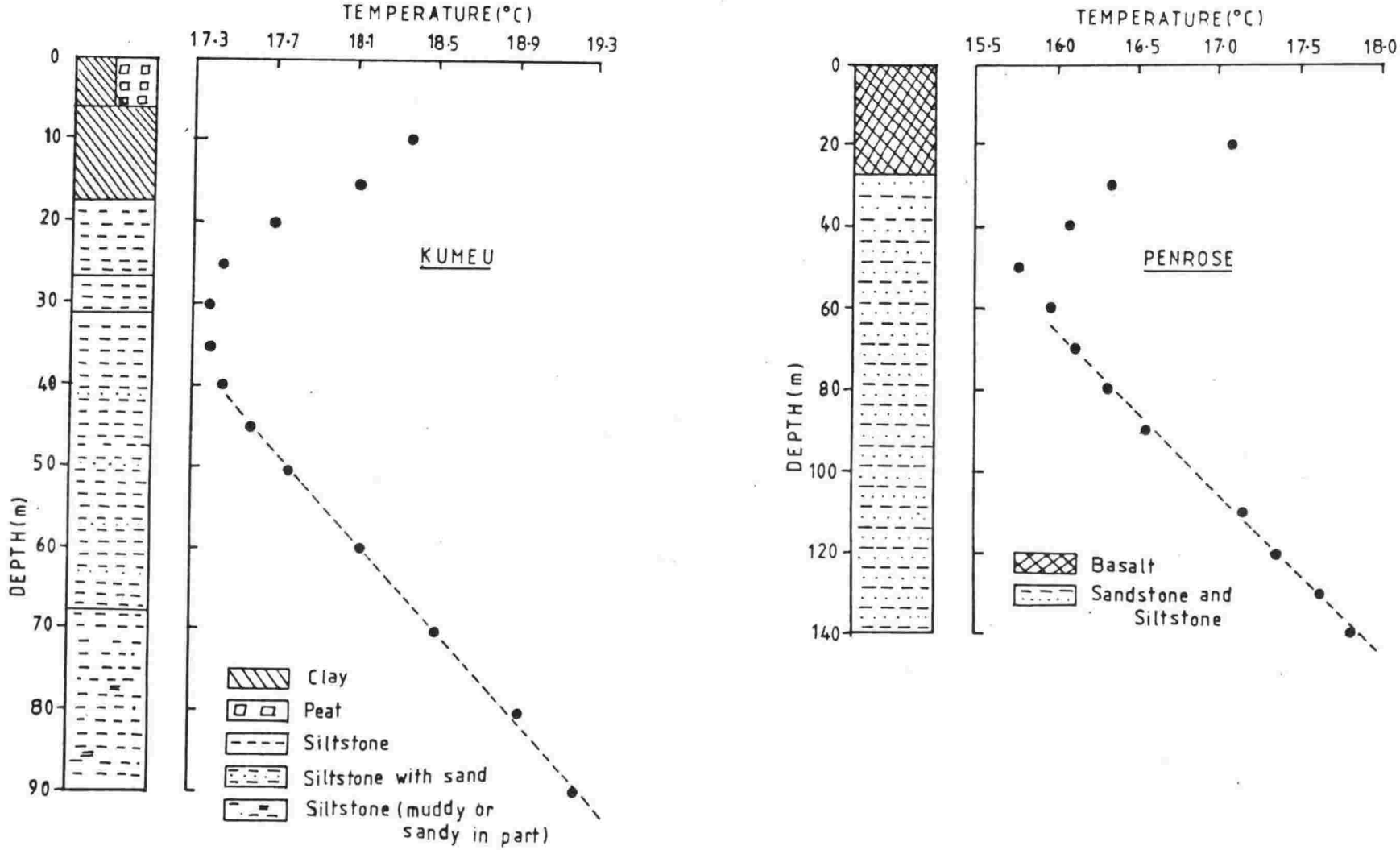
TEMPERATURE(°C)
17·3
17·7
18·1
18·5
18·9
19·3
DEPTH(m)
0
10
20
30
40
50
60
70
80
90
KUMEU
Clay
Peat
Siltstone
Siltstone with sand
Siltstone (muddy or sandy in part)
TEMPERATURE(°C)
15·5
16·0
16·5
17·0
17·5
18·0
DEPTH(m)
0
20
40
60
80
100
120
140
PENROSE
Basalt
Sandstone and Siltstone

Fig. 5.6

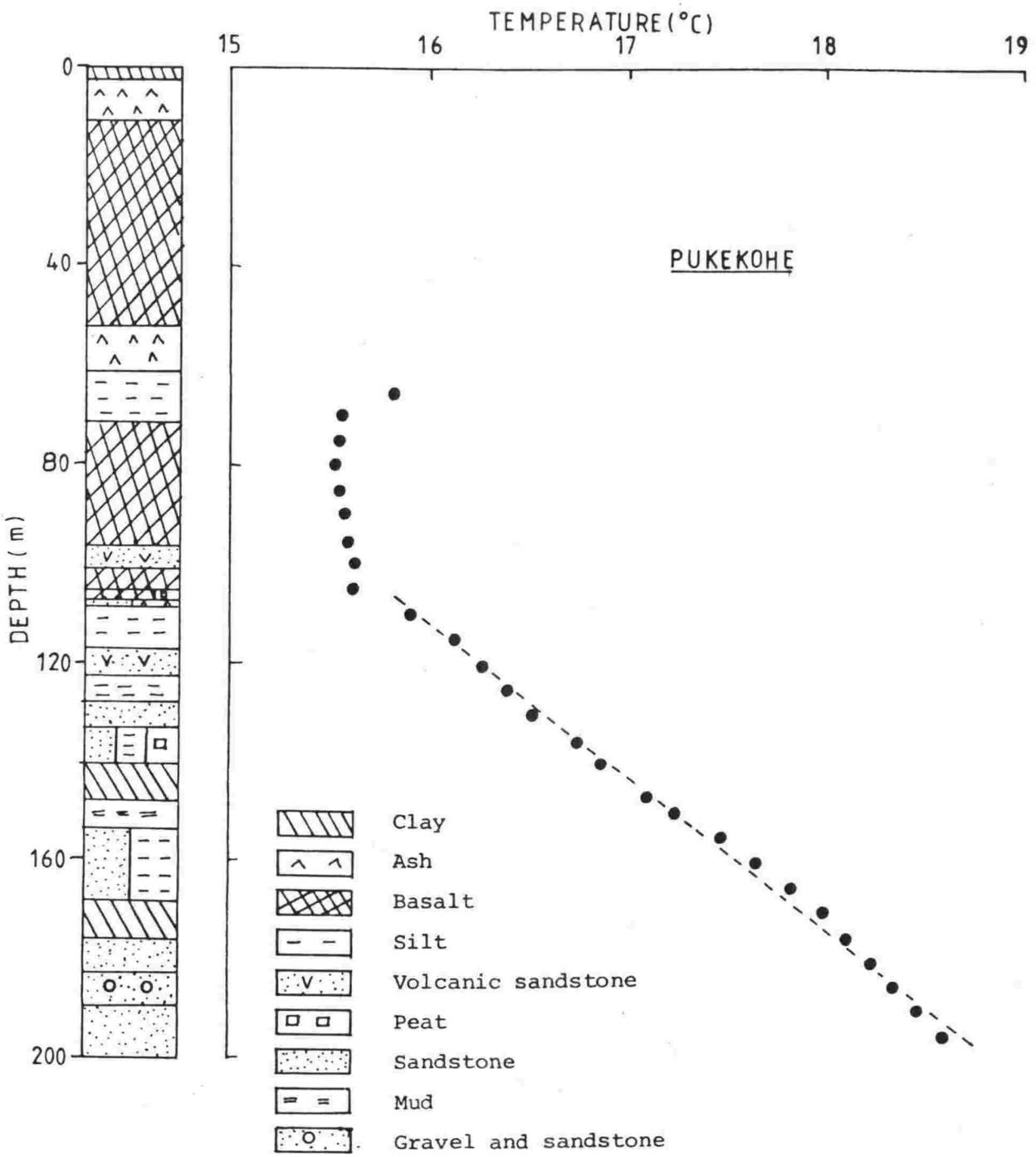
TEMPERATURE (°C)
15
16
17
18
19
0
40
80
120
160
200
DEPTH (m)
PUKEKOHE
Clay
Ash
Basalt
Silt
Volcanic sandstone
Peat
Sandstone
Mud
Gravel and sandstone

Fig. 5.7

to be less than 0.5%, and was therefore neglected.

5.2.2 Waikato Basin

This basin extends through the lower Waikato River - Huntly area; it includes the Hamilton and Hauraki basins, and covers an area of about 9000 sq.km. Basement of mainly folded greywacke is overlain by coal measures, mudstone, sandstone, siltstone and limestone of Upper Eocene to Lower Miocene age, reaching a thickness of over 1500 m. These are overlain by a further Pliocene - Quaternary sequence which is composed of clay, lignite, peat, gravel and sand, and reaches a thickness of about 300 m. A large number of boreholes have been drilled around Huntly in connection with coal, which occurs in the Upper Eocene Waikato coal measures of the Te Kuiti group. Heat flow was determined for 11 locations in the Waikato basin, 6 of these being in the coalfield. Thermal conductivity samples were available only for three coal boreholes and one petroleum hole (Te Rapa -1). It appears that rock formations of this field are fairly uniform in nature from borehole to borehole (N. Fowke, pers. comm.). Therefore in the heat flow calculations the mean conductivity values of the rocks (Table 5.2) have been used, except for the Te Rapa -1 borehole.

Huntly 6534, 8123, 8178, 9022

In these boreholes, temperatures have been used which were recorded continuously with depth about two days after drilling had ceased. The temperature profiles are shown in figs. 5.8 and 5.9 where values taken at 5 m intervals from the continuous records are included along with the litholog of the borehole. Lithologic changes are clearly reflected in these profiles. The upper parts of the profile seem to be disturbed in some holes, while measurements are clearly disturbed below 120 m in borehole 8178, presumably due to ground water circulation; as a result, no heat flow has been evaluated for this location. Heat flow for the other three locations ranges from 63.5 to 99.8 m W/m^2.

Huntly 8333

The temperature-depth profile and the litholog of the borehole is shown in fig. 5.10. In this case the borehole standing time was less than a day.

Huntly 9674

This borehole was drilled to a depth of 135 m but the temperature could be measured only down to 89 m (fig. 5.10), about 55 hours after the completion of drilling. The hole penetrated 74.4 m of peat, sand

Table 5.2 Mean thermal conductivity: Huntly boreholes

Rock Type	Total number of samples	Conductivity ($W/m^{o}C$) Range	Mean
Sandstone	8	1.86-5.75	3.47
Siltstone	6	1.77-3.70	2.67
Mudstone	4	1.55-3.02	2.35
Claystone	4	2.06-2.92	2.49
Greywacke	1	-	3.09
Coal	2	.31-.47	.39

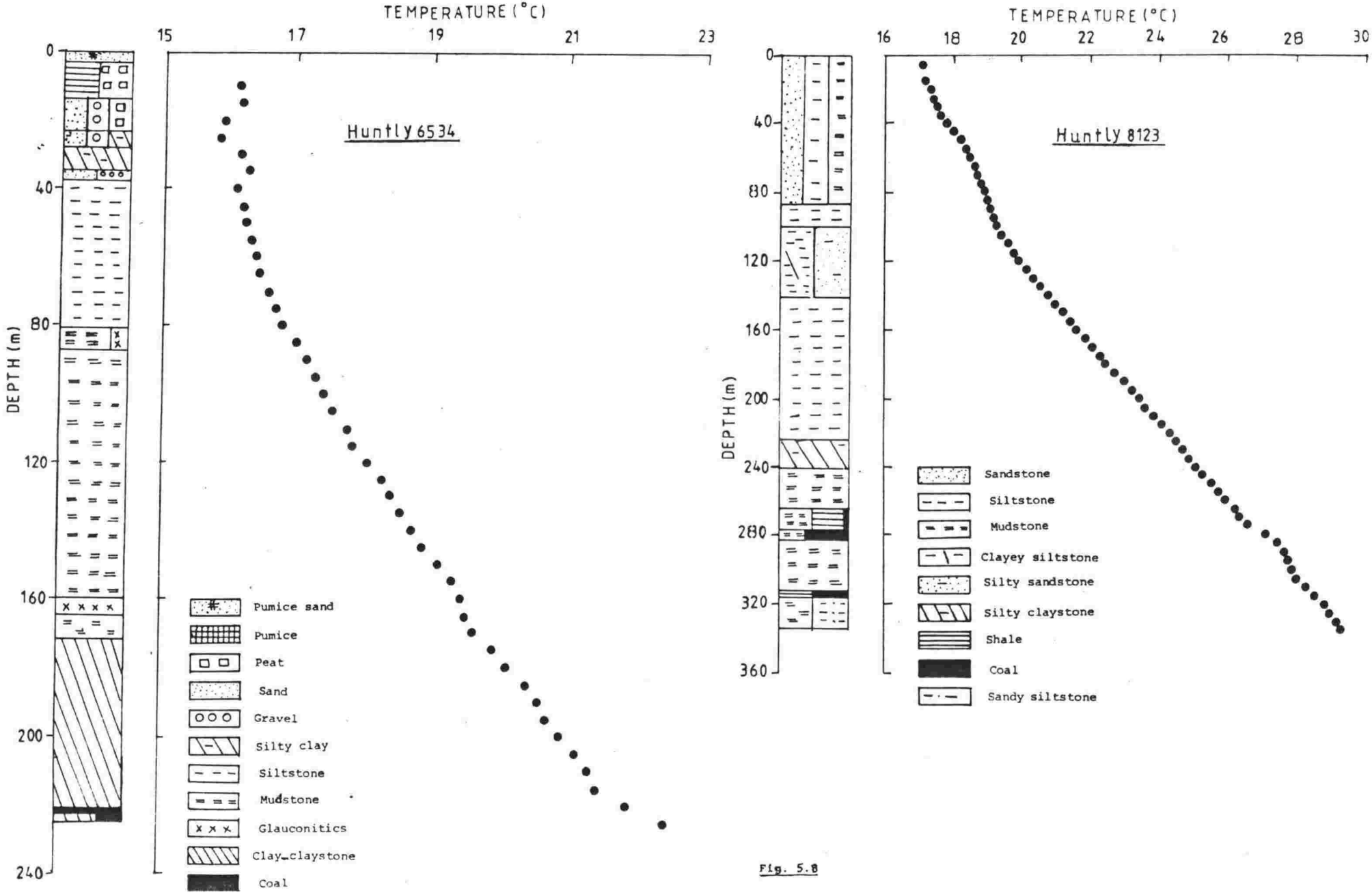
TEMPERATURE (°C)
15
17
19
21
23
0
40
80
120
160
200
240
DEPTH (m)
Huntly 6534
Pumice sand
Pumice
Peat
Sand
Gravel
Silty clay
Siltstone
Mudstone
Glauconitics
Clay_claystone
Coal
TEMPERATURE (°C)
16
18
20
22
24
26
28
30
0
40
80
120
160
200
240
280
320
360
DEPTH (m)
Huntly 8123
Sandstone
Siltstone
Mudstone
Clayey siltstone
Silty sandstone
Silty claystone
Shale
Coal
Sandy siltstone

Fig. 5.8

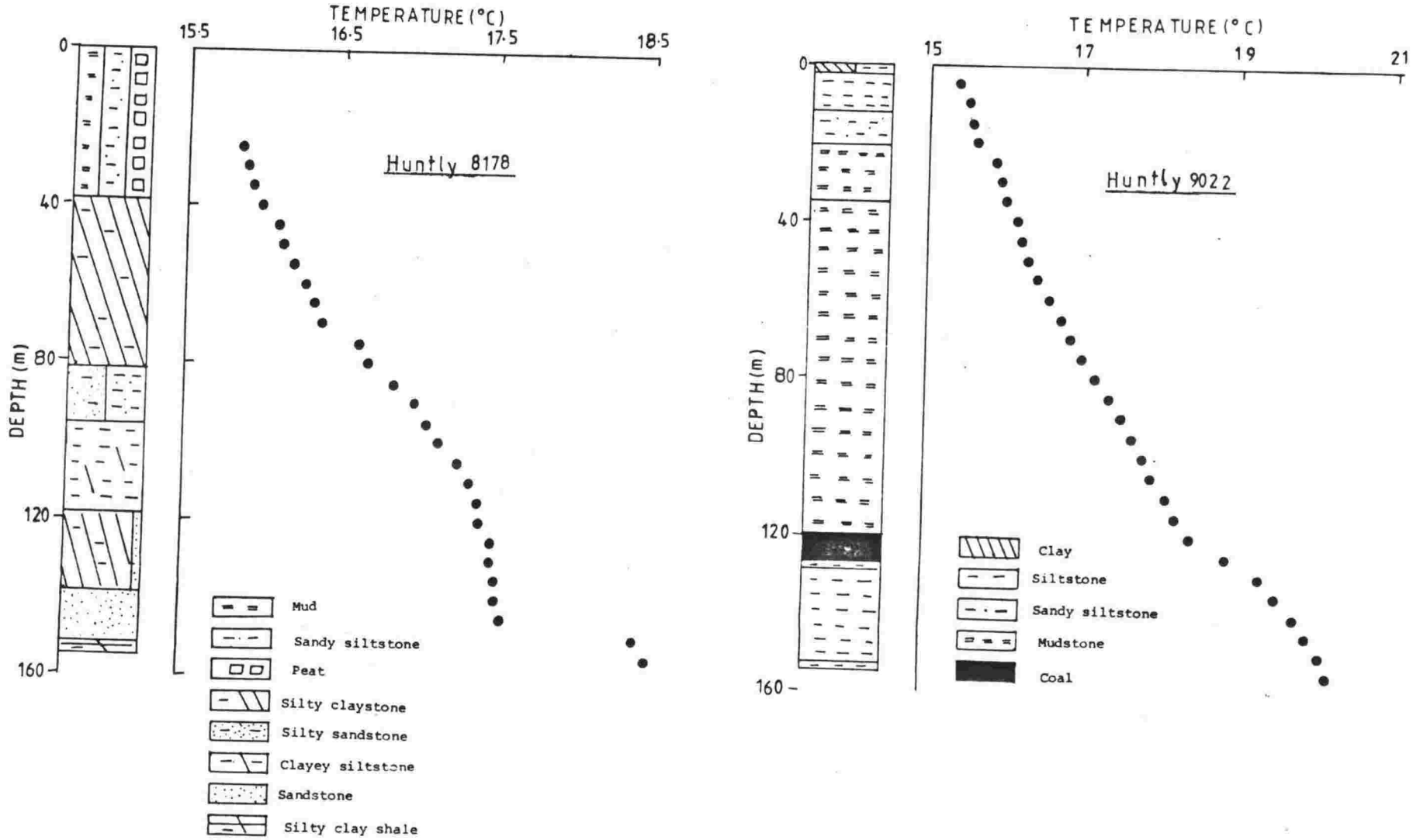

Fig. 5.9 (Data source: M.C. Syms)

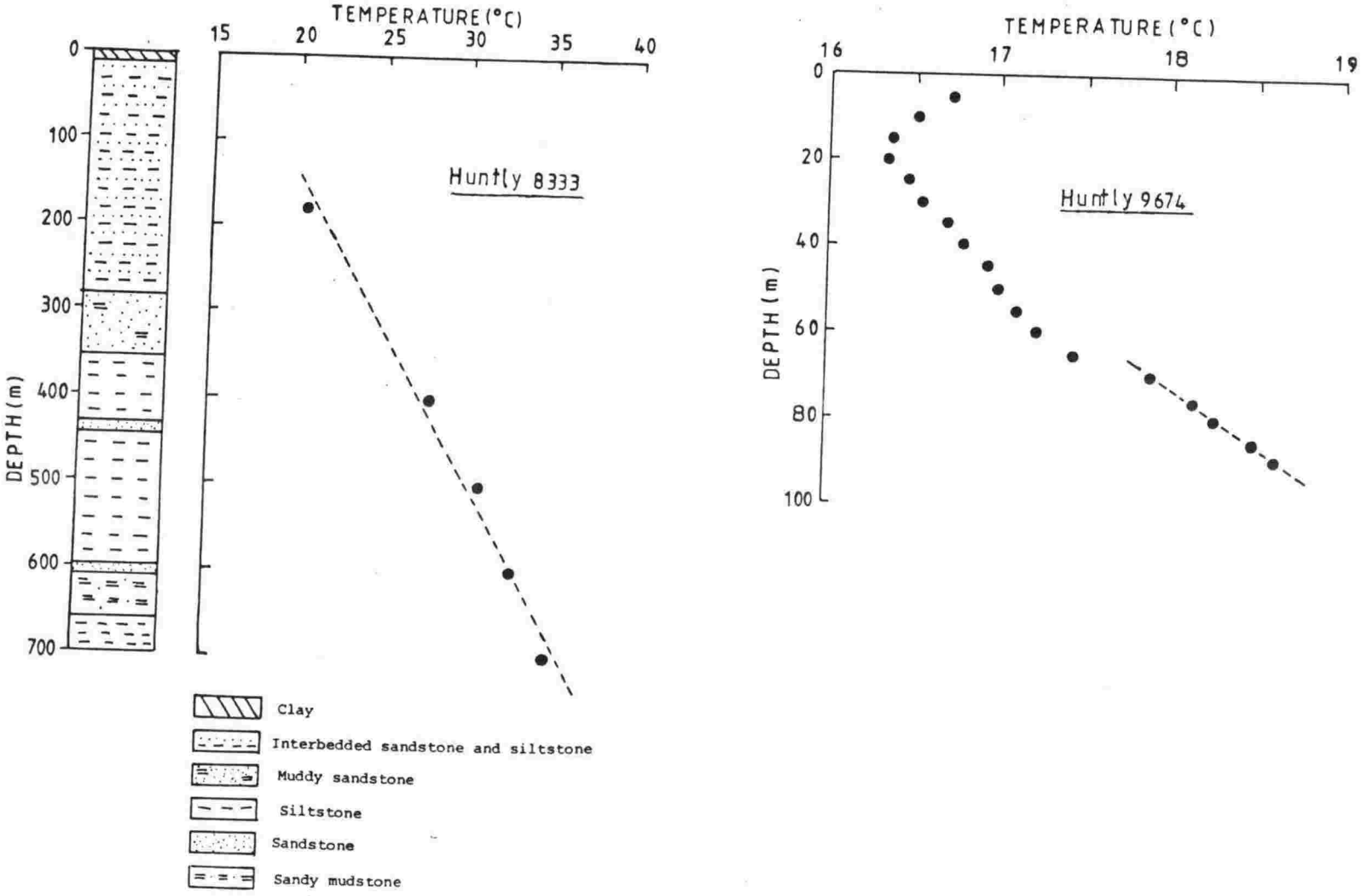

Fig. 5.10 (Data source for Huntly 8333: J. Gumbley)

and clay, followed by mudstone and coal between 74.4 and 89 m.

Waikato -1,2,4,5

These boreholes were drilled to a maximum depth of 1032.1 m, and penetrated mainly sandstone, pumice, siltstone, mudstone and shale with small amounts of lignite, clay and volcanics, before reaching the greywacke basement. A large variation in calculated heat flow, from 62.8 to 113.5 mW/m^2 has been found.

Te Rapa -1

This hole penetrated mainly sandstone, siltstone, clay, and shale, besides some pumice, tuff and lignite of Upper Eocene to Holocene age. The Triassic-Jurassic greywacke basement is at 1645 m.

5.3 COROMANDEL REGION

This region is characterised by the presence of rhyolite, andesite and pumiceous pyroclastics, mainly of Miocene-Pliocene age. Jurassic greywacke basement is exposed at a few places. Heat flow has been determined for a borehole at Whitianga.

DD2 - Whitianga

This hole was drilled to a depth of 209 m and passed through 72 m of Quaternary rocks and 10 m of pumice sand above various pumice sands and silts, lapilli breccias and subwelded tephras of the Whitianga group. The temperatures (measured after one month of drilling) are shown in fig. 5.11. Four samples from this well, obtained between 97.5 and 191.1 m have been used for conductivity determination. Since the borehole is situated in an area of moderate relief, a topographic correction was calculated. This turned out to be less than 2.5% and can thus be neglected.

5.4 TARANAKI-WANGANUI BASIN

This is one of the largest Upper Cretaceous-Cenozoic sedimentary basins in New Zealand, covering an area of about 40,000 sq.km (fig. 5.1). It is located at a considerable distance on the continental side of the subduction zone and contains a Tertiary sequence of estimated thickness 5,000 - 8,000 m. The Basin is divided into two parts by a north-south trending structure, the Tongaporutu-Patea basement high, which is bounded to the west by the large Taranaki Fault, with a throw of about 7km. To the west of this fault lies the Taranaki Basin. On the eastern side of the basement high is a fault with a throw of about 1500 m, which bounds the Wanganui Basin. No hot springs are reported from the entire Taranaki-Wanganui basin. All the boreholes are located in areas of very

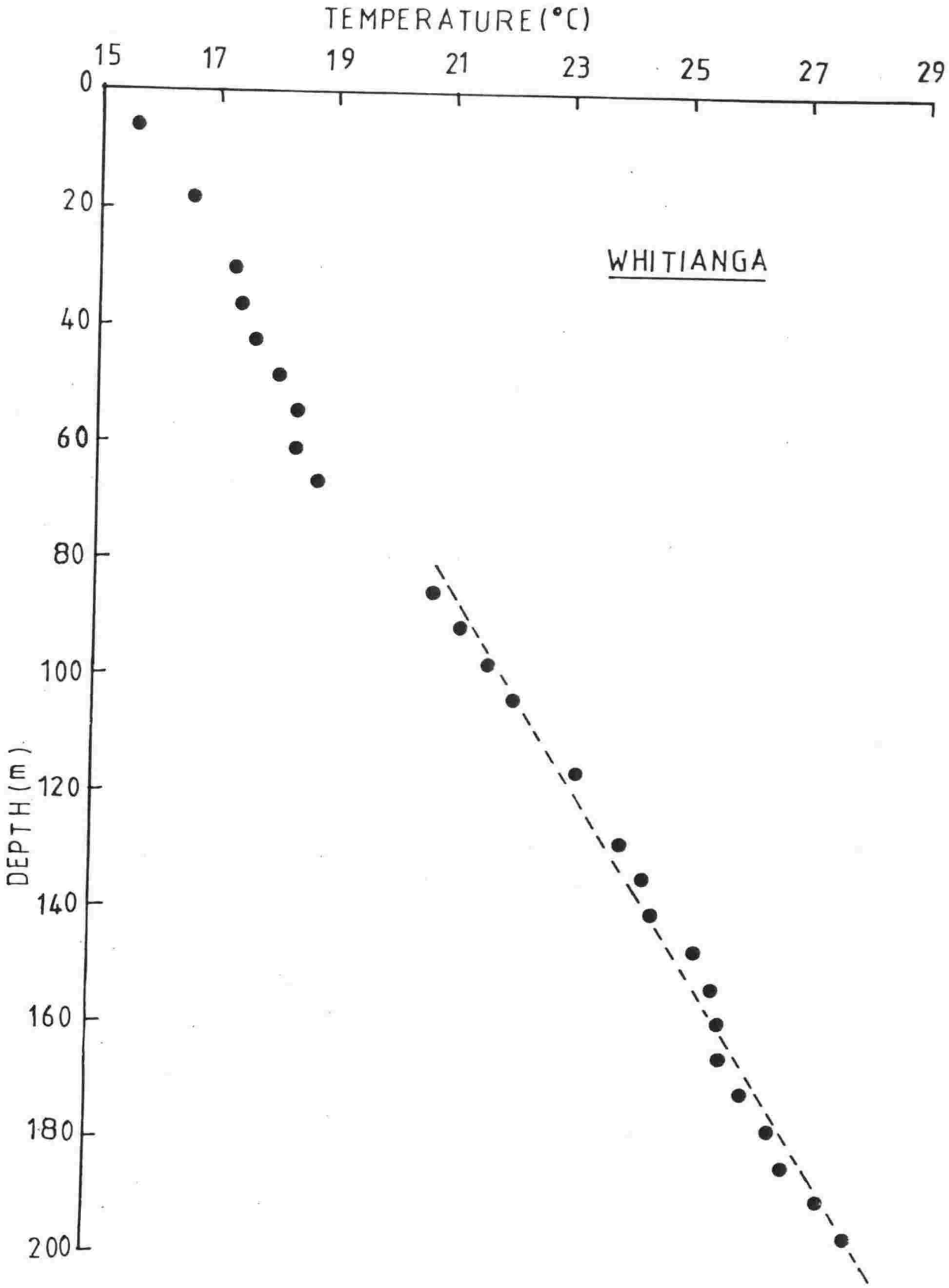

Fig. 5.11 (Data source: Thompson, 1977)

moderate relief. However, since an active andesitic volcano (Mt Egmont 2518 m) is located in the middle of the Taranaki Basin, the topographic effect has been calculated for the nearest location, Kapuni -8, which is situated 14km away. The correction was found to be negligible and has been neglected. No other kind of correction was found necessary.

5.4.1 Taranaki Basin

This basin contains an almost complete succession of Eocene to Recent sediments, and consists of two major structural features; the Western Platform and the Taranaki Graben. Andesitic volcanism has been active in the northern part of the Taranaki Graben. Some structural anticlines are associated with oil - gas condensate (McBeath, 1977). Basement is thought to be made up of Mesozoic-Palezoic sediments, granite, diorite and schist. Stratigraphic sequences penetrated in the onshore part of the Taranaki Basin are shown in fig. 5.12.

Western Platform

Moa -1B

Rock types in the depth interval of the heat flow calculations are Paleocene-Miocene mudstone, sandstone, siltstone and shale, with minor limestone, down to 3349.1 m, where the Lower Devonian-Silurian basement was encountered. This basement is composed of quartz - feldspathic biotite schist grading to a quartz - feldspathic amphibolite gneiss.

Tane -1

Lithologic and temperature variations are shown in fig. 5.13. Basement is composed of fresh pale biotite granite. No corrections were needed to the temperature data, since these had already been applied by the oil company.

Maui -1,2,3

These three boreholes are drilled over the offshore Maui structure, which forms one of the main gas - condensate fields. The formations are similar to those in the onshore Taranaki boreholes (fig. 5.12) and differ from Maui -4, which is drilled in the Taranaki Graben complex. The basement is composed of Upper Cretaceous quartzite and quartz mica schist conglomerate (Maui -1); Paleozoic hornblende diorite (Maui -2); and Paleocene shale, sandstone, siltstone, and conglomerates of quartzite and sodic granite (Maui -3). 19 samples have been measured for conductivity. The mean conductivity of each formation used in the heat flow calculations is given in Table 5.3. Calculated heat flows vary from 77.9 to 88.7 mW/m^2. The temperature profile and litholog of one of the wells (Maui -1) is shown in fig. 5.13.

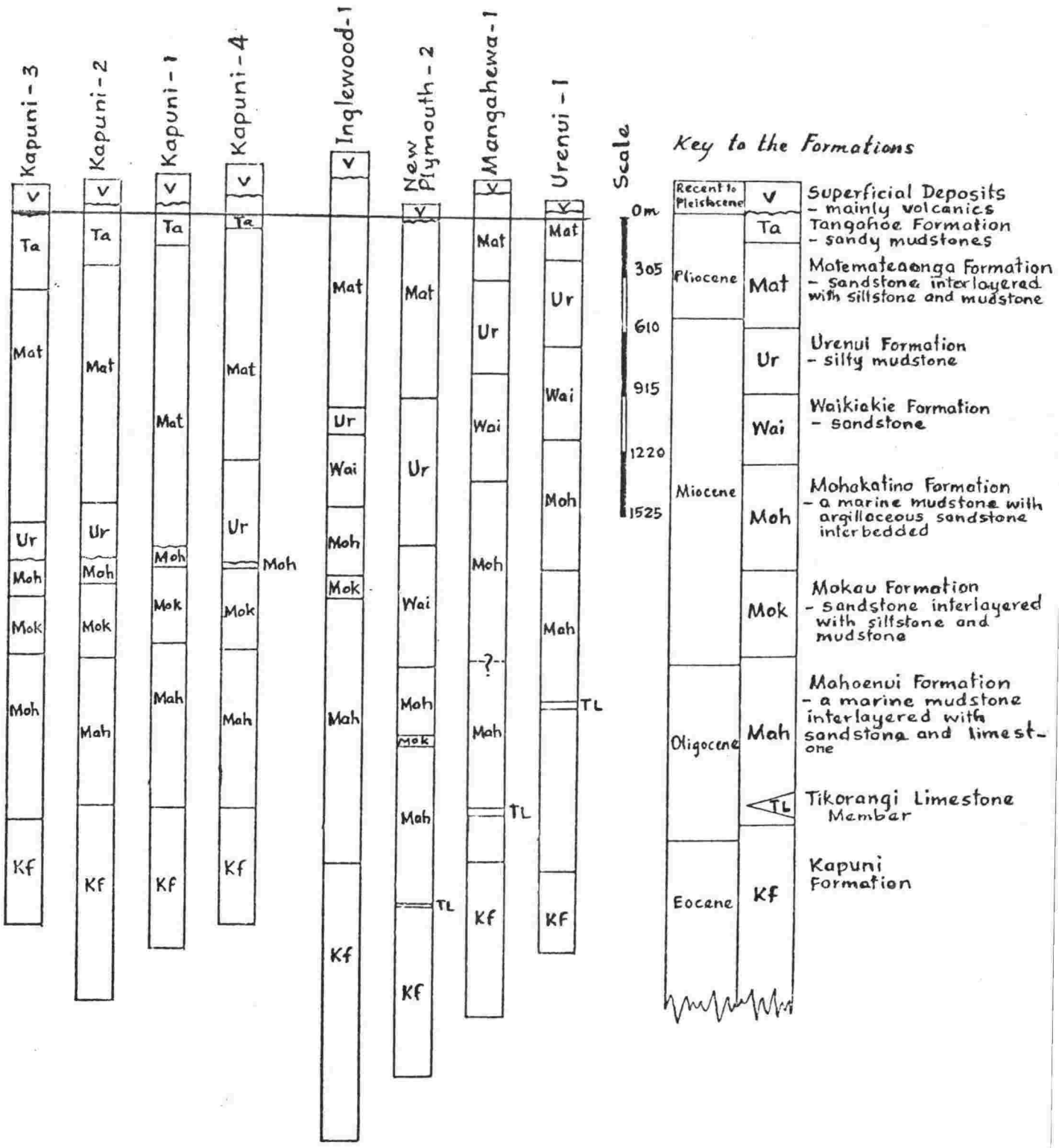

Fig. 5.12 Stratigraphic columns of the boreholes drilled in onshore Taranaki Basin (after Hogan, 1979).

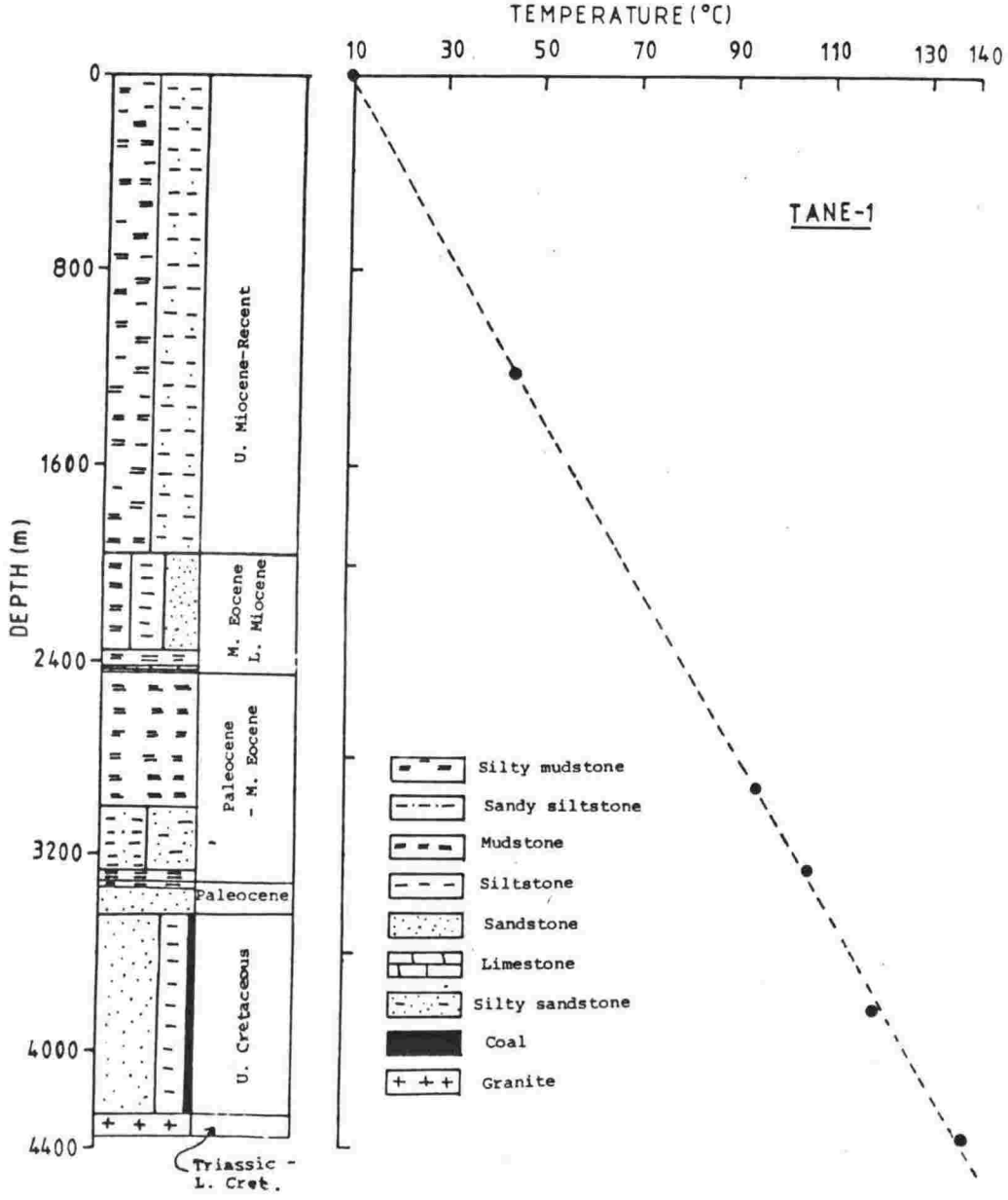
TEMPERATURE (°C)
10 30 50 70 90 110 130 140
TANE-1
DEPTH (m)
0
800
1600
2400
3200
4000
4400
U. Miocene-Recent
M. Eocene L. Miocene
Paleocene - M. Eocene
Paleocene
U. Cretaceous
Triassic - L. Cret.
Silty mudstone
Sandy siltstone
Mudstone
Siltstone
Sandstone
Limestone
Silty sandstone
Coal
Granite

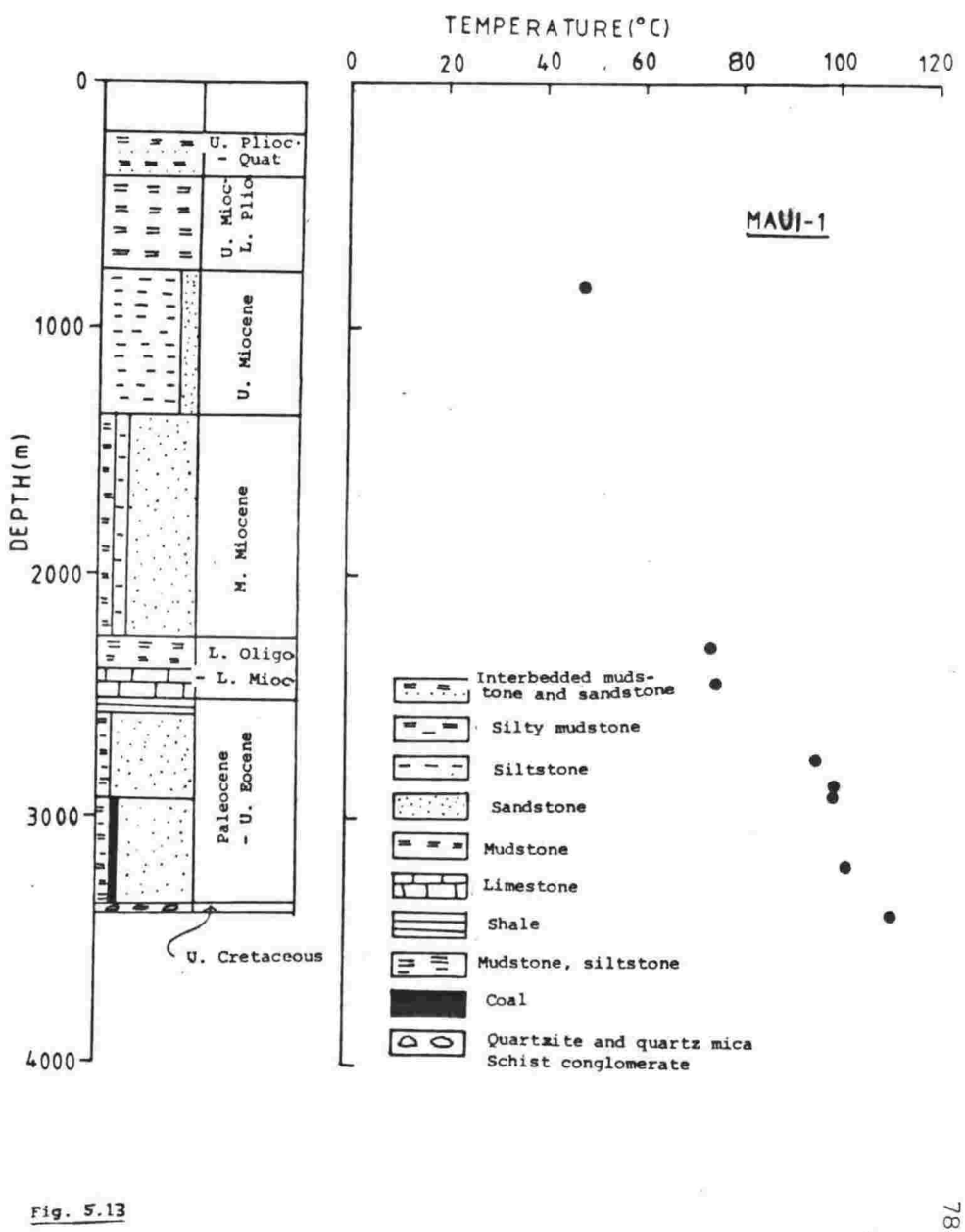
TEMPERATURE (°C)
0 20 40 60 80 100 120
MAUI-1
DEPTH (m)
0
1000
2000
3000
4000
U. Plioc. - Quat
U. Mioc - L. Plio
U. Miocene
M. Miocene
L. Oligo - L. Mioc
Paleocene - U. Eocene
U. Cretaceous
Interbedded mudstone and sandstone
Silty mudstone
Siltstone
Sandstone
Mudstone
Limestone
Shale
Mudstone, siltstone
Coal
Quartzite and quartz mica Schist conglomerate

Fig. 5.13

Table 5.3 Stratigraphy and mean thermal conductivity: Maui - 1,2,3.

Name of formation	Geologic age	Major Rock Type	Mean conductivity ($W/m^{o}C$)
Superficial deposits	Recent	-	-
Matemateaonga/ Tangahoe	Pliocene-Quaternary	Mudstone inter-bedded with sandstone	-
Urenui formation equivalent	U. Miocene-L. Pliocene	Silty mudstone	2.71
Waikiekie formation equivalent	U. Miocene	Siltstone	2.67
Mokau-Mohakatino formation equivalent	M. Miocene	Mainly sandstone, with mudstone and siltstone	4.35
Mahoenui formation equivalent	L. to M. Miocene	Hard mudstone	2.54
Takaka - Te kuiti formation equivalent	Oligocene - L. Miocene	Limestone	3.24
Kapuni formation equivalent	Paleocene - U. Eocene	Sandstone, shale	2.54
Pakawau formation equivalent	U. cretaceous	Conglomerate of quartzite, sand-stone, quartz mica schist, diorite, silt-stone, granite	3.28
Rotoroa Igneous complex equivalent	Paleozoic	Hornblende diorite	3.91

Cook -1

The temperature profile and litholog of the borehole are shown in fig. 5.14. Conductivity ranged from 2.85 to 4.73 $W/m^{o}C$, with a mean of 3.85 ± 0.42 $W/m^{o}C$, which is quite high and seems to be related to the higher SiO_2 content (74.1 to 86.2%). The heat flow of 136.6 ± 16.7 mW/m^2 is also the highest that has been measured in the Taranaki-Wanganui basin.

Taranaki Graben

Republic New Plymouth -1,2,3,4

These boreholes are located in the Moturoa oil field near New Plymouth; the greatest depth reached was 960 m. They penetrate mainly Upper Miocene to Recent mudstone, siltstone and sandstone, with some conglomerate, volcanics, dolomite and quartz. Only one sample of sandy and muddy siltstone was available for conductivity measurement. For other rock types the conductivity value has been taken from New Plymouth -2 borehole, which is less than 2km distant.

It is interesting to note that the equilibrium temperature reported by Studt and Thompson (1969) in a nearby New Plymouth well (less than a kilometre away from this location) agrees very well with that of $40^{o}C$ at 684.4 m in Republic New Plymouth -4.

New Plymouth -2

The temperature data and litholog are shown in fig. 5.16. The heat flow has been calculated using both the G-K method and the resistance integral method. The respective values are 92.3 ± 7.1 mW/m^2 and 90.2 ± 5.6 mW/m^2, which agree quite well. We adopt the latter.

McKee -1

The temperatures and penetrated rock types are shown in fig. 5.16. The temperature data include several formation-test temperatures, besides conventional bottom hole measurements. The conductivity has been estimated from Urenui -1 and Mangahewa -1. The values of heat flow obtained from the two types of data are as follows :-

Depth range (m)	Heat flow (mW/m^2)	Temperatures
1836-3683	81.8±5.3	formation-test
1831-3897.4	80.6±10.7	corrected bottom hole

In view of the close agreement, the data were combined, and gave the value 80.3 ± 5.2 mW/m^2.

Inglewood -1

This is the deepest borehole drilled in New Zealand, reaching 5053.9 m. The temperature profile and litholog are shown in fig. 5.17.

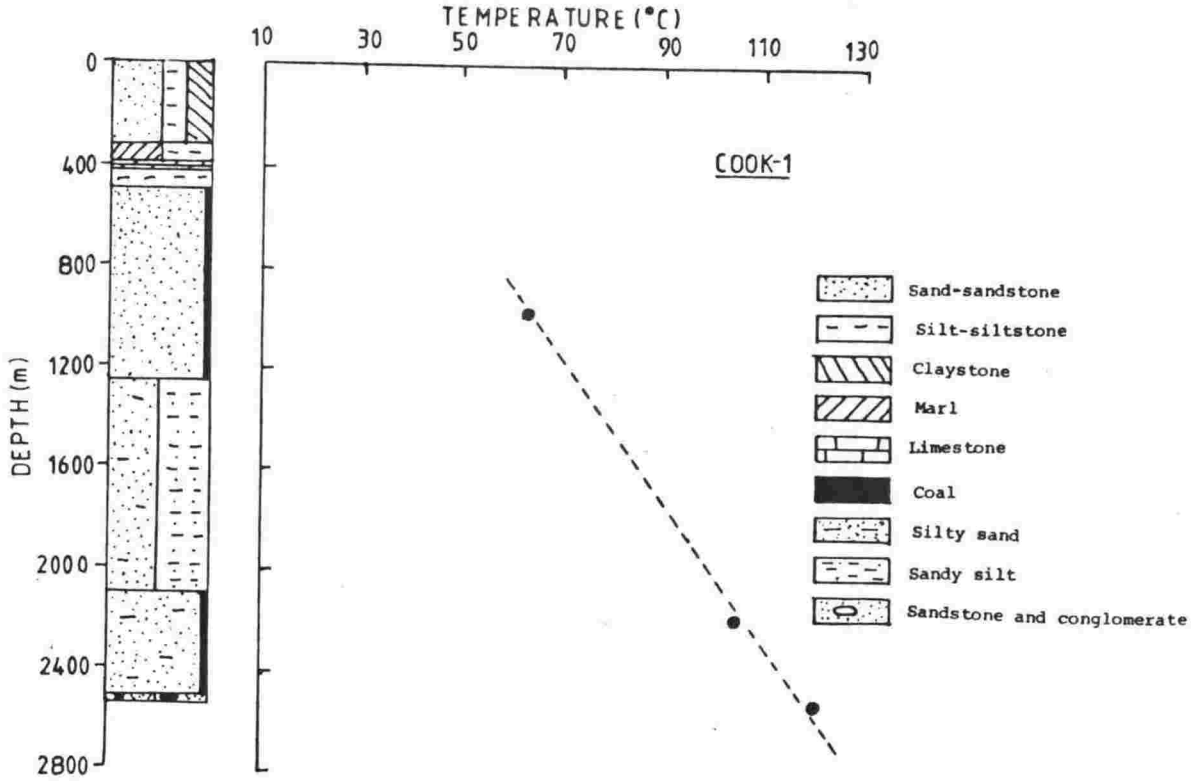
TEMPERATURE (°C)
10
30
50
70
90
110
130
COOK-1
DEPTH (m)
0
400
800
1200
1600
2000
2400
2800
Sand-sandstone
Silt-siltstone
Claystone
Marl
Limestone
Coal
Silty sand
Sandy silt
Sandstone and conglomerate

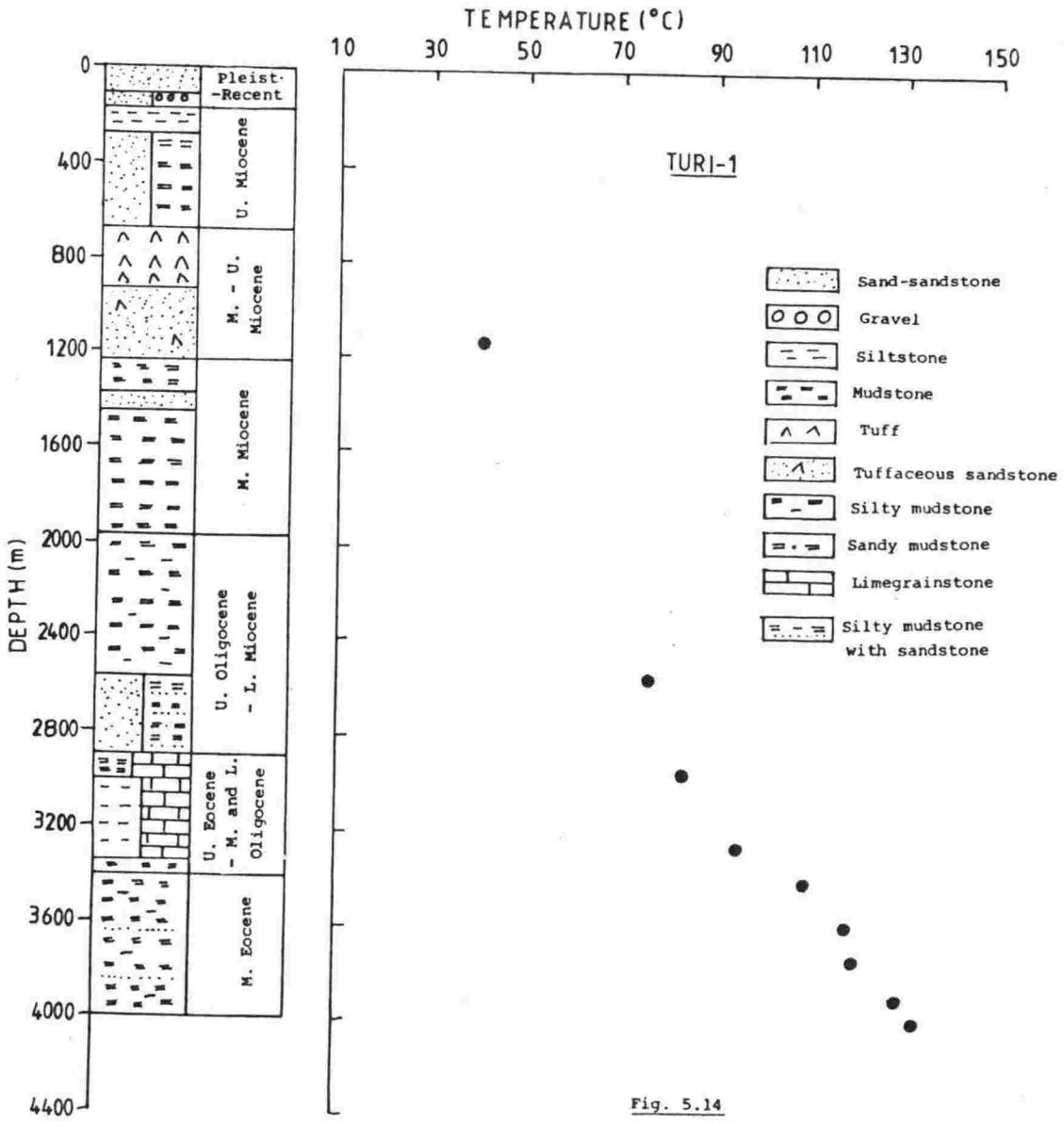
TEMPERATURE (°C)
10
30
50
70
90
110
130
150
TURI-1
DEPTH (m)
0
400
800
1200
1600
2000
2400
2800
3200
3600
4000
4400
Pleist-
-Recent
U. Miocene
M. - U. Miocene
M. Miocene
U. Oligocene
- L. Miocene
U. Eocene
- M. and L.
Oligocene
M. Eocene
Sand-sandstone
Gravel
Siltstone
Mudstone
Tuff
Tuffaceous sandstone
Silty mudstone
Sandy mudstone
Limegrainstone
Silty mudstone
with sandstone

Fig. 5.14

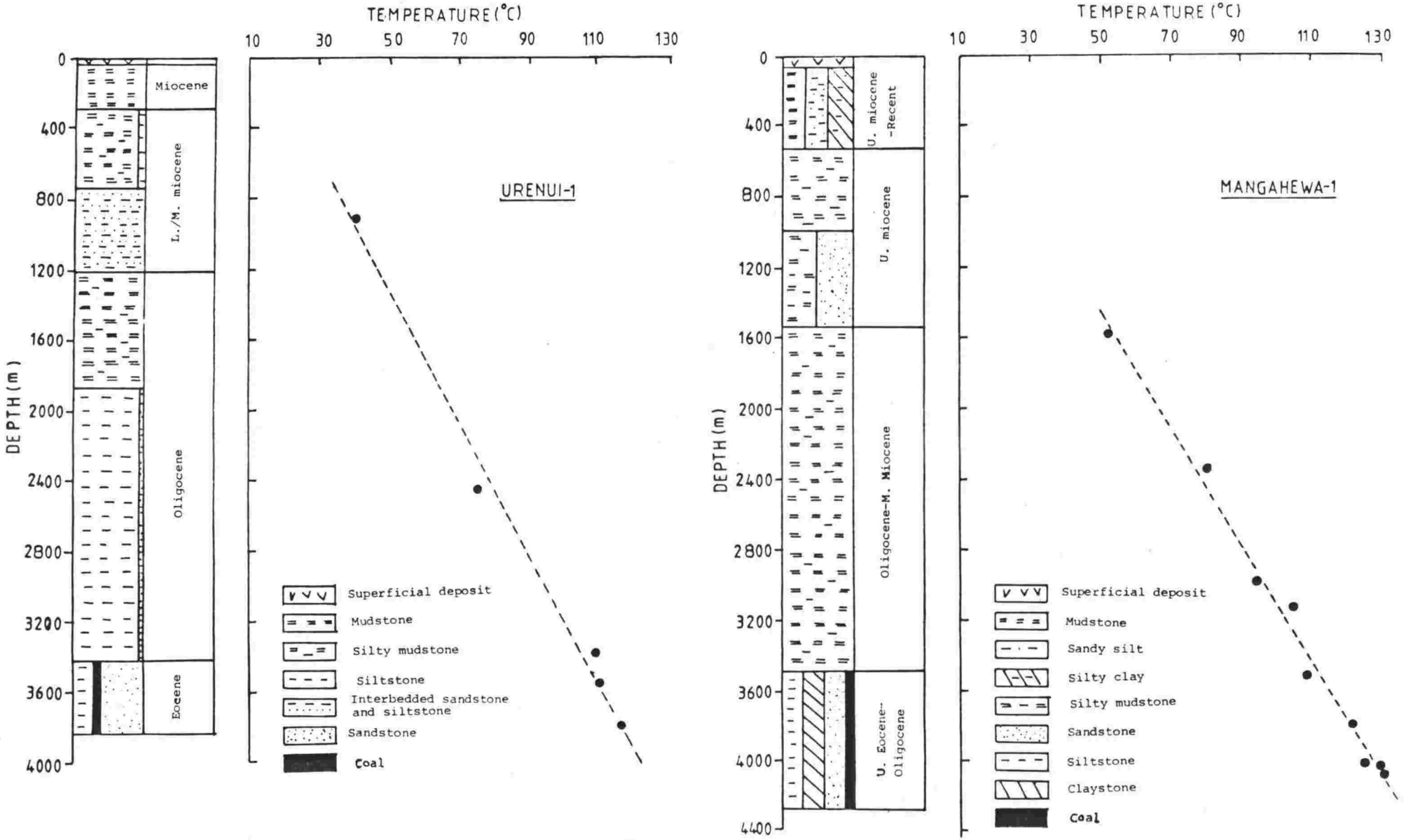
TEMPERATURE (°C)
10
30
50
70
90
110
130
DEPTH (m)
0
400
800
1200
1600
2000
2400
2800
3200
3600
4000
4400
Miocene
L./M. miocene
Oligocene
Eocene
URENUI-1
U. miocene -Recent
U. miocene
Oligocene-M. Miocene
U. Eocene-Oligocene
MANGAHEWA-1
Superficial deposit
Mudstone
Silty mudstone
Siltstone
Interbedded sandstone and siltstone
Sandstone
Coal
Sandy silt
Silty clay
Claystone

Fig. 5.15

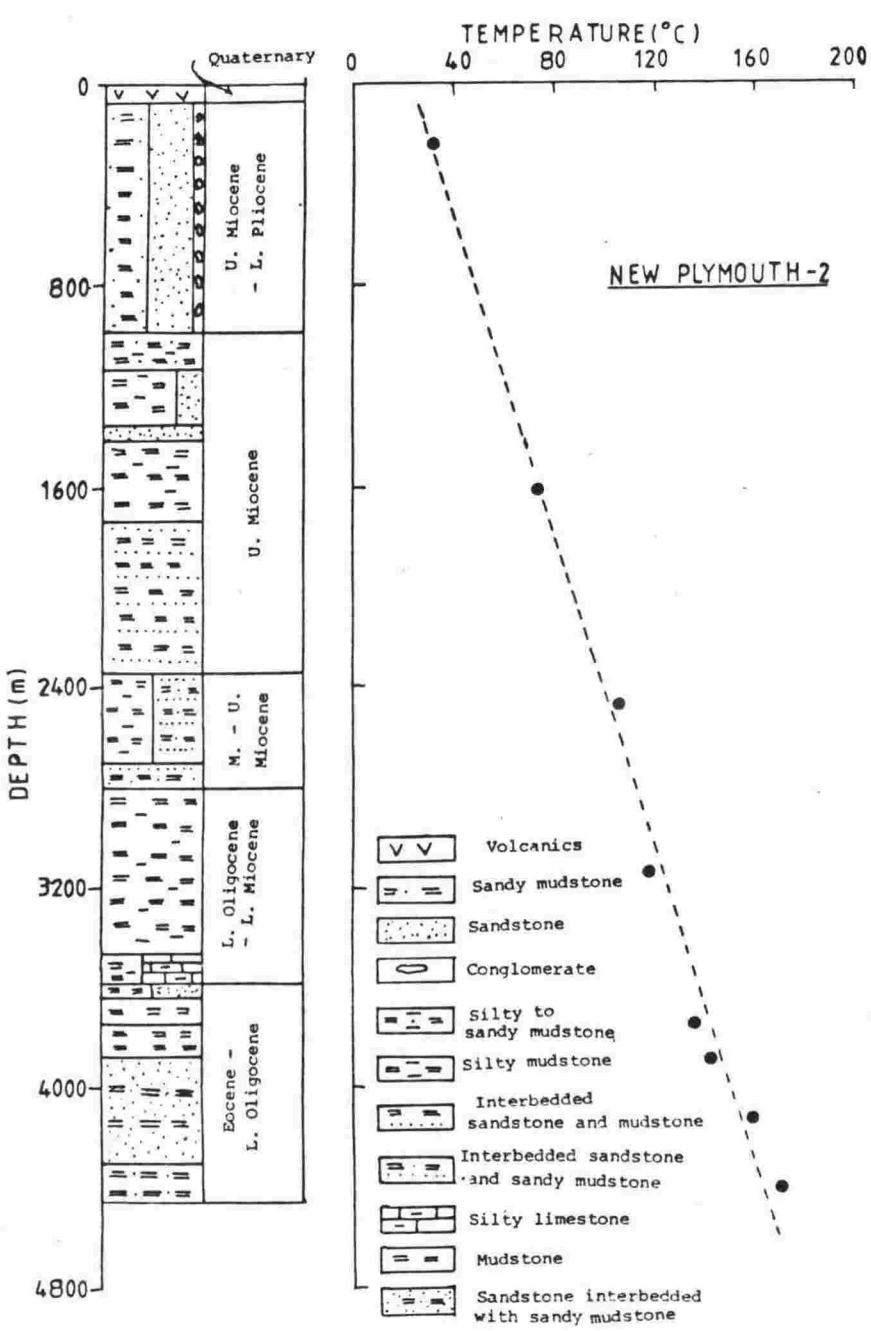
TEMPERATURE (°C)
0
40
80
120
160
200
Quaternary
U. Miocene - L. Pliocene
U. Miocene
M. - U. Miocene
L. Oligocene - L. Miocene
Eocene - L. Oligocene
DEPTH (m)
0
800
1600
2400
3200
4000
4800
NEW PLYMOUTH-2
Volcanics
Sandy mudstone
Sandstone
Conglomerate
Silty to sandy mudstone
Silty mudstone
Interbedded sandstone and mudstone
Interbedded sandstone and sandy mudstone
Silty limestone
Mudstone
Sandstone interbedded with sandy mudstone

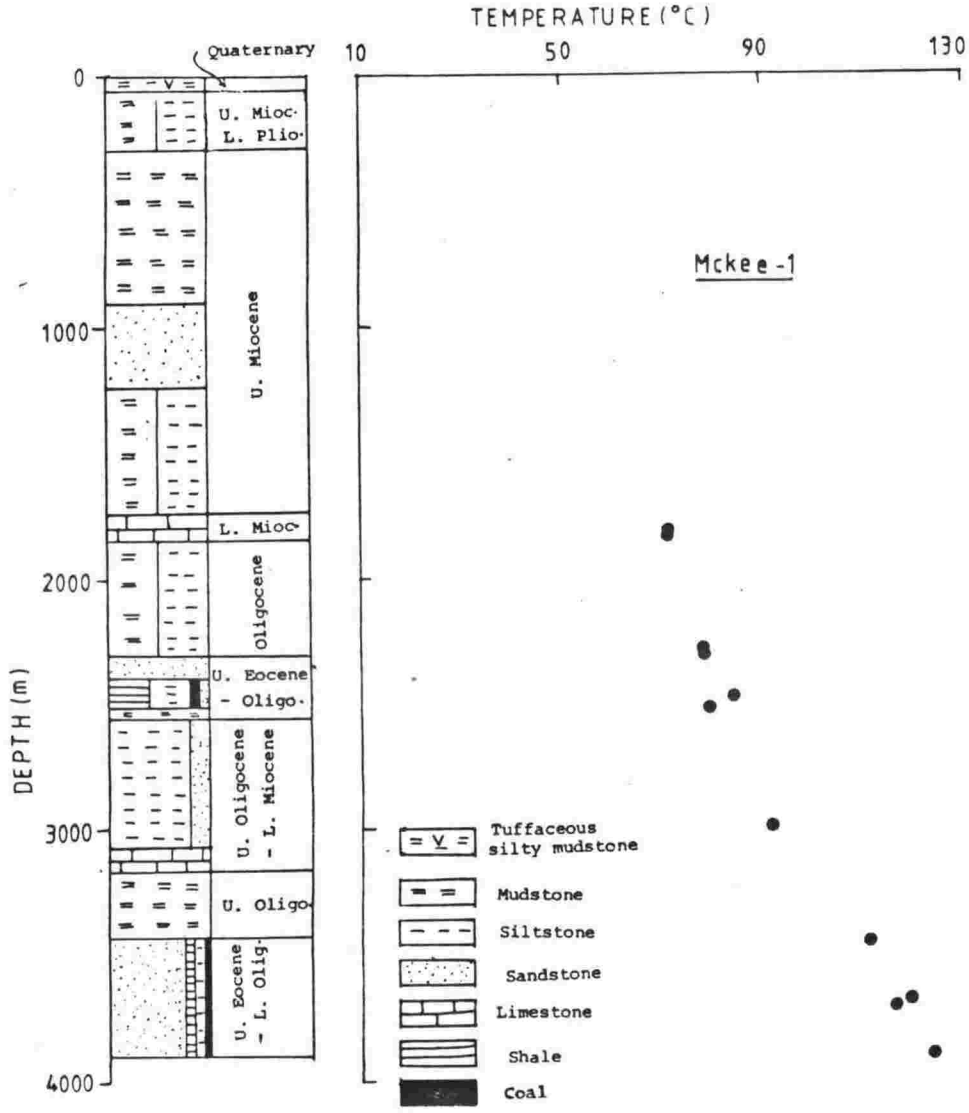
TEMPERATURE (°C)
10
50
90
130
Quaternary
U. Mioc - L. Plio
U. Miocene
L. Mioc
Oligocene
U. Eocene - Oligo
U. Oligocene - L. Miocene
U. Oligo
U. Eocene - L. Olig
DEPTH (m)
0
1000
2000
3000
4000
Mckee-1
Tuffaceous silty mudstone
Mudstone
Siltstone
Sandstone
Limestone
Shale
Coal

Fig. 5.16

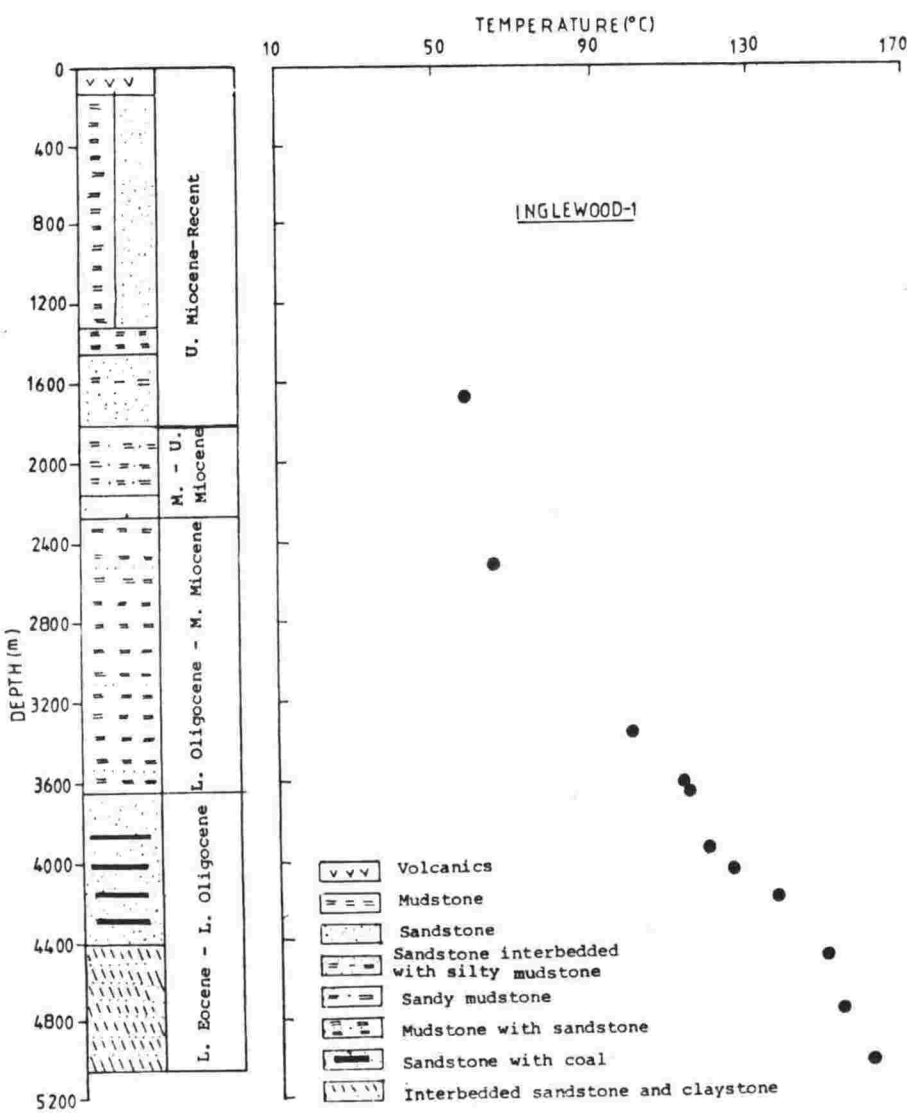
TEMPERATURE (°C)
10
50
90
130
170
INGLEWOOD-1
DEPTH (m)
0
400
800
1200
1600
2000
2400
2800
3200
3600
4000
4400
4800
5200
U. Miocene-Recent
M. - U. Miocene
L. Oligocene - M. Miocene
L. Eocene - L. Oligocene
Volcanics
Mudstone
Sandstone
Sandstone interbedded with silty mudstone
Sandy mudstone
Mudstone with sandstone
Sandstone with coal
Interbedded sandstone and claystone

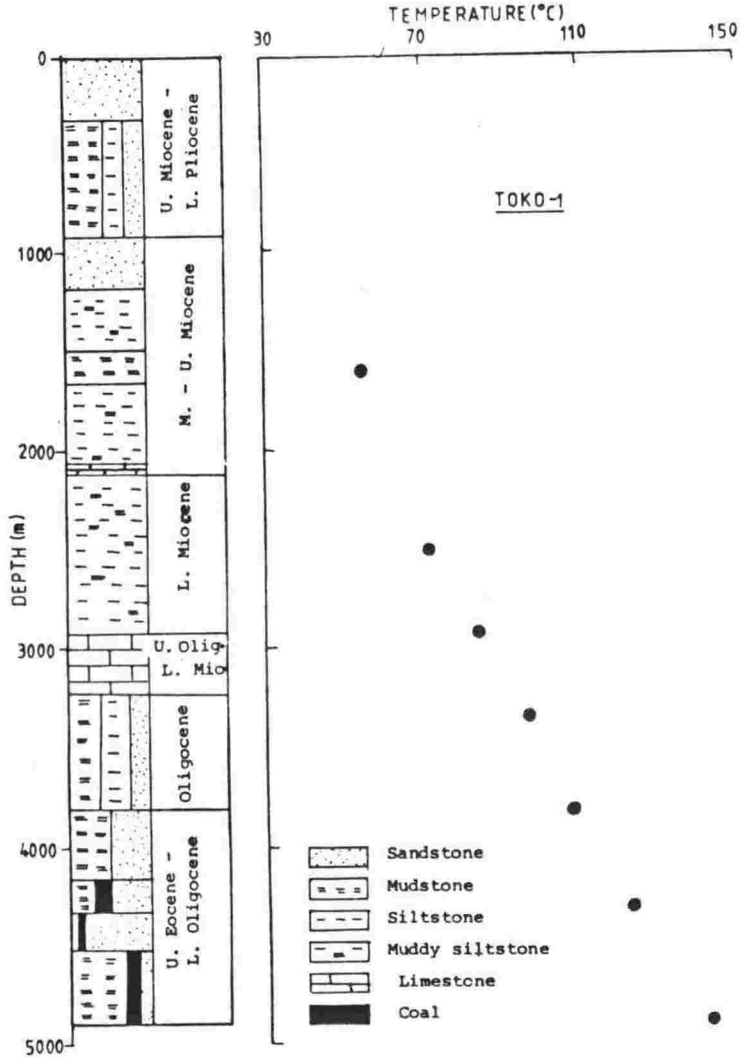
TEMPERATURE (°C)
30
70
110
150
TOKO-1
DEPTH (m)
0
1000
2000
3000
4000
5000
U. Miocene - L. Pliocene
M. - U. Miocene
L. Miocene
U. Olig
L. Mio
Oligocene
U. Eocene - L. Oligocene
Sandstone
Mudstone
Siltstone
Muddy siltstone
Limestone
Coal

Fig. 5.17

A sandstone sample from this well (depth 4508.9 m), which contained 91.1% SiO_2, gave the highest thermal conductivity to be measured in this study — 6.55 $W/m^{o}C$.

Kapuni -1,2,3,3A,4,5,6,7,8,9,10,11

These holes are located about 48km SSE of New Plymouth in an area of about 9km x 3km. The Kapuni structure is described as a north-south trending, slightly asymetrical anticline with a faulted western flank (McBeath, 1977); it is a gas-condensate producer. Except for Kapuni -1,2,4,6 and 8, the boreholes were inclined and appropriate corrections were made for depth. Along with bottom hole measurements, static temperatures had been measured, after periods of several months to years, during pressure/temperature surveys; these were available for 10 boreholes. The static temperatures were always higher because of the absence of drilling effects. A typical temperature profile and litholog of one of the wells (Kapuni -1) is shown in fig. 5.18.

The thermal conductivity has been measured on 32 samples from different formations in five of these wells. Since all wells are located in a small area and penetrate the same formations, we determined an average conductivity for each lithologic formation (Table 5.4).

Maui -4

The temperature profile and rock types are shown in fig. 5.18. The hole penetrated similar sediments to those occurring onshore in Taranaki, before reaching Paleozoic basement composed of albite granite, at 3700.9 m. This granite is a probable equivalent of the Separation Point Granite which outcrops in north-west Nelson.

Kupe -1

This is an interesting offshore location, where the temperature distribution (fig. 5.19) gave a low value of 16.04 ± 3.49$^{o}C/km$ for the geothermal gradient. In the absence of samples, the conductivity has been estimated from the nearest Kapuni wells. Heat flow values calculated by the G-K method (48.4 mW/m^2) and by the resistance integral method (48.1 ± 10.4 mW/m^2) agree closely. In spite of the large scatter in temperature data, a considerably low heat flow for this location compared to others in the graben complex cannot be denied.

North Tasman -1

Rock types in the depth range of heat flow calculation are sandstone, mudstone, shale and siltstone of Upper Cretaceous to Miocene age, which rest on Middle Cretaceous (?) granitic basement at 2551.5 m.

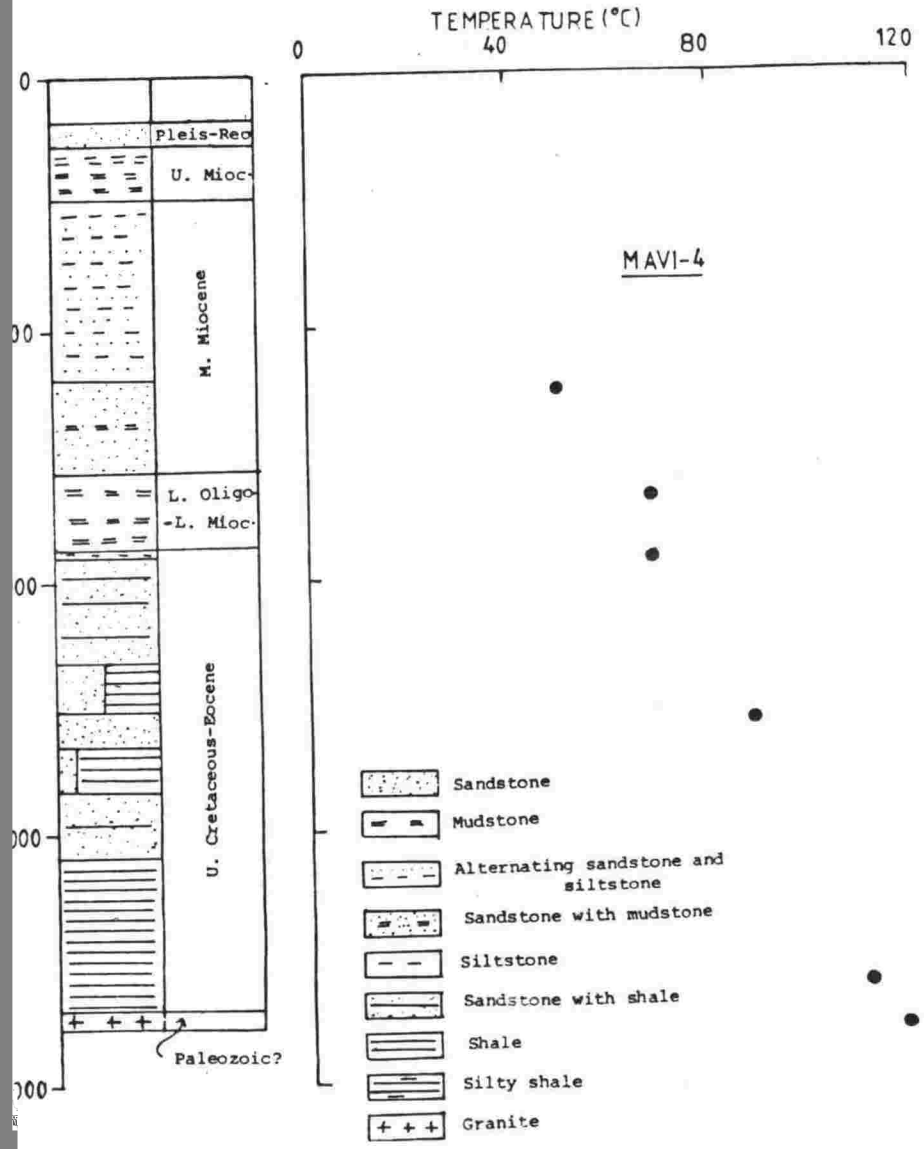
TEMPERATURE (°C)
0
40
80
120
MAVI-4
Pleis-Rec
U. Mioc-
M. Miocene
L. Oligo
-L. Mioc
U. Cretaceous-Eocene
Paleozoic?
Sandstone
Mudstone
Alternating sandstone and siltstone
Sandstone with mudstone
Siltstone
Sandstone with shale
Shale
Silty shale
Granite

5.18

Table 5.4 Stratigraphy and mean thermal conductivity: Kapuni boreholes.

Name of formation	Geologic Age	Major rock type	Mean conductivity ($W/m^{o}C$)
Superficial deposits	Quaternary	Volcanics	1.32
Tangahoe	Pliocene	Mudstone with sand	2.45
Matemateaonga	M.Miocene - Pliocene	Sandstone with mudstone, siltstone	3.27
Urenui	M. to U. Miocene	Siltstone, mudstone	2.81
Mohakatino	M. to U. Miocene	Mudstone	2.69
Mokau	L. Miocene	Sandstone (with siltstone and mudstone)	3.48
Mahoenui	Oligocene - Miocene	Compact and hard silty mudstone	3.04
Kapuni	Eocene - L. Oligocene	Sandstone, siltstone, shale, coal	2.97

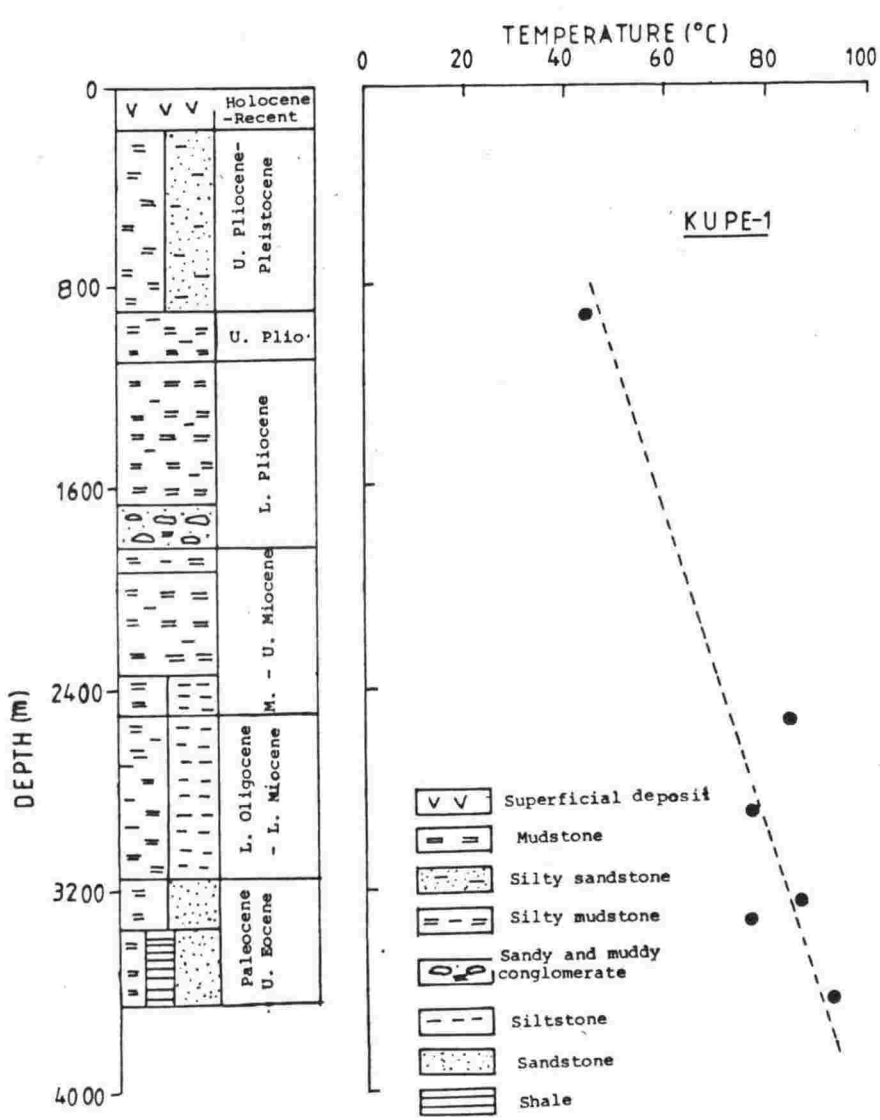
TEMPERATURE (°C)
0
20
40
60
80
100
KUPE-1
DEPTH (m)
0
800
1600
2400
3200
4000
Holocene -Recent
U. Pliocene- Pleistocene
U. Plio·
L. Pliocene
M. - U. Miocene
L. Oligocene - L. Miocene
Paleocene U. Eocene
Superficial deposit
Mudstone
Silty sandstone
Silty mudstone
Sandy and muddy conglomerate
Siltstone
Sandstone
Shale

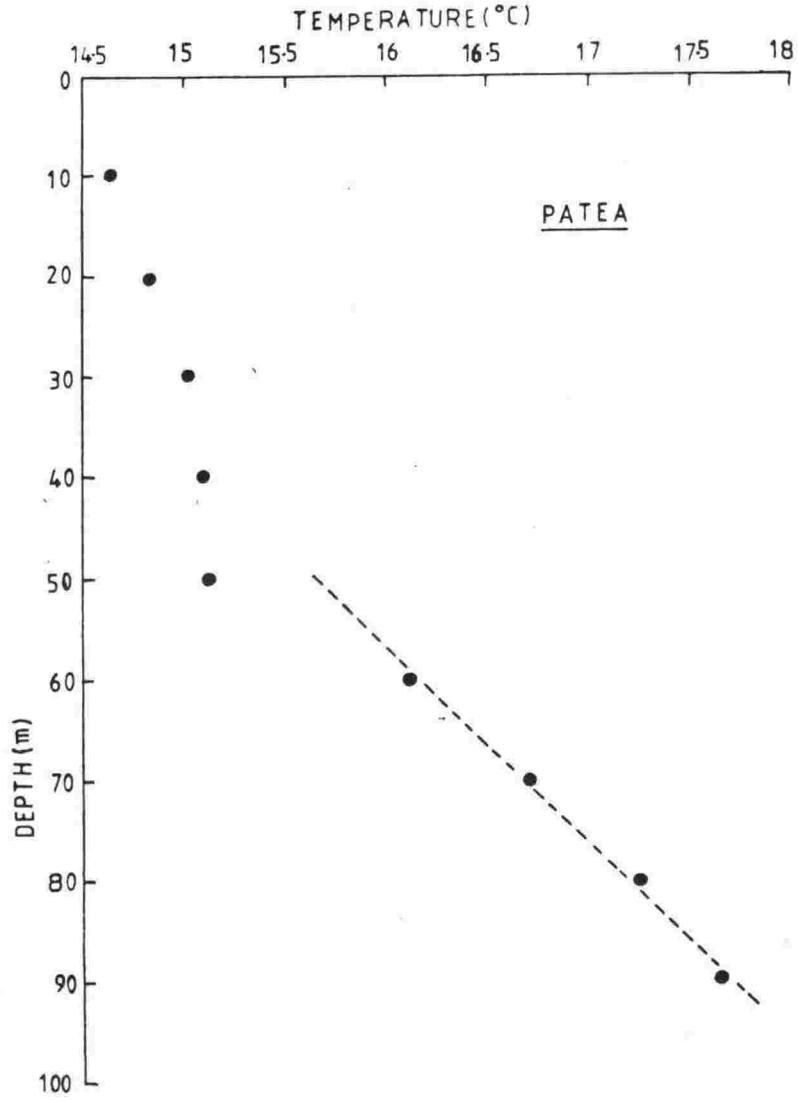
TEMPERATURE (°C)
14·5
15
15·5
16
16·5
17
17·5
18
PATEA
DEPTH (m)
0
10
20
30
40
50
60
70
80
90
100

Fig. 5.19

Tasman -1

This borehole was drilled through silt-siltstone, mudstone, and sandy limestone, with small amounts of shale, marl and sands, all belonging to Eocene - Pleistocene (?) age. It reached the Permian-Triassic basement, composed of hydrothermally altered conglomerates of mafic volcanics and red granite, at 1446 m.

Fresne -1

Rock types between 1183.2 m and 2413 m are Upper Cretaceous - Paleocene sandstone, conglomerate with small amounts of siltstone and coal.

Surville -1

Rock types between 949 m and 2140.5 m consist mainly of sandstone, with some mudstone, limestone, shale and coal of Eocene to Early Miocene age, before reaching the basement of arkose granite at 2002.5 m. A core taken between 2139.5 and 2141.5 m is recognised as biotite microcline granite. This granite is similar to the Separation Point Granite and is of Middle Cretaceous age.

5.4.2 Patea - Tongaporutu High

Kiore -1

This borehole occupies a central position in the structure, and passes through Upper Miocene sandstone and silty to sandy mudstone before reaching the pre-Tertiary basement, composed of fine-grained sandstone grading to siltstone and silty mudstone, at 480.1 m.

Patea

The temperature profile, measured after several years of standing time, is shown in fig. 5.19. Heat flow at this location could not be determined since neither samples nor lithological information were available.

5.4.3 Wanganui Basin

Stratigraphically this basin differs from the adjacent Taranaki basin. It can be divided into two parts; North Wanganui Basin and South Wanganui Basin. No Eocene rocks are reported to occur here. Oligocene - Miocene rocks are restricted to the North Wanganui Basin, while the South Wanganui Basin contains thick piles of Plio-Pleistocene sequences. Basement is composed of Mesozoic greywacke, metaquartzite, argillite and Permian-Triassic schist. The basement schist complex of Marlborough Sound seems to plunge NNE under the offshore Wanganui Basin.

North Wanganui Basin

Waikaka -1

This hole penetrated Oligocene shale, siltstone and interbedded silty shale mudstone down to 942.7 m, then 18.3 m of Oligocene limestone overlying pre-Tertiary greywacke basement. Conductivity has been estimated from the nearest wells.

Ararimu -1

This borehole was drilled through mainly Oligocene shale and siltstone before reaching the pre-Tertiary greywacke basement at 1028.1 m.

Whakamaro -1

At this location, penetrated rock types were Middle to Upper Oligocene shale, mudstone and silty sandstone.

Tatu -1

This hole was drilled through mainly carbonaceous sandstone, sandy siltstone and silty mudstone of Upper Oligocene to Middle Miocene age. At 827.8 m, Jurassic-Cretaceous basement was met which contained very hard sandy mudstone and thin sandstone beds.

Koporongo -1

At this site, the borehole passed through Oligocene-Miocene shale overyling Jurassic basement, composed of metaquartzite and argillite, at 528.5 m.

Tupapakurua -1

This borehole penetrated mainly Oligocene-Miocene shale and mudstone with thin sandstone and siltstone bands. These formations rest on greywacke basement at 1123.5 m.

South Wanganui Basin

Parikino -1

The temperature data and litholog are shown in fig. 5.20. This well bottomed in Permian-Triassic basement composed of Kaimanawa schist. Since the well penetrated 2286.9 m of younger Pliocene-Pleistocene (and possibly some Upper Miocene) rocks, a correction for the sedimentation effect has been applied.

Santoft -1A

This hole is near the Parikino -1 well but is stratigraphically different. It penetrated sand, gravels and clay to 864 m, mudstone with occasional sand to 2295.6 m, and greywacke conglomerate to 2623.3 m, where the Mesozoic argillite basement was encountered. Above the basement all rocks were of Pliocene-Quaternary age. Here too, the

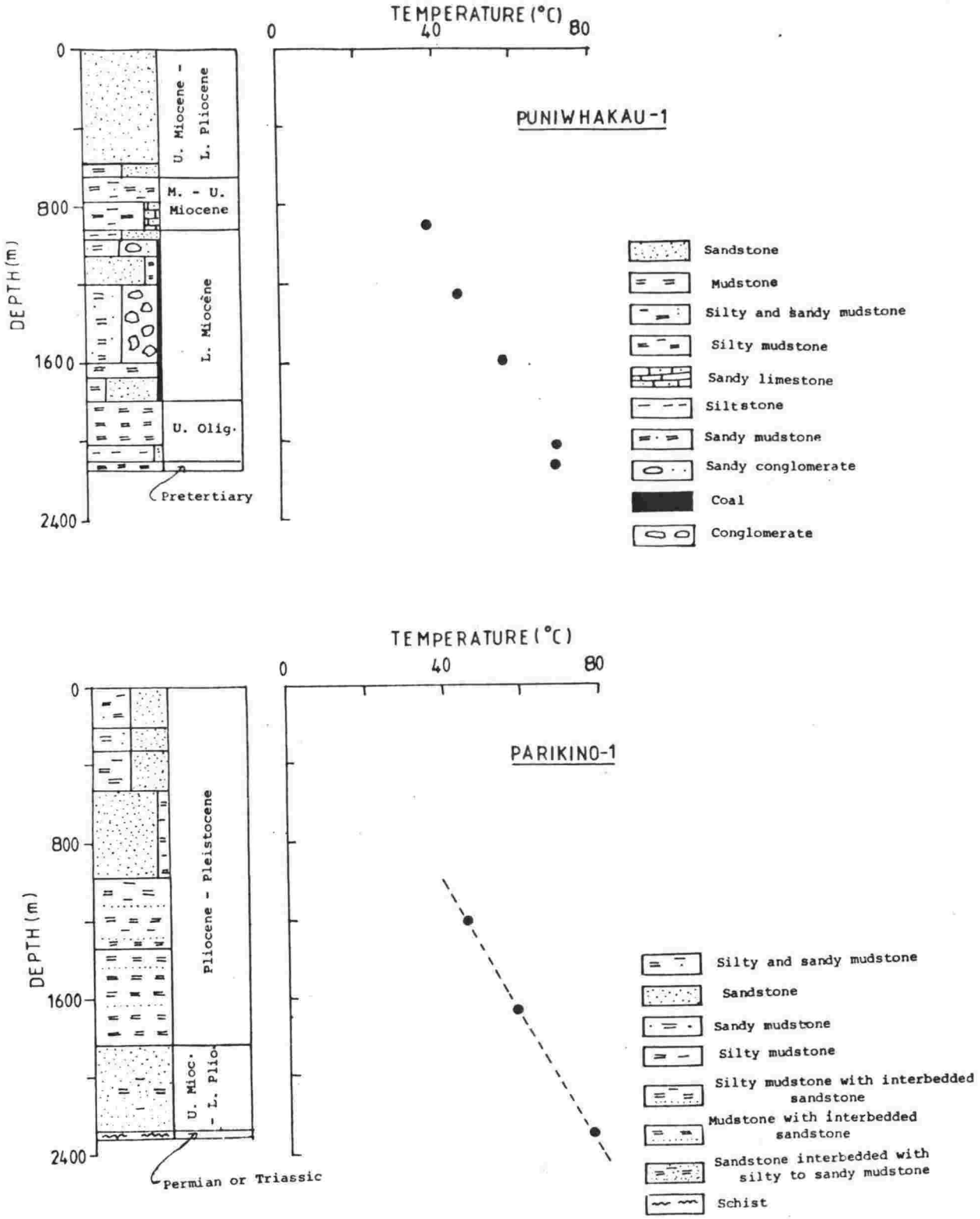
TEMPERATURE (°C)
0
40
80
PUNIWHAKAU-1
DEPTH (m)
0
800
1600
2400
U. Miocene - L. Pliocene
M. - U. Miocene
L. Miocene
U. Olig.
Pretertiary
Sandstone
Mudstone
Silty and sandy mudstone
Silty mudstone
Sandy limestone
Siltstone
Sandy mudstone
Sandy conglomerate
Coal
Conglomerate
TEMPERATURE (°C)
0
40
80
PARIKINO-1
DEPTH (m)
0
800
1600
2400
Pliocene - Pleistocene
U. Mioc. - L. Plio
Permian or Triassic
Silty and sandy mudstone
Sandstone
Sandy mudstone
Silty mudstone
Silty mudstone with interbedded sandstone
Mudstone with interbedded sandstone
Sandstone interbedded with silty to sandy mudstone
Schist

Fig. 5.20

temperature gradient needed a correction for sedimentation effects. The corrected gradient and heat flow for this location are about half those for Parikino -1.

5.5 EAST COAST BASIN

This is a huge, elongated, complex sedimentary basin covering an area of about 38,400 sq.km. along the east coast of the North Island. It contains thick Middle to Late Cretaceous marine deposits, along with even thicker Cenozoic sequences. The Upper Cretaceous has a combined thickness of about 4,600 m (Kingma, 1965). In the Hawkes Bay depression, Tertiary sediments directly overlap the greywacke basement, and Cretaceous sediments are absent in large areas.

The East Coast Basin has been affected by several diastrophic movements, complicating the geological structure of the area, where abrupt changes in facies are found. In some cases complete Cretaceous-Tertiary sequences are present, while large sequences are missing in other parts (Kingma, 1959b). Geotectonically the Basin can be divided into two parts. In the northern part extensive block movements have taken place, along with gravity sliding, from Late Cretaceous to Late Tertiary. This part is also associated with Late Cenozoic diapiric intrusions and mud-volcanic activity. Further south the geological structures are relatively simple. Basement in the entire Basin is thought to be greywacke. A few hot springs occur in the northeastern part.

Some parts of the Basin (e.g. Cape Kidnappers, East Cape, Mahia Peninsula) have been affected by uplift rates of 1 to 3 mm/yr for the past 400,000 yrs (P. Froggatt, K. Berryman, A. Hull, pers. comm.; Lewis, 1971; Singh, 1971; Wellman, 1971a,b; Garrick, 1979). However, these locations are remote from the heat flow locations, and in view of the structural complexity of the region the uplift rates cannot be adopted on a regional basis. Moreover, in many parts of the basin sedimentation has been rapid due to deepening of the trough, and the rates are expected to be around zero, or negative (A. Hull, pers. comm.). Thus the correction has been neglected.

A topographic correction has been attempted for the shallow hole Rotokautuku -1, which is located in an area of rugged topography. The amount of the correction was less than 3.5%, and can be neglected. Other sites had moderate relief. A correction for the sedimentation effect was found necessary at three locations.

Te Horo -1

This borehole penetrated mainly siltstone, mudstone and sandstone of Upper Cretaceous-Eocene age. A mean conductivity has been estimated from Rotokautuku -1 and Te Puia -1.

Rotokautuku -1

This hole was drilled over the southeast flank of the Rotokautuku dome, which has been interpreted as a diapiric structure. The hole passed through gas-charged argillaceous siltstone with sandstone, of Upper Cretaceous-Paleocene age, and give a high geothermal gradient of 55.56^{o}C/km. The topographic correction was found to be negligible.

Te Puia -1

This borehole penetrated mudstone, siltstone and sandstone of Lower Cretaceous-Eocene age.

Waitangi Station -1

Rock formation between 1051 m and 2128.1 m are grey to green bentonitic, glauconitic mudstone of mainly Middle to Upper Eocene age.

Opoutama -1

This is the deepest borehole drilled in this basin. Only three temperatures had been measured during logging (fig. 5.22). A puzzling feature of this borehole has been the decrease of temperature from 87.43^{o}C at 2743 m to 80.89^{o}C at 3651.7 m; this remains unexplained. The most likely causes are trouble with the thermometer, or excessive circulation. The temperature at 3651.7 m is rejected. Gradients of 31.88^{o}C/km and 16.77^{o}C/km were found between the surface and 1722.3 m, and in the interval 1722.3 m - 2743 m, respectively. The upper interval consisted mainly of silty, sandy, and bentonitic mudstone, with little sandstone. A single available sample of mudstone from this interval gave a conductivity of 2.13 W/m^{o}C corresponding to a heat flow of 67.9 mW/m^{2}. For the other interval, which consisted entirely of Upper Cretaceous rocks, 13 Upper Cretaceous samples obtained from below 1722.3 m gave a mean conductivity of 3.56 ± 0.28 W/m^{o}C and a heat flow of 59.7 ± 4.7 mW/m^{2}, which is the preferred value for this site.

Hawke Bay -1

Geologically this site differs considerably from the nearest other borehole (Opoutama -1); this well penetrated 1133 m of Pleistocene-Pliocene sediments and a further 980 m of Upper Miocene rocks. The geothermal gradient is calculated between 1294.3 m and 1762.1 m, where the rocks are Upper Miocene silty to sandy clays. In the absence of samples, the conductivity of the clays is taken from Mangaone -1.

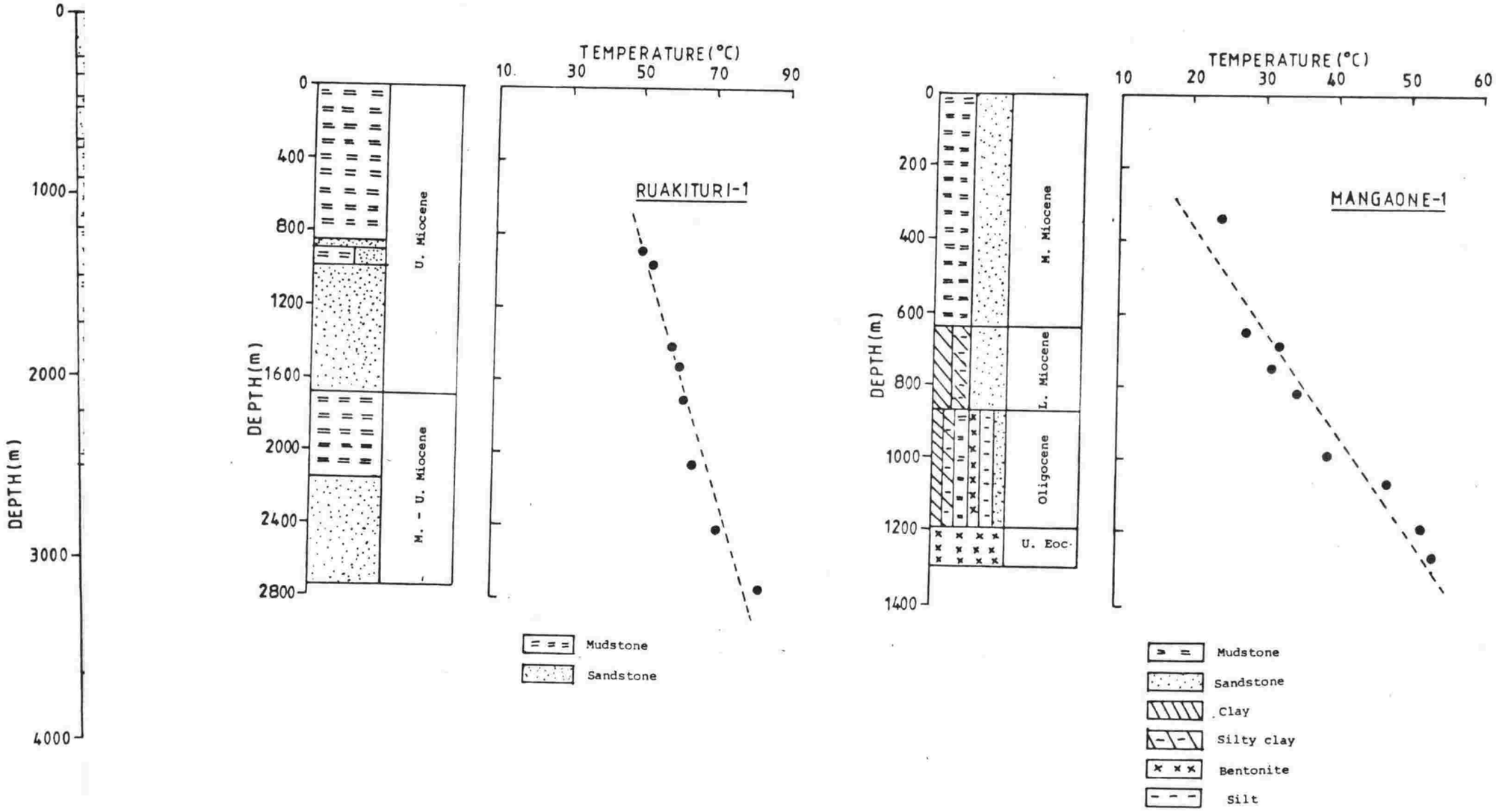
DEPTH(m)
0
1000
2000
3000
4000
DEPTH(m)
0
400
800
1200
1600
2000
2400
2800
U. Miocene
M. - U. Miocene
TEMPERATURE(°C)
10
30
50
70
90
RUAKITURI-1
Mudstone
Sandstone
DEPTH(m)
0
200
400
600
800
1000
1200
1400
M. Miocene
L. Miocene
Oligocene
U. Eoc.
TEMPERATURE(°C)
10
20
30
40
50
60
MANGAONE-1
Mudstone
Sandstone
Clay
Silty clay
Bentonite
Silt

Fig. 5.21

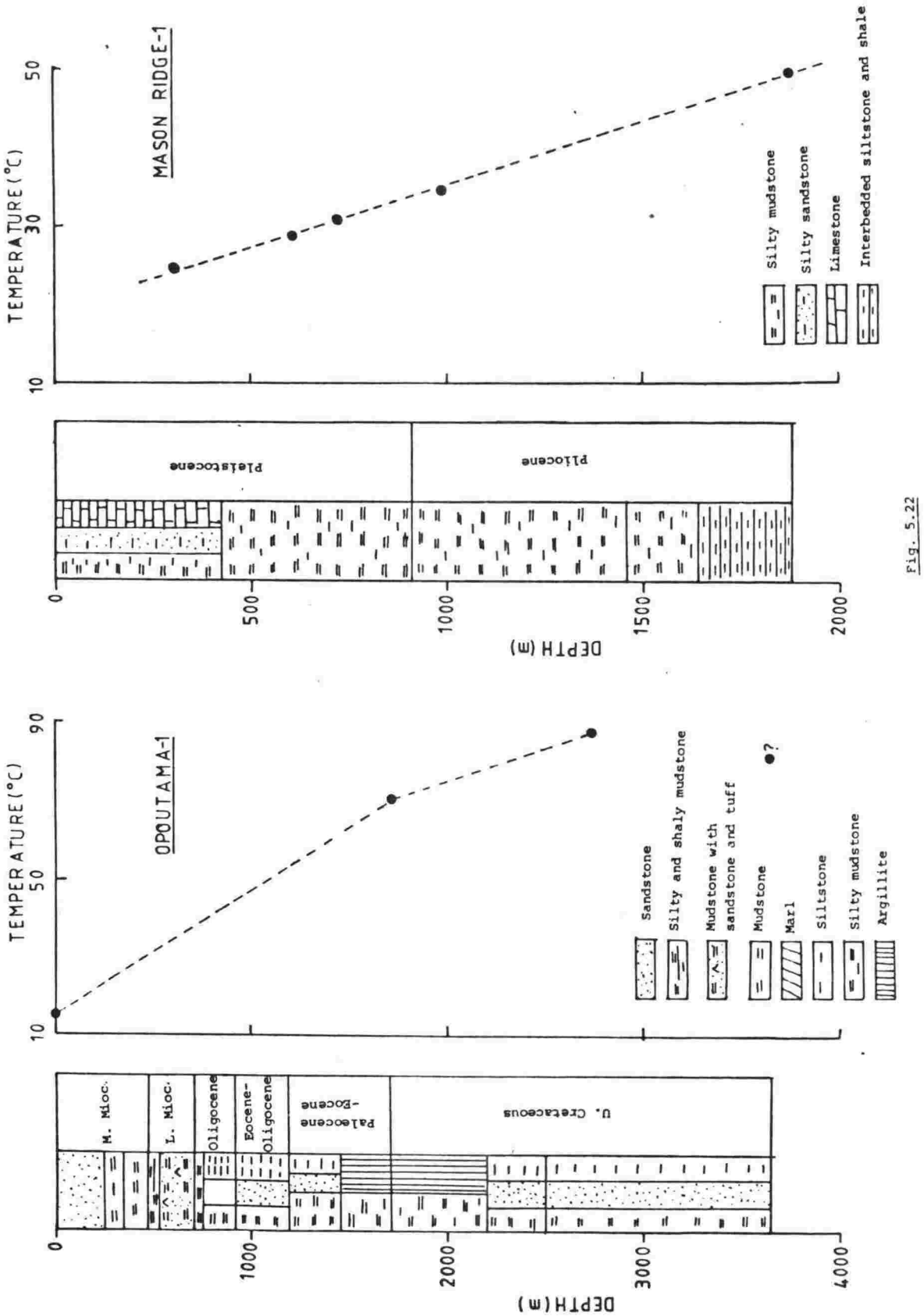
MASON RIDGE-1
TEMPERATURE (°C)
10
30
50
Silty mudstone
Silty sandstone
Limestone
Interbedded siltstone and shale
Pleistocene
Pliocene
0
500
1000
1500
2000
DEPTH (m)
OPOUTAMA-1
TEMPERATURE (°C)
10
50
90
Sandstone
Silty and shaly mudstone
Mudstone with sandstone and tuff
Mudstone
Marl
Siltstone
Silty mudstone
Argillite
M. Mioc.
L. Mioc.
Oligocene
Eocene-Oligocene
Paleocene-Eocene
U. Cretaceous
0
1000
2000
3000
4000
DEPTH (m)

Fig. 5.22

Taradale -1

This is a unique borehole, in which the measured temperatures decrease with depth (Appendix - I). The reasons for this decrease are not known. The borehole is reported to contain explosive gases. No heat flow could be determined for this location.

Mason Ridge -1, Ongaonga -1, Takapau -1

The temperature - depth relations and the lithologs of these boreholes are shown in figs. 5.22 and 5.23. A sedimentation correction has been applied to the measured geothermal gradients of all three boreholes. The corrected heat flow ranged from 35.6 mW/m^2 to 36.8 mW/m^2.

5.6 RANGIPO

This region is situated adjacent to the southern end of the Central Volcanic Region, in steep mountainous terrain. Permian-Triassic basement composed of greywacke and argillite is overlain by Waikoko alluvium (cobbles and pebbles), Taupo Pumice formation (rhyolitic pumice, boulders), and andesitic gravel and sands at some places. Heat flow has been measured at one location.

R-240

The temperature was measured about four years after drilling was completed to a depth of 99 m (fig. 5.24). Temperatures are disturbed in the upper 30 m. The heat flow has been calculated for the depth interval 55 - 89 m. A topographic correction was found necessary; the corrected heat flow is 87.6 mW/m^2.

5.7 CENTRAL VOLCANIC REGION

This region is considered to be a complex volcano-tectonic rift zone; it is flanked on both sides by mountain ranges consisting mainly of Mesozoic greywacke and argillites. The region contains numerous hot springs and geothermal fields associated with upflowing hot water at temperatures up to 300°C. Surface geothermal gradients elsewhere are often near zero because of the downflowing meteoric water (Studt and Thompson, 1969; Thompson, 1977). Heat flow is thus predominantly convective, with an average of about 700 mW/m^2 (Allis, 1979a), a value which is probably related to rhyolitic volcanism and a thin crust.

We have measured some further temperature profiles at a number of locations, and have found that the gradients are either zero or negative. Some typical profiles from non-geothermal areas, and two from geothermal areas, are shown in figs. 5.25 and 5.26 respectively. Temperatures from three boreholes in the vicinity of Mt Tihia have been used for heat flow

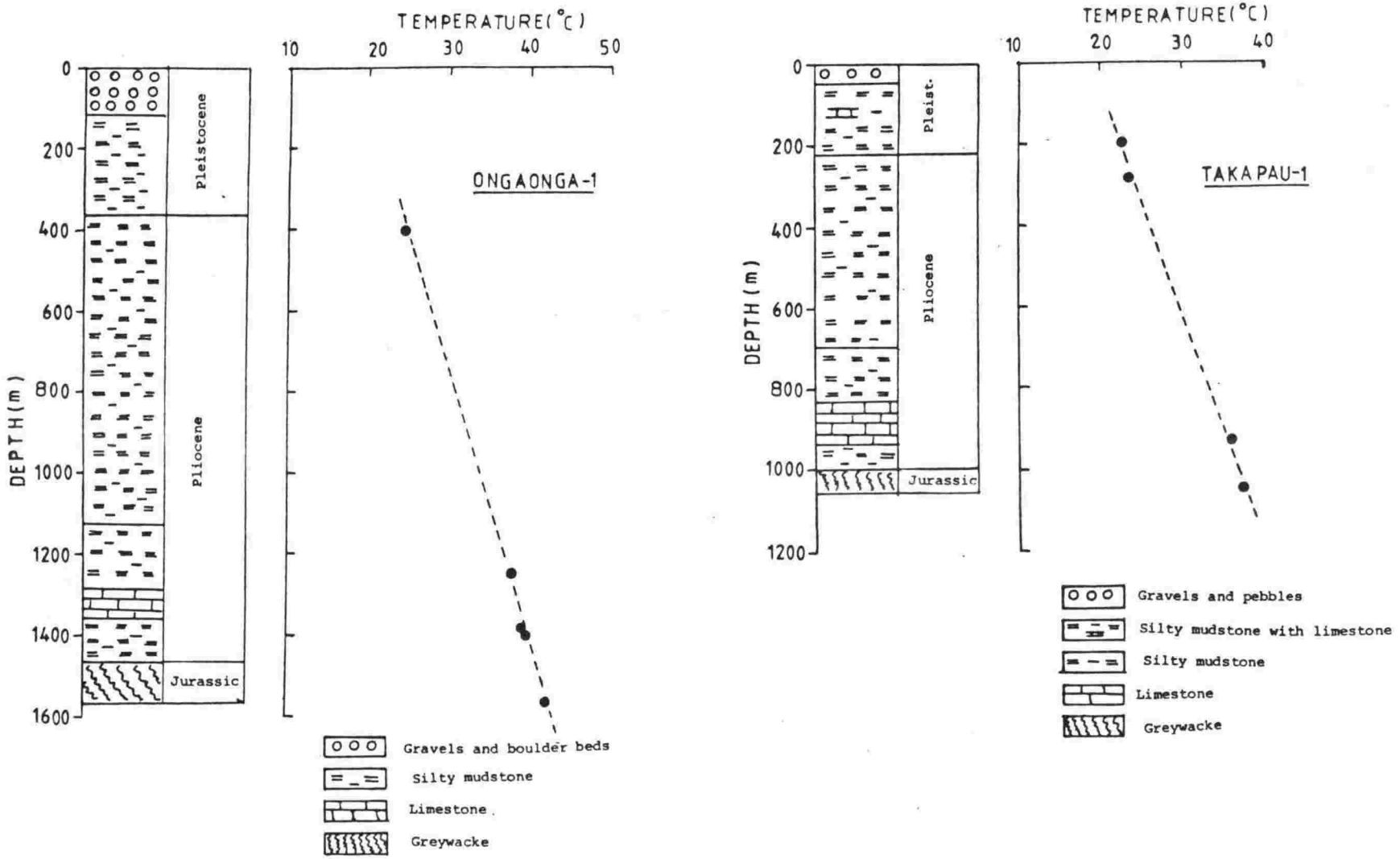
TEMPERATURE(°C)
10
20
30
40
50
0
200
400
600
800
1000
1200
1400
1600
DEPTH(m)
Pleistocene
Pliocene
Jurassic
ONGAONGA-1
Gravels and boulder beds
Silty mudstone
Limestone
Greywacke
TEMPERATURE(°C)
10
20
30
40
0
200
400
600
800
1000
1200
DEPTH(m)
Pleist.
Pliocene
Jurassic
TAKAPAU-1
Gravels and pebbles
Silty mudstone with limestone
Silty mudstone
Limestone
Greywacke

Fig. 5.23

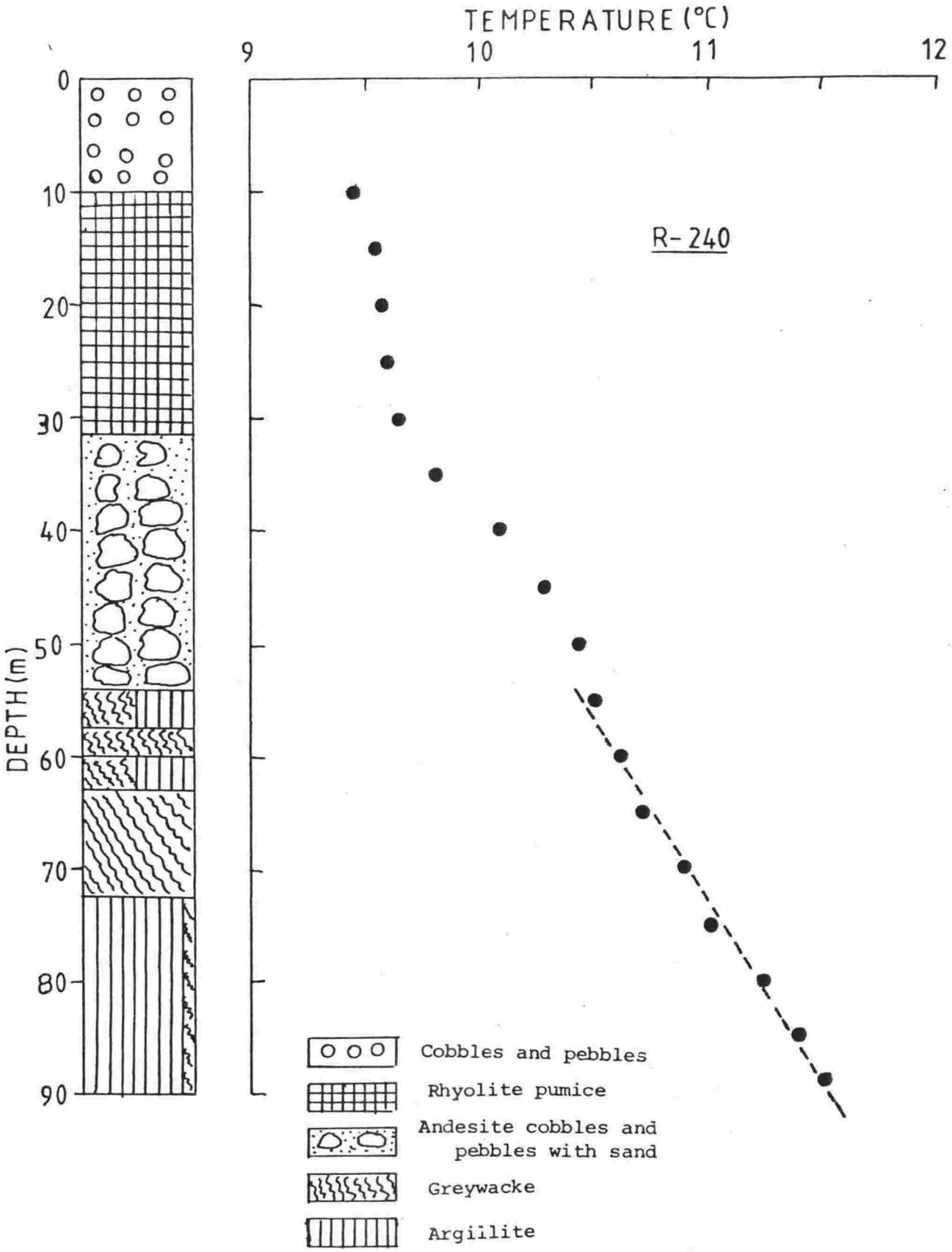
TEMPERATURE (°C)
9
10
11
12
0
10
20
30
40
50
60
70
80
90
DEPTH (m)
R-240
Cobbles and pebbles
Rhyolite pumice
Andesite cobbles and pebbles with sand
Greywacke
Argillite

Fig. 5.24

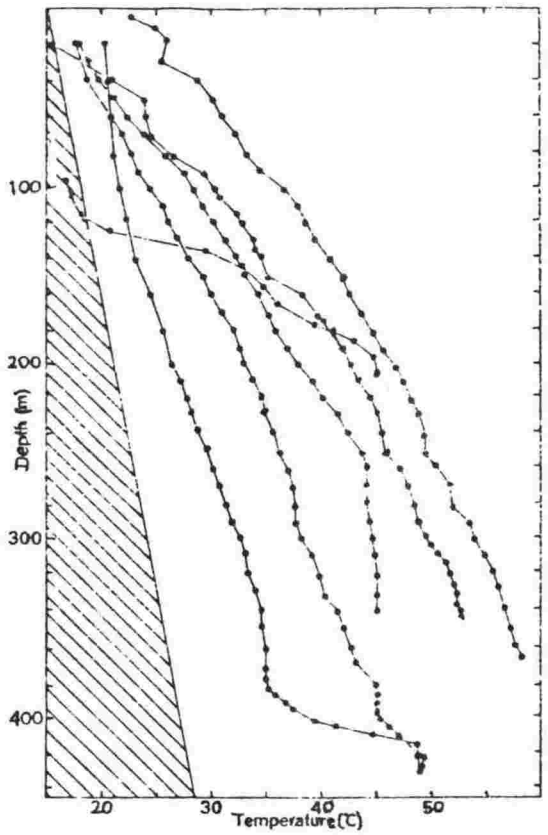

Fig. 5.25 Typical temperature profiles from Tauranga region. Right hand boundary of the shaded area shows a gradient of 30°C/km (after Thompson, 1980).

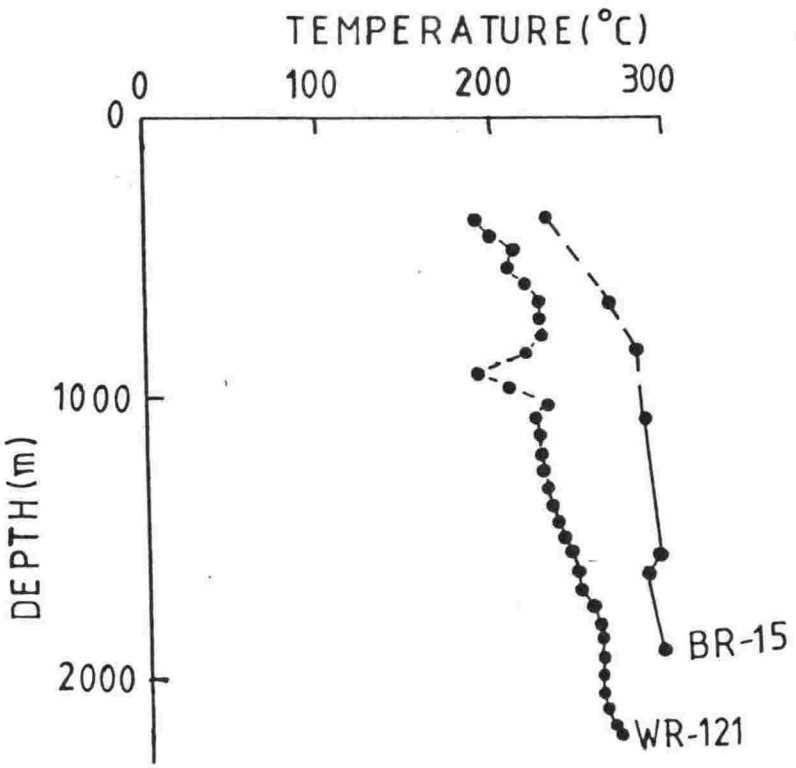

Fig. 5.26 Wairakei borehole WR-121 and Broadlands borehole BR-15 (after Smith, 1970).

determinations. These boreholes were drilled along the axis of the Tokaanu penstock tunnel, and passed through unaltered to highly altered andesites and andesite breecia. Samples for conductivity measurement were available from two boreholes.

Tokaanu F-5A, F-5C, F-10

Measured gradients were high, ranging from 189.66°C/km to 213.29°C/km. A topographic correction calculated for borehole F-5A comes to less than 1.5% and is thus neglected. Calculated heat flow values vary from 367.9 mW/m^2 to 415.9 mW/m^2. A temperature profile for one of the boreholes (F-5A) is shown in fig. 5.27.

5.8 PETONE - LOWER HUTT AREA

Temperatures have been measured in three unused exploratory boreholes which are located in a valley-like structure composed of young sediments. The valley is flanked on both sides by greywacke hills, and greywacke also forms the basement. Temperatures were unsatisfactory in one of the boreholes, which was blocked at 89 m.

UW -1 (Petone)

This hole was drilled to a depth of 311.2 m. Equilibrium temperatures were measured after 18 years of standing time, to a depth of 150 m, below which the hole seems to have collapsed. The measured profile is shown in fig. 5.28. Temperatures are disturbed to a depth of about 100 m, and exhibit a curvature around 60 m. For the depth interval in which the geothermal gradient was calculated, the litholog shows mainly greywacke, sand, sandy silt, clay and silty clay. Greywacke basement was met at 299 m. The conductivity has been measured on five representative specimens of the penetrated rock types collected from cliffs and surface outcrops in the area. A correction for the effect of sedimentation has been applied to the measured gradient.

UW -3 (Lower Hutt)

Equilibrium temperatures (fig. 5.28) were measured about 15 years after drilling finished. As with UW -1, the temperatures are disturbed in the upper parts. It is remarkable to see that the temperatures in the two wells, which are about 4km apart, are within about 0.15°C. The temperature gradient has been calculated between 115-175 m, where the rocks consist of silty to sandy clay, clay, claysand, peat, silt, sandy silt and greywacke. Greywacke basement was met at 175.3 m. The same conductivity is used as in the UW -1 borehole. A topographic correction was calculated but found to be insignificant (less than 3.5%). However, a sedimentation correction was found necessary.

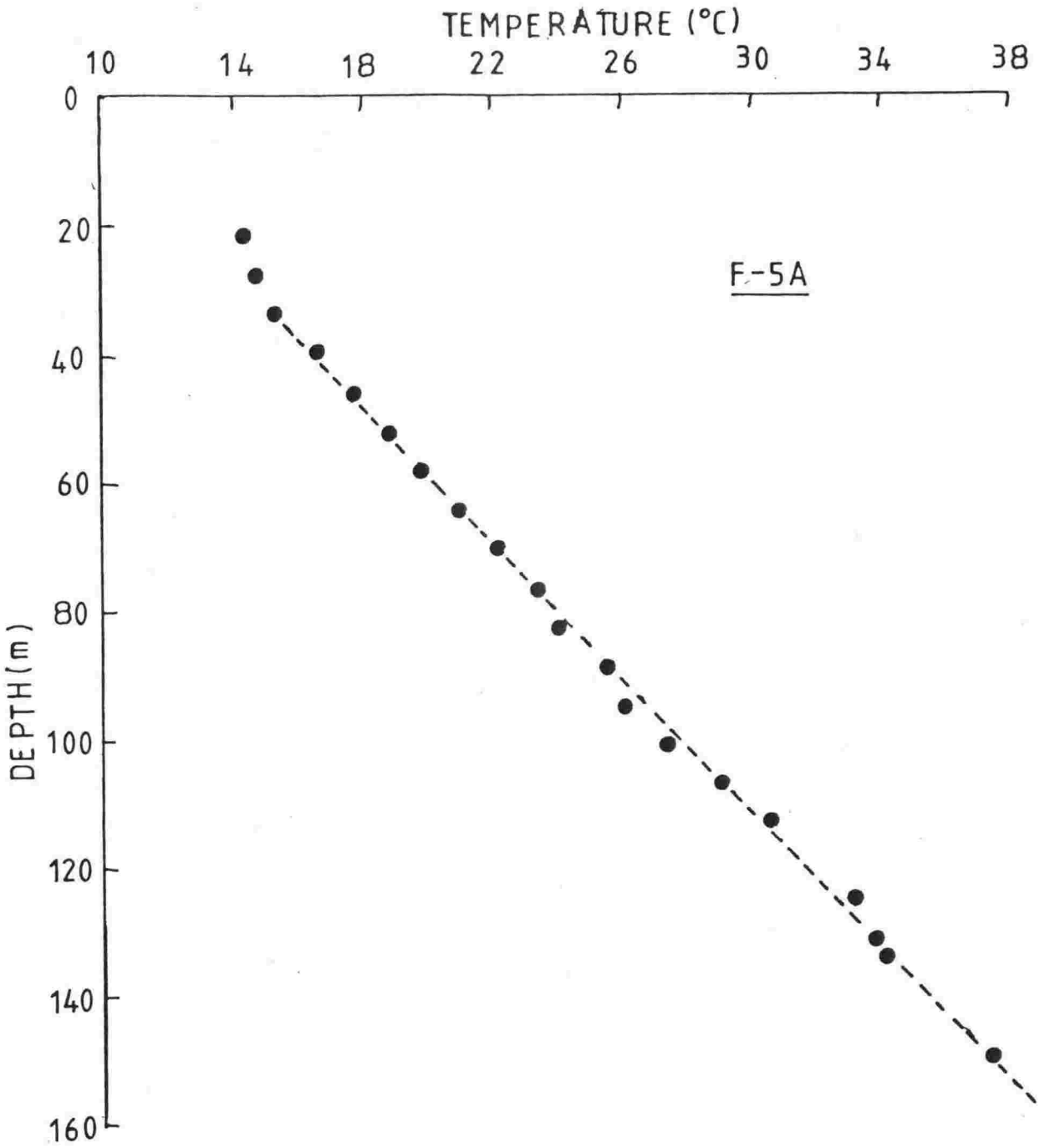

Fig. 5.27 (Data source: B. Hegan)

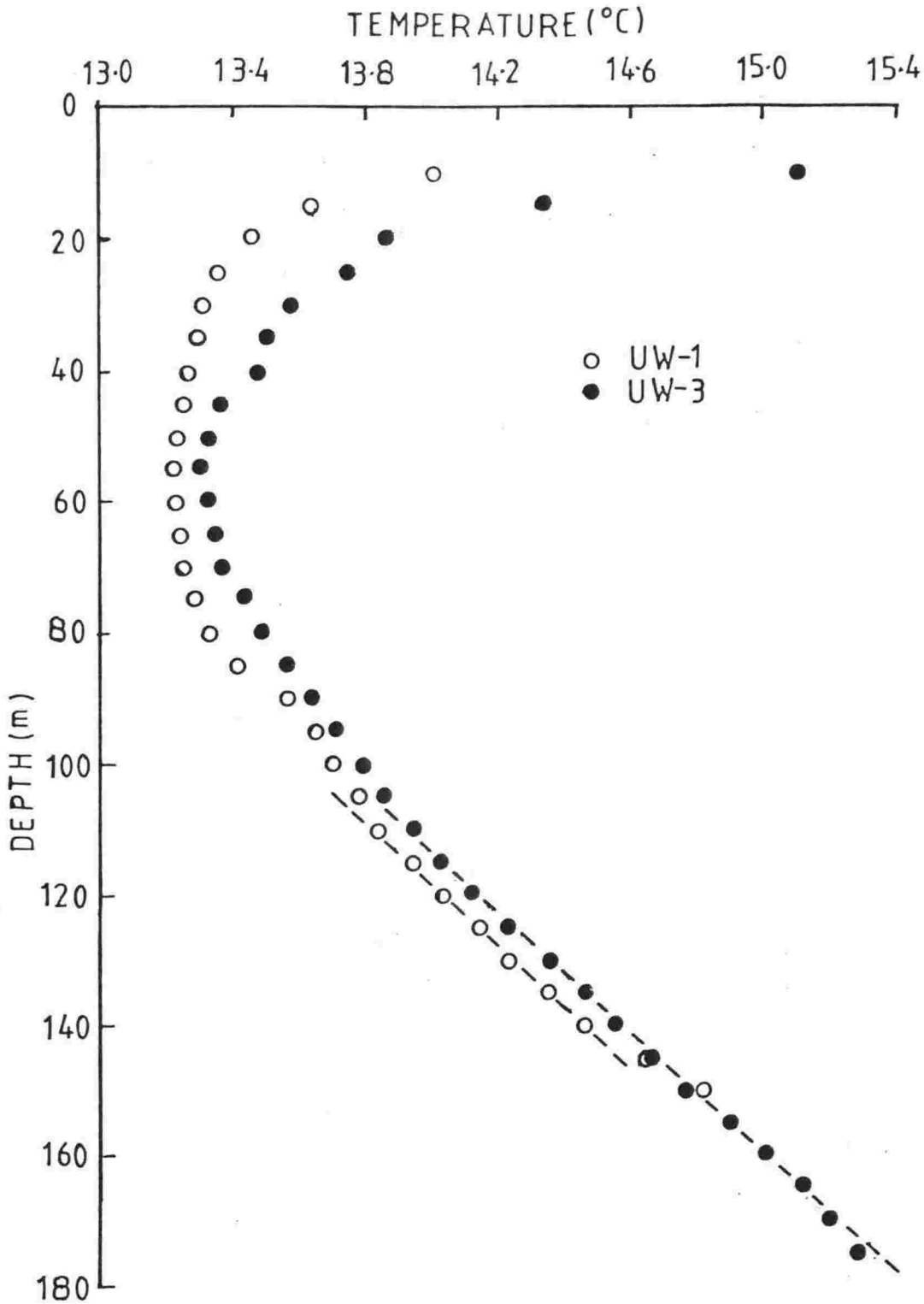
TEMPERATURE (°C)
13·0
13·4
13·8
14·2
14·6
15·0
15·4
0
20
40
60
80
100
120
140
160
180
DEPTH (m)
UW-1
UW-3

Fig. 5.28

CHAPTER 6

TERRESTRIAL HEAT FLOW IN THE SOUTH ISLAND

6.1 INTRODUCTION

The geology of the South Island differs considerably from that of the North Island, as mentioned in chapter 2. Except one, all the heat flow sites are located in four major sedimentary basins (fig. 5.1) — West Coast, Canterbury, Southland-Solander, and Great South Basin. The Great South Basin is wholly offshore while the others extend both onshore and offshore. The East and West Coast Basins of the North Island have been interpreted as continuing into the Canterbury and Westland Basins respectively (Kingma, 1959b; Katz, 1968). All the heat flow measurements are summarised in table 6.1, and the regional distributions of geothermal gradient and heat flow are shown in figs. 6.1 and 6.2 respectively. Temperature profiles and lithologs of specimen boreholes are shown in figs. 6.3 to 6.11, to which reference is included in the table. Temperature-depth data for all locations can be found in Appendix -2. Additional details for some bore holes are given in following sections.

6.2 BLENHEIM

Thompsons Ford

In a borehole which is situated a few kilometres away from Blenheim, temperature measurements were made about 4 years after drilling. The temperature profile, as shown in fig. 6.3, is disturbed to a depth of about 50 m.

6.3 WEST COAST BASIN

This major basin includes three smaller basins: the Westport-Karamea Basin, the Greymouth Basin and the Murchison Basin. Sediment thicknesses reaching more than 6000 m overlie a basement of paleozoic and Mesozoic sedimentary and volcanic rocks, granite and metamorphics. The area is stratigraphically complex. Throughout the Cretaceous and Tertiary, movements of some kind or other were in progress (Kingma, 1959b). Strong deformation has occurred over much of the area.

Due to extreme subsidence, Tertiary sedimentation (Upper Eocene - Upper Miocene) seems to be thickest in the Murchison Basin. The sediments of this basin are much denser (wet density 2.49 - 2.69 g/cm^3) and have lower porosities than most Tertiary rocks found in New Zealand. The most likely basement rocks are the Tuhua and Separation Point granite and the

Table 6.1 Heat flow data: South Island

Name of borehole	Location Lat.(S)	Location Long.(E)	Elevation (m)	Depth range (m)	N	Mean thermal conductivity (W/m°C)	Geothermal gradient (°C/km)	Heat flow (mW/m²)	Type of temperature data	Fig.
Blenheim										
Thompsons Ford	41°29'	173°56'	-	60-109.5	1	3.65	12.89±.39	47.0	Probe+	6.3
Westport-Karamea and Greymouth Basins										
Haku -1	42°13'	171°13'	-26.5	0-1618.5	5	2.51±.20	35.31	88.6±7.1	BHT+	-
Ahaura -2	42°22'	171°34'	55	0-1062.3	1	2.42	38.3	92.7	BHT+	-
Aratika -2	42°33'	171°26'	91	611.1-1142.6	-	3.10	34.05	105.6	BHT+	-
Aratika -3	42°33'	171°29'	116	0-1722.1	2	2.94	30.75	90.4	BHT+	-
Taramakau -1	42°35'	171°08'	31.4	1214.3-2117.1	11	3.12	32.60	101.7±10.5	BHT*	6.4
Arahura -1	42°44'	171°06'	45.4	522.4-1732.5	11	2.87	37.28	107±3.5	BHT*	6.4
Harihari -1	43°07'	170°28'	28.9	912.1-2519.6	8	2.40	25.47±1.42	61.1	BHT+	-
Waiho -1	43°18'	170°02'	3.9	1761.4-3744.5	5	2.79±.33	28.58±2.51	79.7±11.7	BHT+	6.5
Murchison Basin										
Murchison -1	41°49'	172°24'	-	249.9-396.2	-	2.85	30.78±.54	87.7	Probe+	6.6
Blackwater -1	41°51'	172°24'	-	176.8-420.6	6	2.86±.08	33.51±.36	95.8±2.9	Probe+	6.7
Bounty -1	41°52'	172°24'	269.1	1061.2-3116.4	17	2.91±.14	31.79±.74	92.5±4.9	BHT+	6.5
Canterbury Basin										
Kowai -1	43°10'	172°36'	130.8	393.1-1412.1	3	2.21	26.33	58.2±2.3	BHT*	6.8
Christchurch	43°33'	172°39'	-	125-150	-	1.95	22.8±1.08	44.5	Probe+	6.9
Leeston -1	43°41'	172°18'	43.9	0-1153.2	8	2.03	26.18	53.1	BHT+	-
Pendarves	43°57'	171°59'	-	110-151	9	1.95±.10	15.13±.13 18.25S	29.5±1.5 35.6S	Probe+	6.10
Resolution -1	44°11'	172°38'	-64	1135.3-1886.1	6	2.43±.21	24.76±4.25	60.2±11.6	BHT+	-
The Great South Basin										
Endeavour -1	45°14'	171°08'	-38.7	1170.4-2667.3	10	2.67±.34	32.86±.30	87.7±11.2	BHT+	-
Takapu -1A	46°10'	170°26'	-60.4	0-799.2	1	2.07	57.91	119.9	BHT+	-
Tara -1	47°19'	169°10'	-123.4	1235-4262	4	2.82±.28	30.91±2.02	87.2±10.4	BHT+	-
Toroa -1	47°27'	169°29'	-480.1	1234.7-4040.4	-	3.34	30.27	101.1±12.9	BHT*	6.8
Pakaha -1	48°15'	169°33'	-684.9	1173.8-2673.4	6	2.85	34.94	99.6	BHT+	-
Kawau -1A	48°56'	169°06'	-683.1	1235.4-3113.3	10	3.20	36.03	115.3±6.9	BHT*	6.11
Hoiho -1C	49°37'	169°37'	-656.8	822.4-1697.7	3	3.37	48.61	163.8	BHT+	-
Southland -Solander Basin										
J.T. Benny -1	46°10'	168°18'	42.7	817.8-1007.1	8	2.31	32.91	76.0	BHT+	-
Parara -1	46°37'	167°10'	-147.5	924.8-3619.5	6	2.47±.22	28.34±3.06	70.0±9.8	BHT+	6.11

± Refers to standard error

N Total number of samples

+ G-K method

* Resistance integral method

BHT Bottom hole temperature

Probe Conventional temperature probe

S Corrected for sedimentation effects

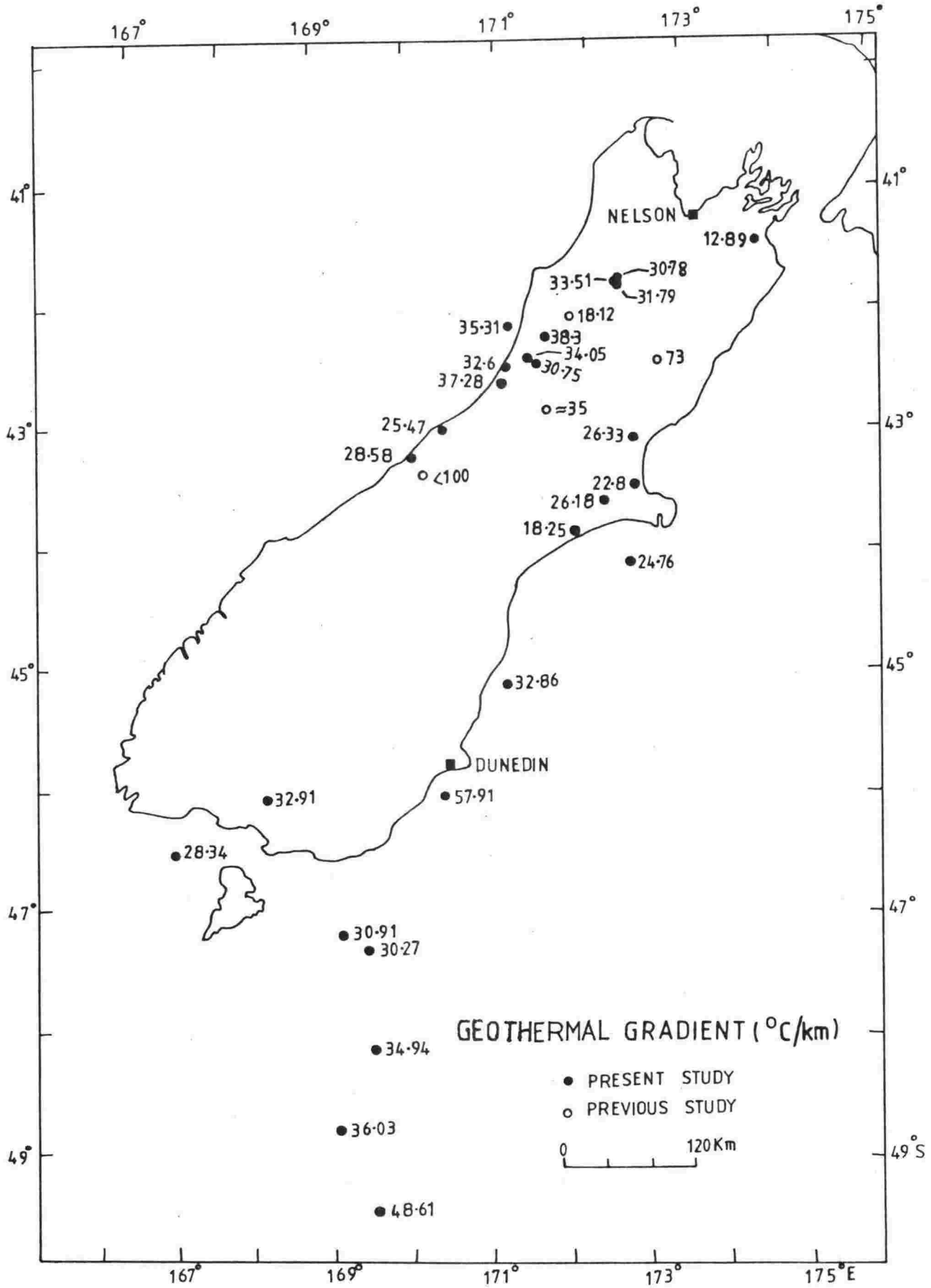

Fig. 6.1 Geothermal gradients: South Island. Data from previous studies are derived from Henderson (1917), Hilgendorf et al. (1919), Thompson (1966) and Dr R. Allis (pers. comm.).

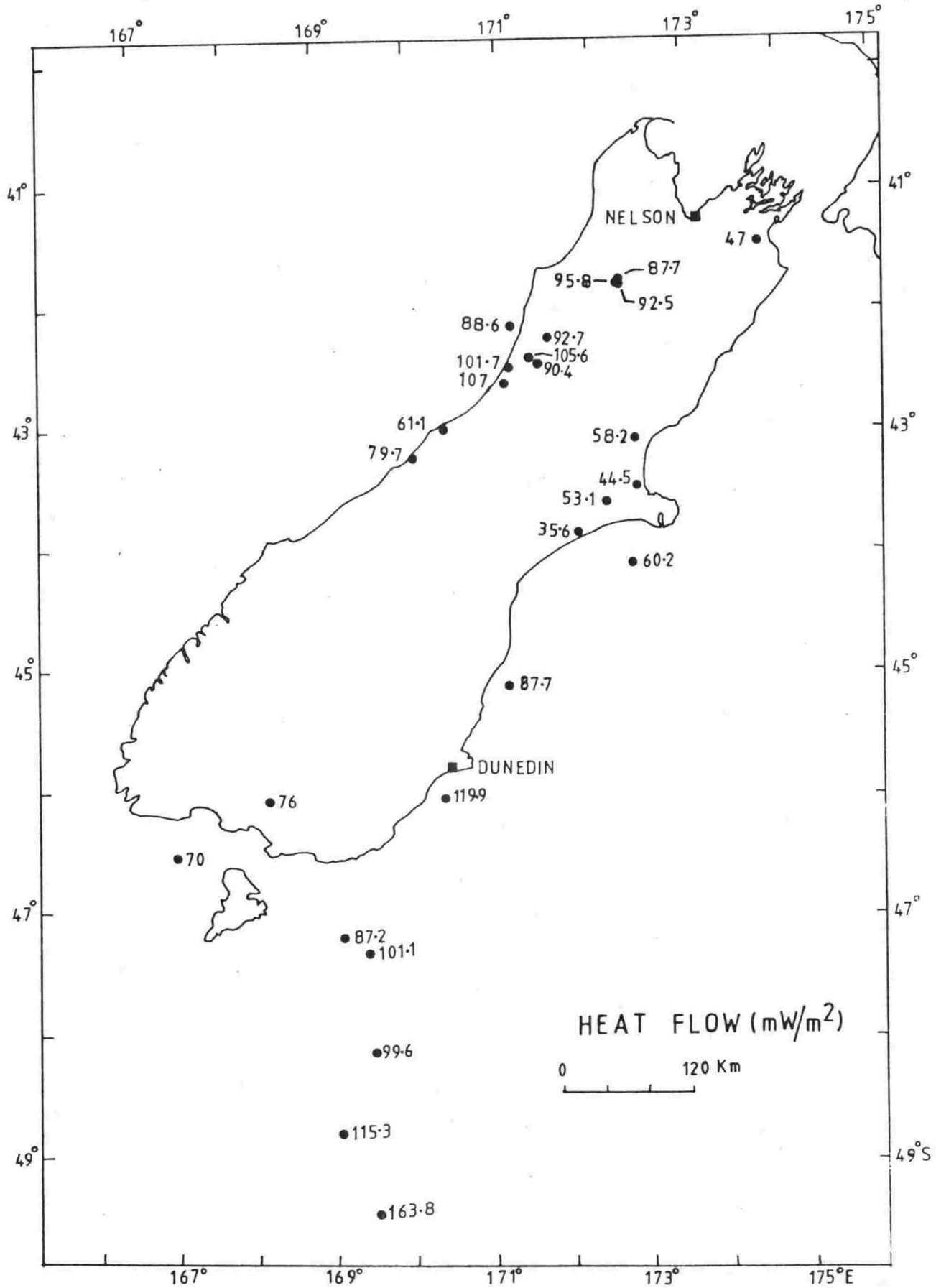

Fig. 6.2 Terrestrial heat flow: South Island.

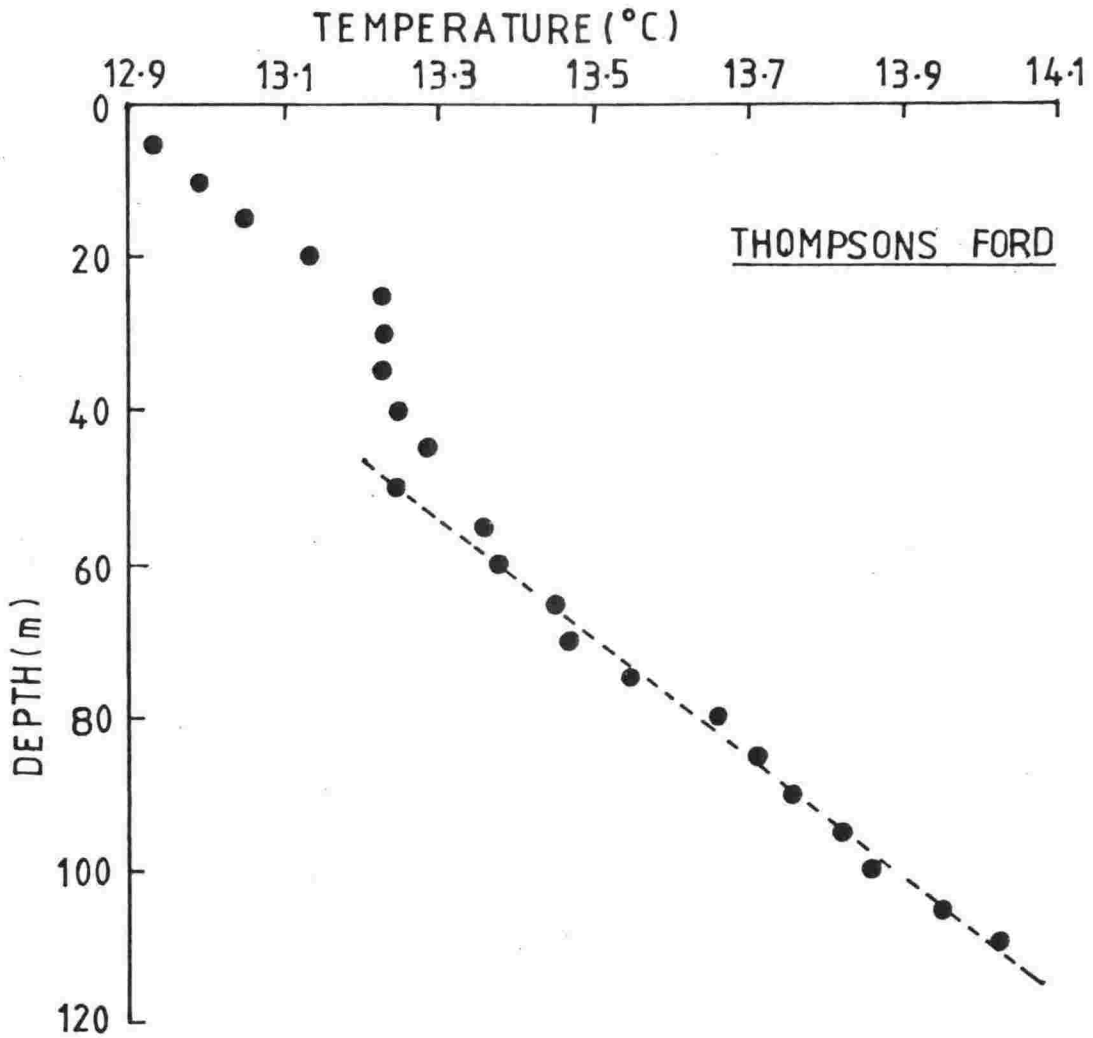
TEMPERATURE (°C)
12·9
13·1
13·3
13·5
13·7
13·9
14·1
0
20
40
60
80
100
120
DEPTH (m)
THOMPSONS FORD

Fig. 6.3

Rotoroa Igneous Complex, comprising diorite, granite and granodiorite.

Heat flow, which has been evaluated at 11 locations, ranged from 61.1 to 107 mW/m^2.

Westport-Karamea-Greymouth Basin

Haku -1

This borehole penetrated Eocene-Pleistocene mudstone, with small amounts of sandstone and siltstone, until it reached the Paleozoic basement at 1615.1 m. The basement is composed of quartzose green schist. No Oligocene rocks are found, Miocene rocks resting directly on the Eocene formation.

Ahaura -2

The rock types penetrated were mainly sandy conglomerates, sandstone and mudstone with small amounts of alluvial gravels, limestone and lignite. These formations are of ages up to Oligocene and rest on the Paleozoic basement of interbedded sandstone and argillite at 1043.1 m.

Aratika -2

The rock types between 631.6 m and 785.06 m are sandstone, silty shale, coal and conglomerate of Upper Cretaceous age. These overlie the Ordovician basement, which comprises interbedded sandstone and argillites of the Greenland group, and was drilled to 1142.06 m. The conductivity has been estimated from the nearest boreholes penetrating similar rocks.

Aratika -3

Lithologically this borehole differs considerably from the nearby Aratika -2, in that the entire Upper Cretaceous sequence is missing. The borehole penetrated mainly mudstone, sandstone, and conglomerate, with small amounts of gravels, siltstone and limestone (Oligocene - Recent), before reaching the Cambro-Ordovician basement, consisting of metasediments, at 1708.1 m.

Harihari -1

The geothermal gradient was determined between 912.1 m and 2519.6 m. The rocks are mainly mudstone and shale, with a little sandstone and limestone, until 2502.5m where argillite basement of the Greenland Group was reached.

Murchison Basin

Murchison -1

The temperature profile, measured several years after drilling, is shown in fig. 6.6, along with the litholog. The conductivity was estimated from Blackwater -1 borehole, which is situated within 2km.

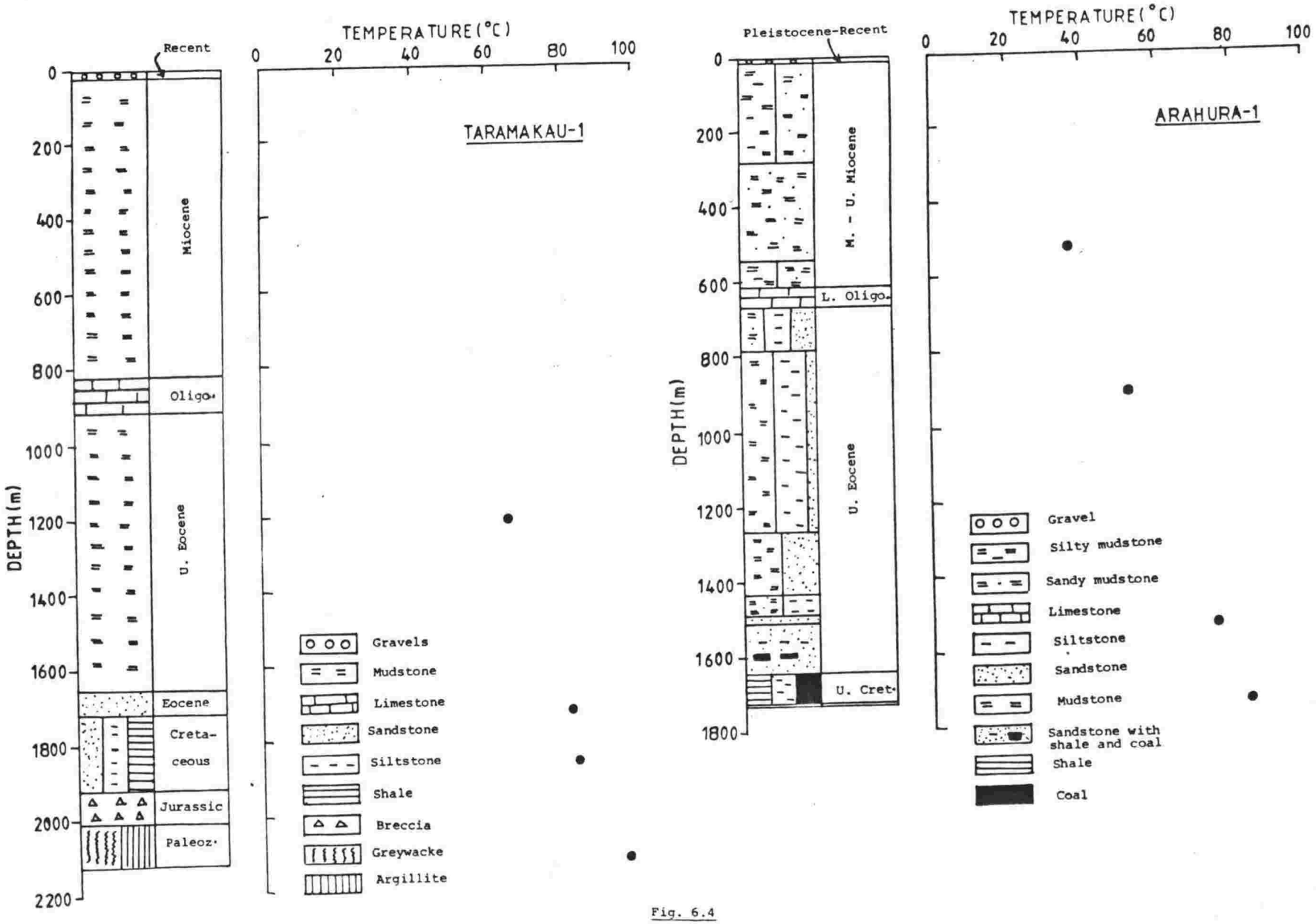
TEMPERATURE (°C)
0
20
40
60
80
100
TARAMAKAU-1
Recent
Miocene
Oligo.
U. Eocene
Eocene
Creta-ceous
Jurassic
Paleoz.
DEPTH (m)
0
200
400
600
800
1000
1200
1400
1600
1800
2000
2200
Gravels
Mudstone
Limestone
Sandstone
Siltstone
Shale
Breccia
Greywacke
Argillite
Pleistocene-Recent
M. - U. Miocene
L. Oligo.
U. Eocene
U. Cret.
ARAHURA-1
Gravel
Silty mudstone
Sandy mudstone
Limestone
Siltstone
Sandstone
Mudstone
Sandstone with shale and coal
Shale
Coal

Fig. 6.4

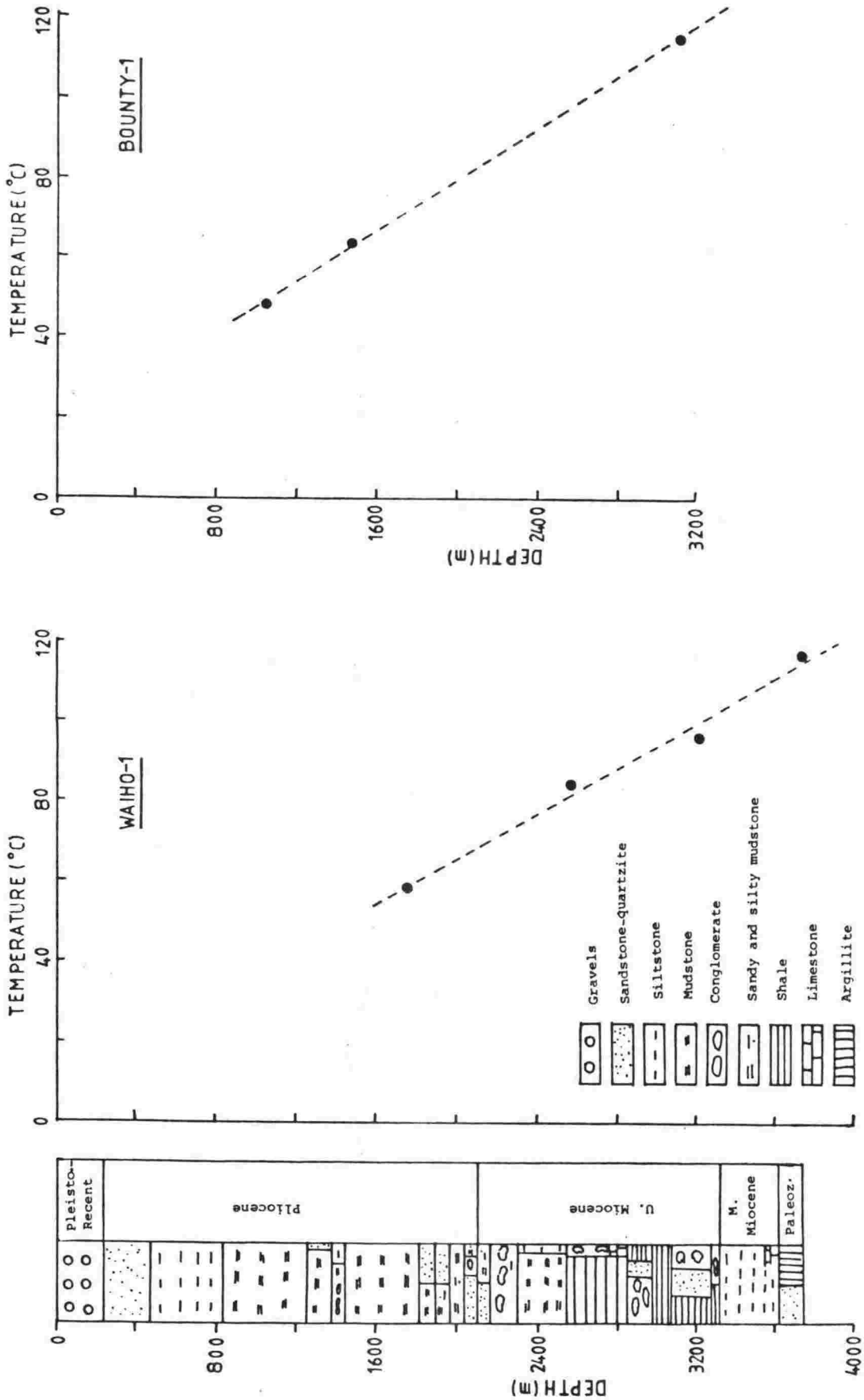
BOUNTY-1
TEMPERATURE (°C)
0
40
80
120
DEPTH (m)
800
1600
2400
3200
WAIHO-1
TEMPERATURE (°C)
0
40
80
120
DEPTH (m)
800
1600
2400
3200
4000
Pleisto-Recent
Pliocene
U. Miocene
M. Miocene
Paleoz.
Gravels
Sandstone-quartzite
Siltstone
Mudstone
Conglomerate
Sandy and silty mudstone
Shale
Limestone
Argillite

Fig. 6.5

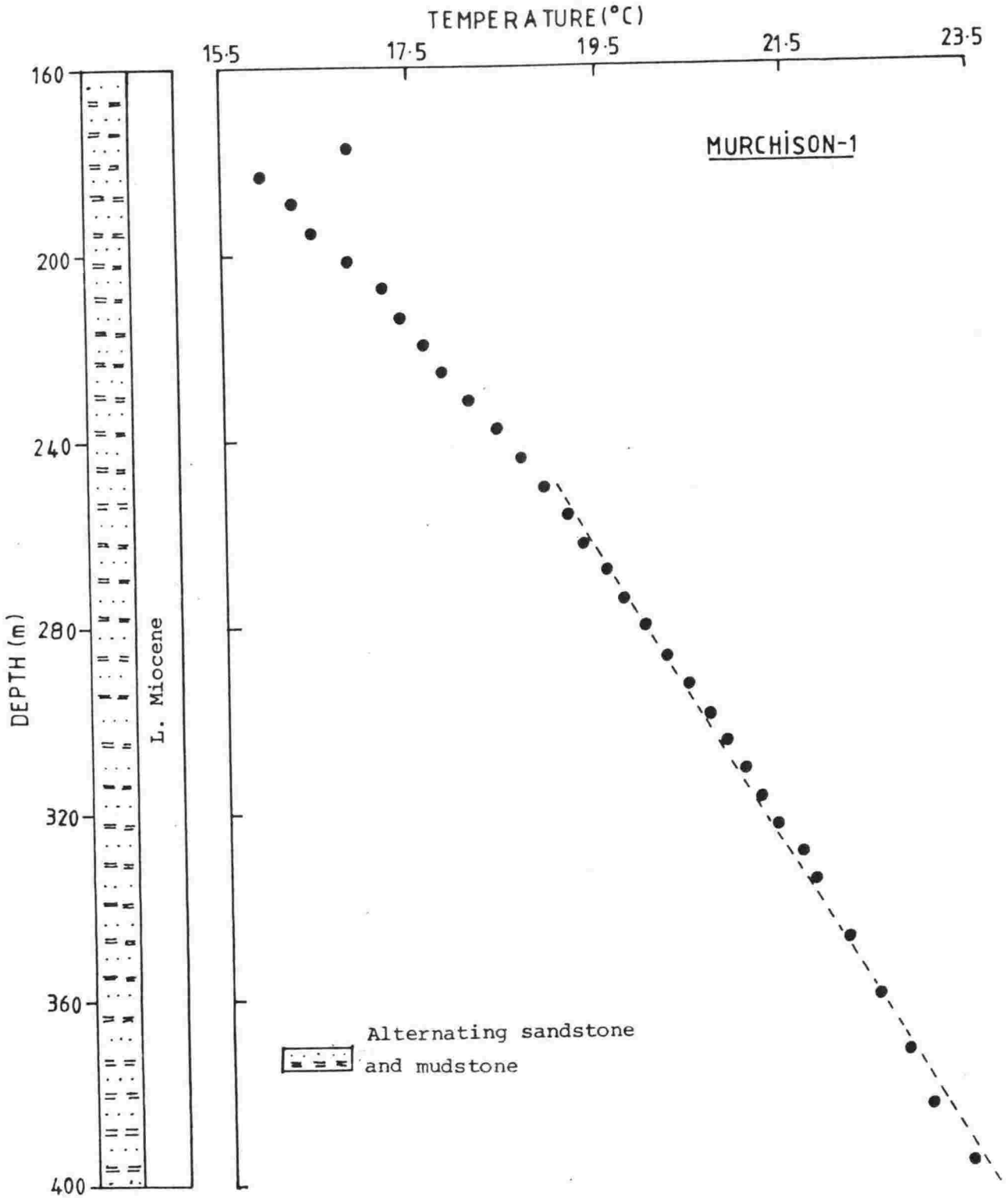

Fig. 6.6 (Data source: Mr G.E.K. Thompson)

Blackwater -1

As fig. 6.7 shows, the upper section of the profile seems to be disturbed to a depth of about 120 m.

Bounty -1

This borehole is located approximately 1.6 km from Blackwater -1 and 4km south of Murchison -1. It penetrated heavily indurated siltstone and mudstone with sandstone bands, of Oligocene-Miocene age. The temperature profile is shown in fig. 6.5. It is interesting to see that the heat flow of 92.5 ± 4.9 mW/m^2 obtained at this location, using bottom-hole temperatures, agrees quite well with the heat flow of 87.7 mW/m^2 and 95.8 ± 2.9 mW/m^2 measured at Murchison -1 and Blackwater -1 respectively, where temperatures have been used which were measured after several months or more.

6.4 CANTERBURY BASIN

This basin extends about 320km along the central eastern region of the South Island. A great thickness of sedimentary rocks, the shallowest being young alluvial gravels, lie on a basement consisting of folded Triassic-Jurassic greywacke, argillite, basic volcanics, rhyolitic and andesitic complexes, and syenitic to gabbroic intrusions. Heat flow has been determined for five locations in this Basin.

Kowai -1

Stratigraphically this well differs from the nearby Leeston -1 well in that no volcanics were found. Penetrated rock types and temperatures are shown in fig. 6.8.

Christchurch

The temperature measurement was performed several years after drilling. The measured profile is shown in fig. 6.9; it is disturbed in the upper section, presumably because of groundwater circulation. The borehole penetrated clay, sand and gravel. In the absence of samples, the thermal conductivity has been adopted from the Pendarves borehole.

Leeston -1

This borehole penetrated gravels, volcanics, sandstone and siltstone of Pliocene - Pleistocene age, overlying the Mesozoic greywacke basement at 1108.4 m.

Pendarves

This borehole penetrated silty to sandy clay, silts, sands and silty to sandy gravels. The temperature was measured about 5 months after drilling (fig. 6.10). The upper part of the profile shows a curvature at about 65 m. A sedimentation correction has been applied

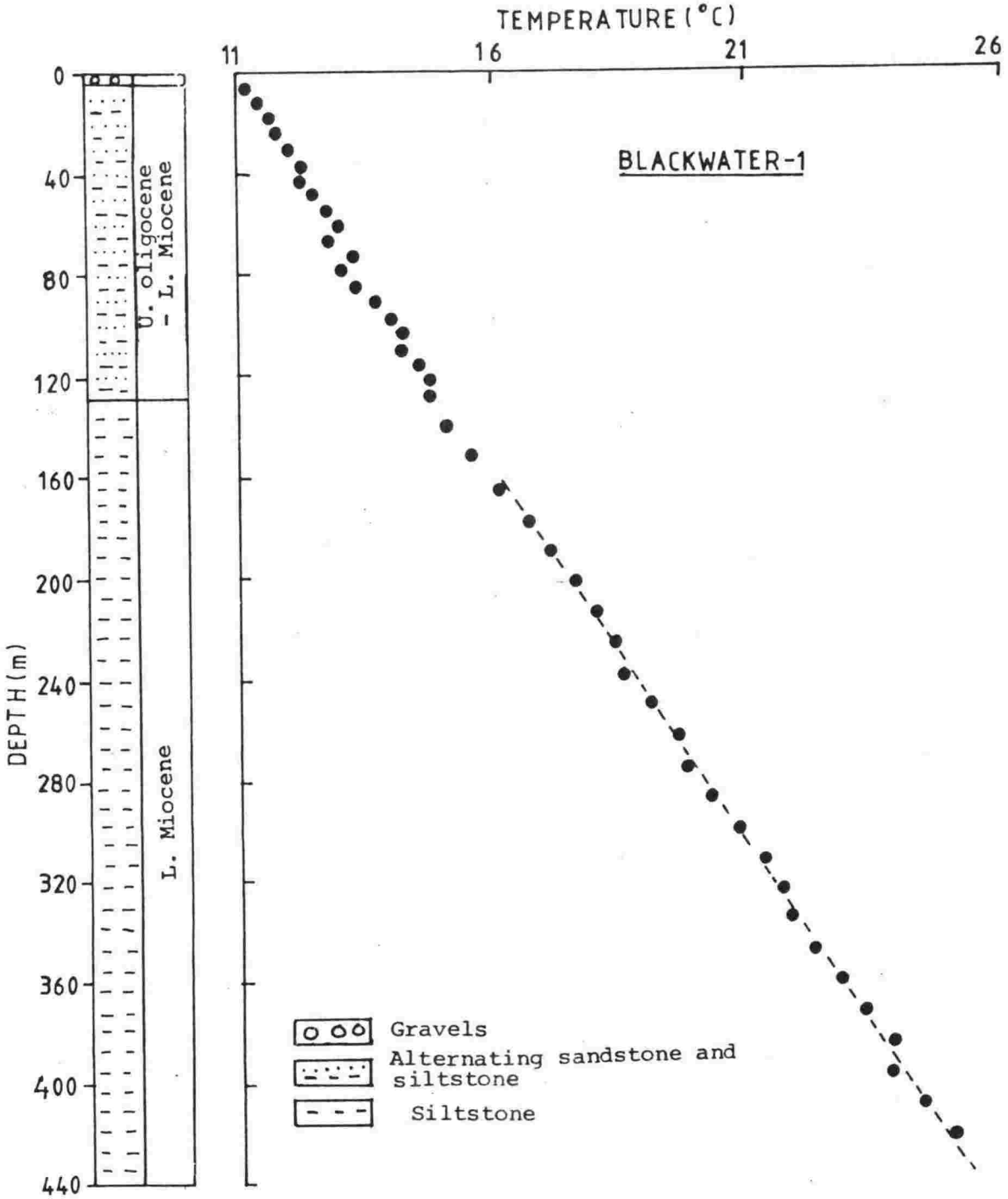

Fig. 6.7 (Data source: Mr G.E.K. Thompson)

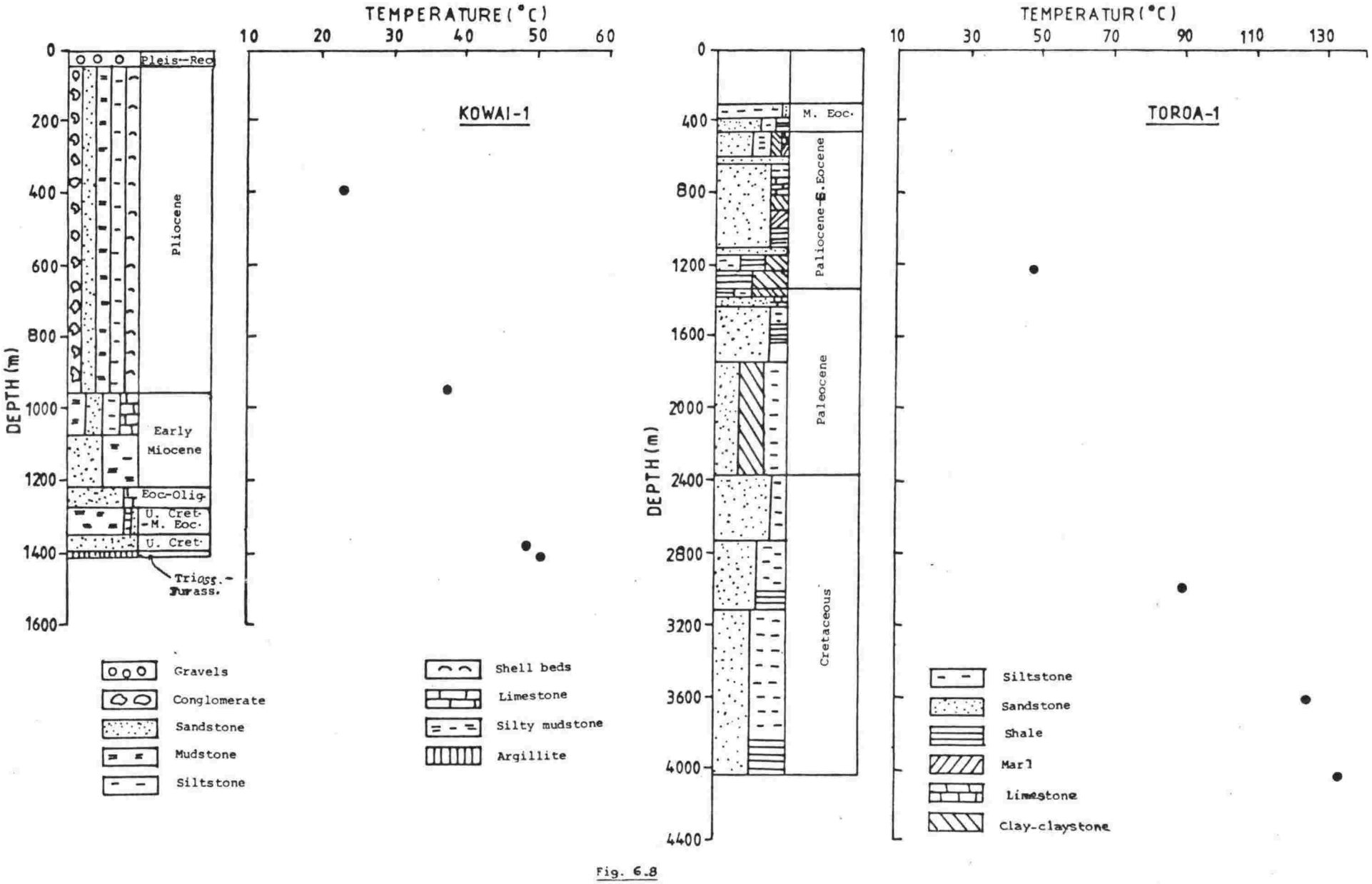
TEMPERATURE (°C)
10 20 30 40 50 60
KOWAI-1
DEPTH (m)
0 200 400 600 800 1000 1200 1400 1600
Pleis-Rec
Pliocene
Early Miocene
Eoc-Olig
U. Cret-M. Eoc.
U. Cret
Triass.-Jurass.
Gravels
Conglomerate
Sandstone
Mudstone
Siltstone
Shell beds
Limestone
Silty mudstone
Argillite
TEMPERATUR (°C)
10 30 50 70 90 110 130
TOROA-1
DEPTH (m)
0 400 800 1200 1600 2000 2400 2800 3200 3600 4000 4400
M. Eoc.
Paliocene-E. Eocene
Paleocene
Cretaceous
Siltstone
Sandstone
Shale
Marl
Limestone
Clay-claystone

Fig. 6.8

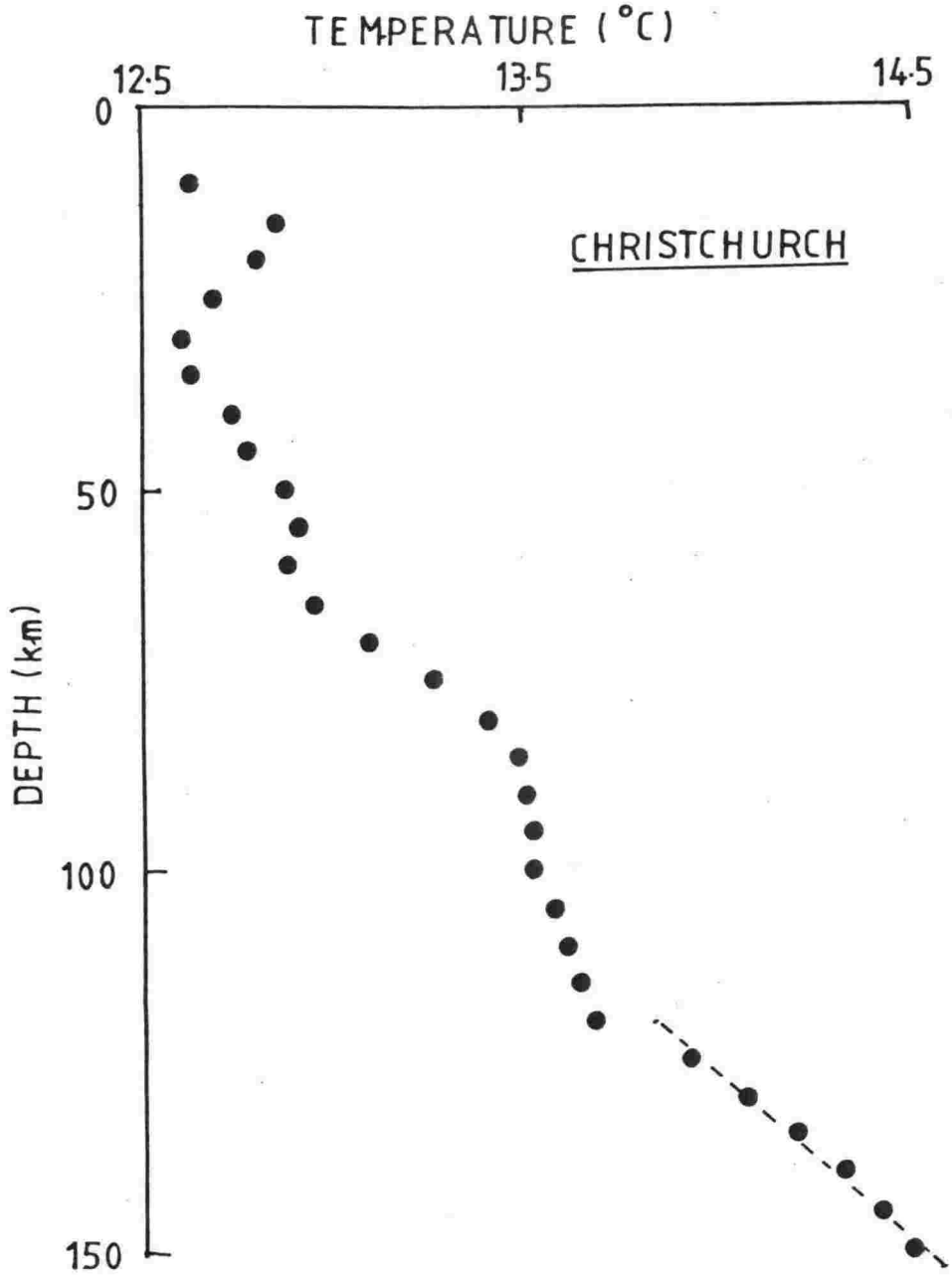

Fig. 6.9

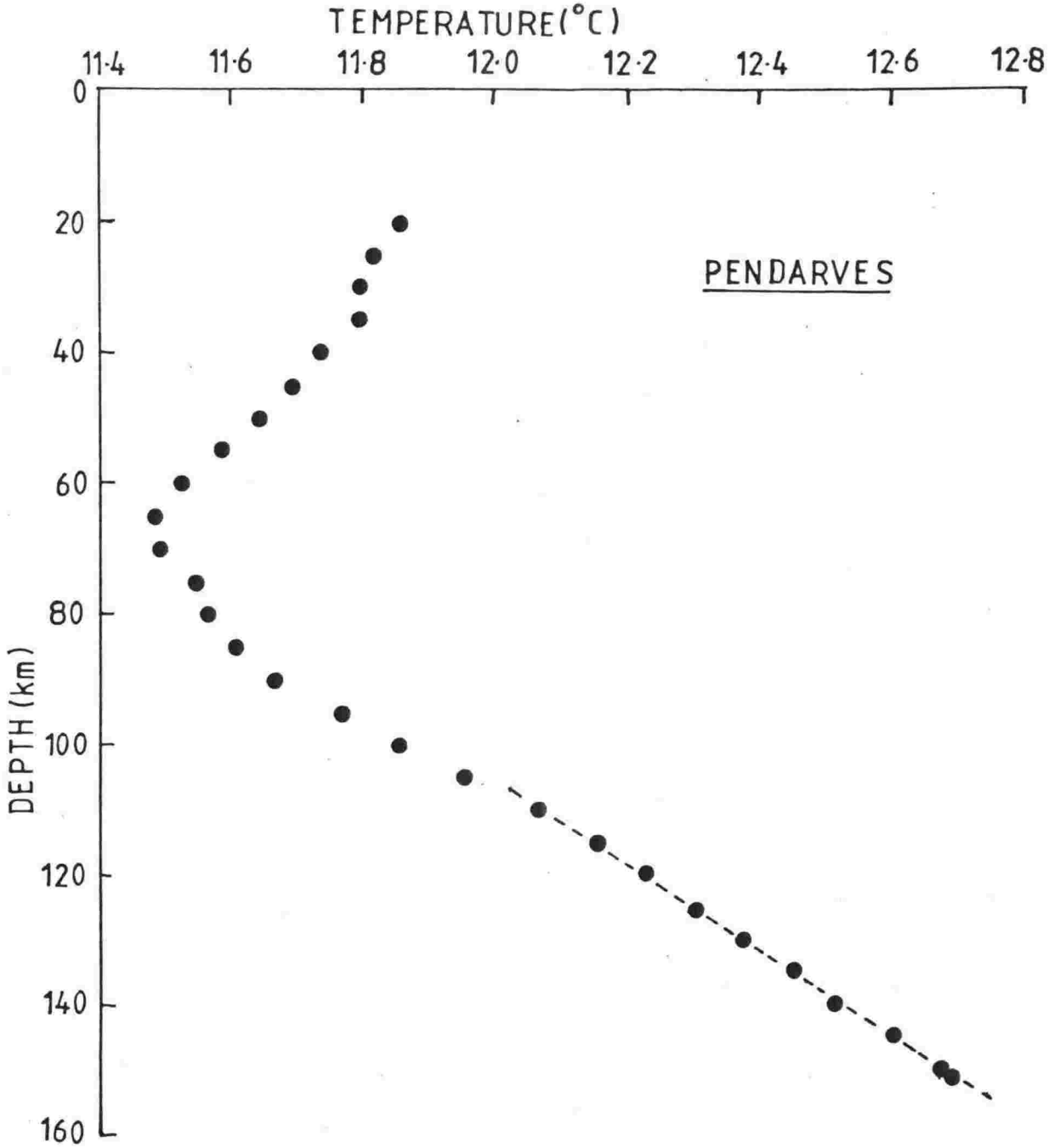
TEMPERATURE(°C)
11·4
11·6
11·8
12·0
12·2
12·4
12·6
12·8
0
20
40
60
80
100
120
140
160
DEPTH (km)
PENDARVES

Fig. 6.10

to the measured gradient.

Resolution -1

Penetrated rock types in the interval 1135.3 and 1886.1 m are silts, sandy siltstone, silty clay, limestone, mudstone and sandstone extending back to Upper Cretaceous in age. The borehole bottomed in a Miocene igneous intrusion which consists of quartz syenogabbro and teschenite. The nearest igneous rocks, at Banks Peninsula, are dated as 5.8 to 12 Myr old (Stipp and McDougall, 1968).

6.5 GREAT SOUTH BASIN

This basin is the largest submarine structural basin off the South Island, covering an area of 98500 sq. km., and bordering the canterbury Basin in the North. It contains more than 5000 m of Tertiary and Cretaceous sediments (Sanford, 1980), which rest on Jurassic-Paleozoic basement, mainly composed of metasediments, schist, granite and gneiss. The basin has its origin in the Upper Cretaceous to Early Tertiary. 7 boreholes drilled for petroleum exploration have been utilised for heat flow determinations.

Endeavour -1

The temperature gradient has been determined between 1174 m and 2667.3 m, where the strata are mainly mudstone with some siltstone, sandstone, tuff, coal and schist. The hole terminated in quartz-feldspathic sandstone of Upper Cretaceous age.

Takapu -1A

Penetrated rock types are sandstone, clay, marl, shale, sandy silt and siltstone of Eocene - Miocene age down to 759 m, where the drill struck Late Paleozoic Otago Schist basement.

Tara -1

Rock types in the interval of the temperature gradient calculation are Upper Cretaceous - Eocene sequences of sandstone, shale, clay-claystone, siltstone and coal. These formations overlie a granitic basement, which is dated as 115 Myr old, at 4233.4 m.

Toroa -1

Temperatures and lithologs are shown in fig. 6.8. The conductivity has been estimated from Pakaha -1 and Tara -1. Seismic and magnetic investigations have indicated the occurrence of an ultrabasic dike near this location.

Pakaha -1

This borehole was drilled in water 684.9 m deep over a prominent, seismically mapped, horst feature. Heat flow has been calculated between 1173.8 m and 2673.4 m, where the rock types are Cretaceous - Eocene siltstone, sandstone, shale and clay-claystone. The granitic basement, 92 Myr old, is at 2599 m. This granite is muscovite-bearing and is similar to that found at Stewart Island and The Snares. It probably forms a part of a batholith extending from Stewart Island towards The Snares and Auckland Islands.

Kawau -1A

Fig. 6.11. A sample from 3111.7 m was found to be pale grey indurated quartzose siltstone dated 291.7 ± 6.4 Myr this is possibly an equivalent of the Greenland Group.

Hoiho -1C

This is the southernmost borehole in the Basin. A high geothermal gradient has been found between 822.4 and 1697.7 m, where the rocks consist mainly of sandstone and shale with some limestone, cherts, clay-claystone and conglomerates of Cretaceous-Miocene age. These rocks overlie Ordovician schist of the Greenland group at 1590.1 m. The metamorphic grade of the rock is very low and the likely cause of the metamorphism is the thermal effect of a nearby Cretaceous intrusive body (Hunt International Petroleum Company, 1978). Seismic surveys have shown a very strong reflection at 1811.4 m depth. The observed heat flow of 163.8 mW/m^2 is the highest so far recorded in New Zealand, if we exclude the Central Volcanic Region.

6.6 SOUTHLAND - SOLANDER BASINS

These basins are situated at the southern tip of the South Island. The Southland Basin covers an area of about 5600 sq km; the basement is made up of Paleozoic metamorphic and igneous rocks, and Permian-Jurassic sediments. There are more than 2km of sediments. In the Solander Basin, which lies offshore, the sedimentary thickness is greater than 3km. Complete Tertiary sequences have been encountered and they probably overlie the same Paleozoic gneissic basement found in Parara -1 (fig. 6.11). Heat flow has been determined at two places, one in each Basin.

J.T. Benny -1

The temperature gradient has been measured between 817.8 m and 1007.1 m, where the rocks are Oligocene sandstone, shale and lignite overlying Mesozoic greywacke basement at 995.8 m.

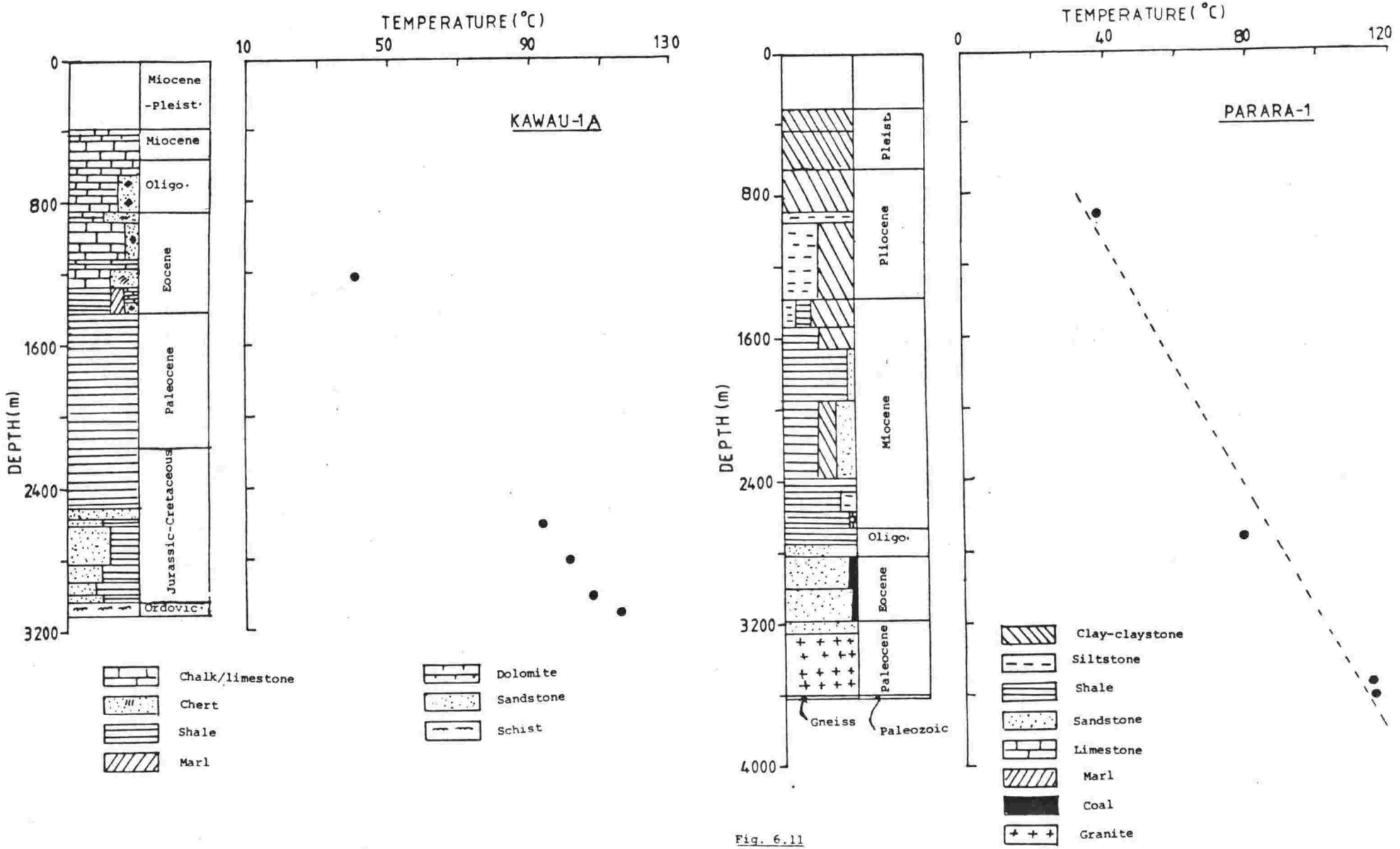
TEMPERATURE (°C)
10
50
90
130
KAWAU-1A
DEPTH (m)
0
800
1600
2400
3200
Miocene -Pleist.
Miocene
Oligo.
Eocene
Paleocene
Jurassic-Cretaceous
Ordovic.
Chalk/limestone
Chert
Shale
Marl
Dolomite
Sandstone
Schist
TEMPERATURE (°C)
0
40
80
120
PARARA-1
DEPTH (m)
0
800
1600
2400
3200
4000
Pleist.
Pliocene
Miocene
Oligo.
Eocene
Paleocene
Gneiss
Paleozoic
Clay-claystone
Siltstone
Shale
Sandstone
Limestone
Marl
Coal
Granite

Fig. 6.11

CHAPTER 7

RADIOACTIVE HEAT GENERATION, HEAT FLOW AND TEMPERATURE PROFILES

7.1 INTRODUCTION

Of the parameters to which heat flow is related, radioactive heat generation of the crustal rocks is one of the most important. It is the main source of the heat flow and any anomaly within a heat flow province is mainly attributable to differences in the heat-generating elements of the crustal rocks. Radioactive heat generation (A) depends upon the amount of uranium, thorium and potassium present in the rock. Uranium and thorium are normally present as trace elements and their concentration does not exceed a few tens of parts per million (ppm), while potassium is often present as a major element. Heat generation is known to be the highest in acid rocks and lowest in ultrabasics; thus the deeper parts of the crust, and the upper mantle, contain very low radioactivity. Heat generation plays an important role in the calculation of the deep temperature profile.

In New Zealand little work has been done in this field apart from the studies by Duncan (1970), Ewart and Stipp (1968), and Ewart et al. (1968), on rocks of the Central Volcanic Region. We therefore have carried out a detailed study of the radioactive content of different rocks in order to examine its relationship with heat flow and other parameters.

7.2 MEASUREMENTS OF URANIUM, THORIUM AND POTASSIUM

Concentrations of uranium (U), thorium (Th) and potassium (K) can be measured by means of γ-ray spectrometer, neutron activation, XRF spectrometer, or isotope dilution. In this study measurements of U, Th and K by the XRF method were performed at the University's Analytical Facility. For the U and Th measurements, after an initial calibration, seven rock samples were run at a time along with one "Spetrosil" (ultra pure SiO_2 glass blank) and one international rock standard. The rock standard was used to determine repeatability; the mean and standard deviations are shown in table 7.1 where recommended values are also included. For the K determinations a linear calibration was set up using approximately ten international rock standards. Measured and recommended values of the standards are also given in table 7.1 With the rocks collected for this thesis, the same sample was used for both determinations. Abundance of U, Th and K were

Table 7.1 Measurements of U, Th and K on the international rock standards by XRF method.

(A) Measurements of U and Th

NAME OF STANDARD	N	MEAN U (ppm)	RECOMMENDED* U (ppm)	MEAN Th (ppm)	RECOMMENDED* Th (ppm)
STM-1	30	10.18 ± 1.30	9.07 ± .07	30.11 ± .90	33 ± 5
RGM-1	16	6.93 ± 0.50	5.84 ± .07	16.33 ± 0.53	16 ± 2
SDC-1	8	3.69 ± 0.70	3.02 ± .10	13.13 ± 0.73	12 ± .4

(B) Measurements of K

NAME OF STANDARD	MEASURED K (%)	RECOMMENDED+ K (%)
AGV-1	2.41	2.42
GSP-1	4.40	4.57
BCR-1	1.41	1.41
JB-1	1.25	1.18
JG-1	3.32	3.29
BEN	1.25	1.16
ANG	0	.11
SDC-1	2.66	2.74
STM-1	3.65	3.57
NIM-S	13.03	12.74
BHVO-1	.41	.44
BR	1.22	1.17
QLO-1	2.97	3.01
RGM-1	3.76	3.57
NIM-G	4.24	4.14
GA	3.25	3.34

N is the number of observations

± refers to standard deviation

* Gladney and Goode (1981)

+ Abbey (1980), Govindaraju (1980)

transformed into heat generation according to the relations given by Birch (1954).

7.3 RESULTS OF HEAT GENERATION MEASUREMENTS

Results for 439 samples are summarised in table 7.2, which reveals a large variation in heat generation among different rocks. Among basement rocks, argillites and sandstones show the highest radioactivity, followed by granites. The average U content of 2.86 ppm for granite is lower than the 4.75 ppm reported by Kappelmeyer and Haenel (1974). The lowest radioactivity was found for diorites and gneisses. Gneissic rocks, which normally constitute much of the "granitic" crustal layer, have considerably lower heat production than granite. A similar observation has been made by Clark et al. (1966). A very uniform result has been found for greywacke, with a mean of 1.89 ± 0.08 $\mu W/m^3$. The K concentration in this rock (2.39 ± 0.08%) is much higher than the average value of 1.4% reported by Clark et al. (1966). In rocks above basement, sandstone has the highest heat generation and the andesites the lowest. It is interesting to note that our measurements on andesites for the Central Volcanic Region agree well with those of Ewart and Stipp (1968), who used the γ-ray spectrometer method.

In table 7.3 heat generation values are presented for the locations where heat flow is known. The highest heat generation of 14.13 $\mu W/m^3$, which was found for a greywacke sample from Ongaonga -1, is almost entirely due to a high Th content of 195.13 ppm. This heat generation value is about four times higher than the greatest heat generation measured elsewhere on the same rock type (table 7.3). It seems to represent a very localised anomaly since in the same borehole a value of 1.07 $\mu W/m^3$ has been obtained for a deeper interval (table 7.3), which is within the range of the values measured on greywacke at two nearby locations. Therefore the value of 1.07 $\mu W/m^2$ will be used in the heat flow - heat generation analysis, rather than the value from the shallow level.

7.4 RELATIONSHIP BETWEEN HEAT FLOW AND HEAT GENERATION

The observed relationship between surface heat flow (q_o) and heat generation (A_o) led to the concept of heat flow provinces (Lachenbruch, 1968; Roy et al. 1968), which added a new dimension to the interpretation of continental heat flow data. The relationship was first reported by Birch et al. (1968) and then by Roy et al. (1968), Lachenbruch (1968),

Table 7.2 Summary of heat generation measurements on New Zealand rocks.

Rock Types	U (ppm)		Th (ppm)		K(%)		Th/U		K/U($X10^4$)		Heat generations (μ W/m^3)	
	N(n)	Mean	N(n)	Mean	N(n)	Mean	N(n)	Mean	N(n)	Mean	N(n)	Mean
Basement Rocks												
Granite	51(15)	2.86±.63	51(15)	16.66±5.77	51(15)	3.64±.45	46(13)	7.79	47(14)	4.63	51(15)	2.27±.56
Gneiss	16(6)	1.21±.24	16(6)	6.75±1.67	16(6)	1.98±.33	8(4)	5.85	8(4)	1.53	16(6)	1.05±.23
Schist	49(9)	2.90±.31	49(9)	14.58±2.33	49(9)	2.42±.27	49(9)	8.05	49(9)	1.25	49(9)	2.01±.22
Basalt	11(2)	1.77±1.77	11(2)	12.56±3.29	11(2)	1.88±1.73	5(1)	6.03	5(1)	1.35	11(2)	1.53±.86
Diorite	11(3)	1.33±1.09	11(3)	5.15±1.83	11(3)	1.82±.42	1(1)	2.46	1(1)	.76	11(3)	.88±.44
Greywacke	117(74)	3.06±.19	117(74)	12.22±.42	117(74)	2.39±.08	117(74)	5.56	117(74)	1.11	117(74)	1.89±.08
Argillite	42(9)	3.89±.28	42(9)	15.62±1.13	42(9)	3.21±.26	42(9)	4.32	42(9)	.91	42(9)	2.42±.14
Mudstone	15(4)	3.16±.50	15(4)	11.97±.76	15(4)	2.77±.29	15(4)	4.58	15(4)	1.04	15(4)	1.93±.16
Sandstone	18(3)	2.26±.57	18(3)	22.87±11.75	18(3)	2.86±.03	18(3)	54.83	18(3)	3.41	18(3)	2.48±.69
Claystone	3(1)	2.53	3(1)	10.43	3(1)	1.99	3(1)	4.15	3(1)	.79	3(1)	1.59
Conglomerate	10(2)	4.17±1.59	10(2)	9.28±1.61	10(2)	2.58±.02	10(2)	2.71	10(2)	.84	10(2)	1.99±.57
Mixed Rocks	7(2)	3.58±.11	7(2)	6.78±1.00	7(2)	1.80±.41	7(2)	2.79	7(2)	.72	7(2)	1.57±.08
Non Basement Rocks												
Argillite	1(1)	3.3	1(1)	6.2	1(1)	1.69	1(1)	1.88	1(1)	.51	1(1)	1.45
Mudstone	6(5)	3.24±.84	6(5)	21.29±11.09	6(5)	1.88±.22	6(5)	15.7	6(5)	.89	6(5)	2.52±.67
Sandstone	29(22)	2.65±.49	29(22)	31.19±10.18	29(22)	2.02±.21	24(17)	30.26	24(17)	1.66	29(22)	3.09±.69
Limestone	7(4)	2.23±.89	7(4)	8.8 ±6.97	7(4)	.78±.25	6(3)	4.98	6(3)	.73	7(4)	1.27±.74
Silt-siltstone	5(3)	1.40±.67	5(3)	9.33±2.28	5(3)	1.65±.24	3(2)	7.41	3(2)	1.60	5(3)	1.17±.33
Shale	1(1)	2.5	1(1)	10.1	1(1)	1.33	1(1)	4.04	1(1)	.53	1(1)	1.49
Bentonite	1(1)	1.7	1(1)	12.5	1(1)	1.25	1(1)	7.35	1(1)	.74	1(1)	1.44
Coal	1(1)	2.9	1(1)	3.6	1(1)	.35	1(1)	1.24	1(1)	.12	1(1)	1.04
Breccia	2(1)	3.3	2(1)	9.65	2(1)	1.64	2(1)	3.04	2(1)	.52	2(1)	1.68
Andesite	3(3)	.67±.27	3(3)	6.93±.92	3(3)	1.00±.24	3(3)	12.94	3(3)	1.94	3(3)	.76±.13
Ignimbrite	2(2)	1.7±.20	2(2)	8.7±.80	2(2)	1.95±.04	2(2)	5.14	2(2)	1.17	2(2)	1.25±.11
Rhyolite	2(2)	2.00±0.00	2(2)	6.05±2.05	2(2)	1.00±.83	2(2)	3.03	2(2)	.51	2(2)	1.04±.06
Dolerite	1(1)	1.9	1(1)	11.7	1(1)	.78	1(1)	6.16	1(1)	.41	1(1)	1.39
Mixed Rocks	25(11)	4.54±.42	25(11)	11.27±1.44	25(11)	2.16±.17	25(11)	2.63	25(11)	.60	25(11)	2.19±.18

N is total number of samples measured
n is the number of depths or sites
Mean refers to n and ± indicates a standard error

Table 7.3 Summary of radioactive heat generation data and heat flow.

Name of Borehole	Rock Type	Depth of Sample (m)	No. of Sample	U (ppm)	Th (ppm)	K (%)	Th/U	K/U (X104)	Heat generation ($\mu W/m^3$)	Heat Flow (mW/m^2)
Northland-1	Basalt	581.9	6	0.0	9.27±2.58	.15±.02	∞*	∞*	0.67*	98.7
Waimamaku-2	Mudstone	3348.8-3351.8	2	2.15±.25	13.5±0	2.30±.06	6.37	1.08	1.73±.07	90.8
Orewa	Greywacke	860-875.5	6	0.81	6.57±.08	1.96±.02	8.11*	2.42*	0.86*	64.7
Ararimu	Greywacke	100-150	3	1.87±.81	10.93±.15	2.19±.03	10.55	2.11	1.47±.20	38.0+
	Greywacke	100-150	3	1.5±.20	9.7±.35	2.11±.03	6.71	1.45	1.28±.04	
	Greywacke	—	3	1.93±.87	11.8±.35	2.38±.03	21.57	4.44	1.57±.25	80.1
Huntley	Claystone	498-500.2	3	2.53±.15	10.43±.12	1.99±0.0	4.15	.79	1.59±.03	
Mavi-4	Albite granite	3730.1-3778.9	5	3.64±.71	10.84±.59	2.06±.01	3.63	.68	1.91±.18	52.8
Tasman-1	Hydrothermally altered conglomerate	1461.2-1517.6	5	5.76±.54	11.48±.51	2.56±.03	2.05	.46	2.55±.17	76.1
Surville-1	Granite	2099.5-2122.2	8	2.06±.44	7.84±.52	3.05±.04	12.00	5.52	1.38±.12	54.3
	Granite	2126.5-2139.5	4	2.98±.59	13.0±1.02	3.24±.04	4.79	1.24	2.0±.21	
MoA-1B	Quartz Oligoclase Biotite Schist	3349.8-3377.2	10	3.81±.42	10.95±.43	2.12±.01	5.08	.64	1.96±.10	80.3
Tane-1	Biotite Granite	4292-4352	11	0.18	4.15±.16	1.67±.02	23.05*	9.28*	.50*	85.3
Mavi-1	Quartzite and Quartz mica Schist conglomerate	3385.1-3389.7	5	2.58±.60	7.08±.63	2.59±.03	3.36	1.22	1.42±.17	77.9
Mavi-2	Hornblende diorite	3361.6-3419.6	9	≤0.5	2.36±.45	1.33±.02	—	—	0.42*	88.7
Mavi-3	Shale with sandstone and siltstone	3251.9-3255	3	3.47±.57	7.77±.52	2.21±.03	2.32	.67	1.65±.17	77.9
Kiore-1	Sandstone grading to siltstone	532.5	4	1.20±.90	46.23±12.47	2.85±.04	155.45	7.98	3.86±.67	112.3
	Sandstone grading to siltstone	531.6	4	3.15±.49	9.03±.55	2.81±.04	3.03	.94	1.72±.14	
Ararimu-1	Greywacke	1033-1048.2	4	2.53±.31	8.75±.30	2.18±.07	59.38	3.68	1.48±.07	75.1
Tatu-1	Sandy Mudstone	852.8	4	2.65±.68	10.53±.29	2.96±.09	5.43	1.49	1.72±.16	116.1
	Sandy Mudstone	854-856.8	4	4.43±.54	13.03±.46	3.52±.06	3.08	.84	2.40±.17	
Tupapakurua-1	Greywacke	1126.5-1132.6	3	3.47±.15	8.9±.78	1.74±.03	2.59	.50	1.69±.05	80.8
Puniwhakau-1	Indurated mudstone	2140.5	5	3.40±.50	10.80±.49	2.30±.02	3.45	.75	1.86±.16	83.9
Parikino-1	Schist	2307.8	10	1.76±.33	21.09±.94	2.54±.04	31.46	3.94	2.19±.09	99.0
Santoft-1A	Argillite	2623.3-2626.3	3	4.67±.41	14.8±.50	2.90±.04	3.22	.63	2.53±.11	49.1

Table 7.3 Summary of radioactive heat generation data and heat flow (Continued).

Name of Borehole	Rock Type	Depth of Sample (m)	No. of Sample	U (ppm)	Th (ppm)	K (%)	Th/U	K/U (X104)	Heat generation ($\mu W/m^3$)	Heat Flow (mW/m^2)
Cngaonga-1	Greywacke	1488.3-1489.6	3	≤.5	195.13±.35	2.08±.05	—	—	14.13*	35.6
	Greywacke	1568.5-1569.1	5	1.42±.50	8.06±.40	1.33±.01	54.14	22.00	1.07±.14	
Takapau-1	Greywacke	997.9-998.8	2	2.05±.05	18.8±14.4	.82±.03	9.35	.41	1.95±1.01	36.4
	Greywacke	1053.1-1054	7	0.87	5.0±.30	1.38±.06	5.75*	1.59*	0.71*	
Rangipo	Argillite	61	2	3.25±.15	16.85±.35	3.57±.08	5.2	1.10	2.38±.03	87.6
	Argillite	74	2	4.1±.30	16.0±.60	3.36±.04	3.94	.82	2.52±.04	
	Argillite	85	2	4.35±.45	15.45±.25	2.91±.34	3.6	.67	2.5±.13	
Petone-Lower Hutt	Greywacke	-	22	4.67±.26	13.59±.69	2.87±.15	3.05	.64	2.44±.12	46.0
Haku-1	Schist	1613.6-1620.9	2	4.0±.40	12.25±.95	2.53±.06	3.12	.64	2.14±.03	88.6
Ahaura-2	Argillite	1062.1	5	2.64±.18	13.62±.32	3.77±.02	5.25	1.45	2.01±.05	92.7
Aratika-3	Sandstone (Meta sediment)	1719.1	10	2.43±.23	13.35±.23	2.91±.02	6.00	1.30	1.85±.06	90.4
Taramakau-1	Argillite	2040.3-2049.5	7	4.17±.52	17.89±.38	2.66±.02	4.71	.70	2.60±.14	101.7
Arahura-1	Basalt	1730-1731	5	3.54±.92	15.84±.43	3.60±.26	6.03	1.35	2.38±.26	107.0
Harihari	Argillite	2504.6-2522.9	8	2.76±.44	9.09±.34	1.94±.03	4.43	.98	1.54±.12	61.1
Waiho-1	Argillite	3729.8-3742	6	5.00±.46	15.1±.72	3.07±.02	3.11	.64	2.66±.14	79.7
Murchison basin	Granite	-	1	1.4	≤.5	6.97	-	4.98	1.06	92.0
Kowai-1	Argillite	1412.1	7	4.06±.20	21.77±.27	4.70±.05	5.45	1.17	3.04±.06	58.2
Leeston-1	Greywacke	1109.3-1155.3	7	4.43±.54	12.86±.32	2.18±.02	3.13	.53	2.26±.15	53.1
	Greywacke	1152-1155.3	3	6.23±.59	13.43±.54	1.87±.04	2.21	.30	2.74±.12	
Resolution-1	Sandstone, Syenogabbro, teschenite	1716.3-1884.3	4	3.68±1.27	5.78±.34	1.39±.02	3.26	.77	1.49±.33	60.2
Takapu-1A	Schist	759-798.6	6	1.65±.24	8.5±.27	1.94±.02	5.77	1.32	1.21±.06	119.9
Tara-1	Granite gneiss	4246.8-4255.9	3	1.67±.18	8.1±.57	2.10±.07	4.92	1.29	1.65±.29	87.2
	Granite gneiss	4255.9-4261.4	3	1.20±.26	7.33±.09	2.11±.03	6.75	1.92	1.03±.07	
Pakaha-1	Granite	2606.3-2672.2	9	3.41±.25	11.03±.23	3.97±.03	3.44	1.24	2.04±.07	99.6
Kawau-1A	Schist	3034.9-3111.7	9	2.38±.29	12.49±.33	2.42±.03	5.84	1.14	1.73±.09	115.3
Hoiho-1C	Schist	1588.9-1698.7	7	2.56±.34	13.83±.19	3.13±.03	6.12	1.38	1.94±.08	163.8
J.T. Benny-1	Greywacke	995.8-1001.9	8	5.36±.50	13.0±.47	2.71±.09	2.58	.54	2.57±.16	76.0
Parara-1	Granite wash	3482-3564.3	4	≤0.5	1.4±.32	2.24± 0	—	—	0.44*	70.0
	Granite wash and gneiss	3573.5-3621	7	≤0.5	4.37±.31	2.29±.03	—	—	0.66*	

* calculated from average U, Th and K. + Dr Rick. Allis (pers. commn.)

Jaeger (1970), Swanberg et al. (1974) Rao and Jessop (1975), Rao et al. (1976), Kutas (1977) and Jessop and Lewis (1978). Initially the relationship was established for plutonic rocks but it is applicable to non-plutonic settings as well. The relationship for a heat flow province can be written as :

$$q_o = q_r + D A_o \qquad (4.1)$$

where the intercept q_r is called the "reduced heat flow", and the slope D is the "characteristic depth" (actually a thickness) related to the near-surface radioactivity. In simple terms, D corresponds to the thickness of the surface layer of the crust in which the heat generation would be uniform at the value A_o (Roy et al., 1968). In another interpretation, which also satisfies equation 4.1, D is the logarithmic decrement for an exponentially decreasing radioactive concentration (Lachenbruch, 1968, 1970). In this case heat production (A) and depth (Z) are related as :

$$A(z) = A_o e^{-z/D} \qquad (4.2)$$

The exponential model has some advantage in the sense that it maintains the linear relationship under differential erosion. It has been supported by the studies of Swanberg (1972), Hawkesworth (1974) and Lachenbruch and Bunker (1971). It also looks more realistic from a geochemical point of view. Sometimes a very rapid decrease in heat generation with depth is observed (Dolgushin and Amshinsky, 1966).

In the studies cited above, values of q_r normally ranged from 10.9 mW/m^2 to 59.0 mW/m^2, and D from 7 to 15km, for major heat flow provinces. Pollack and Chapman (1977a,b) recently discovered that an empirical relationship exists between q_o and q_r :

$$q_r \simeq 0.6\, q_o \qquad (4.3)$$

The relationship expressed in equation 4.1 is well established for the heat flow provinces of the U.S.A. Among these provinces, the Basin and Range Province is considered representative of active, high heat flow regions, and the Eastern United States representative of stable continental regions (Roy et al., 1968). The parameters for these provinces are included in table 7.4; results for newly studied regions are often compared with these.

Table 7.4 Heat flow regions: thermal parameters

HEAT FLOW REGION	AVERAGE HEAT FLOW (mW/m^2)	AVERAGE HEAT GENERATION ($\mu W/m^3$)	REDUCED HEAT FLOW (mW/m^2)	D (km)	TEMPERATURE AT 35 km (^oC)		REFERENCE
					UNIFORM MODEL	EXPONENTIAL MODEL	
Northland-Waikato	74.2	1.24	61.8+	10*	894	939	Present study
Hikurangi	40.9	1.69	29.9	7.1	442	488	"
Taranaki	86.4	1.77	71.9	9.6	1021	1079	"
Western Cook Strait	61.3	2.15	39.8+	10*	623	682	"
West Coast (S. Island)	91.2	2.03	70.9+	10*	1039	1095	"
Marlborough-Canterbury	49.8	2.42	25.6+	10*	419	487	"
The Great South Basin	110.7	1.59	94.8+	10*	1341	1390	"
Basin and Range (Western United States)	92	-	59	9.4	937	857	Blackwell (1971), Pollack and Chapman (1977)
Eastern United States	57	-	33	7.5	541	478	"

* Adopted

\+ Calculated from equation 4.4 using D = 10 km.

It will be of interest to see how such a relationship fits with the New Zealand data, since none of the U.S.A. studies was carried out in an active subduction region. New Zealand has been divided into eight heat flow regions, based on the observed level of heat flow, as shown in fig. 7.1. Values of A_o have been determined for 42 locations in all. A summary of heat flow - heat generation data for these locations is given in table 7.3.

A general increase of q_o with A_o was found for the Taranaki and Hikurangi regions only, as shown in fig. 7.2. The calculated values of q_r and D for these regions are given in table 7.4. The relationship for the Basin and Range Province and the Eastern United States are included in fig. 7.2 for comparison. For the Taranaki region, although all the data points fall above the Basin and Range line, and the value of q_r is thus higher, the value of D is similar. The four data points for the Hikurangi region plot very close to the Eastern United States line. It thus appears that there are some similarities in the thermal characteristics of (i) Taranaki Region and the Basin and Range Province, and (ii) Hikurangi Region and the Eastern United States, although in both cases there is little similarity from the viewpoint of geologic structure and plate tectonics. It may be noted, however, that upper mantle temperatures are high and Pn velocities are low (7.8 - 7.9 km/s) under the Taranaki Region and the Basin and Range Province, while temperatures are low and Pn velocities are high under the Hikurangi Region and the Eastern United States.

Wide scatter was found for the Northland-Waikato, West Coast and Great South Basin regions, as shown in fig. 7.3. This figure also includes the Basin and Range line and Eastern United States line for reference. Data from the Great South Basin plot considerably above the Basin and Range line; the distribution is somewhat similar to that of the Cordilleran thermal anomaly zone (U.S.A.), where volcanism is young (<17 Myr old) and the heat flow - heat generation relationship is non-existent (fig. 7.4) (Blackwell, 1978). There is evidence of young volcanism in the Great South Basin also (C. Adams and R. Cook, pers. comm.). It may be mentioned here that in some earlier studies (Kutas, 1972; Sass et al., 1972; Chapman and Pollack, 1974), usual relationship between heat flow and heat generation was not apparent for some regions. There are too few data to support a correlation for the Canterbury-Marlborough and Southland-Solander regions, or for the Central Volcanic Region (fig. 7.3).

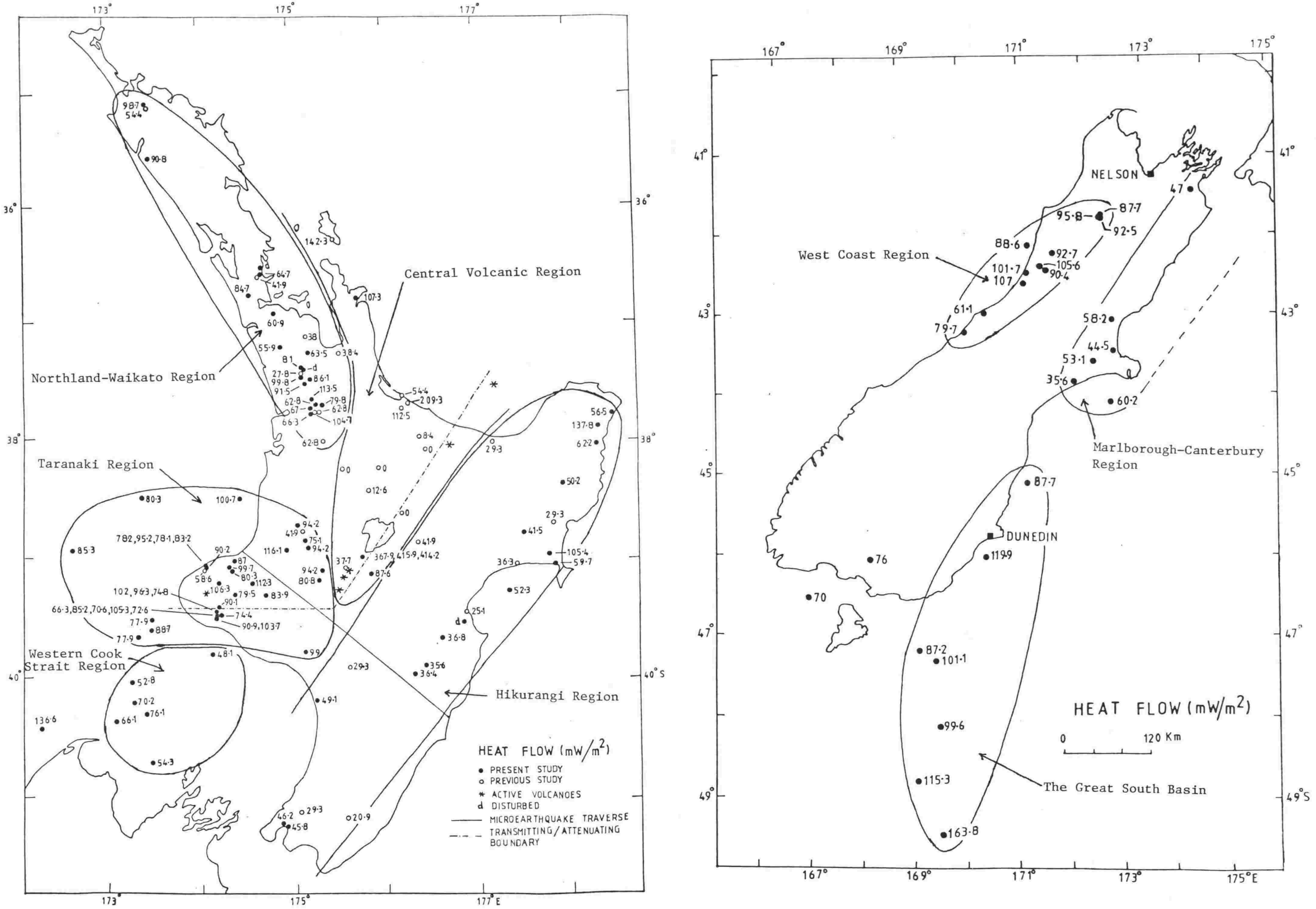

Fig. 7.1 Heat flow regions.

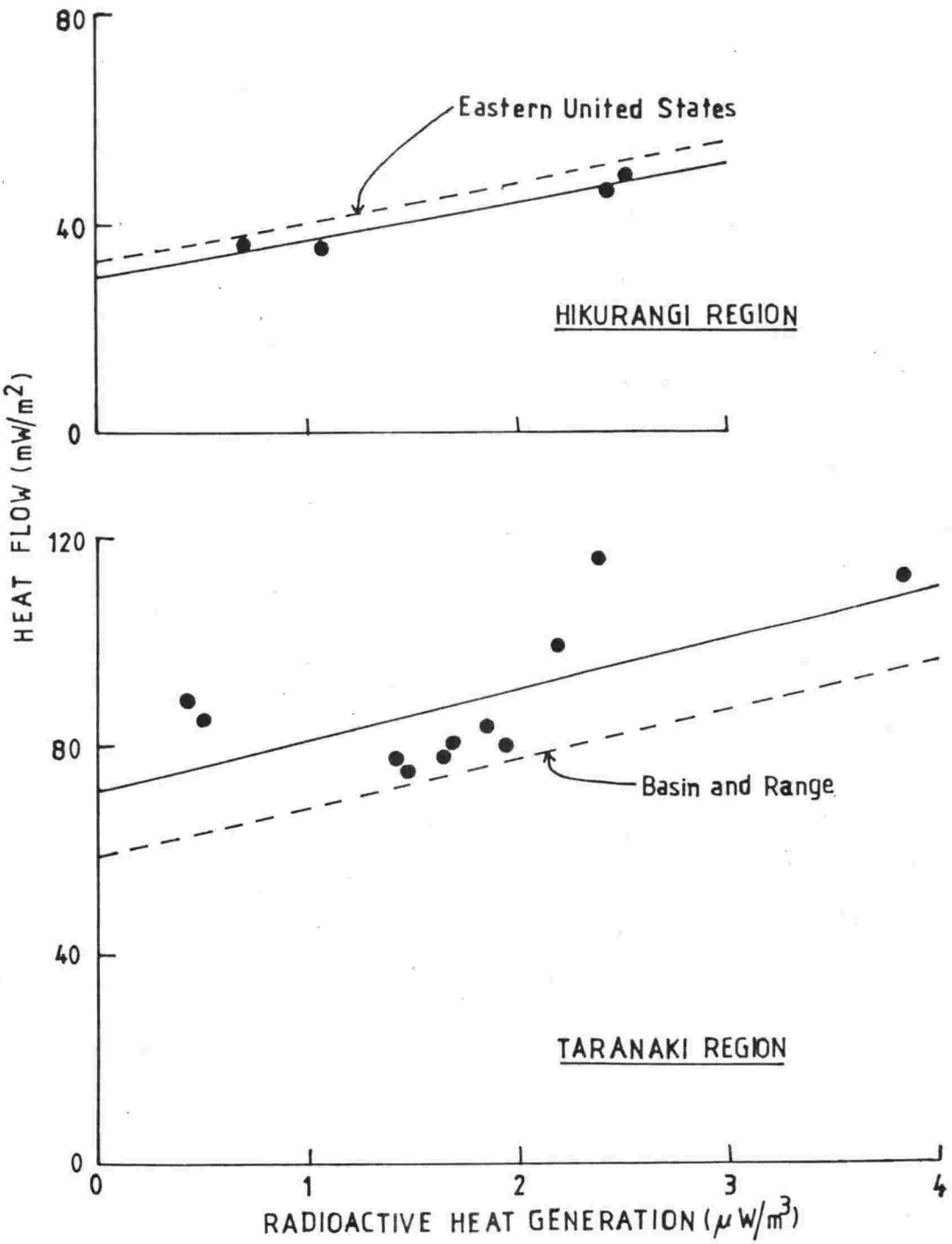

Fig. 7.2 Heat flow vs heat generation for the Hikurangi and Taranaki regions.

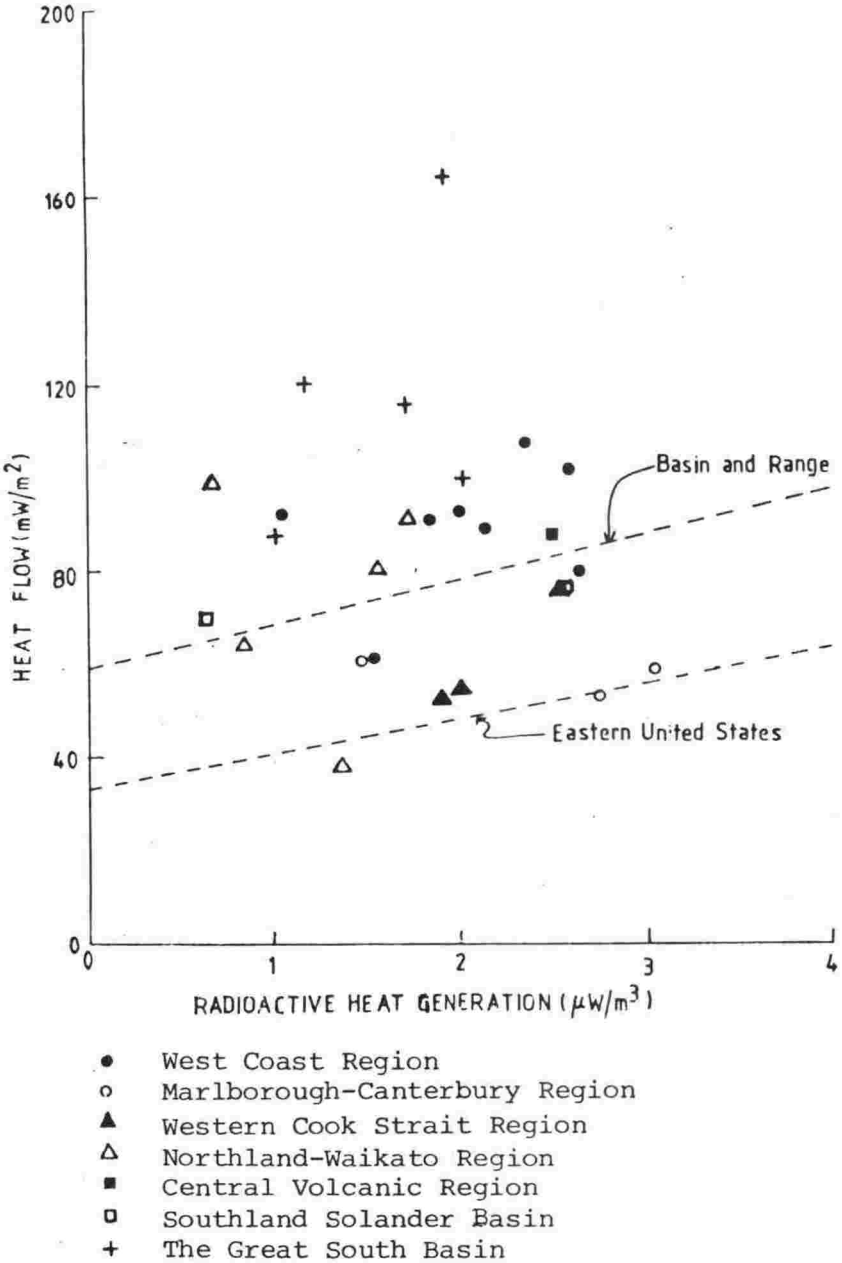

Fig. 7.3 Heat flow vs heat generation: other heat flow regions.

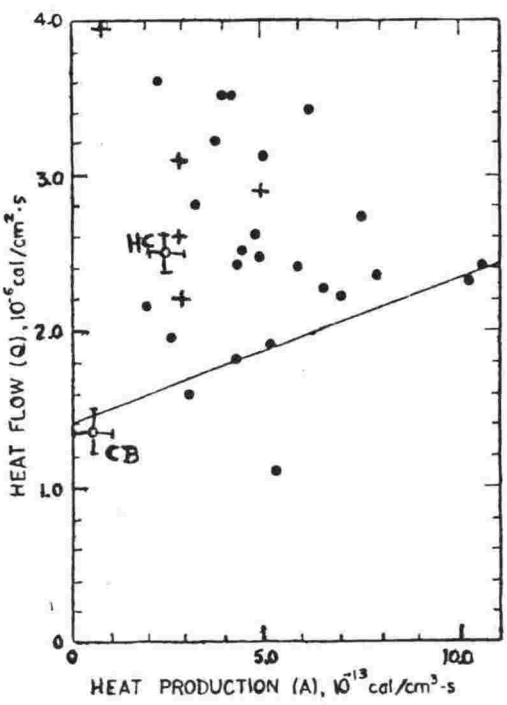

Fig. 7.4 Heat flow vs heat generation for the Cordilleran thermal anomaly zone (excluding California) for areas where volcanism is less than 17 Myr old. HC is for the western border of the High Cascades, and CB is for the Columbia Basin portion of the Columbia Plateau. Plus signs represent data along the margin of the Western Snake River Plain. The Basin and Range line is shown for reference (Blackwell, 1978).

7.5 REDUCED HEAT FLOW (q_r)

This is normally interpreted as the heat flowing from depths ranging from D to three or four times D, depending upon the heat production model. For regions other than Taranaki and Hikurangi, q_r values can be calculated from following equation (Sass and Lachenbruch, 1978):

$$\bar{q}_r = \bar{q}_o - D\,\bar{A}_o \qquad (4.4)$$

where $\bar{q}_r$, $\bar{q}_o$ and $\bar{A}_o$ are the average values of reduced heat flow, observed heat flow and surface radioactive heat generation, respectively, for the region. In the calculation, D is conventionally taken as 10km (Roy et al., 1972; Smith, 1974; Decker and Smithson, 1975; Smith et al., 1979 etc.), a value similar to that obtained for the Taranaki region. Calculated $\bar{q}_r$ values are given in table 7.4.

$\bar{q}_r$ for the Taranaki, West Coast and Great South Basin regions is considerably higher than the value of q_r = 59 mW/m^2 for the Basin and Range Province. The value obtained for the Great South Basin compares only with the range of values 83.7 - 104.7 mW/m^2 associated with the Battle Mountain high of the Western United States.

7.6 TEMPERATURE PROFILES

The temperature distribution in the earth plays an important role in the interpretation of various geophysical anomalies. It is possible to approximate the deep-seated temperature distribution in an area if the surface heat flow, the vertical and areal distribution of heat producing elements, and the thermal conductivity are known with sufficient accuracy. Holmes (1915, 1916) was perhaps the first to calculate the deep-seated temperature distribution using measured heat generation values.

The temperature at depth z in a layer of constant heat generation A and conductivity K is given by

$$T(z) = To + \frac{qz}{K} - \frac{Az^2}{2K} \qquad (4.5)$$

where To is the surface temperature and q is the surface heat flow, (Jaeger, 1965). If we assume an exponential decrease of heat production with depth then the temperature T(z) can be calculated from following equation (Lachenbruch, 1968).

$$T(z) = To + \frac{qr}{K}z + \frac{D^2}{K}Ao[1 - \exp(-z/D)] \qquad (4.6)$$

The parameters q_r, Ao and D have been defined in section 7.4 above.

Temperatures calculated to a depth of 35km, using both the above models, for all heat flow regions except the Central Volcanic Region, are presented in table 7.4, and the distribution of temperature with depth is shown in figs. 7.5 to 7.8. In all cases a uniform conductivity of 2.5 $W/m^{\circ}C$ has been adopted as an average for the entire crust, and in the uniform model the heat generation in the lower crust is taken as 0.2 $\mu W/m^3$ (Allis, 1979b). The adopted value for the thermal conductivity is reasonable for the crustal rocks in New Zealand; to have allowed for a variation of conductivity with depth would not have changed the calculated temperatures appreciably. The average sedimentary thickness in these regions varies from 1 to 4 km; the temperature calculations start from the base of the sediments. All other parameters used in the calculation are given in Table 7.4.

A large variation has been found in the temperature at 35km depth (taking the mean for the two models), from $453^{\circ}C$ (Marlborough-Canterbury Region) to $1366^{\circ}C$ (Great South Basin). Calculated temperatures at the same depth in the heat flow provinces of U.S.A. vary from $310^{\circ}C$ (Sierra Nevada) to $1400^{\circ}C$ (Battle Mtn high). For the regions of Taranaki and West Coast the temperatures are close to the basalt-eclogite solidus (figs. 7.6, 7.7). In the Great South Basin, conditions of melting may have been reached at a depth of about 35km (fig. 7.8). On the other hand, temperatures are much lower than the solidus under the Hikurangi, Western Cook Strait and Marlborough-Canterbury regions. As is usual in regions of moderate to high heat flow, radioactive heat generation makes a small to negligible contribution to the temperature at 35km in New Zealand.

7.7 RADIOACTIVITY DISTRIBUTION BENEATH WESTERN CANTERBURY REGION

It is well accepted that the lower crust is depleted in the heat producing elements, heat generation being in the range 0.2 to 0.6 $\mu W/m^3$ (Roy et al., 1968; Decker and Smithson, 1975; Rao and Jessop, 1975; Allis, 1979b; Decker et al., 1980). The radioactivity decreases from the surface down to this low value at depth D in the uniform radioactivity model, and at about 2D in the exponentially decreasing model.

An opportunity to study more directly the variation of heat generation with depth is provided by data from the Central Southern Alps. In this region a continuous section of low grade metagreywacke to high grade schist/gneiss occurs in a 15-20km wide belt along the eastern side of the Alpine Fault. These rocks are exposed continuously along the Franz Josef - Fox Glacier valleys; the location is shown in fig. 7.9(a)

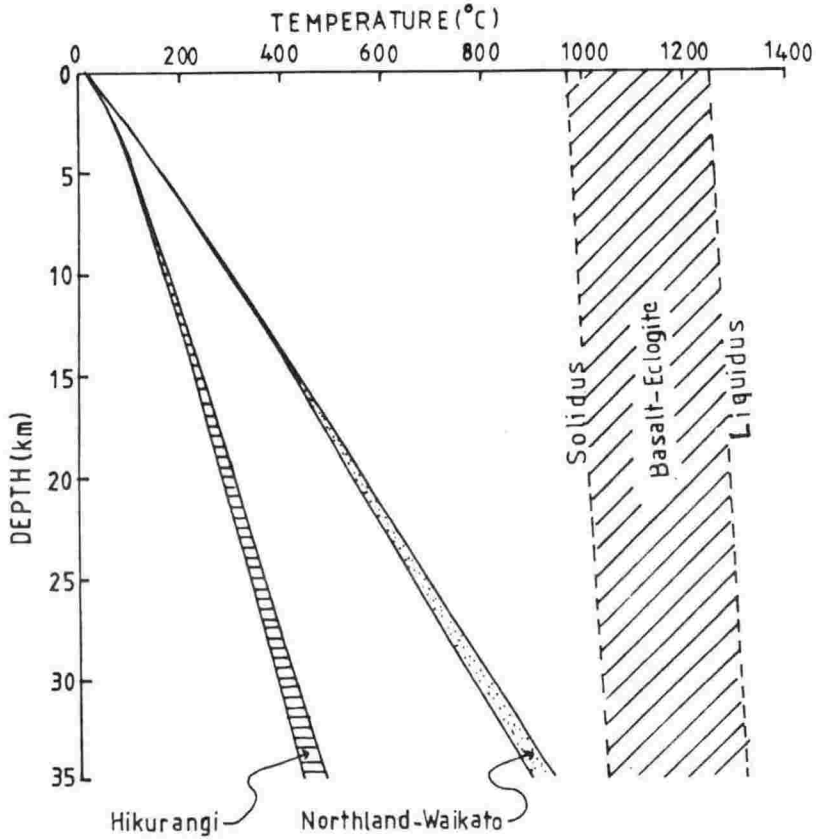

Fig. 7.5 Temperature - depth curves for the Hikurangi and Northland-Waikato regions calculated using uniform (lower bound) and exponentially decreasing (upper bound) radioactivity models. Basalt-Eclogite melting relation is taken from Yoder and Tilley (1962).

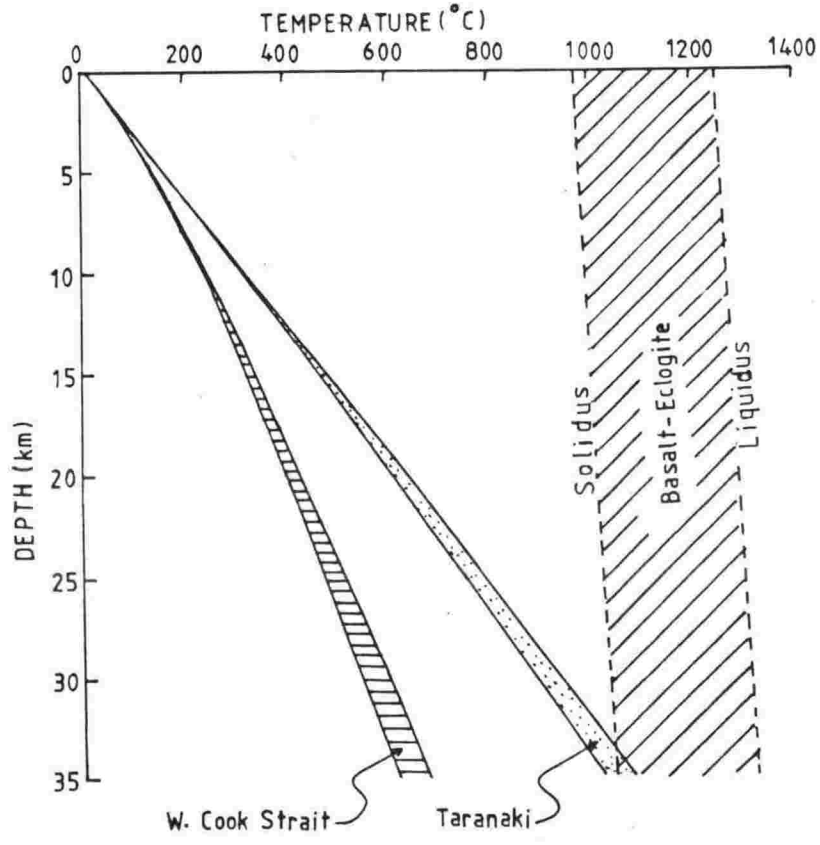

Fig. 7.6 Temperature - depth curves for the Taranaki and Western Cook Strait regions calculated using uniform (lower bound) and exponentially decreasing (upper bound) radioactivity models.

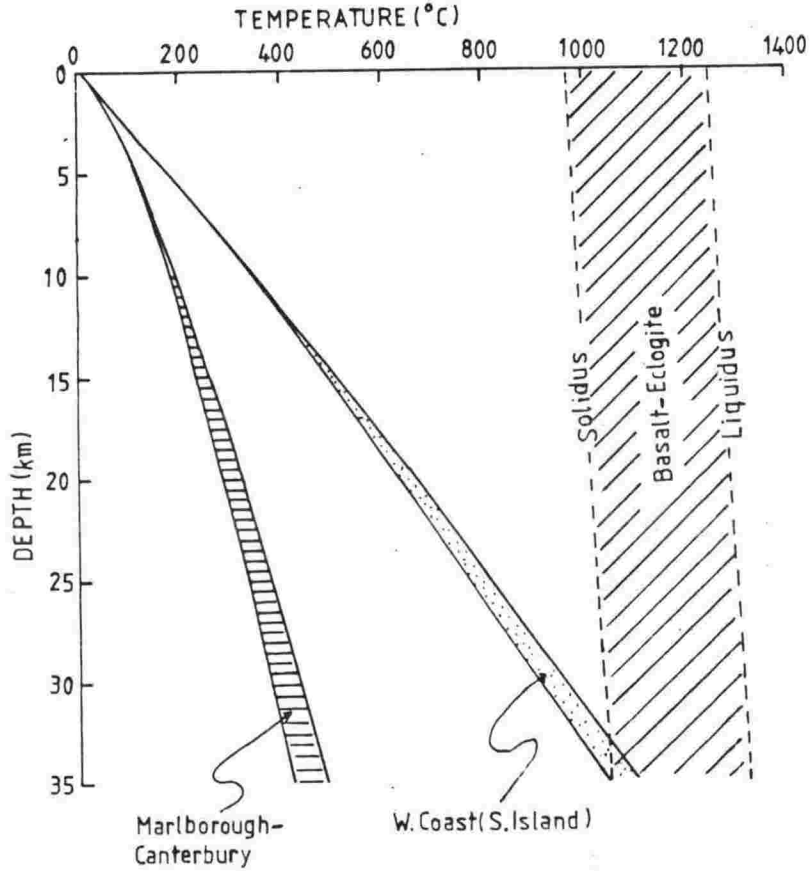

Fig. 7.7 Temperature - depth curves for the West Coast and Marlborough-Canterbury regions calculated using uniform (lower bound) and exponentially decreasing (upper band) radioactivity models.

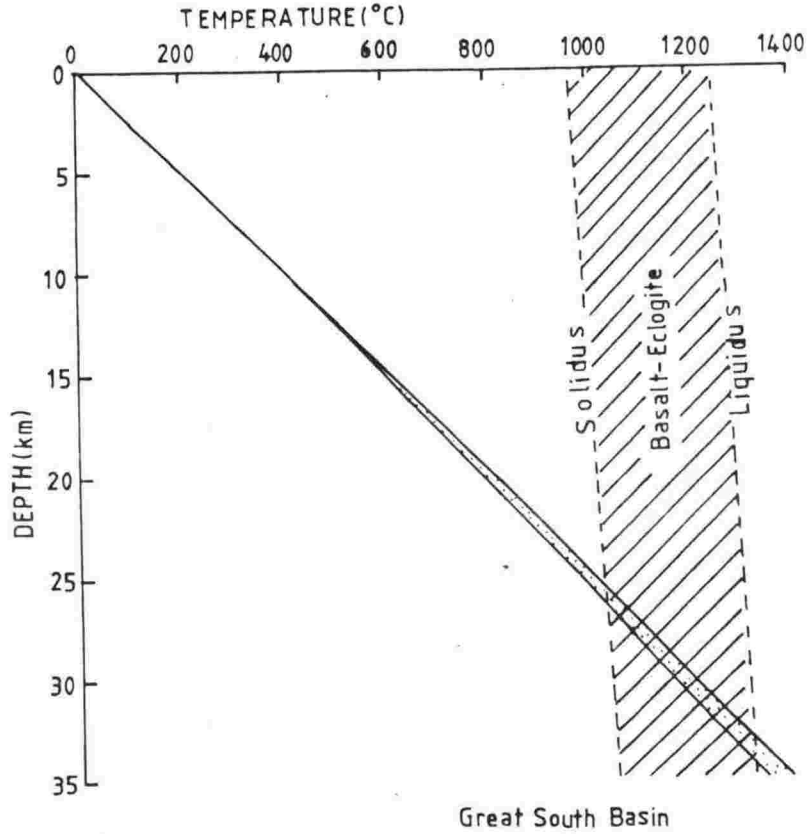

Fig. 7.8 Temperature - depth curves for the Great South Basin calculated using uniform (lower bound) and exponentially decreasing (upper bound) radioactivity models.

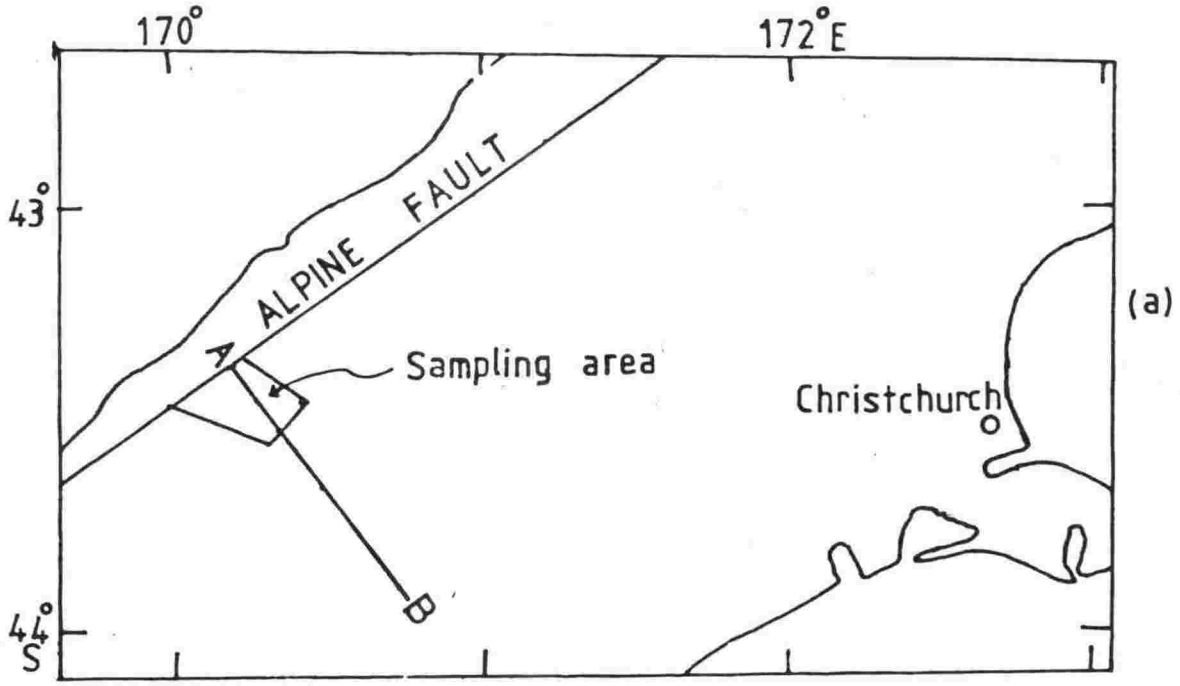

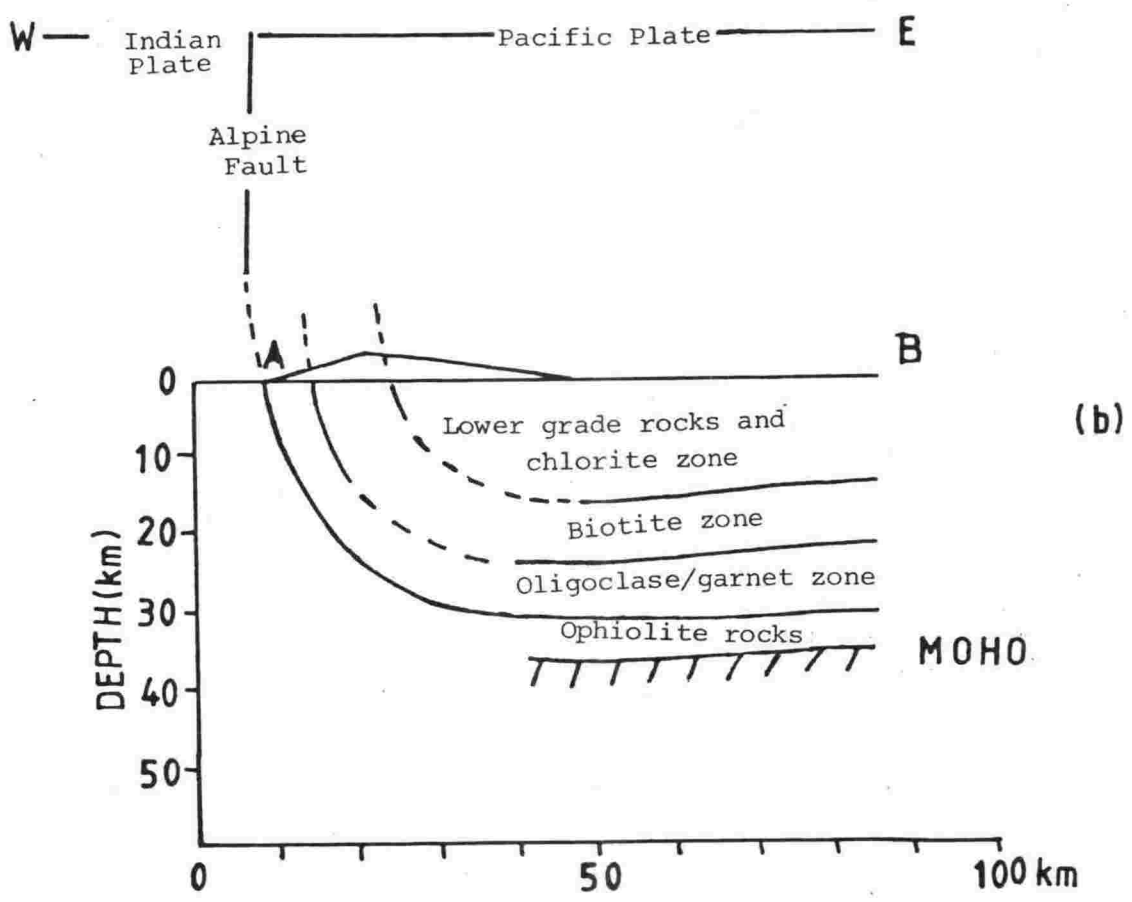

Fig. 7.9 (a) Locations map.
(b) A possible crustal cross section: eastwards from the Central Southern Alps (R. Grapes, pers. comm.).

by a rectangle. The metamorphic grade regularly increases from east to west, the highest grade rocks occurring near the Alpine Fault. A possible crustal section eastwards from the Central Southern Alps is shown in fig. 7.9(b) (R. Grapes, pers. comm.).

Rock samples from the Franz Josef - Fox Glacier valleys have been studied by Dr R. Grapes (Joint Mineral Science Research Laboratory) in connection with an investigation of the metamorphic geothermal gradient. 31 samples have also been measured for U, Th and K concentrations. According to the model proposed by Dr R. Grapes, which relates uplift on the Alpine Fault to plate convergence, these samples correspond to a vertical sequence between 17km and 30km in depth from a distance of about 30km east of Alpine Fault to perhaps 75km further to the east (fig. 7.9b). The variation of measured heat generation with depth corresponding to this vertical sequence is shown in fig. 7.10. The heat generation appears to vary randomly between 0.92 and 2.39 $\mu W/m^3$, with a mean of 1.56 ± 0.07 $\mu W/m^3$. This mean value is very much higher than the usually adopted value of 0.2 to 0.6 $\mu W/m^3$ for the lower crust. Heat generation has also been measured on the greywacke and argillite from boreholes Leeston -1 and Kowai -1 near the east coast. These are the rock types shown between the surface and a depth of 17km in the model of fig. 7.9(b). The heat generation values are included in fig. 7.10.

Taking the heat generation as 2.89 $\mu W/m^3$ for 0-17km and 1.56 $\mu W/m^3$ for 17-30km, and adopting a heat flow contribution of 25.6 mW/m^2 from below 30km, the calculated heat flow at the surface is 95 mW/m^2. No heat flow data are available from the mid-Canterbury area except for four measurements near the east coast; these have a mean of 47.9 mW/m^2, about half of that expected over the proposed section.

Thus it is clear that the proposed sequence - from greywacke through to high grade metamorphics between the surface and 30km depth - is not present under the boreholes located near the east coast. This contributes evidence of the present width of New Zealand Geosyncline rocks, suggesting a vertical section such as is shown in fig. 7.11. A more detailed determination of this section could be obtained by means of a heat flow traverse in the east-west direction across the Canterbury Plains.

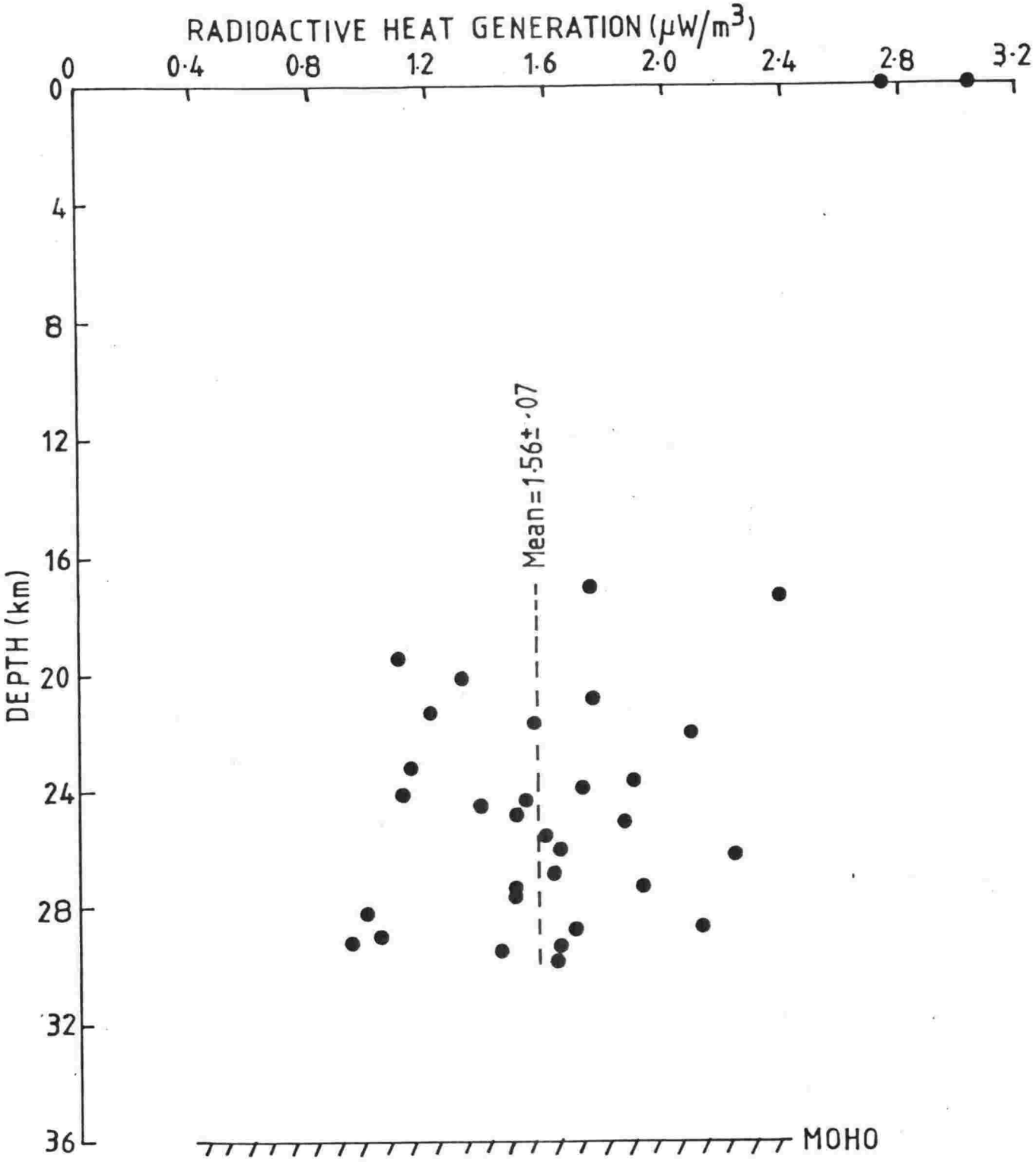

Fig. 7.10 Inferred variation of radioactive heat generation with depth beneath Western Canterbury Region.

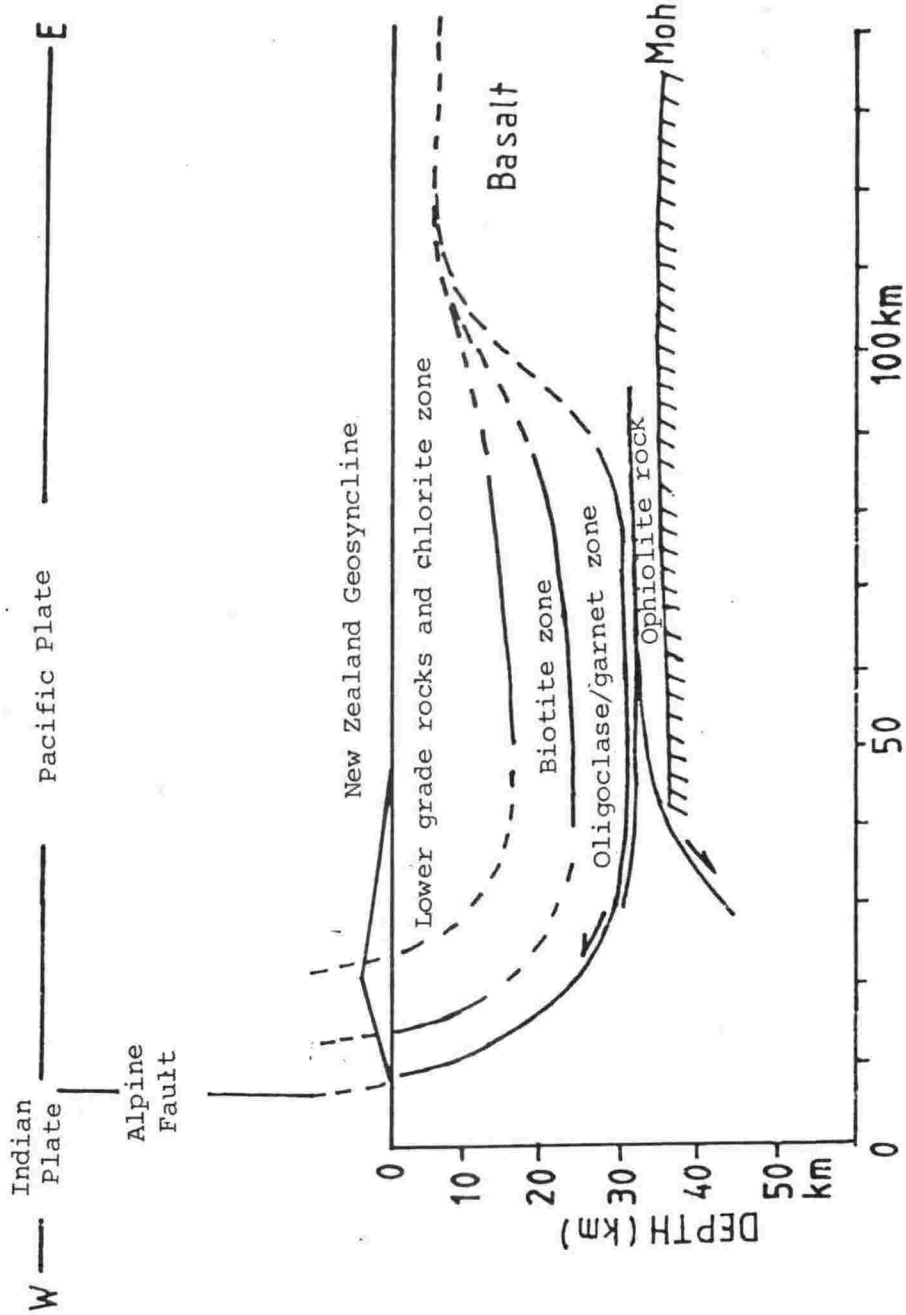

Fig. 7.11 A possible crustal section across the New Zealand Geosyncline.

7.8 HEAT GENERATION AND PETROPHYSICAL PARAMETERS

7.8.1 Seismic velocity and density

Heat generation has been correlated with parameters such as seismic velocity, density, and thermal conductivity. An empirical relationship between heat generation (A) and compressional velocity (Vp) has been obtained for crystalline and metamorphic rocks by Rybach (1973, 1976a,b, 1978/79), showing that A decreases with increasing Vp. As would be expected, a decrease in A with increasing density has also been found (Steinhart et al., 1968; Kutas, 1979; Allis, 1979b).

In this study we have measured the heat generation on selected samples for which the density and conductivity had been measured earlier. The possibility of a correlation of particle density with the measured heat generation is examined in fig. 7.12. There seems to be no such correlation, either using rock averages (fig. 7.12a) or individual values (fig. 7.12b). The data are, however, too few to assert that no correlation exists.

7.8.2 Heat generation and thermal conductivity

Horai and Nur (1970) postulated a positive correlation between these parameters, based on a global analysis. Rybach (1976b) also studied this relation for 110 Alpine rocks, and found no correlation for either igneous or metamorphic rocks, although one was suggested for sedimentary rocks. We have plotted the two parameters for various rock types in fig. 7.13., but again we fail to find any correlation.

7.9 CONCLUSIONS

The following conclusions are drawn from the above analysis:

(i) There is a large variation in heat generation from rock to rock. In basement rocks the highest heat generation is found for argillites and sandstones and the lowest in diorites and gneisses.

(ii) A linear relationship between heat flow and heat generation is found only in the Taranaki and Hikurangi regions, which show some thermal similarity with the Basin and Range Province and Eastern United States respectively.

(iii) Measured heat generation of 1.56 ± 0.07 $\mu W/m^3$, corresponding to a proposed vertical sequence between 17km and 30km under the areas lying 30km to 75km east of the Alpine Fault, is very much higher than the usually adopted value of 0.2 to 0.6 $\mu W/m^3$ for the lower crust. This study suggests that the New Zealand geosynclinal sequences of greywacke through high grade metamorphics are not present near the east coast of Canterbury.

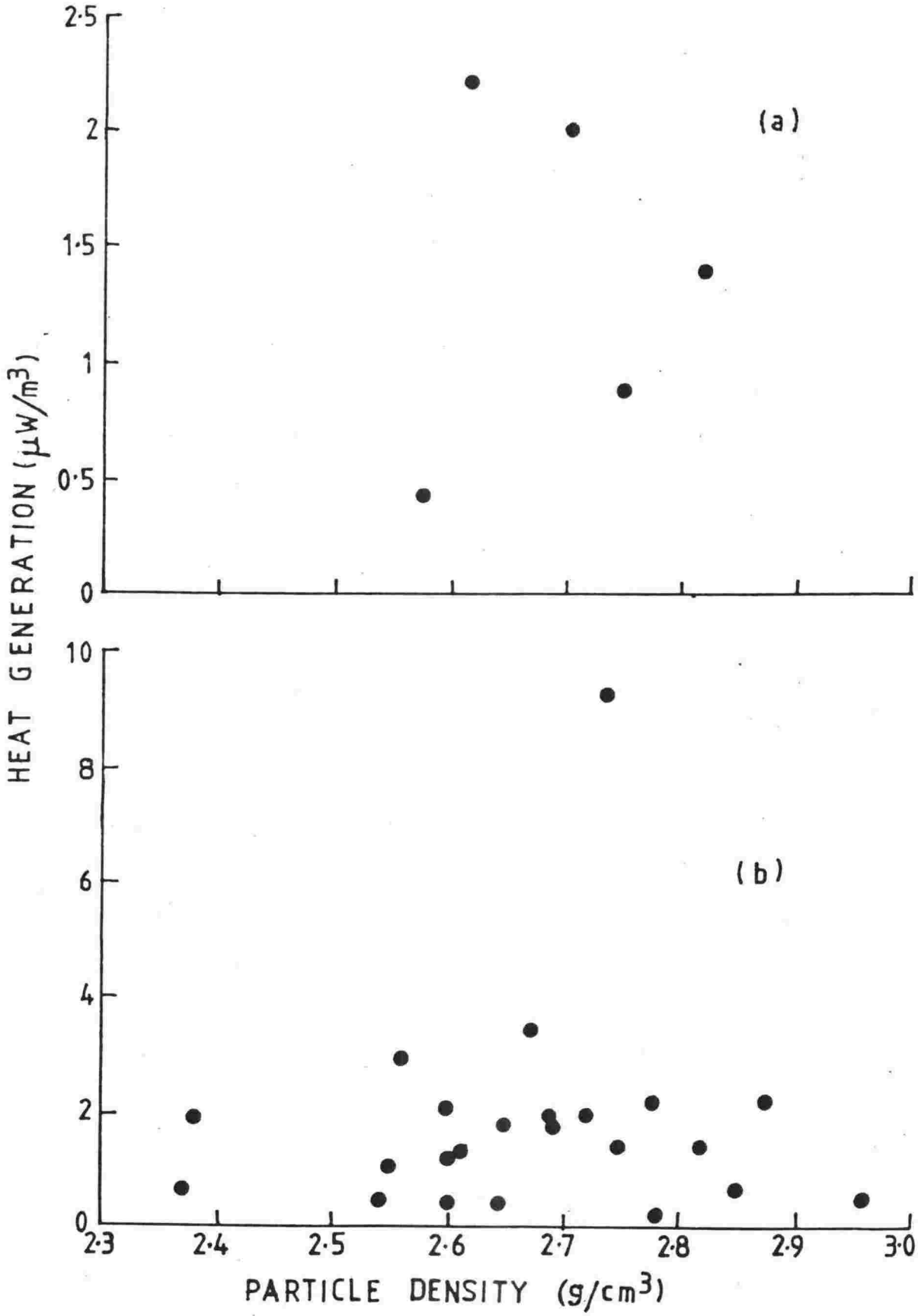

Fig. 7.12 Radioactive heat generation vs Particle density: (a) rock averages, (b) individual samples.

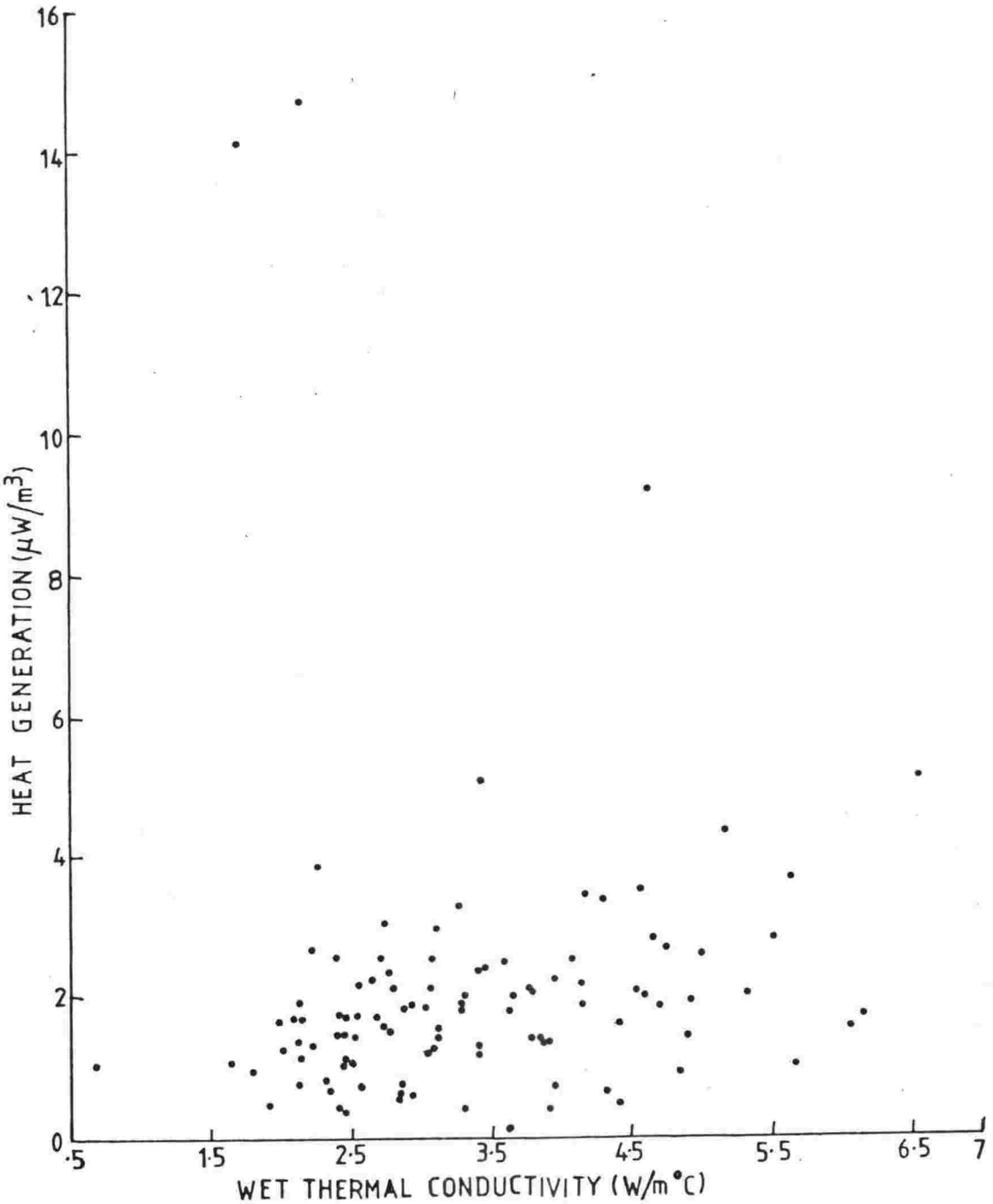

Fig. 7.13 Radioactive heat generation vs wet thermal conductivity.

(iv) q_r values and the temperatures at 35km vary from region to region (table 7.4). The calculated temperatures at 35km in the Taranaki and West Coast regions coincide with the basalt-eclogite solidus, while in the Great South Basin, melting conditions may be reached at a depth of about 35km.

(v) No correlations have been found between the heat generation and either density or thermal conductivity.

CHAPTER 8

HEAT FLOW REGIONS

8.1 INTRODUCTION

In chapters 5 and 6, results of heat flow investigations have been presented and the pertinent details of individual locations have been given briefly. An important feature which has emerged from this study is the distribution pattern of the regional heat flow. In this chapter we discuss this pattern in the light of surface manifestations, regional plate tectonics, geophysical anomalies, and the deep-seated temperature distribution. An attempt is made to find relationships between heat flow and geothermal parameters. The relevance of the thermal field in locating hydrocarbon deposits is also discussed.

8.2 REGIONAL DISTRIBUTION IN THE NORTH ISLAND

Heat flow values in this Island range from 20.9 mW/m^2 to 137.8 mW/m^2 with a mean of 73.3 ± 2.7 mW/m^2, which is higher than the continental mean of 62.3 mW/m^2 (Jessop et al., 1976). In calculating this mean as well as subsequent means all the values from Central Volcanic Region have been omitted, as have three values from a previous study (Thompson, 1977) for which the thermal conductivity was assumed. The North Island contains five heat flow regions as shown in fig. 7.1. Salient features of these regions are discussed below.

(i) Northland - Waikato Region

This region is characterised by young volcanism and a large number of thermal springs (fig. 2.8). The area is associated with abrupt lateral changes in geothermal gradient and heat flow. Temperature profiles are sometimes disturbed due to underground thermal water circulation, as at Waiwera, where temperatures reach 45°C at about 100 m depth (fig. 5.4). Just a few kilometres away from this location, at Orewa, the geothermal gradient is normal.

The measured heat flow varies from 38 mW/m^2 to 113.5 mW/m^2, with an average of 74.2 ± 4.3 mW/m^2. The high reduced heat flow of 61.8 mW/m^2 suggests that the major source of heat lies in the upper mantle. Calculated temperatures (fig. 7.5) suggest the presence of melting conditions at a depth of about 55km. Low seismic velocities, large positive teleseismic residuals, and an attenuating zone may be associated with high temperatures. Midha (1979) has suggested that the North Island Conductivity Anomaly (fig. 2.7), which he relates to an old NW trending

subduction, implies that the 1200°C isotherm occurs at 20km depth. In view of fig. 7.5, however, this temperature seems too extreme. There is a possibility of a weak and thinned crust under this region since the gravity anomalies are positive nearly everywhere (Albert - Beltrán, 1979).

(ii) Taranaki Region

Heat flow in this region varies from 41.9 mW/m^2 to 116.1 mW/m^2, with a mean of 86.4 ± 2.4 mW/m^2, which is substantially higher than in the Northland - Waikato region. The reduced heat flow of 71.9 mW/m^2 is also higher. This region spans the transition from (i) attenuating to transmitting seismic zones (Mooney, 1970), and (ii) positive to negative gravity anomalies. A notable feature which may be associated with this high heat flow anomaly is the presence of an active high-potash and andesitic volcano (Mt Egmont) in the middle of this region. This is the only such volcano in New Zealand. It is also interesting to observe that this is the region from which four exceptionally deep earthquakes have been reported (Adams, 1963; Adams and Ferris, 1976); the focal depths and epicentres are shown in figs. 8.1 and 8.2 respectively.

Calculated temperatures (fig. 7.6) imply favourable thermal conditions for the rocks to be in the liquid state (Pandey, 1981) at about 45km. The presence of high temperatures at such a shallow depth could lead to crustal thinning by subcrustal erosion, but there is no obvious evidence of such thinning in the gravity anomaly map.

(iii) Western Cook Strait

The calculated mean heat flow, reduced heat flow, and temperatures are considerably lower than in the adjacent Taranaki Region (table 7.4) The boundary between the two regions lies about 35km south of the seismic attenuating/transmitting boundary of Mooney (1970). Gravity anomalies are negative over the entire area and overlie the transmitting zone of Mooney (1970). The following factors may be associated with the lack of volcanism and lower heat flow in this region.

(a) Subduction is relatively shallower (fig. 8.1) and younger (Scholz et al., 1973); consequently the total volume of subducted material is smaller. The convergence rate is also lower, and magma generation may not be possible, since this requires the presence of water (Kushiro, 1972) and smaller rates will supply less water from the subducted plate.

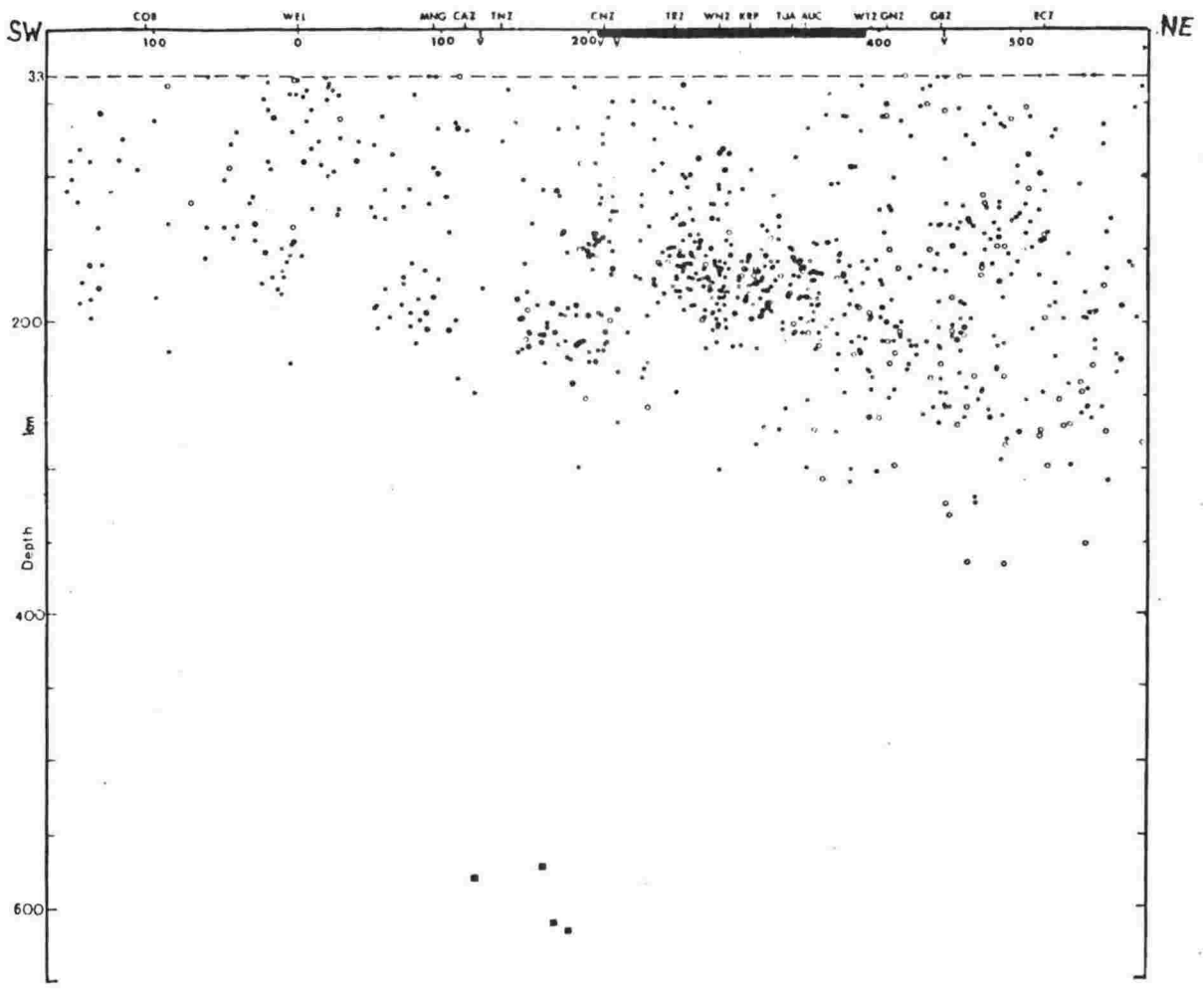

Fig. 8.1 Vertical cross section of foci along strike of Benioff zone, showing positions of seismograph stations, volcanoes (V), volcanic zone (shaded). Large symbols represent earthquakes of magnitute 4.5 or greater, and solid symbols denote those more accurately located (Adams and Ware, 1977).

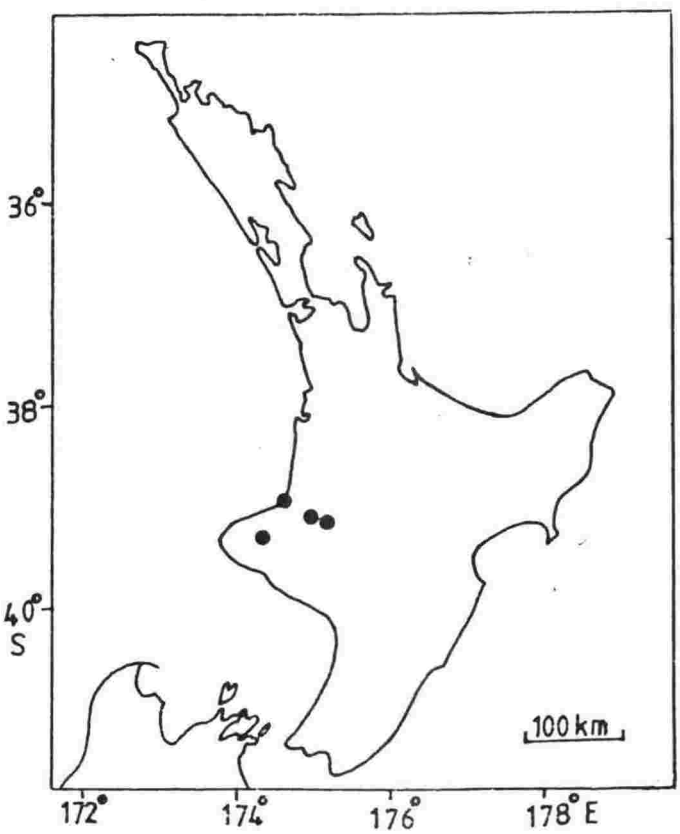

Fig. 8.2 Epicentres of four exceptionally deep earthquakes (after Adams and Ferris, 1976).

(b) There is a possibility of greater crustal thickness under this region, since the isostatic gravity anomaly is everywhere negative. The greater crustal thickness would provide a blanketing effect over the deep-seated heat source (Negi et al., 1974; Negi and Pandey 1976, 1981).

(iv) Hikurangi region

In this region the heat flow is low to normal except for two isolated high values which are probably related to basic intrusives. These two locations are sited close to thermal springs and are associated with larger positive magnetic anomalies. They may be remnants of a high heat flow zone related to an earlier, NW trending, subduction zone, active between 18 Myr and 3 Myr before the present, and extending from Northland to Mahia Peninsula. Midha (1979) mentioned this possible thermal expression of the North Island Conductivity Anomaly. The Pn and Sn velocities are lower, and the seismic residuals are larger, compared to further north.

Excluding these values, the range of heat flow is 20.9 to 62.2 mW/m^2, and the mean is 40.9 ± 2.8 mW/m^2. This is quite low compared to the values found elsewhere in New Zealand. However, it is typical of values found towards the trench side of island arc systems (McKenzie and Sclater, 1968; Watanabe et al., 1977 etc.). The estimated average temperature of 465^{o}C at 35km is about half of that obtained in the Taranaki region. Therefore it appears that the low heat flow of this region, associated with the presently active subduction, is overprinted on the thermal effect of an old subduction.

(v) Central Volcanic Region

This region is characterised by widespread recent volcanism. Heat flow is dominantly convective. Usually, observed gradients are hydrothermally disturbed, ranging from zero, or even negative, to many times normal. The heat flow varies accordingly, reaching such values as 52 W/m^2 for convective heat flow (Calhaem, 1973).

Some high conductive heat flow values have been measured. Heat flow at Mt Tihia (borehole F5A, F5C, F10) is extremely high, ranging from 367.9 mW/m^2 to 415.9 mW/m^2; this is not surprising since the average convective heat flow over the region is estimated to be 700 mW/m^2 (Allis, 1979a). Such high values are indicative of extremely high temperatures, with melting, at shallow depths. This conclusion seems inescapable, despite the results of Robinson et al. (1981), who found no evidence of extensive melting in their studies of P-wave travel-time residuals and of P/S amplitude ratios.

In this region Pn and Sn velocities are very low (7.4 and 3.95 km/s respectively), isostatic gravity anomalies are positive, and volcanic swarms (fig. 8.3) are common.

8.3 REGIONAL DISTRIBUTION IN THE SOUTH ISLAND

Heat flow in this Island is here reported for the first time (table 6.1; fig. 6.2). All but two results are grouped into three heat flow regions, the essential features of which are given below.

(i) West Coast Region

In this region the average heat flow is 91.2 ± 3.9 mW/m^2. There is a possibility that this region may extend northwards to include location Cook -1, which has the highest heat flow (136.6 mW/m^2) in the Taranaki Basin. The heat flow in the region is unusual in having no surface expression, either in the form of volcanism or thermal springs, although one of the boreholes (Arahura -1) terminated in basalt. The calculated reduced heat flow of 70.9 mW/m^2 is also high. The temperature distribution (fig. 7.7) suggests melting conditions at a depth of about 45km. Gravity anomalies are mostly positive over this region.

(ii) Marlborough - Canterbury Region

Heat flow is low to normal (from 35.6 mW/m^2 to 60.2 mW/m^2), despite the late Miocene volcanism at Banks Peninsula (near Christchurch). The average heat flow of 49.8 ± 3.8 mW/m^2 is very low compared to that in the other two regions. The reduced heat flow of 25.6 mW/m^2 is the lowest in New Zealand. The calculated temperature at 35km is less than 40 per cent of that in the adjacent Great South Basin. No hot springs are found here, and Pn and Sn velocities are normal. All these observations indicate that normal stable conditions prevail underneath the region. There seems a possibility that the region may be a continuation of Hikurangi heat flow region.

(iii) The Great South Basin

This is an offshore basin which adjoins the Canterbury Basin. All heat flow values are high, ranging from 87.2 mW/m^2 to 163.8 mW/m^2. The mean of the seven determinations is 110.7 ± 10.0 mW/m^2. The calculated reduced heat flow of 94.8 mW/m^2 compares, in the United States, only to the Cordilleran thermal anomaly zone. Melting conditions are expected at a shallow depth of about 35km (fig. 7.8), which can thus be taken as the base of the lithosphere in this region (Chapman and Pollack, 1977).

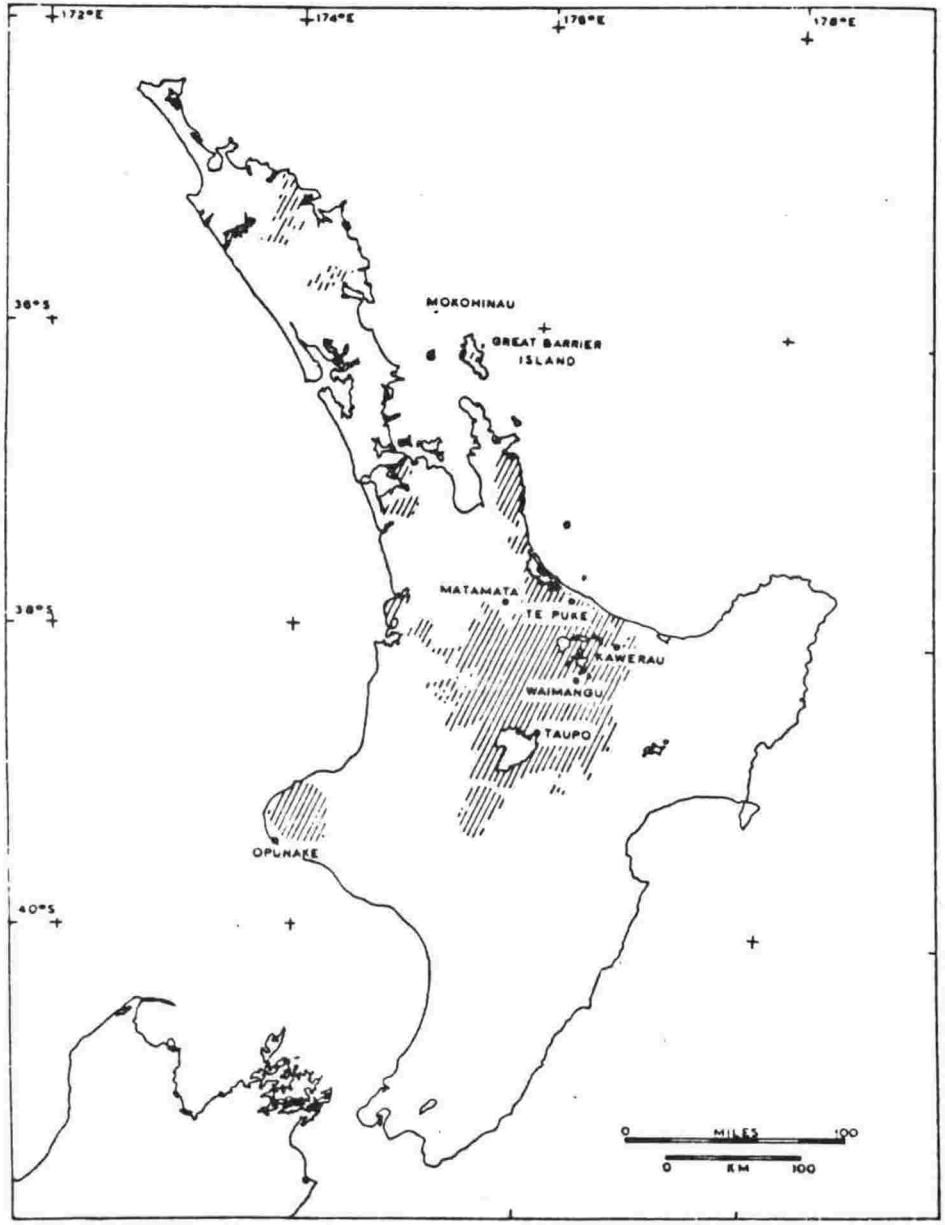

Fig. 8.3 Relationship between districts from which earthquake swarms are reported and the areas of Quaternary volcanic rocks (Eiby, 1966)

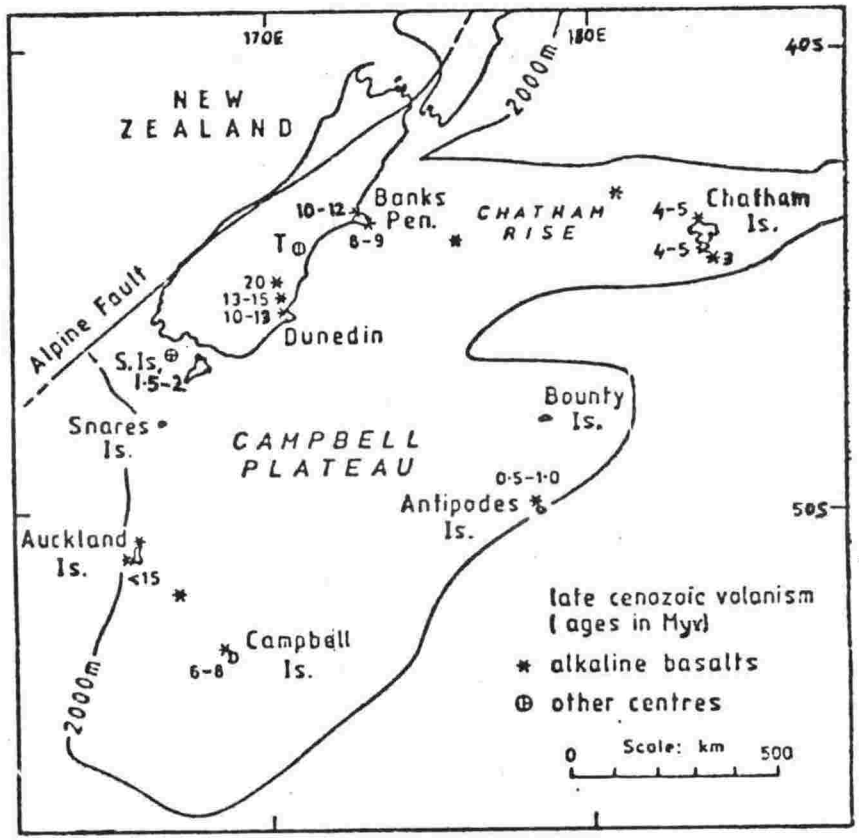

Fig. 8.4 Age data for centres of volcanism in Southern New Zealand and Campbell Plateau. SI = Solander Is., T= Timaru Basalt (C. Adams, pers. comm.)

Other kinds of geophysical observations are limited. There is some seismic evidence of young volcanism in the form of intrusions above basement (R. Cook, pers. comm.). Also in one of the boreholes (Hoiho -1C) a deep reflector, interpreted as a large batholith, has been reported to occur within the basement (Hunt International Petroleum Company, 1978). At this location heat flow is 163.8 mW/m^2, which is the highest so far measured outside the Central Volcanic Region.

Young volcanism has also occurred in the nearby islands surrounding this basin (Adams, pers. comm.). The ages (8-15 Myr BP in the Great South Basin) are shown in fig. 8.4; the suggested process is one of mantle upwelling at sites which have migrated from the Campbell Plateau and Chatham Rise to the present position.

8.4 UPPER MANTLE INHOMOGENEITY

The primary upper mantle inhomogeneity in the North Island is due to the subduction of the Pacific plate. An important though less extensive inhomogeneity also occurs in the Western Cook Strait region, and this will be discussed in detail later. Hatherton (1970b) was first to observe similarities between the seismic attenuating/transmitting regions which Mooney (1970) found in the upper mantle, and other geophysical parameters. The present heat flow distribution seems to correlate well with these regions.

The attenuating area is associated with high heat flow, mainly positive gravity anomalies, quaternary volcanism, low Pn and Sn velocities, large positive teleseismic residuals, thermal springs, a high electrical conductivity anomaly, and volcanic swarms. In the corresponding heat flow regions (Northland-Waikato, Taranaki), the estimated upper mantle temperatures are high.

On the other hand, in Mooney's region of transmission, heat flow is low to normal, gravity is mainly negative, Pn and Sn velocities are higher, volcanic swarms and quaternary volcanism are absent, thermal springs are rare, and estimated upper mantle temperatures are considerably lower.

8.5 HEAT FLOW DISTRIBUTION OVER PLATE SUBDUCTION

The present distribution of heat flow in the main New Zealand subduction zone seems to be consistent with plate tectonic theory. Fig. 8.5 shows a vertical cross-section of the structure of the Benioff Zone beneath a micro-earthquake traverse (figs. 5.2, 5.3)

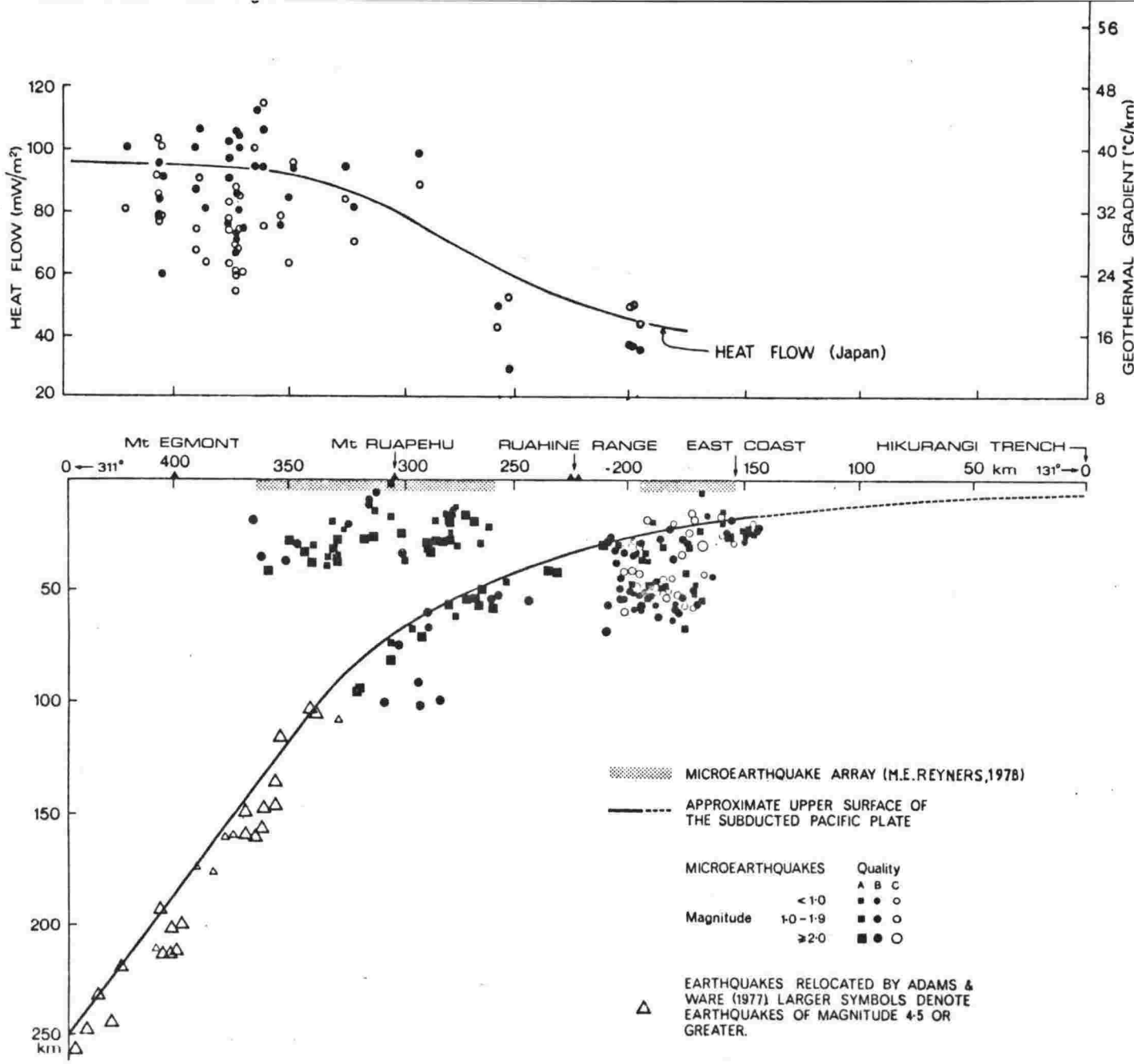

Fig. 8.5 Distribution of heat flow (solid circle) and geothermal gradient (open circle) normal to the Benioff zone. The heat flow profile across Japan is included for comparison.

across the subduction zone (Reyners, 1978). Variations of heat flow and geothermal gradient are shown along the profile. High heat flow and high geothermal gradients correlate with intermediate seismicity and active volcanism, while the considerably lower heat flow and geothermal gradient observed over the Hikurangi Region coincide with the band of shallow seismicity. In fig. 8.5 a heat flow profile across Japan is also included for comparison. The similarity is obvious.

The distribution shown in fig. 8.5 is similar to that observed across the other subduction zone (Uyeda and Horai, 1964; Vacquier et al., 1967; McKenzie and Sclater, 1968; Watanabe, 1974; Watanabe et al., 1977). Some of the profiles from the Western Pacific, and an average heat flow profile across an arc-trench setting (Wang, 1980) are shwon in figs 8.6 and 8.7. It may be mentioned here that in most calculations regarding the thermal regime in a trench-arc setting (e.g. Turcotte and Oxburgh, 1969; Minear and Toksöz, 1970; Toksöz et al., 1971) the kind of profile observed was not predicted.

It is an important problem to find an explanation for the observed heat flow patterns (Sugimura and Uyeda, 1973; Watanabe et al., 1977). In the past this has usually been explained using one of two models (fig. 8.8). One is the frictional heating model (Turcotte and Oxburgh, 1969; Minear and Toksöz, 1970; Hasebe et al., 1970), through which the observed heat flow is explained by shear heating along the slip-plane, which is also taken as the cause of extensive magmatism or diapirism. The other model is the secondary mantle flow model (McKenzie, 1969; Sleep and Toksöz, 1971; Andrews and Sleep; 1974), in which the upper mantle wedge above the slab is considered as a viscous fluid capable of sustaining convective flow caused by the descending slab.

The observed heat flow in the Taranaki region can be better explained through the secondary flow model, since the high heat flow extends at least 80km further northwest than the Benioff Zone, showing some similarity with back-arc basins. This suggests the possibility of convective heat transport under the Taranaki region. However, it is difficult to interpret the low heat flow of the Hikurangi region, which may have been caused by dehydration of the oceanic crust (Anderson et al., 1976), possibly cancelling out the frictional heat. The frictional sliding model of Wang (1980) suggests low frictional heating in the upper 60km.

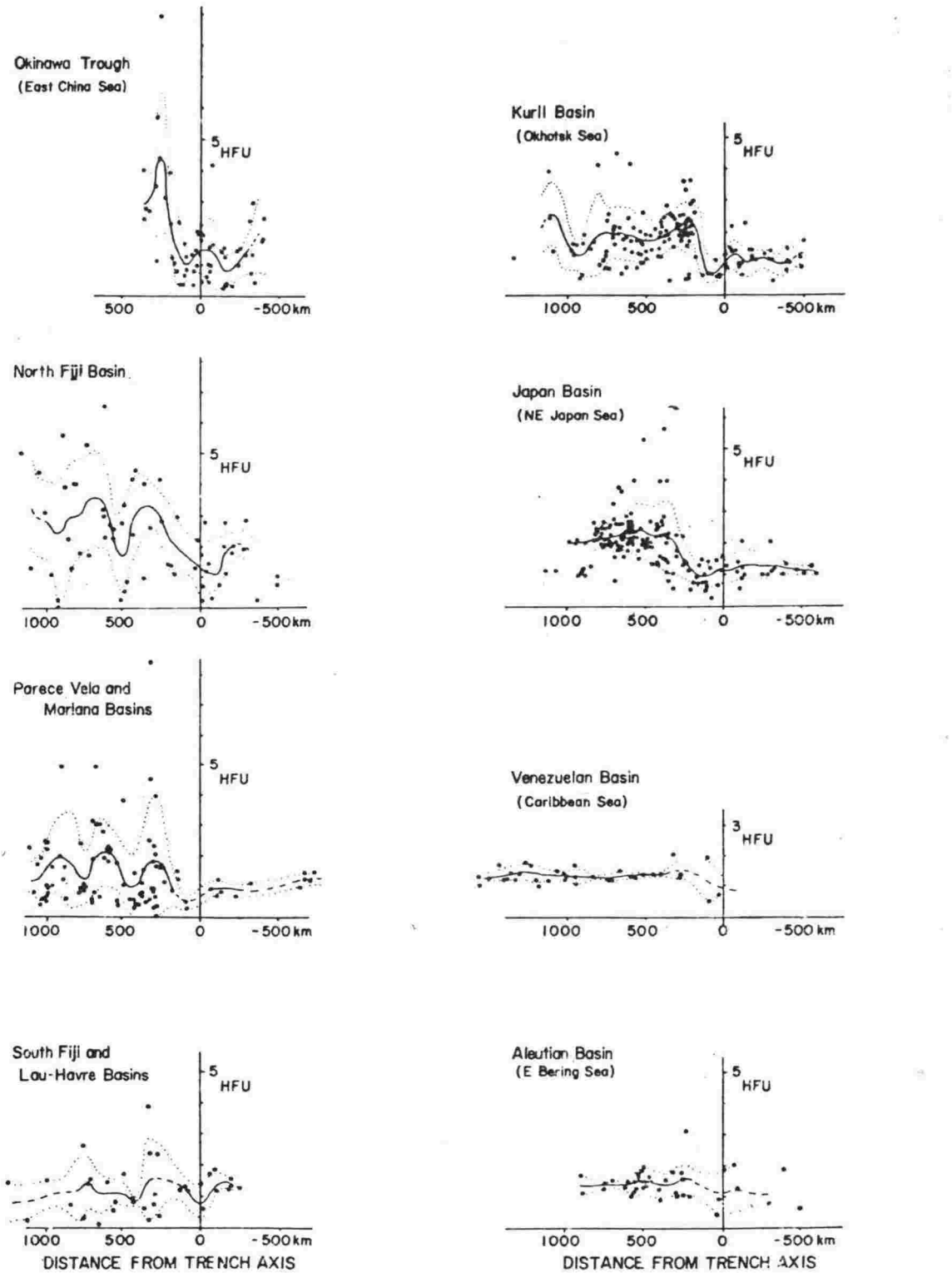

Fig. 8.6 Heat flow distribution across major trench island-arcs and back-arc basins in the Western Pacific (Watanabe et al., 1977).

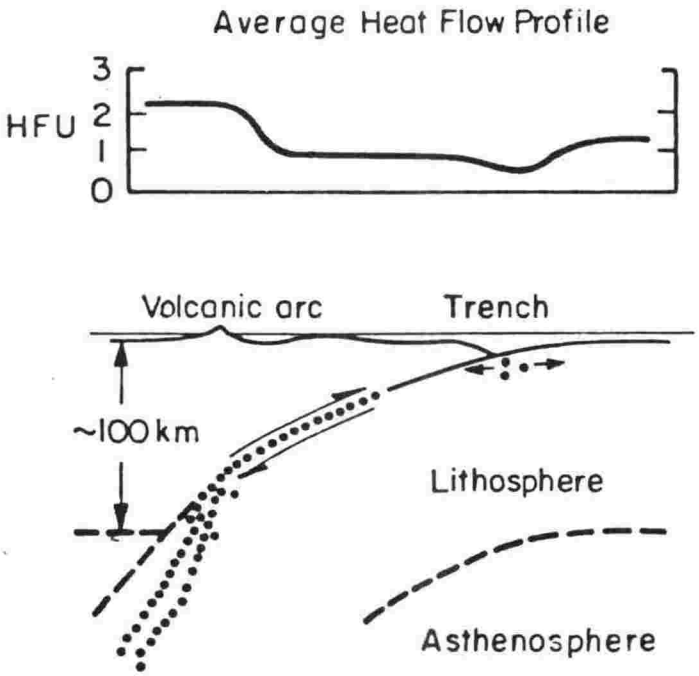

Fig. 8.7 Average heat flow profile across an arc-trench system (Wang, 1980).

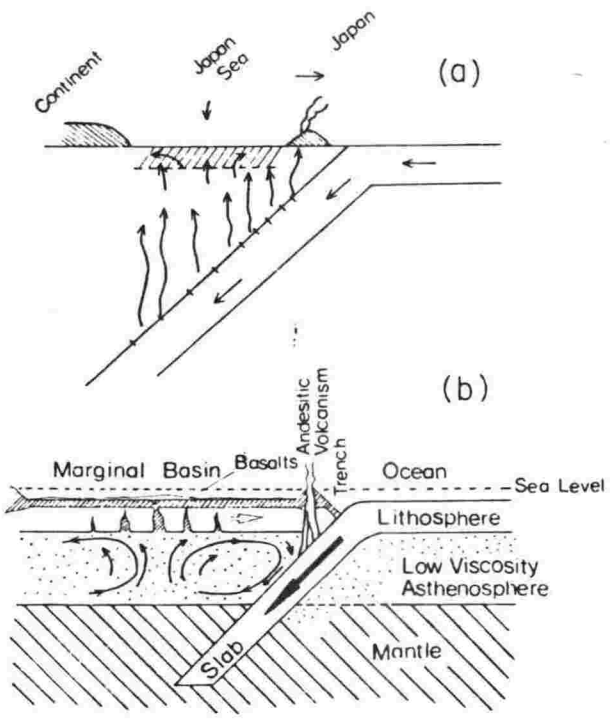

Fig. 8.8 (a) Frictional heating model, and (b) secondary mantle flow model (Uyeda, 1977).

8.6 UPPER MANTLE MODEL BENEATH WESTERN COOK STRAIT REGION

As mentioned earlier, the average heat flow in this region is about normal, in contrast to higher values in the north (Taranaki Region) and lower values in the east (Hikurangi Region). The boundary between the high and normal heat flow regions seems well-defined and is roughly parallel to the zero gravity anomaly and the seismic attenuating/transmitting boundary of Mooney (1970) (fig. 7.1). So far, the cause of the east-west orientation of the Mooney's boundary has remained unexplained. According to Mooney (1970) the boundary is not very well defined. Thus there seems a possibility that it may coincide with the heat flow boundary.

Both phenomena could be due to a reduction of subcrustal temperatures beneath the Western Cook Strait region (fig. 7.6), caused by a thickening of the crust and consequent thickening of the lithosphere to about 90km, by the well-known blanketing effect (Negi et al., 1974; Negi and Pandey, 1976, 1981). Such a lithospheric thickness is in contrast to about 45km beneath the Taranaki region, as shown in fig. 8.9. This model would also satisfy the gravity anomaly being everywhere negative. Thus the high heat flow usually found over a subducted plate is offset by the lithospheric thickening, giving a resultant heat flow about normal. The virtual absence of an asthenosphere in the region (fig.8.9) would account for the good seismic wave transmission obtained by Mooney (1970).

8.7 RELATIONSHIP OF HEAT FLOW WITH GEOTHERMAL GRADIENT AND THERMAL CONDUCTIVITY

Recently, attempts have been made (Gupta and Rao, 1970; Horai and Nur, 1970; Negi et al., 1974; Negi and Pandey, 1981) to find interrelationships between heat flow, thermal conductivity and geothermal gradient, on a regional and a global basis. These studies have led to several interesting conclusions, but sometimes also to inconsistent results, as discussed in detail by Negi et al. (1974) and Negi and Pandey (1981).

According to Negi et al. (1974) and Negi and Pandey (1981) there appears to be a negative correlation between heat flow and thermal conductivity for the sedimentary basins of India and Michigan (N. America), which is in disagreement with the earlier findings of Gupta and Rao (1970) of a null correlation in the Indian Precambrian crystalline regions, and by Horai and Nur (1970) of a positive correlation in many continental geological provinces, as well as in the Indian Peninsular shield.

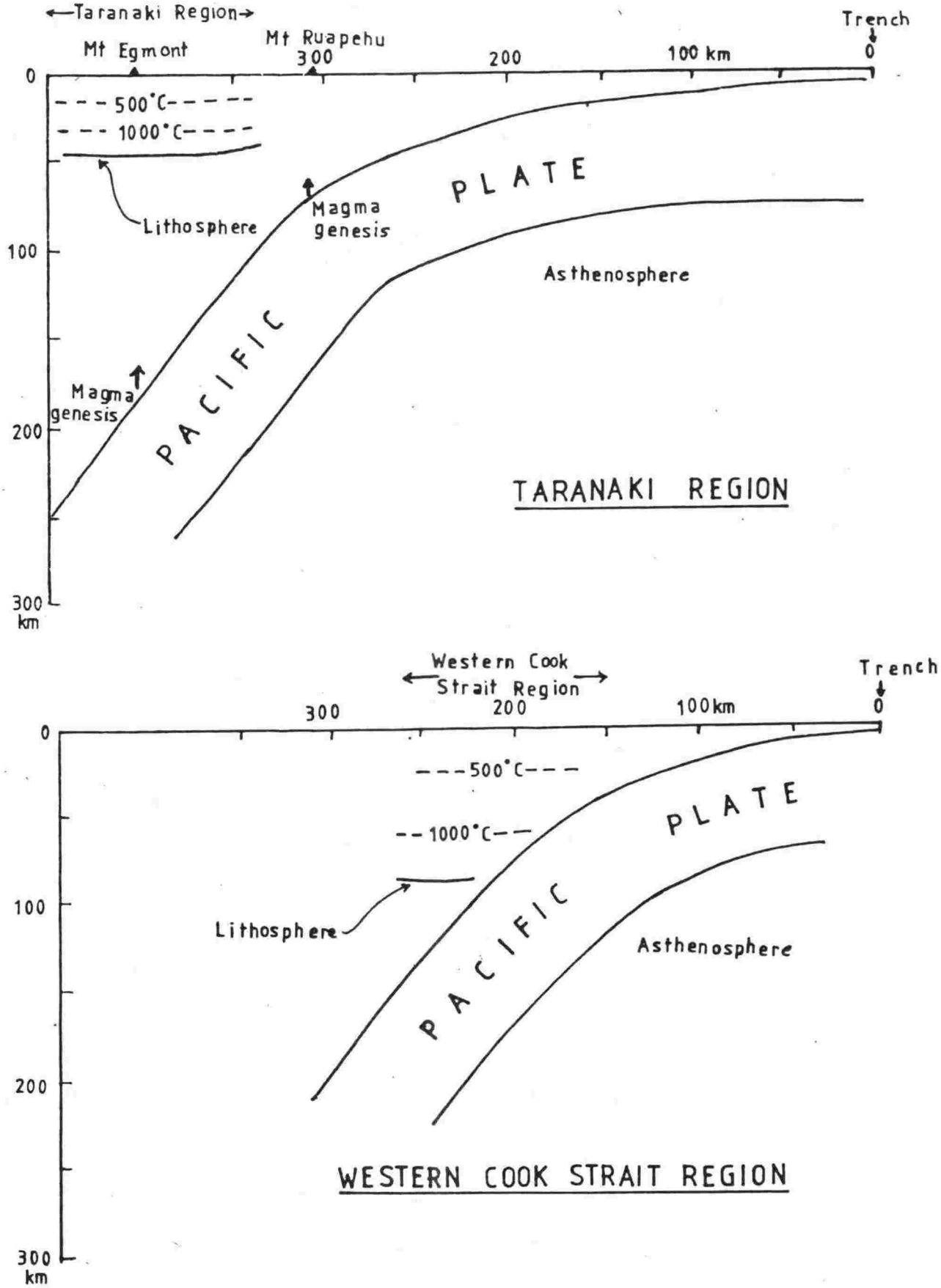

Fig. 8.9 Upper mantle models beneath Taranaki and Western Cook Strait regions.

Here, we examine the nature of the dependence of heat flow on geothermal gradient and thermal conductivity, using only those data from the present study for which the conductivity has been measured. The observed relationship is shown in fig. 8.10, which suggests that the heat flow is not correlated with thermal conductivity.

8.8 RELEVANCE TO PETROLEUM GENERATION

8.8.1 Background

A knowledge of geothermal parameters is essential in studies of thermal and subsidence histories of a sedimentary basin, and is thus relevant to the search for petroleum resources (Hunt, 1979; Keen, 1979). Most of the world's major oil/gas fields are located in areas where the sediments range in age from Jurassic to Cenozoic (Moody, 1975). These areas are also associated with high heat flow (Lee and Uyeda, 1965; Lee 1970; Sclater and Francheteau, 1970; Sclater et al., 1980). A continental mean heat flow of 76.2 mW/m^2 is reported for an age group of 0 to 250 Myr (Sclater et al., 1980), compared to an overall continental mean of 62.3 mW/m^2 (Jessop et al., 1976). Makarenko and Sergiyenko (1974) have considered that the accumulation of hydrocarbon leads to an increased heat flow. On the other hand, Klemme (1975) observed that in the majority of areas associated with large petroleum accumulations, geothermal gradient and heat flow are high, and that this enhances the processes of formation, migration and accumulation of oil or gas. This is consistent with the view that the rate of hydrocarbon generation increases sharply with temperature (Laraskaya and Zhabrev, 1964; Philippi, 1965; Hunt, 1979 etc.).

8.8.2 Temperature - Time relationship

Most major hydrocarbon deposits are known to occur at depths of less than 2750 m and nearly half lie above 1850 m (Klemme, 1975). In fields shallower than 1850 m, temperature alone seems the major factor for hydrocarbon generation, while temperature and time both play a role in deeper fields. The effect of time and temperature on the threshold of the main oil genesis phase is plotted in fig. 8.11 for 12 global locations where the present temperature does not differ too much from the maximum reached in the past. (Basins associated with extensive orogenic activity, erosion, volcanism, hydrothermal activity, etc., are excluded). Data are included for two gas-condensate producing areas of the Taranaki Basin. The basic data for this figure are taken from Connan (1974) but a correction to the temperatures has been made using the solid curve of fig. 3.5, so as

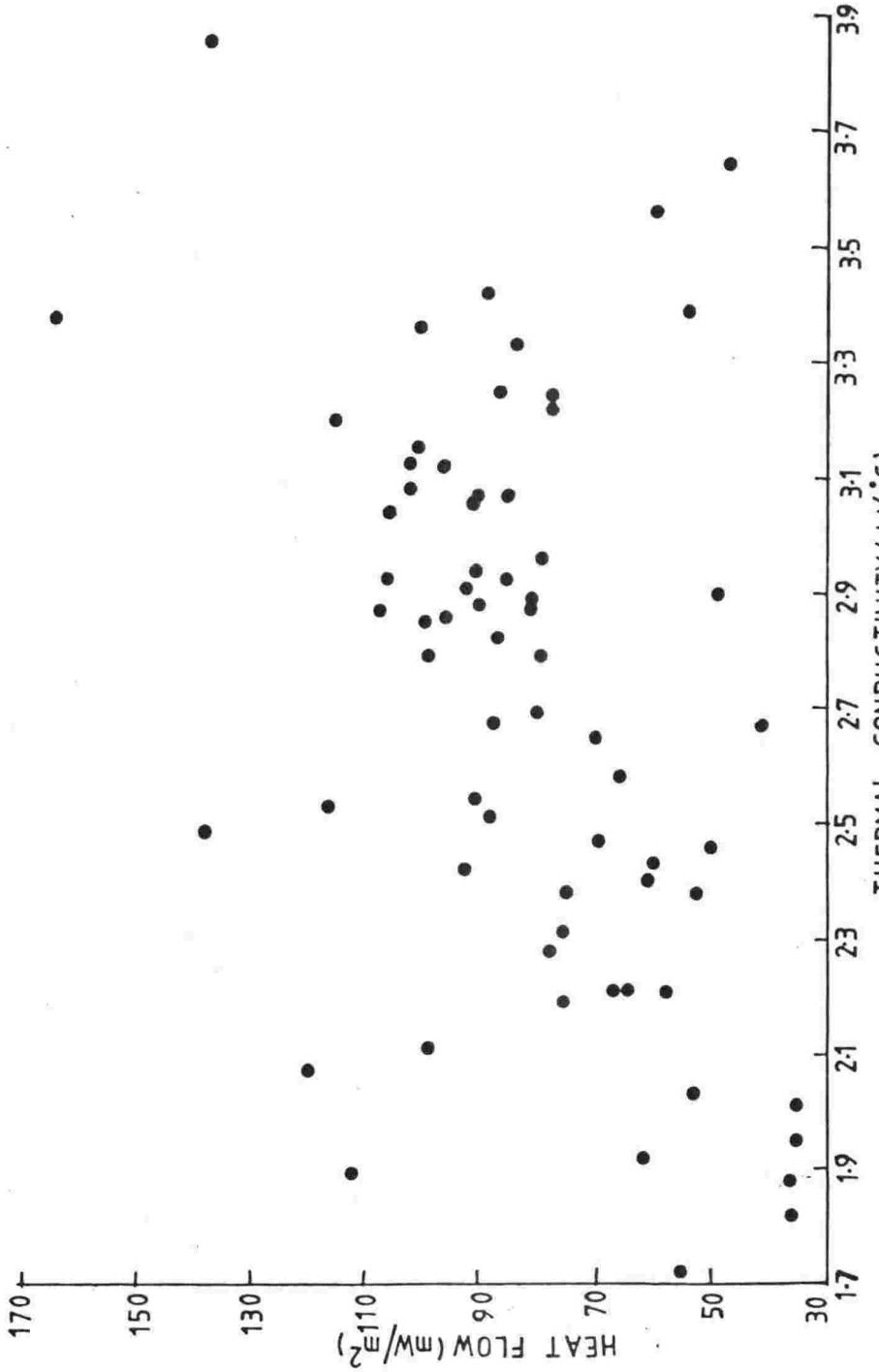

Fig. 8.10 Heat flow vs thermal conductivity.

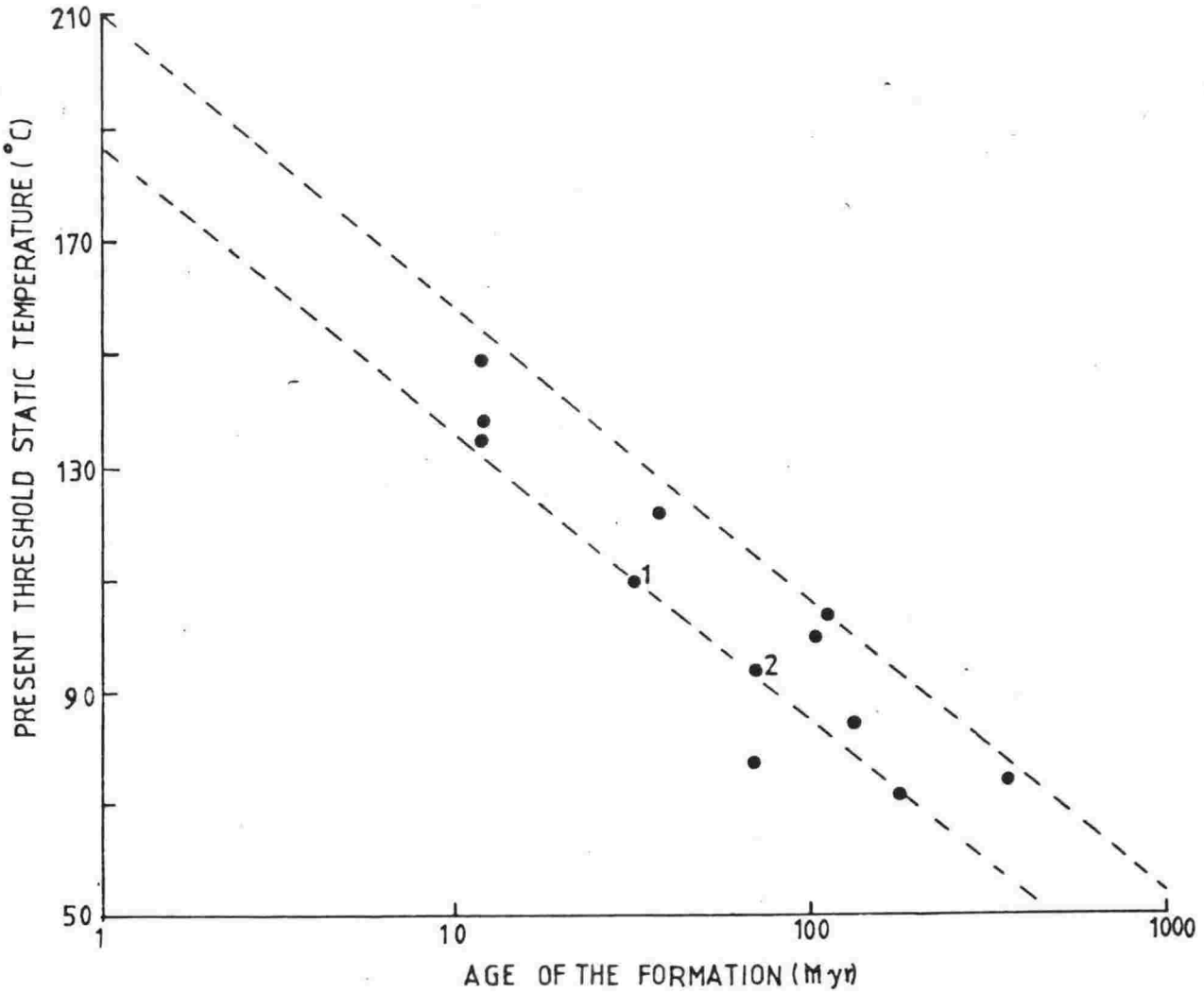

Fig. 8.11 Relationship between present threshold static temperature and age of the corresponding formation for twelve global locations. 1: data point for onshore Taranaki, 2: data point for offshore Taranaki.

to obtain the static formation temperatures.

All the data points in fig. 8.11, except one, fall in a narrow band, and reveal a strong correlation between the present threshold equilibrium temperature and the age of the corresponding formation. It is clear that in younger sedimentary basins a higher formation temperature is needed for the threshold of intense oil genesis, compared to older formations where time seems to compensate for temperature. In other words, higher temperatures are required in the younger rocks compared to older ones to reach equivalent maturities. This agrees with the observations of Connan (1974) and Dow (1977). If we find a temperature window corresponding to the ages of the rock formations in which nearly all of the major oil-gas finds occur (Moody, 1975), we get a range of about 60°C to 170°C, close to the accepted range of about 60° to 150°C in which hydrocarbons can form (Hunt, 1979). It is believed that the formation of hydrocarbons peaks at about 100°C, and the main phase of oil formation probably does not start until 80°C (Carnelius, 1975; Hunt, 1979; etc.).

8.8.3 Relevance to New Zealand

In New Zealand, drilling for oil has mostly been done in formations varying in age from Pliocene - Pleistocene to Late Cretaceous (R. Katz, pers. comm.). In fig. 8.11, this age group corresponds to a temperature range of about 80°C to 170°C for the threshold of intense oil genesis. This means that insitu temperatures of about 100°C and more are required in formations of Eocene age and younger. The present study suggests that there are large areas in some basins, such as Waikato, Wanganui, East Coast, Canterbury and Southland where the required temperatures are not reached in the sediments above the basement; the measured geothermal gradients, and the sedimentary thickness, are too small in these areas. However, older and deeper sections such as the Upper Cretaceous rocks in the East Coast Basin (Hicks, 1980), may provide suitable temperature conditions for hydrocarbon generation. It must be mentioned that these conclusions are valid only for those basins which are sufficiently free from the processes mentioned earlier in section 8.8.2., since the past geothermal gradient also plays an important role in the formation of petroleum (Klemme, 1975).

In view of the known sedimentary thicknesses and underground temperature distributions, the northern part of the Taranaki Basin, the West Coast Basin and the Great South Basin seem to have higher chances of oil generation. Heat flow in these regions is high.

All have a proven hydrocarbon potential, and the Northern Taranaki Basin is a commercial gas-condensate producer. It may also be mentioned here that in the Southern Taranaki Basin, where heat flow is normal, it was found that hydrocarbon generation was not significant in two of the three boreholes studied (Thompson, 1980).

8.9 CONCLUSIONS

In this chapter the results of the heat flow studies, mainly grouped in eight heat flow regions, have been discussed in the light of geological and geophysical parameters, and interpreted in terms of plate tectonics. Large variations in heat flow, from 20.9 to 163.8 mW/m^2 have been found, with a mean of 76.1 ± 2.5 mW/m^2.

In the North Island the heat flow distribution is largely typical of those found in active subduction zones elsewhere. There is a similarity in the heat flow distributions here and in Japan. The effect of an old northwest trending subduction, which was active between 18 and 3 Myr before present, can be seen in the distribution of heat flow. Heat flow is high and variable in the regions of Northland-Waikato, Central Volcanic Region and Taranaki, while the Hikurangi and Western Cook Strait regions have low to normal heat flow. The Taranaki high heat flow anomaly can be better explained with the help of a secondary mantle flow model. The boundary between the Taranaki and Western Cook Strait regions is well defined and may represent the actual attenuating/transmitting boundary of Mooney (1970).

Heat flow distribution in the South Island is less complicated. It is high in the West Coast Region and the Great South Basin. The Canterbury-Marlborough Region has low to normal heat flow and seems a possible continuation of the Hikurangi Region.

The anomalously high heat flow in the regions of Taranaki, West Coast and the Great South Basin seems to be associated with melting conditions in the upper most mantle. The distribution of heat flow correlates well with surface manifestations and regional scale differences in the deep-seated temperature. Upper mantle inhomogeneities deduced from seismological observations are also reflected in the heat flow distributions. In general, heat flow is high over the high frequency attenuating zone and lower above transmitting areas. The occurrence of normal heat flow and of a transmitting zone over the Western Cook Strait region can be explained with the help of lithospheric and crustal thickening.

There seems to be no correlation between heat flow and thermal conductivity. The present study seems to have some relevance to the petroleum search. It is noted that the three areas which have a proven hydrocarbon potential (Northern Taranaki Basin, West Coast Basin and the Great South Basin) are also associated with high heat flow.

CHAPTER 9

CONCLUSIONS

The principle objective of this investigation has been fulfilled to the extent that it has become possible to make some generalised conclusions about the thermal state of the crust and upper mantle beaneath New Zealand and its surrounding offshore region. The significance of bottom hole temperatures has been highlighted; it has been shown that heat flow calculated using bottom hole temperatures agrees well with values obtained by means of conventional probe measurements of temperature. A new conductivity sampling technique applicable to well cuttings has been found very effective.

In New Zealand a large variation in conductive heat flow from 20.9 mW/m^2 to 163.8 mW/m^2 (excluding the central Volcanic Region) has been found, with a mean of 76.1 ± 2.5 mW/m^2, somewhat higher than the global continental mean of 62.3 mW/m^2. A large variation in reduced heat flow, from 25.6 to 94.8 mW/m^2, has also been recorded.

Most of the heat flow determinations have been grouped into 8 heat flow regions. In the North Island, heat flow is clearly influenced by the subduction process; the higher heat flows and geothermal gradients correlate with intermediate depth seismicity and active volcanism. The residual effect of an old NW trending subduction, which was active between 18 and 3 Myr BP, can be seen in the heat flow distribution. Heat flow is especially high in the Taranaki Region and the Central Volcanic Region; in the latter region the heat transfer is mainly convective. Low heat flow has been obtained for the Hikurangi Region, while elsewhere it is low to normal with isolated highs.

The Taranaki and Western Cook Strait Regions meet in a fairly well-defined boundary trending eastwest. This boundary possibly coincides with the attenuating/transmitting boundary of Mooney (1970). A more detailed heat flow study is desirable throughout the Taranaki-Wanganui Basin.

The reason for the seismic wave transmitting region beneath the Western Cook Strait heat flow region has hitherto been unexplained. This phenomenon as well as the heat flow in the region may be attributed to a 90km thick lithosphere, the result of crustal thickening. Under this region the asthenosphere above the Pacific slab is either missing or very thin. This model would also account for the gravity anomaly.

In the South Island, heat flow is high in the West Coast Region and the Great South Basin, and considerably lower in the Marlborough-Canterbury Region. The heat flow anomaly associated with the Great South Basin is a prominent feature of the heat flow map of New Zealand. The reduced heat flow of 94.8 mW/m^2 compares only with the Battle Mountain High region of the Western United States. Melting conditions are expected at about 35km depth.

A linear relationship between heat flow and heat generation has been obtained only for the Taranaki and Hikurangi Regions, which exhibit some thermal similarities with the Basin and Range Province and Eastern United States Region respectively, despite geologic and plate tectonic dissimilarities.

No correlation has been found between heat generation and either density or thermal conductivity. A radioactive heat generation study on the Central Southern Alps rocks suggests that (i) the radioactivity of the lower crust beneath the Western Canterbury Region is much higher than normal, and (ii) New Zealand geosynclinal sequences are not present in such thicknesses beneath the east coast of the Canterbury Region. A heat flow traverse in the east-west direction across the Canterbury Plains should help to determine the present extent of the geosynclinal rocks at depth.

This study further reveals that the density and thermal conductivity of the rocks are primarily functions of age, depth and porosity, and that the conductivity also depends on SiO_2 content. A rough estimate of the conductivity can be made if these parameters are known.

Finally, it appears that heat flow has some direct relevance to petroleum exploration in New Zealand, since in areas of proven hydrocarbon potential, heat flow and the geothermal gradient are high.

APPENDIX 1

Temperature data : North Island boreholes

Depth (m)	Temperature (°C)
Northland-1	
0	(16.5)
620	45.49
Waimamaku-2	
1402.6	54.37
2361.2	77.00
2722.4	95.38
2910.2	105.55
3347.3	124.40
Bridgeman's-2 (Waiwera)	
5	24.16
10	25.85
15	27.10
20	28.21
25.3	29.28
30	30.25
35.1	31.28
40	32.45
45.2	33.58
50	34.74
55.1	35.79
60	36.93
65	38.17
70	39.02
75	40.03
80.2	41.20
85.4	42.16
90	43.12
95.1	44.12
100	45.06
105.1	45.94
110.1	46.62
115	47.23
Bridgeman's-2 (Waiwera) (Continued)	
120.1	47.85
125.2	48.33
130	48.58
135	49.09
140.1	49.32
145.3	49.51
150	49.56
155.1	49.71
160.2	49.85
165.3	49.96
170.3	50.02
175	50.10
180	50.15
185.4	50.18
190.2	50.21
195.2	50.26
200.1	50.30
205	50.34
210	50.37
215	50.53
L. Harvey (Orewa)	
10	16.25
20	16.42
30	16.62
40	16.89
50	17.10
60.5	17.40
70.2	18.01
80	18.63
90	19.29
100.3	19.58
L. Harvey (Orewa) (Continued)	
110.2	19.86
120	20.08
130	20.35
140	20.49
150.3	20.79
160.3	21.04
170	21.41
180.4	21.79
190	22.07
200	22.39
210.3	22.43
220	22.56
230	22.87
240	23.21
250.2	23.46
260	23.74
270	24.06
280	24.39
290.3	24.71
300	25.03
310.5	25.41
320.5	25.71
330	26.02
340	26.21
350.8	26.53
360	26.77
370	27.06
380.2	27.31
390	27.56
400	27.88
410	28.03
420	28.40

Depth (m)	Temperature (°C)
Kumea	
10	18.37
15.4	18.13
20	17.71
25.2	17.46
30.1	17.38
35.2	17.39
40	17.46
45.3	17.60
50.5	17.79
60	18.15
70.2	18.52
80.2	18.93
90	19.21
Penrose (Auckland)	
10.3	18.11
20	17.11
30	16.36
40	16.10
50	15.77
60	15.98
70	16.13
80	16.32
90	16.56
110	17.15
120	17.36
130	17.62
140	17.81
Pukekohe	
65.5	15.82
70	15.56
75	15.55
80	15.53
85.3	15.55
90	15.58
95.4	15.60
100	15.62
105	15.62
110	15.91
115	16.13
120.2	16.27

Depth (m)	Temperature (°C)
Pukekohe (Continued)	
125.1	16.40
130	16.52
135.4	16.75
140	16.87
146.7	17.11
150	17.24
155	17.48
160.2	17.65
165.2	17.84
170	18.00
175	18.11
180.3	18.25
185	18.36
190	18.47
195	18.59
Huntly 6534	
10	16.14
15	16.18
20	15.93
25	15.86
30	16.14
35	16.28
40	16.10
45	16.21
50	16.25
55	16.31
60	16.39
65	16.46
70	16.60
75	16.70
80	16.77
85	17.00
90	17.14
95	17.28
100	17.42
105	17.56
110	17.78
115	17.86
120	18.07

Depth (m)	Temperature (°C)
Huntly 6534 (Continued)	
125	18.28
130	18.39
135	18.53
140	18.70
145	18.85
150	19.07
155	19.28
160	19.42
165	19.49
170	19.60
175	19.90
180	20.10
185	20.37
190	20.56
195	20.70
200	20.90
205	21.10
210	21.28
215	21.42
220	21.86
225	22.42
Huntly 8123	
5	17.14
10	17.18
15	17.15
20	17.35
25	17.46
30	17.56
35	17.63
40	17.77
45	18.00
50	18.21
55	18.35
60	18.49
65	18.63
70	18.70
75	18.81
80	18.93
85	19.00

Depth (m)	Temperature (°C)
Huntly 8123 (Continued)	
90	19.07
95	19.18
100	19.28
105	19.42
110	19.63
115	19.77
120	19.93
125	20.14
130	20.35
135	20.56
140	20.79
145	21.00
150	21.21
155	21.42
160	21.63
165	21.84
170	22.07
175	22.28
180	22.49
185	22.70
190	23.00
195	23.21
200	23.42
205	23.60
210	23.84
215	24.07
220	24.28
225	24.46
230	24.67
235	24.86
240	25.07
245	25.25
250	25.49
255	25.72
260	25.90
265	26.14
270	26.32
275	26.56
280	27.07

Depth (m)	Temperature (°C)
Huntly 8123 (Continued)	
285	27.42
290	27.63
295	27.74
300	27.79
305	27.93
310	28.21
315	28.49
320	28.79
325	28.93
330	29.09
335	29.21
Huntly 8178	
25	15.86
30	15.90
35	15.93
40	16.00
45	16.10
50	16.14
55	16.21
60	16.28
65	16.35
70	16.40
75	16.63
80	16.70
85	16.86
90	17.00
95	17.07
100	17.14
105	17.28
110	17.35
115	17.42
120	17.42
125	17.49
130	17.49
135	17.53
140	17.53
145	17.56
150	18.42
155	18.49

Depth (m)	Temperature (°C)
Huntly 9022	
5	15.35
10	15.49
15	15.56
20	15.63
25	15.85
30	15.93
35	16.00
40	16.14
45	16.21
50	16.28
55	16.42
60	16.56
65	16.72
70	16.86
75	17.00
80	17.18
85	17.35
90	17.49
95	17.63
100	17.79
105	17.90
110	18.07
115	18.21
120	18.42
125	18.86
130	19.28
135	19.49
140	19.72
145	19.90
150	20.04
155	20.18
Huntly 8333	
180	20.5
400	28.00
500	31.00
600	33.00
700	35.10

Depth (m)	Temperature (°C)
Huntly 9674	
5	16.71
10	16.51
15	16.37
20	16.36
25	16.47
30	16.56
35	16.70
40	16.79
45	16.95
50	17.00
55	17.11
60	17.23
65	17.45
70	17.89
75	18.14
80	18.27
85	18.49
89	18.62
Waikato -1	
0	(14.17)
1032.1	41.62
Waikato -2	
0	(13.99)
1018	40.46
Waikato -4	
0	(14.28)
594.4	34.39
Waikato -5	
0	(14.34)
1012.2	63.02
Te Rapa -1	
0	(14.2)
1566.1	61.69
DD2 (Whitianga)	
6.1	15.64
18.29	16.55
30.48	17.27
36.58	17.39
42.67	17.65

Depth (m)	Temperature (°C)
DD2 (Whitianga) (Continued)	
48.76	18.09
54.86	18.36
60.96	18.36
67.06	18.73
85.34	20.69
91.44	21.18
97.54	21.64
103.63	22.09
115.82	23.23
128.02	24.00
134.11	24.36
140.21	24.55
146.30	25.27
152.40	25.55
158.50	25.64
164.59	25.75
170.69	26.09
176.78	26.55
182.88	26.82
188.98	27.45
195.07	27.90
Moa -1B	
1964.4	63.13
2040.6	65.14
2806.6	84.95
3375.7	106.13
Tane -1	
0	10.00
1211.0	44.44
2935.4	94.44
3265	105.84
3830.6	118.89
4354.1	137.78

Depth (m)	Temperature (°C)
Maui -1	
827.5	47.96
2287.8	73.82
2438.1	75.04
2745	95.56
2851.7	98.89
2895.9	98.89
3180.6	101.43
3380.5	110.91
Maui -2	
950.4	54.85
2026.6	70.47
2437.8	80.25
2675.8	99.83
2855.7	103.10
3041.6	105.92
3424.1	119.40
Maui -3	
1697.4	73.63
2987.6	108.31
3253.1	112.34
Cook -1	
969.9	63.55
2182.1	104.40
2534.4	120.06
Turi -1	
1140.3	41.22
2554.3	76.39
2949.9	83.36
3260.5	95.00
3405.6	109.71
3585.1	118.11
3738.2	119.22
3904.9	128.80
4004.5	132.60
Urenui -1	
913.5	40.78
2458.8	74.98
3390.3	108.97
3544.5	109.13
3803.9	116.00

Depth (m)	Temperature (°C)
Republic New Plymouth -1	
0	(15.00)
906	40.56
962.4	46.70
Republic New Plymouth -2	
0	(15.00)
911	52.69
Republic New Plymouth -3	
0	(15.00)
745.8	42.22
Republic New Plymouth -4	
0	(15.00)
684.4	40.00
947.2	46.96
Mangahewa -1	
1584.4	52.40
2350	80.00
2984.3	93.96
3123.6	104.44
3508.9	107.80
3796.9	120.68
4033.7	124.44
4040.4	128.80
4086.8	129.44
New Plymouth -2	
239.4	32.11
1615.3	72.97
2483.1	105.71
3149	116.20
3767.8	134.81
3902.5	141.87
4132.3	159.11
4420.7	170.48
McKee -1	
1831	71.09
1836	71.11
2295	77.78
2324	78.33
2487	83.89
2535	78.73

Depth (m)	Temperature (°C)
McKee -1 (Continued)	
2994.2	90.98
3457	110.00
3683	118.33
3710.5	115.38
3897.4	122.31
Inglewood -1	
1670.3	58.37
2514.0	65.26
3370.5	99.50
3618.3	112.78
3656.1	114.27
3956.6	118.89
4058.1	125.02
4202.3	136.38
4503.1	149.64
4783.2	153.43
5051.1	160.53
Toko -1	
1666	54.54
2513	71.21
2929	83.33
3360.5	95.37
3832	107.09
4313	121.51
4882	141.66
Kapuni -1	
1339.6	38.47
1826.4	47.09
2410.4	63.94
3010.8	78.71
3046.8	78.96
3292.1	88.59
3562.5	104.00
3792.6	112.34
3967.9	119.40

Depth (m)	Temperature (°C)
Kapuni -2	
1639.2	47.76
3503.7	82.17
3742	102.22
3787.1	106.56
3995.6	114.27
4112.1	118.70
Kapuni -3	
1708.1	48.43
3530.5	104.5
3682.9	105.83
Kapuni -3A	
2332.9	64.25
3541.1	105.00
3565.1	106.18
3649.4	110.00
Kapuni -4	
1671.5	43.78
2482.6	61.33
3264.4	73.18
3417.1	82.17
3702.7	118.12
3895.3	119.40
Kapuni -5	
761.5	45.32
2414.2	62.69
3309.7	90.10
3630.1	108.00
3638	109.11
3698.8	110.00
Kapuni -6	
754	44.94
3516.4	104.00
3723.7	109.00
Kapuni -7	
0	(12.6)
3503.1	102.00
3543.3	104.00
3728.9	109.00

Depth (m)	Temperature (°C)
Kapuni -8	
2437.7	67.21
3276.6	89.00
3324.8	92.00
3413.8	93.00
3611.8	101.78
4071.7	114.97
Kapuni -9	
912.4	42.79
2120.1	60.45
2544.5	70.44
3583.2	103.00
3665	105.49
3741.7	107.00
Kapuni -10	
2354.5	61.86
3567.4	104.00
3626.4	106.98
3689.9	108.00
Kapuni -11	
0	(13.00)
3291.8	96.00
3535.7	103.00
3688.1	105.00
Maui -4	
1253.0	49.44
1684.3	68.41
1931.2	68.33
2575.9	88.09
3611.9	110.13
3784.7	116.76
Kupe -1	
925.9	44.44
2531.9	84.34
2894.8	76.83
3254.6	86.59
3333.3	76.67
3641.9	93.10

Depth (m)	Temperature (°C)
North Tasman -1	
448.2	31.71
1431.5	60.90
2613.5	89.25
Tasman -1	
0	(13.5)
1520.6	66.34
Fresne -1	
1183.2	47.27
2036.3	71.81
2413.0	77.97
Surville -1	
949.0	45.75
2140.5	64.84
Kiore -1	
0	(12.5)
532.8	44.15
Patea	
10	14.64
20	14.83
30	15.02
40	15.10
50	15.13
60	16.11
70	16.70
80	17.25
90	17.64
Waikaka -1	
0	(13.9)
975.1	52.84
Ararimu -1	
0	(12.60)
1054	45.86
Whakamaro -1	
0	(13.9)
912.3	48.83
Tatu -1	
0	(13.00)
854	52.17

Depth (m)	Temperature (°C)
Koporongo -1	
0	(12.50)
586.7	32.11
Tupapakurua -1	
0	(12.1)
1146	44.15
Puniwhakau -1	
903.4	38.32
1257.9	45.77
1590.8	57.05
2031.5	70.47
2135.1	70.47
Parikino -1	
1222.9	45.77
1670.9	57.78
2311.0	77.00
Santoft -1A	
1628.1	51.74
2301.4	60.69
2627.5	63.94
Te Horo -1	
0	(15.9)
1800.8	61.11
Rotokautuku -1	
350.3	50.17
619.4	65.12
Te Puia -1	
0	(13.76)
1474.5	65.48
2035	78.32
Waitangi Station -1	
1051	45.57
2128.1	67.55
Ruakituri -1	
887.3	50.17
963.2	53.51
1408.5	59.03
1521.6	61.03
1702.9	62.35

Depth (m)	Temperature (°C)
Ruakituri -1 (Continued)	
2058.9	65.26
2421.0	71.77
2740.8	83.52
Mangaone -1	
339.5	24.08
648.3	27.78
688.5	32.22
745.8	31.11
815.3	34.44
991.5	38.89
1065.0	47.09
1187.5	51.74
1264.0	53.06
Opoutama -1	
0	(15.40)
1722.3	70.31
2743.0	87.43
3651.7	80.89
Hawke Bay -1	
1294.3	47.11
1762.1	55.15
Taradale -1	
526.4	76.67*
1117.1	71.11*
1215.2	65.56*
1652.0	54.44*
Mason Ridge -1	
310.0	24.75
610.8	28.76
724.5	30.77
993.0	34.14
1877.0	49.08
Ongaonga -1	
403.3	24.75
1249.4	37.81
1389.3	39.14
1399.6	39.80
1567.0	42.14

Depth (m)	Temperature (°C)
Takapau -1	
198.1	22.74
284.7	23.41
932.7	36.12
1053.4	37.08
R-240 (Rangipo)	
10	9.44
15	9.54
20	9.57
25	9.59
30	9.65
35	9.81
40	10.09
45	10.29
50	10.46
55	10.51
60	10.63
65	10.72
70	10.91
75	11.02
80	11.26
85	11.41
89	11.52
Tokaanu F-5A	
21.34	14.44
27.43	14.76
33.53	15.33
39.62	16.67
45.72	17.81
51.82	18.89
57.91	19.91
64.01	21.05
70.10	22.19
76.20	23.46
82.30	24.09
88.39	25.62
94.49	26.13
100.58	27.46
106.68	29.17
112.78	30.63

Depth (m)	Temperature (°C)
Tokaanu F-5A (Continued)	
124.97	33.24
131.06	33.87
134.11	34.26
149.96	37.43
Tokaanu F-5C	
30.48	10.83
42.67	12.22
54.86	13.33
67.06	14.72
79.25	16.94
91.44	17.50
97.54	17.78
103.63	18.06
109.73	18.06
115.82	18.06
128.02	20.83
134.11	21.94
140.21	22.83
146.30	24.28
152.40	24.83
158.50	24.72
164.59	25.44
170.69	26.22
176.78	27.61
182.88	27.78
188.98	29.94
195.07	32.06
201.17	32.22
Tokaanu F-10	
182.88	21.28
188.98	21.83
219.46	23.22
225.55	25.39
231.65	26.53
260.60	32.78

Depth (m)	Temperature
UW-1 (Petone)	
5	15.26
10	13.99
15	13.63
20	13.46
25	13.36
30	13.32
35	13.30
40	13.27
45	13.25
50	13.24
55	13.23
60	13.24
65	13.25
70	13.26
75	13.29
80	13.34
85	13.42
90	13.57
95	13.65
100	13.70
105	13.77
110	13.83
115	13.94
120	14.03
125	14.14
130	14.23
135	14.35
140	14.46
145	14.65
150	14.82
UW-3 (Lower Hutt)	
5	16.83
10.5	15.11
15	14.34
20	13.86
25	13.75
30	13.58
35	13.51
40	13.48
45	13.37

Depth (m)	Temperature (^{o}C)
UW-3 (Lower Hutt)	
50	13.33
55	13.31
60	13.33
65	13.35
70	13.37
75	13.44
80	13.49
85	13.56
90	13.64
95	13.71
100	13.79
105	13.86
110	13.94
115	14.02
120	14.12
125	14.22
130	14.35
135	14.46
140	14.55
145	14.66
150	14.77
155	14.90
160	15.01
165	15.12
170	15.20
175	15.28

Estimated temperatures are shown in brackets. Uncorrected temperatures are shown by asterisks.

APPENDIX 2

Temperature data : South Island boreholes

Depth (m)	Temperature (°C)
Thompsons Ford Blenheim	
5	12.93
10.1	12.99
15	13.05
20	13.14
25	13.23
30	13.23
35	13.23
40	13.25
45	13.29
50	13.25
55	13.36
60	13.38
65	13.45
70	13.47
75	13.55
80	13.66
85.1	13.71
90	13.76
95	13.82
100	13.86
105	13.95
109.5	14.03
Haku -1	
0	(12.5)
1618.5	69.65
Ahaura -2	
0	(12.20)
1062.3	52.89
Aratika -2	
631.6	43.74
1142.6	61.14
Aratika -3	
443.9	34.95
1722.1	65.45

Depth (m)	Temperature (°C)
Taramakau -1	
1214.3	65.67
1721.8	82.78
1853.8	84.25
2117.1	97.87
Arahura -1	
522.4	37.22
911.7	52.17
1530.4	75.00
1732.5	83.58
Harihari -1	
912.1	50.83
2255.9	83.52
2519.6	92.66
Waiho -1	
1761.4	58.37
2572.2	84.79
3221.4	96.57
3744.5	117.45
Murchison -1	
176.78	16.86
182.89	15.91
188.98	16.24
195.07	16.46
201.2	16.84
207.3	17.19
213.4	17.41
219.5	17.66
225.6	17.86
231.6	18.11
237.7	18.39
243.8	18.68
249.9	18.91
256	19.14
262.1	19.30

Depth (m)	Temperature (°C)
Murchison -1 (Continued)	
268.2	19.55
274.3	19.75
280.4	19.97
286.5	20.20
292.6	20.45
298.7	20.65
304.8	20.84
310.9	21.04
317	21.19
323.1	21.37
329.2	21.62
335.3	21.76
347.5	22.11
359.7	22.43
371.9	22.73
384	23.00
396.2	23.42
Blackwater -1	
6.1	11.22
12.2	11.47
18.3	11.68
24.4	11.83
30.5	12.06
36.6	12.33
42.7	12.31
48.8	12.54
54.9	12.77
60.9	13.02
67	12.84
73.2	13.29
79.2	13.09
85.3	13.34
91.4	13.75
97.5	14.05

Depth (m)	Temperature (°C)
Blackwater -1 (Continued)	
103.6	14.25
109.7	14.25
115.8	14.55
121.9	14.80
128	14.80
140.2	15.08
152.4	15.56
164.6	16.09
176.8	16.69
189	17.09
201.2	17.56
213.4	18.01
225.6	18.33
237.7	18.56
249.9	19.08
262.1	19.60
274.3	19.75
286.5	20.25
298.7	20.79
310.9	21.29
323.1	21.59
335.3	21.78
347.5	22.28
359.7	22.80
371.9	23.27
384	23.78
396.2	23.81
408.4	24.40
420.6	25.04
Bounty -1	
1061.2	48.43
1491.2	63.68
3116.4	114.27
Kowai -1	
393.1	23.19
950.9	37.78
1381.1	49.00
1412.1	50.93

Depth (m)	Temperature (°C)
Christchurch	
10	12.64
15	12.86
20	12.82
25	12.70
30	12.62
35	12.64
40	12.75
45	12.79
50	12.88
55	12.92
60	12.89
65	12.96
70	13.10
75	13.27
80	13.41
85	13.49
90	13.51
95	13.53
100	13.53
105	13.58
110	13.61
115	13.64
120	13.69
125	13.93
130	14.07
135	14.20
140	14.32
145	14.41
150	14.50
Leeston -1	
0	(11.95)
1153.2	42.14
Pendarves	
20	11.86
25	11.82
30	11.80
35	11.80
40	11.74

Depth (m)	Temperature (°C)
Pendarves (Continued)	
45	11.70
50	11.65
55	11.59
60	11.53
65	11.49
70	11.50
75	11.55
80	11.57
85	11.61
90	11.67
95	11.77
100	11.86
105	11.96
110	12.07
115	12.16
120	12.23
125.5	12.31
130	12.38
135	12.46
140	12.52
145	12.61
150	12.68
151	12.70
Resolution -1	
1135.3	47.28
1590.1	61.11
1886.1	65.48
Endeavour -1	
1170.4	59.35
2572.2	105.69
2667.3	108.31
Takapu -1A	
0	(11.50)
799.2	57.78

Depth (m)	Temperature (^{o}C)
Tara -1	
1235	47.37
3144	111.20
4262	140
Toroa -1	
1234.7	48.17
2988.9	89.86
3608.5	123.89
4040.4	132.22
Pakaha -1	
1173.8	52.33
2673.4	104.72
Kawau -1A	
1235.4	41.34
2614.9	93.33
2812.1	101.11
3010.5	107.80
3113.5	115.56
Hoiho -1C	
822.4	41.34
1697.7	83.89
J.T. Benny -1	
817.8	48.83
1007.1	55.06
Parara -1	
924.8	37.84
2721.9	78.04
3551.5	113.08
3619.5	113.65

Estimated temperatures
are shown in brackets

APPENDIX 3

Note on corrections to previously published heat flow values

Forty-two values of heat flow in the North Island were given in a preliminary report (Pandey, 1981). These values are tabulated below together with the values for the same locations given in this thesis. The earlier values have been corrected in several ways.

(i) The static temperature correction (see section 3.2.4) has been applied to all values. The effect of this correction has been to increase the heat flow value in most cases. The four largest corrections are:

Northland -1	+26.3 mW/m^2
Maui -2	+13.5 "
Fresne -1	+9.2 "
Kapuni -4	+9.2 "

(ii) Thermal conductivity has been measured on many additional samples. At some sites this enabled superior estimates of heat flow to be obtained for different depth ranges from those used previously. The main corrections are:

Tasman -1	+42.1 mW/m^2
Te Puia -1	+23.2 "

The five largest corrections for estimates made for the same depth ranges as before are:

Turi -1	-23.0 mW/m^2
Ararimu -1	-16.4 "
Waimamaku -2	+15.7 "
Toko -1	-9.9 "
Waitangi Station -1	+9.4 "

(iii)Additional static and bottom-hole temperatures became available for a few sites. The three largest corrections are:

Kapuni -3	+33.1 mW/m^2
Mangaone -1	+20.6 "
Ruakituri -1	-10.5 "

(iv) The sedimentation correction has been applied (see section 3.2.6). The two largest corrections are:

Parikino -1	+18.7 mW/m^2
Santoft -1A	+13.2 "

The nett changes in the estimated value of heat-flow were 20% or greater at 12 locations of the 42 locations discussed by Pandey (1981). A total of 105 locations are discussed in the thesis. The estimated value

of mean heat flow is changed for two of the heat-flow regions, as follows:

Region	Mean heat flow (mW/m^2)	
	Pandey (1981)	Thesis
Taranaki	92 ± 3	86.4 ± 2.4
Hikurangi	40 ± 4	40.9 ± 2.8

Thus the revisions do not appreciably affect the regional pattern.

The data available for the thesis are much more extensive than were available to Studt and Thompson (1969). The value provided by Allis (pers.comm.) is also subject to amendment. It might therefore have been considered appropriate to base the regional mean heat-flow values solely on the new data. If this were done, the means given in the thesis would be altered as follows:

Region	Mean heat flow (mW/m^2)	
	Including earlier values	Excluding earlier values
Northland-Waikato	74.2 ± 4.3	79.2 ± 4.2
Taranaki	86.4 ± 2.4	88.4 ± 2.0
Hikurangi	40.9 ± 2.8	47.7 ± 2.6

Here too the regional pattern is not appreciably affected by the inclusion of the earlier values.

The rather large changes which have been made to some individual estimates, as detailed in this note, demonstrate the value in heat-flow studies of securing the best and most numerous data possible.

Table : Comparison of heat-flow values

Borehole	Heat Flow (mW/m^2)	
	Pandey (1981)	Thesis
Northland -1	65	98.7
Waimamaku -2	70	90.8
Te Rapa -1	76	67.0
Moa -1B	80	80.3
Tane -1	106	85.3
Maui -1	77	77.9
Maui -2	78	88.7
Maui -3	69	77.9
Cook -1	129	136.6
Turi -1	120	100.7
Urenui -1	79	87.0
Mangahewa -1	105	99.7

Borehole	Heat Flow (mW/m^2)	
	Pandey (1981)	Thesis
New Plymouth -2	94	90.2
Inglewood -1	109	106.3
Toko -1	94	79.5
Kapuni -1	88	96.3
Kapuni -2	81	85.2
Kapuni -3	56	90.9
Kapuni -4	93	102.0
Maui -4	56	52.8
Kupe -1	57	48.1
Tasman -1	34	76.1
Fresne -1	57	66.1
Surville -1	56	54.3
Kiore -1	91	112.3
Ararimu -1	95	75.1
Tatu -1	115	116.1
Koporango -1	80	94.2
Tupapakurua -1	84	80.8
Puniwhakau -1	101	83.9
Parikino -1	74	99.0
Santoft -1A	40	49.1
Te Puia -1	39	62.2
Waitangi Station -1	37	50.2
Ruakituri -1	53	41.5
Mangaone -1	71	105.4
Opoutama -1	62	59.7
Hawke Bay -1	60	52.3
Taradale -1	45	disturbed
Mason Ridge -1	34	36.8
Ongaonga -1	30	35.6
Takapau -1	31	36.4

REFERENCES

Abbey, S., 1980. Studies in "standard samples" for use in the general analysis of silicate rocks and minerals. Part 6: 1979 edition of "Usable" values. Energy Mines and Resources Canada, Geol. Surv. paper 80-14, 30 pp.

Adam, A., 1978. Geothermal effects in the formation of electrically conducting zones and temperature distribution in the earth. Phys. Earth Planet. Int., 17: 21-28.

Adams, C.J.D., 1975. Discovery of Precambrian rocks in New Zealand: Age relations of the Greenland group and constant gneiss, West Coast, South Island. Earth Planet. Sci. Lett., 28: 98-104.

Adams, R.D., 1963. Source characteristics of some deep New Zealand earthquakes. N.Z. J. Geol. Geophys., 6: 209-220.

Adams, R.D. and Ferris, B.G. 1976. A further earthquake at exceptional depth beneath New Zealand (Note). N.Z. J. Geol. Geophys., 19: 269-273.

Adams, R.D. and Ware, D.E., 1977. Subcrustal earthquakes beneath New Zealand; locations determined with a laterally inhomogeneous velocity model. N.Z. J. Geol. Geophys., 20: 59-83.

Albert-Beltrán, J.F., 1979. Heat flow and temperature gradient data from Spain. In: Terrestrial heat flow in Europe, Editors V. Cermák and L. Ryback, Springer-Verlag, Berlin. Heidelberg, pp. 261-266.

Albright, J.N., 1976. A new and more accurate method for the direct measurement of earth temperature gradients in deep boreholdes. Proc. Sec. U.N. Symposium on the development and use of geothermal resources, San Francisco, California, U.S.A., Vol. 2, pp. 847-851.

Allis, R.G., 1978. The effect of Pleistocene climatic variations on the geothermal regime in Ontario: a reassessment. Can. J. Earth Sci., 15: 1875-1879.

Allis, R.G., 1979a. Heat Flow. In: Scientific excursion A5, volcanic and geothermal areas of the North Island, New Zealand. Compiler M.P. Hochstein and T.M. Hunt, The R. Soc. N.Z., Wellington, pp. 49-50.

Allis, R.G., 1979b. A heat production model for stable continental crust. Tectonophysics, 57: 151-165.

Anderson, R.N., Uyeda, S. and Miyashiro, A., 1976. Geophysical and geochemical constraints at converging plate boundaries. Pt. I: Dehydration in the downgoing slab. Geophys. J.R. Astr. Soc., 44: 333-357.

Andrews, D.J. and Sleep, N.H., 1974. Numerical modeling of tectonic flow behind island arcs. Geophys. J. R. Astr. Soc., 38: 237-251.

Arabasz, W.J. and Robinson, R., 1976. Microseismicity and geologic structure of the northern South Island, New Zealand. N.Z.J. Geol. Geophys., 19: 569-601.

Auckland Regional Water Board, 1980. Waiwera Water Resource Survey, A.R.W.B. Technical Publ. No. 17.

Ballance, P.F., 1976. Evolution of the Upper Cenozoic magmatic arc and plate boundary in northern New Zealand. Earth Planet. Sci. Lett., 28: 356-370.

Balling, N., 1979. Subsurface temperatures and heat flow estimates in Denmark. In: Terrestrial heat flow in Europe, Editors V. Cermák and L. Rybach, Springer-Verlag, Berlin Heidelberg, pp. 161-171.

Beck, A.E., 1957. A steady state method for the rapid measurement of the thermal conductivity of rocks. J. Sci. Instr., 34: 186-189.

Beck, A.E. 1965. Techniques of measuring heat flow on land. In: Terrestrial heat flow. Editor W.H.K. Lee, Am. Geophys. Un., Washington, D.C., Geophys. Monograph 8, pp. 24-57.

Beck, A.E., 1977. Climatically perturbed temperature gradients and their effect on regional and continental heat flow means. Tectonophysics, 41: 17-39.

Beck, A.E., Jaeger, J.C. and Newstead, G.N., 1956. The measurement of the thermal conductivities of rocks by observations in boreholes. Aust. J. Phys., 9: 286-296.

Benfield, A.E., 1939. Terrestrial heat flow in Great Britain. Proc. Roy. Soc. London, A, 173: 428-450.

Birch, F., 1950. Flow of heat in the Front Range, Colorado. Bull. Geol. Soc. Am., 61: 567-630.

Birch, F., 1954. Heat from radioactivity. In: Nuclear Geology, Editor H. Faul, John Wiley, New York, pp. 148-175.

Birch, F. and Clark, H., 1940. The thermal conductivity of rocks and its dependance upon temperature and composition. Am. J. Sci., 238: 529-558.

Birch, F., Roy, R.F. and Decker, E.R., 1968. Heat flow and thermal history in New England and New York. In: Studies of Appalachian Geology: Northern and Maritime, Editors E. Zen, W.S. White, J.B. Hadley and J.B. Thompson, Jr., Interscience, New York, pp. 437-451.

Blackwell, D.D., 1971. The thermal structure of the continental crust. In: The structure and physical properties of the Earth's crust. Editor J.G. Heacock, Am. Geophys. Un., Washington, D.C. Geophys. Monograph 14, pp. 169-184.

Blackwell, D.D., 1978. Heat flow and energy loss in the Western United States. In: Cenozoic Tectonics and regional geophysics of the Western Cordillera. Editors R.B. Smith and G.P. Eaton, The Geological Society of America, Inc., memoir 152, pp. 175-208.

Blackwell, J.H., 1954. A transient heat flow method for determination of thermal constants of insulating materials in bulk. J. Appl. Phys., 25: 137-144.

Blackwell, J.H., 1956. The axial flow error in the thermal conductivity probe. Can. J. Phys., 34: 412-417.

Boccaletti, M., Fazzuoli, M., Loddo, M. and Mongelli, F., 1977. Heat-Flow measurements on the Northern Apennine arc. Tectonophysics, 41: 101-112.

Brown, D.A., Campbell, K.S.W. and Crook, K.A.W., 1968. The geological evolution of Australia & New Zealand. Pergamon Press, London, 409 pp.

Bullard, E.C., 1938. The disturbance of temperature gradient in the earth's crust by inequalities of height. Month. Not. R. Astr. Soc., Geophys. Suppl., 4: 360-362.

Bullard, E.C., 1939. Heat flow in South Africa. Proc. R. Soc. London, A, 173: 474-502.

Bullard, E.C., 1947. The time necessary for a borehole to attain temperature equilibrium. Monthly Notices Roy. Astr. Soc., Geophys. Suppl., 5: 127-130.

Bullard, E.C., 1954. The flow of heat through the floor of the Atlantic Ocean. Proc. R. Soc. London, A, 222: 408-429.

Bullard, E.C., 1965. Historical introduction to terrestrial heat flow. In: Terrestrial heat flow. Editor W.H.K. Lee, Am. Geophys. Un., Washington, D.C., Geophys. Monograph 8, pp. 1-6.

Bullen, K.E., 1939. The crustal structure of the New Zealand region as inferred from studies of earthquake waves. Proc. 6th Pacif. Sci. Congr., 1: 103-110.

Calhaem, I.M., 1973. Heat flow measurements under some lakes in North Island, New Zealand. Ph.D. Thesis, Victoria University of Wellington.

Calhaem, I.M., Haines, A.J. and Lowry, M.A., 1977. An intermediate-depth earthquake in the central region of the South Island used to determine a local crustal thickness. N.Z. J. Geol. Geophys., 20: 353-361.

Carslaw, H.S. and Jaeger, J.C., 1959. Conduction of heat in solids second edition, Oxford University Press, London, 510 pp.

Carvalho, H.S., Purwoko., Siswoyo., Thamrin, M. and Vacquier, V., 1980. Terrestrial heat flow in the Tertiary basin of Central Sumatra. Tectonophysics, 69: 163-188.

Cermák, V., 1971. Undergraound temperature and inferred climatic temperature of the past millenium. Palaeography, Palaeoclimatol., Palaeoecol, 10: 1-20.

Cermák, V., 1973. Thermal conductivity of rocks, its measurement and role in heat flow investigation. Mineralia Slovaca, 5: 507-513.

Cermák, V. and Jessop, A.M., 1971. Heat flow, heat generation and crustal temperature in the Kapuskasing area of the Canadian Shield. Tectonophysics, 11: 287-303.

Chapman, D.S. and Pollack, H.N., 1974. 'Cold spot' in West Africa: anchoring the African plate. Nature, 250: 477-478.

Chapman, D.S. and Pollack, H.N., 1977. Regional geotherms and lithospheric thickness. Geology, 5: 265-268.

Chase, C.G., 1978. Plate kinematics: the Americas, East Africa, and the rest of the world. Earth Planet. Sci. Lett., 37: 355-368.

Cheremenski, G.A., 1960. Time of re-establishing the thermal conditions disturbed by drilling a borehole. Izv. Akad. Nauk SSSR, ser. Geofiz., 1801-1805.

Christoffel, D.A. and Calhaem, I.M., 1969. A geothermal heat flow probe for insitu measurement of both temperature gradient and thermal conductivity. J. Sci. Instr., 2: 457-465.

Clark, S.P., 1941. The effects of simple compression and wetting on the thermal conductivity of rocks. Trans. Am. Geophys. Un., 543-544.

Clark, S.P., 1966. Thermal conductivity. In: Handbook of physical constants, Editor S.P. Clark, The Geol. Soc. Am., Inc., Memoir 97, New York, pp. 459-482.

Clark, S.P., Peterman, Z.E. and Heier, K.S., 1966. Abundances of Uranium Thorium, and Potassium. In: Handbook of Physical Constants, Editor S.P. Clark, The Geol. Soc. Am., Inc., Memoir 97, New York, pp. 521-541.

Combs, J. and Simmons, G., 1973. Terrestrial heat flow determinations in the North Central United States. J. Geophys. Res., 78: 441-461.

Connan, J., 1974. Time - temperature relation in oil genesis. Am. Assoc. Petroleum Geologists Bull., 58: 2516-2521.

Cooper, L.R. and Jones, C., 1959. The determination of virgin strata temperatures from observations in deep survey boreholes. Geophys. J.R. Astron. Soc., 2: 116-131.

Cornelius, C.-D., 1975. Geothermal aspects of hydrocarbon exploration in the North Sea Area. Norges Geol. Unders., 316: 29-67.

Crain, I.K., 1968. The glacial effect and the significance of continental terrestrial heat-flow measurements. Earth Planet Sci. Lett., 4: 69-72.

Daly, R.A., Manger, G.E. and Clark, S.P., 1966. Density of Rocks. In: Handbook of Physical constants, Editor S.P. Clark, The Geol. Soc. Am. Inc., Memoir 97, New York, pp. 19-26.

Dawson, G.B., 1964. The nature and assessment of heat flow from hydrothermal areas. N.Z. J. Geol. Geophys., 7: 155-171.

Dawson, G.B. and Dickinson, D.J., 1970. Heat flow studies in thermal areas of the North Island of New Zealand. Geothermics, 2: 466-473.

Decker, E.R., 1966. Terrestrial heat flow in Colorado and New Mexico, Ph.D. thesis, Harvard University, Cambridge, Mass.

Decker, E.R. and Smithson, S.B., 1975. Heat flow and gravity interpretation across the Rio Grande Rift in Southern New Mexico and West Texas J. Geophys. Res., 80: 2542-2552.

Decker, E.R., Baker, K.R., Bucher, G.J. and Heasler, H.P., 1980. Preliminary heat flow and radioactivity studies in Wyoming. J. Geophys. Res., 85: 311-321.

Dickinson, W.R. and Hatherton, T., 1967. Andesitic volcanism and seismicity around the Pacific. Science, 157: 801-803.

Dolgushin, S.S. and Amshinsky, N.N., 1966. Uranium distribution in certain Altay granitoid intrusives. Geokhimiya, 9: 1081-1086.

Dow, W.G., 1977. Petroleum source beds on continental slopes and rises. In: Geology of continental margins, AAPG continuing Education course note series 5, AAPG continuing education programme. Tulsa, Okla. Am. Assoc. Petroleum geologists, 37 pp.

Duncan, A.R., 1970. The petrology and petrochemistry of andesite and dacite volcanoes in Eastern Bay of Plenty, New Zealand, Ph.D. Thesis, Victoria University of Wellington.

Eiby, G.A., 1955. New Zealand crustal structure. Nature, 176: 32.

Eiby, G.A., 1957. Crustal structure project. Geophys. Mem. N.Z., 5, 40 pp.

Eiby, G.A., 1958. The structure of New Zealand from seismic evidence. Geol. Rundsch., 47: 647-662.

Eiby, G.A., 1964. The New Zealand sub-crustal rift. N.Z. J. Geol. Geophys., 7: 109-133.

Eiby, G.A., 1966. Earthquake swarms and volcanism in New Zealand. Bull. Volcan., 29: 61-74.

Eiby, G.A., 1970. Seismic regions of the South Island of New Zealand. Trans. R. Soc. N.Z., Earth Sciences, 8: 29-39.

Eiby, G.A., 1971. Seismic regions of New Zealand. In: Recent Crustal Movements. Editors B.W. Collins and R. Fraser, R. Soc. N.Z. Bull., 9, pp. 153-160.

Ensor, 1931. The determination of thermal conductivity and its temperature variation for medium conductors. Proc. Phys. Soc., 43: 581- 591.

Evans, T.R., 1977. Thermal properties of North Sea Rocks. The Log Analyst, 18: 3-12.

Evans, T.R. and Tammemagi, H.Y., 1974. Heat flow and heat production in north east Africa. Earth Planet. Sci. Lett., 23: 349-356.

Evison, F.F., Robinson, R. and Arabasz, W.J., 1976. Micro earthquakes, geothermal activity and structure, central North Island, New Zealand. N.Z. J. Geol. Geophys., 19: 625-637.

Ewart, A. and Stipp, J.J., 1968. Petrogenesis of the volcanic rocks of the Central North Island, New Zealand, as indicated by a study of Sr^{87}/Sr^{86} ratios, and Sr, Rb, K, U and Th abundances. Geochimica et Cosmochimica Acta 32: 699-735.

Ewart, A., Taylor, S.R. and Capp, A.C., 1968. Trace and minor element geochemistry of rhyolitic volcanic rocks, central North Island, New Zealand - total rock and residual liquid data. Contr. Mineral. Petrol., 18: 76-104.

Fertl, W.H. and Wichmann, P.A., 1977. How to determine static BHT from well log data. World Oil, January: 105-106.

Gable, R., 1979. Draft of a geothermal flux map of France. In: Terrestrial heat flow in Europe, Editors V. Cermák and L. Ryback, Springer-Verlag, Berlin Heidelberg, pp. 179-185.

Garrick, R.A., 1968. A reinterpretation of the Wellington crustal refraction profile (Letter). N.Z. J. Geol. Geophys., 11: 1280-1294.

Garrick, R.A., 1969. Some physical properties of rocks in the East Cape - Mahia Peninsula region, North Island, New Zealand. N.Z. J. Geol. Geophys., 12: 738-760.

Garrick, R., 1979. Late Holocene uplift at Te Araroa, East Cape, North Island, New Zealand. N.Z. J.Geol. Geophys., 22: 131-139.

Gibowicz, S.J., 1972. Amplitude of P-waves recorded at New Zealand stations from shallow earthquakes at less than 30^{o}. N.Z. J. Geol. Geophys., 15: 336-359.

Gibowicz, S.J., 1974. Frequency-magnitude, depth, and time relations for earthquakes in an island arc: North Island, New Zealand. In: Focal Processes and the prediction of earthquakes. Editor T. Rikitake, Tectonophysics, 23: 283-297.

Girdler, R.W., 1970. A review of Red sea heat flow. Phil. Trans. R. Soc. London, A,, 267: 191-203.

Gladney, E.S. and Goode, W.E., 1981. Elemental concentrations in eight new United States Geol. Surv. rock standards: A review. Geostandards News letter, 5: 31-64.

Govindaraju, K., 1980. Report (1980) on three GIT-IWG rock reference samples: Anorthosite from Greenland, AN-G; Basalte d'Essey-la-Côte, BE-N; Granite de Beauvoir, MA-N. Geostandards Newsletter, 4: 49-138.

Gupta, M.L. and Rao, G.V., 1970. Heat flow studies under Upper mantle project. In: NGRI's contribution to the upper mantle project, Spec. Issue, Bull NGRI, 8: 87-112.

Haines, A.J., 1979. Seismic wave velocities in the uppermost mantle beneath New Zealand. N.Z. J. Geol. Geophys., 22: 245-257.

Hamilton, R.M., 1969. Seismological studies of the Gisborne earthquake sequence, 1966. In: Gisborne Earthquake, New Zealand, March 1966. N.Z. D.S.I.R. Bull. 194, pp. 7-23.

Hamilton, R.M. and Evison, F.F., 1967. Earthquakes at intermediate depths in south-west New Zealand. N.Z. Jl. Geol. Geophys., 10: 1319-1329.

Hamilton, R.M. and Gale, A.W., 1968. Seismicity and structure of North Island, New Zealand. J. Geophys. Res., 73: 3859-3876.

Hamilton, R.M. and Gale, A.W., 1969. Thickness of the mantle seismic zone beneath the North Island of New Zealand. J. Geophys. Res., 74: 1608-1613.

Hasebe, K., Fujii, N. and Uyeda, S., 1970. Thermal processes under island arcs. Tectonophysics, 10: 335-355.

Hatherton, T., 1969. The geophysical significance of calc-alkaline andesites in New Zealand. N.Z. J. Geol. Geophys., 12: 436-459.

Hatherton, T., 1970a. Gravity, seismicity, and tectonics of the North Island, New Zealand. N.Z. J. Geol. Geophys., 13: 126-144.

Hatherton, T., 1970b. Upper mantle inhomogeneity beneath New Zealand: surface manifestations. J. Geophys. Res., 75: 269-284.

Hatherton, T., 1978. Astride two plates - An account of current tectonics in New Zealand. Endeavour, 2: 180-185.

Hatherton, T., 1980. Shallow seismicity in New Zealand 1956-75. J. R. Soc. N.Z., 10: 19-25.

Hatherton, T. and Leopard, A.E., 1964. The densities of New Zealand Rocks. N.Z. J. Geol. Geophys., 7: 605-614.

Hatherton, T. and Syms, M., 1975. Junction of Kermadec and Hikurangi negative gravity anormalies (Note). N.Z. J. Geol. Geophys., 18: 753-756.

Hawkesworth, C.J., 1974. Vertical distribution of heat production in the Basement of the Eastern Alps. Nature, 249: 435-436.

Hegan, B.D., 1978. Engineering geology of Kaimai Tunnel. New Zealand Inst. of Engineers Conference.

Henderson, J., 1917. The Geology and Mineral resources of the Reefton subdivision, Westport and North Westland divisions. N.Z. Geol. Surv. Bull., 18, p. 129-130.

Hicks, S.R., 1980. Basement structures relevant to the oil search in the Dannevirke region. Report 172, Geophyscis Divn., Dept. Sci. Industrial Res., 16 pp.

Hilgendorf, F.W., Farr, C.C., Hogg, E.G., Page, S. and Wild, L.J., 1919. Report on the natural features of the Arthur's Pass Tunnel. Trans. and Proc. N.Z. Inst., 51: 422-426.

Hogan, J.A., 1979. Stratigraphy and sedimentology of the Kapuni formation, Taranaki, New Zealand. M.Sc. Thesis, Victoria University of Wellington.

Holmes, A., 1915. Radioactivity in the Earth and the Earth's thermal history. Geol. Mag., 2: 60-71 and 102-112.

Holmes, A., 1916. Radioactivity in the Earth's thermal history. Geol. Mag., 3: 265-274.

Horai, K., 1969. Effect of past climatic changes on the thermal field of the earth. Earth Planet. Sci. Lett., 6: 39-42.

Horai, K., 1971. Thermal conductivity of rock-forming minerals. J. Geophys. Res., 76: 1278-1308.

Horai, K. and Baldridge, S., 1972a. Thermal conductivity of nineteen igneous rocks, I Application of the needle probe method to the measurement of the thermal conductivity of rock. Phys. Earth Planet. Interiors, 5: 151-156.

Horai, K. and Baldridge, S., 1972b. Thermal conductivity of nineteen igneous rocks, II Estimation of the thermal conductivity of rock from the mineral and chemical compositions. Phys. Earth Planet. Interiors, 5: 157-166.

Horai, K. and Nur, A., 1970. Relationship among terrestrial heat flow, thermal conductivity and geothermal gradient. J. Geophys. Res., 75: 1985-1991.

Horai, K. and Simmons, G., 1969. Spherical harmonic analysis of terrestrial heat flow. Earth Planet. Sci. Lett., 6: 386-394.

Hunt International Petroleum Company, 1978. Well completion Report Hoiho -1C, P.P.L. 863. N.Z. Geol. Surv. Open-File Petroleum Report No. 730.

Hunt, J.M. 1979. Petroleum geochemistry and geology, W.H. Freeman and Comp., San Francisco, 617 pp.

Hurst, A.W., 1974. Magnetic effects in volcanic Regions. Ph.D. Thesis, Victoria University of Wellington.

Hurtig, E. and Schlosser, P., 1976. Vertical changes of the heat flow in boreholes in the North-German sedimentary basin. In: Geoelectric and Geothermal studies, KAPG Geophysical Monograph, Editor-in-Chief A. Ádám, Akadémiai Kiadó, Budapest, pp. 395-401.

Ingersoll, L.R., Zobel, O.J. and Ingersoll, A.C., 1954. Heat conduction with engineering, geological, and other applications. The University of Wisconsin Press, 325 pp.

Jaeger, J.C., 1955-1956. Numerical values for the temperature in radial heat flow. J. Math. Phys., 34: 316-321.

Jaeger, J.C., 1956. Conduction of heat in an infinite region bounded internally by a circular cylinder of a perfect conductor. Aust. J. Phys., 9: 167-179.

Jaeger, J.C., 1961. The effect of the drilling fluid on temperatures measured in boreholes. J. Geophys. Res., 66: 563-569.

Jaeger, J.C., 1965. Application to the theory of heat conduction to geothermal measurements. In: Terrestrial heat flow. Editor W.H.K. Lee, Am. Geophys. Un., Washington, D.C., Geophys. Monograph 8, pp. 7-23.

Jaeger, J.C., 1970. Heat flow and radioactivity in Australia. Earth Planet. Sci. Lett., 8: 285-292.

Jaeger, J.C., and Sass, J.H., 1964. A line source method for measuring the thermal conductivity and diffusivity of cylindrical specimens of rock and other poor conductors. Brit. J. Appl. Phys., 5: 1-8.

Jessop, A.M. and Lewis, T., 1978. Heat flow and heat generation in the superior province of the Canadian shield. Tectonophysics, 50: 55-77.

Jessop, A.M., Hobart, M.A. and Sclater, J.G., 1976. The world heat flow data collection - 1975. Geothermal series number 5, Earth Physics Branch, Energy, Mines and Resources, Canada, 125 pp.

Kappelmeyer, O. and Haenel, R., 1974. Geothermics with special reference to Application. Grebrüder Borntraeger, Berlin, Stuttgart, 238 pp.

Katz, H.R., 1968. Potential oil formations in New Zealand, and their stratigraphic position as related to basin evolution. N.Z. J. Geol. Geophys., 11: 1077-1133.

Lachenbruch, A.H., 1968. Preliminary geothermal model of the Sierra Nevada. J. Geophys. Res., 73: 6977-6989.

Lachenbruch, A.H., 1970. Crustal temperature and heat production: Implications of the linear heat flow relation. J. Geophys. Res., 75: 3291-3300.

Lachenbruch, A.H. and Brewer, M.C., 1959. Dissipation of the temperature effect in drilling a well in Arctic Alaska. U.S. Geol. Surv. Bull., 1083-C, 73-109.

Lachenbruch, A.H. and Bunker, C.M., 1971. Vertical gradients of heat production in the continental crust, 2. Some estimates from borehole data. J. Geophys. Res., 76: 3852-3860.

Langseth, M.G. 1965. Techniques of measuring heat flow through the ocean floor. In: Terrestrial heat flow. Editor W.H.K. Lee, Am. Geophys. Un., Washington, D.C., Geophys. Monograph 8, pp. 58-77.

Larskaya, Ye. S. and Zhabrev. D.V., 1964. Effects of stratal temperatures and pressures on the composition of dispersed organic matter (from the example of the Mesozoic-Cenozoic deposits of the Western Ciscaspian region). Dokl. Akad. Nauk SSSR, 157: 135-138.

Lawrence, P., 1967. New Zealand region; bathymetry, 1: 6,000,000. N.Z. Oceanogr. Inst. Chart, Miscellaneous Series, 15.

Lee, W.H.K., 1970. On the global variations of terrestrial heat flow. Phys. Earth Planet. Int., 2: 332-341.

Lee, W.H.K. and Uyeda, S., 1965. Review of heat flow data. In: Terrestrial heat flow. Editor W.H.K. Lee, Am. Geophys. Un., Washington, D.C., Geophys. Monograph 8, 87-190.

Lewis, K.B., 1971. Growth rate of folds using tilted wave-planed surfaces: coast and continental shelf, Hawke's Bay, New Zealand. In: Recent Crustal Movements, Editors B.W. Collins and R. Fraser, R. Soc. N.Z. Bull., 9,pp. 225-231.

Lubimova, E.A., Lusova, L.M., Firsov, F.V., Starikova, G.N. and Shushpanov, A.P., 1961. Determination of surface heat flow in Mazesta (USSR). Ann. Geophys., 14: 157-167.

Macfadyen, K.A., 1963. A physics laboratory handbook for students. Univ. of Lond. Press Ltd., Warwick Square, London E.C.4., 136 pp.

Makarenko, F.A. and Sergiyenko, S.I., 1974. Heat flow in oil, gas and gas-condensate fields of continents. Dokl. Akad. Nauk SSSR, 214: 45-47.

Marriot, W.G., 1969. A magnetotelluric investigation of the North Island Volcanic Plateau. M.Sc. Thesis, Victoria University of Wellington.

Matsubayashi, O. and Uyeda, S., 1979. Estimation of heat flow in certain exploration wells in offshore areas of Malaysia. Bull. Earthquake Res. Inst., 44: 31-44.

McBeath, D.M., 1977. Gas-condensate fields of the Taranaki Basin, New Zealand. N.Z. J. Geol. Geophys., 20: 99-127.

McKenzie, D.P., 1969. Speculations on the consequences and causes of plate motions. Geophys. J.R. Astr. Soc., 18: 1-32.

McKenzie, D.P. and Sclater, J.G., 1968. Heat flow inside the island arcs of the north western Pacific. J. Geophys. Res., 73: 3173-3179.

Meyer, S.L., 1975. Data analysis for scientists and engineers, John Wiley & Sons, Inc., New York. London. Sydney. Toronto, 513 pp.

Middleton, M.F., 1979. A model for bottom-hole temperature stabilization. Geophysics, 44: 1458-1462.

Midha, R.K., 1979. Geoelectromagnetic induction studies in the North Island volcanic region, New Zealand. Ph.D. Thesis, Victoria University of Wellington.

Minear, J.W. and Toksöz, M.N., 1970. Thermal regime of a downgoing slab and new global tectonics. J. Geophys. Res., 75: 1397-1419.

Misener, A.D. and Beck, A.E., 1960. The measurement of heat flow over land. In: Methods and techniques in geophysics. Editor S.K. Runcorn, Interscience Publishers, New York, pp. 10-61.

Moiseenko, U.I., 1968. Wärmeleitfähigkeit der Gesteine bei hohen Temperaturen. Freiberger Forrsch. -H. C238, Geophysit: 89-94, Leipzig.

Moody, J.D., 1975. Distribution and geological characteristics of giant oil fields. In: Petroleum and global tectonics. Editors A.G. Fischer and S. Judson, Princeton Univ. Press, pp. 307-320.

Mooney, H.M., 1970. Upper mantle inhomogeneity beneath New Zealand: seismic evidence. J. Geophys. Res., 75: 285-309.

Negi, J.G. and Pandey, O.P., 1974. Lateral isoflux-gradient map of the world heat flow data. Geophys. Res. Bull., 12: 155-156.

Negi, J.G. and Pandey, O.P., 1976. Correlation of heat flow and crustal topography in the Indian region. Geophys. J. R. Astr. Soc., 45: 201-217.

Negi, J.G. and Pandey, O.P., 1981. Correlation analysis of geothermal data in North America. Geothermics (in press).

Negi, J.G. and Panda, P.K. and Pandey, O.P., 1974. Correlation analysis of geothermal data for the sedimentary basins of India. Earth Planet. Sci. Lett., 21: 143-148.

Nie, N.H., Hull, C.H., Steinbrenner, K., Jenkins, J.G. and Bent, D.H., 1975. The statistical Package for the social sciences. Univ. of Chicago, McGraw Hill, 2nd Ed., 661 pp.

Nwachukwu, S.O., 1976. Approximate geothermal gradients in Niger delta sedimentary basin. Am. Assoc. Petroleum Geologists Bull., 60: 1073-1077.

N.Z. Geol. Surv., 1973. Geological map of New Zealand, 1972. E.C. Keating, Govt. Printer, Wellington, New Zealand.

N.Z. Geol. Surv., 1977. Faults and volcanoes - New Zealand Geological Survey. Earthquakes and Gravity Anomalies -Geophysics Division, Department of Scientific and industrial Research, E.C. Keating, Govt. Printer, Wellington, New Zealand.

N.Z. Met. Serv., 1978. Temperature Normals 1941 to 1970. N.Z. Met. S. Misc. Pub. 149, E.C. Keating, Govt. printer, Wellington, New Zealand.

Officer, C.B., 1955. Southwest Pacific crustal structure. Trans. Am. Geophys. Un., 36: 449-459.

Oxburgh, E.R., Richardson, S.W., Turcotte, D.L. and Hsui, A., 1972. Equilibrium bore hole temperatures from observations of thermal transients during drilling. Earth Planet. Sci. Lett., 14: 47-49.

Pandey, O.P., 1981. Terrestrial heat flow in the North Island of New Zealand. J. Volcan. Geoth. Res., 10 : 309-316.

Parasnis, D.S., 1976. Thermal parameters of some Precambrian Rocks in Sweden. Pageoph, 114: 319.

Philippi, G.T., 1965. On the depth, time and mechanism of petroleum generation. Geochm. Cosmochim. Acta., 29: 1021-1049.

Plewa, S., 1976. Correlation between thermal conductivity and other physical parameters of rocks. In: Geoelectric and Geothermal studies, KAPG Geophysical Monograph, Editor-in-chief A. Ádám, Akadémiai Kiadó, Budapest, pp. 48-52.

Pollack, H.N. and Chapman, D.S., 1977a. On the regional variation of heat flow, geotherms, and lithospheric thickness. Tectonophysics, 38: 279-296.

Pollack, H.N. and Chapman, D.S., 1977b. Mantle heat flow. Earth Planet. Sci. Lett., 34: 174-184.

Powell, R.W., 1957. Experiments using a simple thermal comparator for measurements of thermal conductivity, surface roughness and thickness of foils or of surface deposits. J. Sci. Instr., 34: 485-492.

Rao, R.U.M. and Jessop, A.M., 1975. A comparison of the thermal characters of shields. Can. J. Earth Sci., 12: 347-360.

Rao, R.U.M., Verma, R.K., Rao, G.V., Hamza, V.M., Panda, P.K. and Gupta, M.L., 1970. Heat flow studies in the Godavari valley (India). Tectonophysics, 10: 165-181.

Rao, R.U.M., Rao, G.V. and Narain, H., 1976. Radioactive heat generation and heat flow in the Indian shield. Earth Planet. Sci. Lett., 30: 57-64.

Reilly, W.I., 1962. Gravity and crustal thickness in New Zealand, N.Z. J. Geol. Geophys., 5: 228-233.

Reilly, W.I., 1965. Gravity map of New Zealand 1: 4,000,000, isostatic anomalies (1st Ed.). Dept. Sci. Indust. Res., Wellington, N.Z.

Revelle, R. and Maxwell, A., 1952. Heat flow through the ocean floor. Nature, 170: 199-200.

Reyners, M.E., 1978. A microearthquake study of the plate boundary, North Island, New Zealand. Ph.D. Thesis, Vcitoria University of Wellington.

Robertson, E. I. and Reilly, W.I., 1958. Bouguer anomaly map of New Zealand. N.Z. J. Geol. Geophys., 1: 560-564.

Robinson, R. 1976. Relative teleseismic travel-time residuals, North Island, New Zealand, and their relation to upper mantle structure. Tectonophysics, 31: T41-T48.

Robinson, R., Smith, E.G.C. and Latter, J.H., 1981. Seismic studies of the crust under the hydrothermal areas of the Taupo Volcanic Zone, New Zealand. J. Volcan. Geoth. Res., 9: 253-267.

Roy, R.F., Blackwell, D.D. and Birch, F., 1968. Heat generation of Plutonic rocks and continental heat flow provinces. Earth Planet. Sci. Lett., 5: 1-12.

Roy, R.F., Blackwell, D.D. and Decker, E.R., 1972. Continental heat flow. In: The nature of the solid earth. Editor E.C. Robertson, McGraw-Hill Book Comp., New York, pp. 506-543.

Rybach, L., 1973. 'Radioactive heat production of rocks from the Swiss Alps; geophysical implications.' 1st European Geophysical Society Meeting, Zurich (Abstract).

Rybach, L., 1976a, Radioactive heat production; A physical property determined by the chemistry of rocks. In: The Physics and Chemistry of Minerals and Rocks, Editor R.G.J. Strens, Wiley and Sons, London, pp. 309-318.

Rybach, L., 1976b. Radioactive heat production in rocks and its relation to other petrophysical parameters. Pageoph, 114: 309-317.

Rybach, L., 1978/79. The relationship between seismic velocity and radioactive heat production in crustal rocks: An exponential law. Pageoph, 117: 75-82.

Sanford, R.M., 1980. Exploration results off S. New Zealand. Oil and Gas J., 78: 83-90.

Sass, J.H. and Lachenbruch, A.H., 1978. Thermal regime of the Australian continental crust. In: The Earth-its origin, structure and evolution. Editor M.W. McElhinny, Academic Press (in press).

Sass, J.H., Munroe, R.J. and Lachenbruch, A.H., 1968. Measurement of geothermal flux through poorly consolidated sediments. Earth Planet. Sci. Lett., 4: 293-298.

Sass, J.H., Lachenbruch, A.H. and Jessop, A.M., 1971a. Uniform heat flow in a deep hole in the Canadian Shield and its paleoclimatic implications. J. Geophys. Res., 76: 8586-8596.

Sass, J.H., Lachenbruch, A.H. and Munroe, R.J., 1971b. Thermal conductivity of rocks from measurements on fragments and its application to heat-flow determinations. J. Geophys. Res., 76: 3391-3401.

Sass, J.H., Nielsen, B.L., Woollenberg, H.A. and Munroe, R.J., 1972. Heat flow and surface radioactivity at two sites in South Greenland. J. Geophys. Res., 77: 6435-6444.

Schofield, J.C., 1968. Regional aspects of cainozoic volcanology in the North Island of New Zealand - Crustal fusion produces intermediate magma. N.Z. J. Geol. Geophys., 11: 277-290.

Scholz, C.H., Rynn, J.M.W., Weed, R.W. and Frohlich, C., 1973. Detailed seismicity of the Alpine fault zone and Fiordland region, New Zealand. Geol. Soc. Am. Bull., 84: 3297-3316.

Schröder, J., 1963. Apparatus for determining the thermal conductivity of solids in the temperature range from 20 to 200°C. Rev. Sci. Instr., 34: 615-621.

Sclater, J.G. and Francheteau, J., 1970. The implications of terrestrial heat flow observations on current tectonic and geochemical models of the crust and upper mantle of the earlth. Geophys. J.R. Astr. Soc., 20: 509-542.

Sclater, J.G., Jaupart, C. and Galson, D., 1980. The heat flow through oceanic and continental crust and the heat loss of the earth. Rev. of Geophysics and space physics, 18: 269-311.

Simmons, G. and Horai, K., 1968. Heat flow data 2. J. Geophys. Res., 73: 6608-6629.

Simpson, B.M., 1980. An interpretation of hydrogeological data from Waiwera. N.Z.G.S. Report G42, 32pp.

Singh, L.J., 1971. Uplift and tilting of the Oterei Coast, Wairarapa, New Zealand, during the last ten thousand years. In: Recent Crustal Movements, Editors B.W. Collins and R. Fraser, R. Soc. N.Z. Bull., 9, pp. 217-219.

Sleep, N. and Toksöz, M.N., 1971. Evolution of marginal basins. Nature, 233: 548-550.

Smith, D.L., 1974. Heat flow, radioactive heat generation, and theoretical tectonics for northwestern Mexico. Earth Planet. Sci. Lett., 23: 43-52.

Smith, D.L., Nuckels III, C.E., Jones, R.L. and Cook, G.A., 1979. Distribution of heat flow and radioactive heat generation in Northern Mexico. J. Geophys. Res., 84: 2371-2379.

Smith, E.G.C., 1979. A micro-earthquake survey of the Rangitikei and Manawatu Basins. N.Z. J. Geol. Geophys., 22: 473-478.

Smith, J.H., 1970. Geothermal development in New Zealand. In: Proc. U.N. Symp. on the development and Utilization of Geothermal Resources. Pisa, Vol. 2, Part I, Geothermics, special issue 2, pp. 232-247.

Smith, W.D., 1970. S to P conversion as an aid to curstal studies. Geophys. J. R. Astr. Soc., 19: 513-519.

Smith, W.D., 1971. Earthquakes at shallow and intermediate depths in Fiordland, New Zealand. J. Geophys. Res., 76: 4901-4907.

Spiegel, M.R., 1961. Schaum's outline of Theory and Problems of Statistics. McGraw-Hill Book Comp., New York, 359 pp.

Steinhart, J.S., Hart, S.R. and Smith T.J., 1968. Heat flow. Carnegie Inst. Washington, Yearb., 67: 306-367.

Stipp, J.J. and McDougall, I., 1968. Geochronology of the Banks Peninsula Volcanoes, New Zealand. N.Z. J. Geol. Geophys., 11: 1239-1260.

Stipp, J.J. and Thompson, B.M., 1971. K/Ar ages from the volcanics of North Island, New Zealand. N.Z. J. Geol. Geophys., 14: 403-413.

Studt, F.E. and Thompson, G.E.K., 1969. Geothermal heat flow in the North Island of New Zealand. N.Z. J. Geol. Geophys., 12: 673-683.

Suggate, R.P., Stevens, G.R. and Te Punga, M.T. (Editors)., 1978. The Geology of New Zealand. Government Printer, Wellington, 2 Vols., 920 pp.

Sugimura, A. and Uyeda, S., 1973. Island Arcs: Japan and its Environs. Elsevier, Amsterdam, 247 pp.

Swanberg, C.A., 1972. Vertical distribution of heat generation in the Idaho batholith. J. Geophys. Res., 77: 2508-2513.

Swanberg, C.A., Chessman, M.D., Simmons, G., Smithson, S.B., Grønlie, G. and Heier, K., 1974. Heat flow - heat generation studies in Norway. Tectonophysics, 23: 31-48.

Thompson, G.E.K., 1966. Temperature survey at Hanmer, November 1962. Rep. 42., Geophysics Divn., DSIR, New Zealand.

Thompson, G.E.K., 1977. Temperature gradients within and adjacent to the North Island volcanic belt. N.Z. J. Geol. Geophys., 20: 85-97.

Thompson, G.E.K., 1980. Temperature gradients within and adjacent to the Taupo Volcanic Zone. N.Z. J. Geol. Geophys., 23: 407-412.

Thompson, J.G., 1980. A source rock analysis of cuttings and outcrop of the Kapuni formation and its correlatives. B.Sc. Hons. Thesis, Victoria University of Wellington.

Thompson, A.A. and Evison, F.F., 1962. Thickness of the earth's crust in New Zealand. N.Z. J. Geol. Geophys., 5: 29-45.

Timko, D.J. and Fertl, W.H., 1972. How downhole temperatures, pressures affect drilling. World Oil, October: 73-88.

Toksöz, M.N., Minear, J.W. and Julian, B.R., 1971. Temperature and geophysical effects of a downgoing slab. J. Geophys. Res., 76:1113-1138.

Turcotte, D.L. and Oxburgh, E.R., 1969. A fluid theory for the deep structure of dip-slip fault zones. Phys. Earth Planet. Interiors, 1: 381-386.

Uydea, S., 1977. Some basic problems in the Trench-Arch-Back Arc System. In: Island Arcs, Deep Sea Trenches and Back - arc Basins, Editors M. Talwani and W.C. Pitman III, Am. Geophys. Un., Washington, D.C., pp. 1-14.

Uyeda, S. and Horai, K., 1964. Terrestial heat flow in Japan. J. Geophys. Res., 69: 2121-2141.

Vacquier, V., Uyeda, S., Yasui, M. Sclater, J., Corry, C. and Watanabe, T., 1967. Heat flow measurements in the Northwestern Pacific, Bull. Earthquake Res. Inst., 44: 1519-1535.

Veliciu, S., Cristian, M., Paraschiv, D. and Visarion, M., 1977. Preliminary data of heat flow distribution in Romania. Geothermics, 6: 95-98.

Von Herzen, R.P. and Maxwell, A.E., 1959. The measurement of thermal conductivity of deep sea sediments by a needle probe method. J. Geophys. Res., 64: 1557-1563.

Walcott, R.I. 1978. Present tectonics and Late Cenozoic evolution of New Zealand. Geophys. J. R. Astro. Soc., 52: 137-164.

Wang, C., 1980. Sediment subduction and frictional sliding in a subduction zone. Geology, 8: 530-533.

Watanabe, T., 1974. Heat flow in the Western Pacific and marginal seas. Marine Sci. Monthly, 6,7,13-17.

Watanabe, T., Epp, D., Uyeda, S., Langseth, M. and Yasui, M., 1970. Heat flow in the Philippine Sea. Tectonophysics, 10: 205-224.

Watanable, T., Langseth, M.G. and Anderson, R.N., 1977. Heat flow in Back-Arc basins of the Western Pacific. In: Island Arcs, Deep Sea Trenches and Back - arc Basins, Editors M. Talwani and W.C. Pitman III, Am. Geophys. Un., Washington, D.C., pp. 137-161.

Wellman, H.W., 1956. Structural outline of New Zealand. N.Z. Dept. Sci. Indust. Res. Bull., 121: 36 pp.

Wellman, H.W., 1971a. Holocene tilting and uplift on the White Rock Coast, Wairarapa, New Zealand. In: Recent Crustal Movements, Editors B.W. Collins and R. Fraser, R. Soc. N.Z. Bull., 9 pp. 211-215.

Wellman, H.W., 1971b. Holocene tilting and uplift on the Glenburn Coast, Wairarapa, New Zealand. In: Recent Crustal Movements, Editors B.W. Collins and R. Fraser, R. Soc. N.Z. Bull., 9 pp. 221-223.

Wellman, H.W., 1979. An uplift map for the South Island of New Zealand, and a model for uplift of the Southern Alps. In: The Origin of the Southern Alps. Editors R.I. Walcott and M.M. Cresswell. R. Soc. N.Z. Bull., 18, pp. 13-20.

Winkler, H.G., 1952. In: Landolf-Börnstein, Zahlenwerte und Funktionen. Bd. III, Astronomie und Geophysik, 324, Springer, Berlin, Wien, Heidelberg.

Woodside, W., and Messmer, J.H. 1961. Thermal conductivity of porous media, 1, unconsolidated sands, 2, consolidated rocks. J. Appl. Phys., 32: 1688-1706.

Woodward, D.J., 1979. The crustal structure of the Southern Alps, New Zealand, as determined by gravity. In: The origin of the Southern Alps, Editors R.I. Walcott and M.M. Cresswell, R. Soc. N.Z. Bull., 18, pp. 95-98.

Yasui, M., Epp, D., Nagasaka, K. and Kishii, T., 1970. Terrestrial heat flow in the seas round the nansei shoto (Ryukyu Islands). Tectonophysics, 10: 225-234.

Yoder, H.S. and Tilley, C., 1962. Origin of basalt magmas, and experimental studies of natural and synthetic rock systems. J. Petrol., 3: 342-532.

Zierfuss, H., 1963. An apparatus for the rapid dtermination of the heat conductivity of poor conductors. J. Sci. Instr. 40: 69-71.